University of Southampton

The significance of abnormalities of p53 expression in lymphoma associated with coeliac disease

Monika Phelps

A thesis submitted for the award of the degree of

Doctor of Philosophy

Division of Cancer Sciences

Faculty of Medicine, Health and Biological Sciences

December 2000

UNIVERSITY OF SOUTHAMPTON

ABSTRACT

FACULTY OF MEDICINE, HEALTH AND BIOLOGICAL SCIENCES

DIVISION OF CANCER SCIENCES

Doctor of Philosophy

THE SIGNIFICANCE OF ABNORMALITIES OF P53 EXPRESSION IN LYMPHOMA ASSOCIATED WITH COELIAC DISEASE

by Monika Phelps

The aim of this study was to investigate pathological tissue from cases of enteropathy-associated T cell lymphoma (EATL), previously shown to over-express p53 protein, for the presence of p53 mutations with the view of correlating over-expression of the protein with the presence of genetic alterations.

Single-stranded conformation polymorphism analysis was used to screen a series of formalin-fixed, paraffin-embedded EATL tissue samples and histologically uninvolved tissue from the same patients for the presence of p53 mutations in exons 5-8. DNA sequence analysis was performed on cases showing PCR fragments with mobility shifts to confirm the presence of mutations. Immunohistochemistry was used to assess expression of p53 and related cell cycle regulatory proteins in the same cases. Mobility shifts were detected in 10/29 (34.5%) tumour (T) samples and in 3/20 (15%) samples of adjacent (A) uninvolved tissue. Only 2 samples (1 T and 1 A sample) showing mobility shifts showed no over-expression of p53. DNA sequence analysis identified the presence of mutations in 3/29 (10%) T samples and in 2/20 (10%) A samples. Additional silent mutations were also detected in 2 T samples from different cases.

The DNA sequencing results suggest that p53 over-expression is associated with p53 mutations in a small proportion of EATL cases. An alternative mechanism may be responsible for the stabilisation of p53 protein in the remaining cases. The detection of multiple mutations in samples from some individual patients may indicate that mutations arise in more than one T cell clone within enteropathic bowel.

CONTENTS

LIST OF TABLES

LIST OF FIGURES

PUBLICATION ARISEN AS A RESULT OF THIS STUDY:

Phelps, M., Wilkins, B.S., and Jones, D.B. (2000). Selective genetic analysis of p53 immunostain positive cells. J.Clin.Pathol.: Mol.Pathol. *53*, 159-161.

ACKNOWLEDGEMENTS

I would like to thank my supervisors Dr. D.B. Jones and Dr. B.S. Wilkins for their guidance and advice during this study.

I am grateful to all the technical staff in the Pathology department, especially Sue Harris, Sammy Reynolds, Kathy Higginson, Tony Carr and Ron Lee, for their valuable assistance.

Thanks also to all my colleagues for their help, patience and friendship. I would especially like to thank Nveed Chaudhary for his patience and accuracy in proof-reading the manuscript and offering his valuable advice.

I am also thankful to the Association for International Cancer Research for providing the funds to carry out this study.

Finally, I would like to say a big thank you to my husband for his exceeding patience and support throughout.

LIST OF ABBREVIATIONS

A	Adenine
A	Adjacent tissue
A_{260}	Absorbance at 260 nm
A_{280}	Absorbance at 280 nm
aa	Amino acid
AEA	Anti-endomysium antibodies
AGA	Anti-gliadin antibodies
APC	Antigen presenting cell
APES	Aminopropyltriethoxysilane
APS	Ammonium persulfate
ARF	Alternative reading frame
ATM	Ataxia telangiectasia mutated gene
BAI1	Brain-specific angiogenesis inhibitor 1
Bax	Bcl-2-associated protein X
BLAST	Basic local alignment search tool
bp	Base pairs
BSA	Bovine serum albumin
C	Cytosine
C	Constant region gene
C	Carboxyl terminus
CD	Cluster of differentiation
CD	Coeliac disease
CDK	Cyclin dependent kinase
CDR	Complementarity determining region
CIP1	CDK2 interacting protein 1
CKI	Cyclin dependent kinase inhibitor
CLL	Chronic lymphocytic leukaemia
cM	Centimorgans
CTCL	Cutaneous T cell lymphoma
CTLA	Cytotoxic T lymphocyte-associated

D	Diversity gene
DAB	Diaminobenzidine
dATP	Deoxyadenosine triphosphate
dCTP	Deoxycytidine triphosphate
ddNTP	Dideoxynucleoside triphosphate
dGTP	Deoxyguanosine triphosphate
DNA	Deoxyribonucleic acid
DNA-PK	DNA-dependent protein kinase
dNTP	Deoxynucleoside triphosphate
DOP-PCR	Degenerate oligonucleotide-primed-PCR
dsDNA	Double stranded DNA
dTTP	Deoxythymidine triphosphate
EATL	Enteropathy associated T cell lymphoma
EDTA	Ethylenediaminetetraacetic acid
EEC	Ectrodactyly, ectodermal dysplasia and cleft lip with or without cleft palate
EF-1α	Elongation factor-1 alpha
EI24	Etoposide-induced 24
F	Forward primer
G	Guanine
G0	Gap 0 phase
G1	Gap 1 phase
G2	Gap 2 phase
GADD45	Growth arrest and DNA damage inducible gene 45
GFD	Gluten free diet
Gln	Glutamine
Glu	Glutamic acid
HCl	Hydrogen chloride
HD	Heteroduplex
H&E	Haematoxylin and eosin
HIC-1	Hypermethylated in cancer 1
HLA	Human leukocyte antigen
HPV	Human papilloma virus

HTLV-I	Human T cell lymphotropic virus type I
IEL	Intraepithelial lymphocyte
IFN	Interferon
Ig	Immunoglobulin
IGF-BP3	Insulin-like growth factor binding protein 3
IHC	Immunohistochemistry
IHSA	Immunohistoselective analysis
IHSS	Immunohistoselective sequencing
IL	Interleukin
INK4	Inhibitor of CDK4
ITAM	Immunoreceptor tyrosine-based activation motif
J	Joining region gene
Kb	Kilobase
kDa	Kilodalton
ln	Lymph node
LOH	Loss of heterozygosity
LP	Lamina propria
M	Mitosis
M	Molecular weight marker
MALT	Mucosa-associated lymphoid tissue
mda-6	Melanoma differentiation associated gene
MDE	Mutation detection enhancement
mdm2	Murine double minute 2 gene
MDM2	Murine double minute 2 protein
MDR1	Multidrug resistance gene 1
MHC	Major histocompatibility complex
MPF	Mitosis promoting factor
N	Amino terminus
NA	Not available
ND	Not done
neg	Negative
NER	Nucleotide excision repair
NBS	Nijmegen Breakage Syndrome

NHL	Non-Hodgkin's lymphoma
NSD	No shifts detected
P	Phosphorus
PEP	Primer-extension pre-amplification
PBS	Phosphate buffered saline
PCR	Polymerase chain reaction
PIG	P53-induced gene
PKC	Protein kinase C
pRB	Retinoblastoma gene product
Pro	Proline
R	Arginine
R	Reverse primer
RFLP	Restriction fragment length polymorphism
RS	Refractory sprue
S	Sulphur
S	Synthesis phase
Sdi 1	Senescent derived inhibitor 1
Ser	Serine
SSCP	Single-strand conformation polymorphism
ssDNA	Single-stranded DNA
STAT5	Signal transducer and activator of transcription
SURF	Selective ultraviolet radiation fractionation
SV40	Simian virus 40
T	Thymine
T	Tumour tissue
T_a	Annealing temperature
T_m	Melt temperature
TAE	Tris acetate EDTA
TBE	Tris borate EDTA
TBP	Tata box binding protein
TBS	Tris buffered saline
TcR	T cell receptor
TEMED	Tetramethylethylenediamine

Th1	T helper cell type 1
Th2	T helper cell type 2
Tsp 1	Thrombospondin 1
tTG	Tissue transglutaminase
U	Uracil
UV	Ultraviolet
V	Variable region gene
VEGF	Vascular endothelial growth factor
W	Whole tissue
WAF1	Wild-type p53 activated fragment 1
wig-1	Wild-type p53 induced gene 1
WT	Wild type DNA

1 - INTRODUCTION

1.1 COELIAC DISEASE

1.1.1 Clinical and histological features

Coeliac disease (CD) is a malabsorptive disorder caused by a genetically determined abnormal immune reaction to ingested gluten in the mucosa of the small intestine (Marsh, 1992). Symptoms show great variation from patient to patient, but classic presentation includes diarrhoea, flatulence, weight loss and fatigue (Trier *et al.*, 1978).

Malabsorption is accompanied by loss of the normal villous architecture, with a flat mucosa due to subtotal villous atrophy in severe cases, crypt hyperplasia, infiltration of the lamina propria by plasma cells and lymphocytes, and an increased number of intra-epithelial lymphocytes (Fig.1.1.1). The total thickness of the mucosa may be increased as a result of crypt hyperplasia and a lymphoplasmocytic infiltrate in the lamina propria (Ciclitira and Hall, 1990).

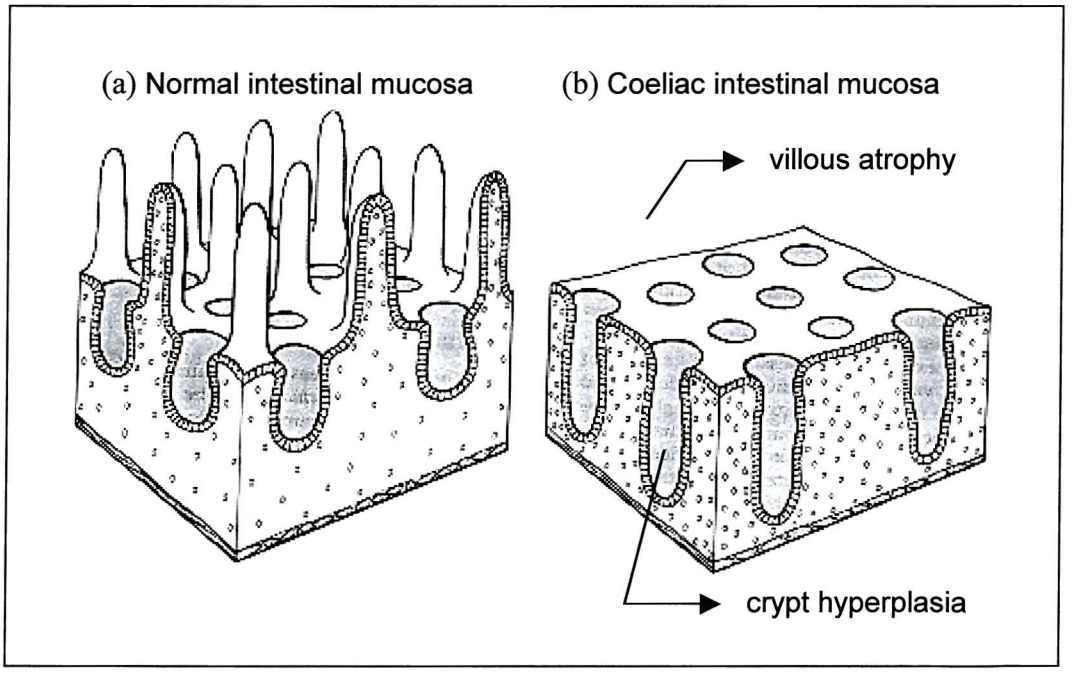

Fig.1.1.1. Changes in small intestinal architecture from a normal jejunal mucosa (a) to severe villous atrophy (b) in coeliac disease. Reproduced with permission from Dixon, 1996.

Figures 1.1.3 and 1.1.4 depict different stages of villous atrophy in CD. A section of normal intestinal mucosa (Fig. 1.1.2) has been added for comparison.

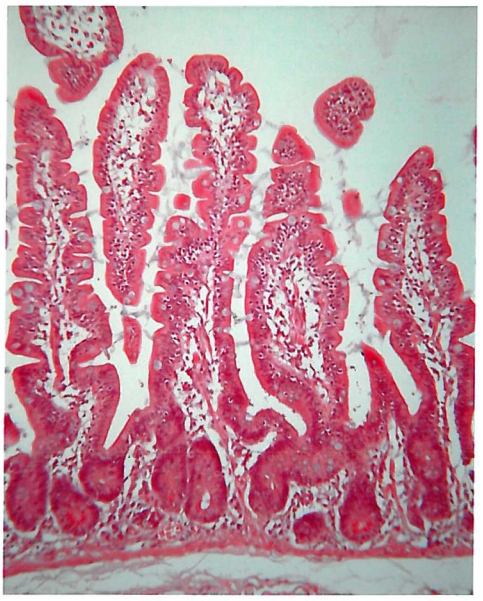

Fig. 1.1.2. Small intestinal mucosa showing normal villous architecture with short crypts between the bases of the villi (H&E, x100).

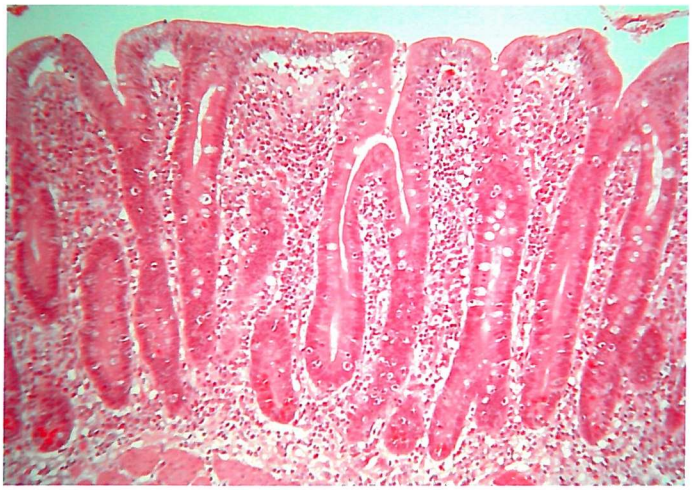

Fig. 1.1.3. Mucosa of enteropathic bowel showing partial villous atrophy, crypt hyperplasia and plasmocytic infiltrate of the lamina propria (H&E, x100).

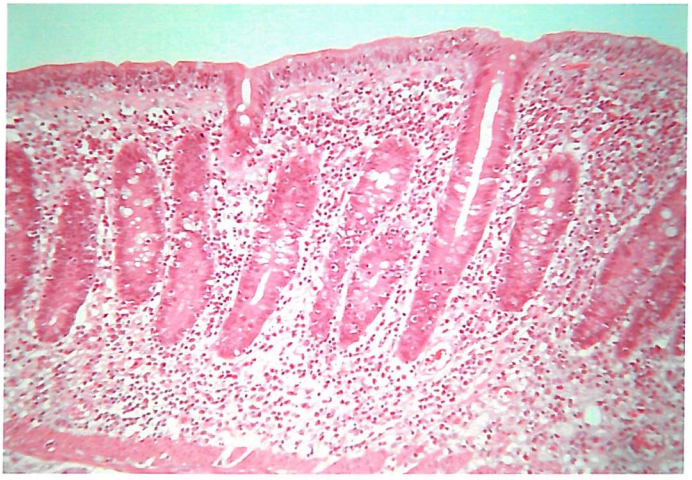

Fig. 1.1.4. Mucosa of enteropathic bowel showing subtotal villous atrophy making it resemble colonic mucosa (H&E, x100).

1.1.2 Incidence

The prevalence of this condition in the United Kingdom is approximately 1 in 1500, while in the west of Ireland it rises to 1 in 300 (Ciclitira and Hall, 1990). It has become apparent recently that clinically manifest cases of CD represent only a small proportion of the total population with this disorder and that the incidence of CD is higher than previously thought, remaining unrecognised in a large number of cases (Unsworth and Brown, 1994).

1.1.3 Diagnosis

Coeliac disease classically presents in infants after weaning and the introduction of cereals into their diets (early onset disease). A second peak of incidence occurs during the third decade, with adults frequently having been asymptomatic until shortly before presentation (late onset disease) (Ciclitira and Hall, 1990).

Small intestinal biopsy with the demonstration of a flat mucosa, which is restored to normal after gluten withdrawal, is considered essential for the diagnosis of classical CD. Re-appearance of mucosal abnormalities upon gluten challenge confirms the diagnosis (Mathus-Vliegen, 1996). Detection of serum IgA antibodies reactive with gliadin (a component of gluten) and with endomysium (a structure of the smooth muscle connective tissue – see section 1.1.5.2) are also valuable tools for the confirmation of CD (Ladinser *et al.*, 1994; Volta *et al.*, 1991).

1.1.4 Treatment

Patients with CD are placed on a gluten-free diet, after which there is usually resolution of all the pathological abnormalities and the normal pattern of villous structure returns. In adult patients, however, resolution is slower and in some cases the villous architecture never returns to normal (Ciclitira and Hall, 1990).

1.1.5 The toxic component: gliadin

Wheat flour contains many water-soluble components (albumins, globulins and starch) and insoluble gluten (Howdle and Losowsky, 1987). Gluten contains two types of storage proteins: prolamins and non-toxic glutenins. The ethanol-soluble fraction of gluten contains prolamins and, in wheat flour, is called gliadin. These are thought to be

the toxic component to the small intestinal mucosa in CD (Kamer, 1953). Other cereals such as rye, barley and oats also contain toxic prolamins, although oats may be tolerated by some individuals (Marsh, 1992; Ciclitira and Hall, 1990).

1.1.5.1 Anti-gliadin antibodies in coeliac disease

The proposal that gliadin is responsible for activation of the immune system is supported by the presence of gliadin-specific T cells in the mucosa of CD patients (Lundin *et al.*, 1993) and the detection of serum IgA anti-gliadin antibodies (Kelly *et al.*, 1991; O'Farrelly *et al.*, 1986).

In untreated CD, both IgG and IgA serum antigliadin antibodies (AGA) have been found to be markedly raised and to fall when patients are placed on a gluten-free diet. Serum IgA AGA levels are thought to fall more quickly than IgG AGA levels, which show a more gradual, progressive decline. Serum IgA has also been found to be more sensitive and specific than IgG in screening for untreated CD (Kelly *et al.*, 1991). In contrast to serum AGA levels, IgA AGA levels in intestinal aspirates remain increased even in patients who have been on a gluten-free diet for over two years and show excellent histological response with normal or near normal small intestinal morphology (Kelly *et al.*, 1991).

1.1.5.2 Anti-endomysium antibodies and tissue transglutaminase enzyme

Another subgroup of serum IgA antibodies, IgA anti-endomysium antibodies (AEA), has been described in a high number of patients with CD (Chorzelsky *et al.*, 1984) and is now used as a tool for screening and follow-up of CD patients. These antibodies have high specificity and sensitivity; their measurement permits the detection of clinical and subclinical disease (Ladinser *et al.*, 1994; Volta *et al.*, 1991). These antibodies are species-specific and react only with endomysium in the oesophagus of primates, targeting the intermyofibril substance of smooth muscle (Volta *et al.*, 1991). More recently, a more specific and sensitive technique has been described for AEA measurement using the more easily available human umbilical cord smooth muscle instead of primate oesophagus (Ladinser *et al.*, 1994).

Gliadin is thought to drive the secretion of AEA, as these antibodies have been shown to be produced in biopsy samples cultured with a peptic/tryptic digest of gliadin (Picarelli *et al.*, 1996). The antigen recognised by AEA has been identified as tissue transglutaminase (tTG), a calcium-dependent enzyme that catalyses the crosslinking of proteins resulting in formation of an ε-(γ-glutamyl)-lysine bond (Dieterich *et al.*, 1997). It is widely distributed in human organs and is normally localized in the cytoplasm of cells but can be released during tissue damage, following which it may associate with cell surfaces or extracellular matrix molecules.

Gliadin is a preferred substrate for tTG and it has been hypothesized that neo-epitopes are created in crosslinked gliadin-gliadin or gliadin-tTG complexes when damage or hyperpermeability of the intestinal epithelium triggers abundant extracellular release of cytosolic tTG, mainly from lamina propria mononuclear or mesenchymal cells. These neo-epitopes could then initiate an immune response, in genetically susceptible individuals, directed against both gliadin and tTG (Dieterich *et al.*, 1997).

1.1.5.3 Disease-precipitating epitopes of gliadin

The identification of disease-precipitating epitopes has been difficult due to the large heterogeneity and complexity of gluten molecules (Marsh, 1992). *In vitro* studies testing the toxicity of peptides isolated from gliadin digests have identified sequences containing repetitive motifs that could represent disease-inducing domains of the protein. These sequences include -Pro-Ser-Gln-Gln- and -Gln-Gln-Gln-Pro-, which are not cleaved by pepsin, trypsin or chymotrypsin (Wieser, 1995; Marsh, 1992). More recently, a gliadin peptide has been identified which is recognised by T cell clones restricted by HLA-DQ8 molecules from small intestinal biopsies of CD patients (van de Wal *et al.*, 1998a). This peptide is located in the carboxyl-terminal region of gliadin and represents a unique sequence found in only one of the many gliadin variants. The minimal peptide necessary to stimulate the T cell clones must contain at least 11 amino acid residues and the sequence -Pro-Ser-Gln-Gln- at its carboxyl terminus, representing one of the repetitive motifs mentioned above (van de Wal *et al.*, 1998a). Another epitope (Gln-Pro-Gln-Gln-Ser-Phe-Pro-Glu-Gln-Gln), resulting from de-amidation of a distinct glutamine in the native structure of a purified γ-type gliadin, has been identified using DQ2-restricted T cell clones derived from CD patients (Sjostrom *et al.*, 1998).

De-amidation was performed by heating (to 98°C) a chymotrypsin gliadin digest in an acetic acid-HCl solution (pH 1.8) for 60min. Incubation at 37°C, pH 1.8, for 15min also created an epitope recognised by a DQ2-restricted T cell clone, suggesting that sufficient de-amidation can occur in the acidic environment of the stomach to create the epitopes recognised by T cells from the intestinal mucosa of CD patients (Sjostrom *et al.*, 1998).

1.1.5.4 The significance of gliadin de-amidation

The strong association of CD with HLA-DQ2 and –DQ8 indicates a preferential recognition of gliadin fragments bound to these alleles by intestinal T cells (Lundin *et al.*, 1994). The peptide-binding motifs of both DQ2 and DQ8 show a preference for negatively charged residues at several positions of the bound peptides (Vartdal *et al.*, 1996). Although gliadins have a very low content of negatively charged amino acids (usually <2% of the residues), they have a large proportion of Gln (glutamine) residues (≤40%), so that the conversion of Gln to Glu (glutamic acid) residues by de-amidation would result in the presence of relatively large numbers of negatively charged Glu residues in gliadin (van de Wal *et al.*, 1998a; Sjostrom *et al.*, 1998).

1.1.5.5 Selective de-amidation by tissue transglutaminase

De-amidation of gliadin can also be caused by enzymatic processes. Recently, it has been demonstrated that the enzyme tTG can effect the de-amidation of gliadins in an ordered and specific manner, creating epitopes that bind efficiently to DQ2, which results in strongly enhanced T cell stimulatory activity (van de Wal *et al.*, 1998b; Molberg *et al.*, 1998).

Immunohistochemical studies have revealed abundantly expressed extracellular tTG and DQ-expressing cells just under the mucosal epithelium of CD patients, suggesting that tTG might be involved in processing gliadin before it binds to DQ2 molecules (Molberg *et al.*, 1998). The subepithelial region might therefore provide a micro-environment for tTG-mediated modification, DQ2 binding and T cell recognition of gliadin peptides as gliadin-specific T cells have also been detected in this area (Molberg *et al.*, 1998).

1.2 GENETIC SUSCEPTIBILITY TO COELIAC DISEASE

Susceptibility to CD is associated with polymorphisms of the major histocompatibility complex (MHC) genes, which are found on the short arm of chromosome 6 (Marsh, 1992).

1.2.1 The HLA system

The products of the MHC complex are associated with intercellular recognition and with self/nonself discrimination. In humans, the MHC complex is referred to as the Human Leucocyte Antigen (HLA) complex and is organized into three regions encoding different classes of molecules (Janeway and Travers, 1997):

- Class I genes encode glycoproteins expressed on the surface of nearly all nucleated cells and platelets, where they present peptide antigens of largely endogenous origin necessary for the activation of CD8-positive ($CD8^+$)T cells, which are mostly cytotoxic.

- Class II genes encode glycoproteins expressed primarily on antigen-presenting cells, such as macrophages, dendritic cells, B cells and activated T cells. Other cell types can also be induced to express class II molecules by interferon-γ; these include vascular endothelium, fibroblasts, renal tubular epithelial cells and intestinal epithelial cells (Panja and Mayer, 1996; Kagnoff, 1990). Class II molecules present processed antigenic peptides of largely exogenous origin to CD4-positive ($CD4^+$)T cells, predominantly of helper phenotype.

- Class III genes encode somewhat different products, including a number of soluble serum proteins such as components of the complement system.

1.2.1.1 HLA class II genes and molecules

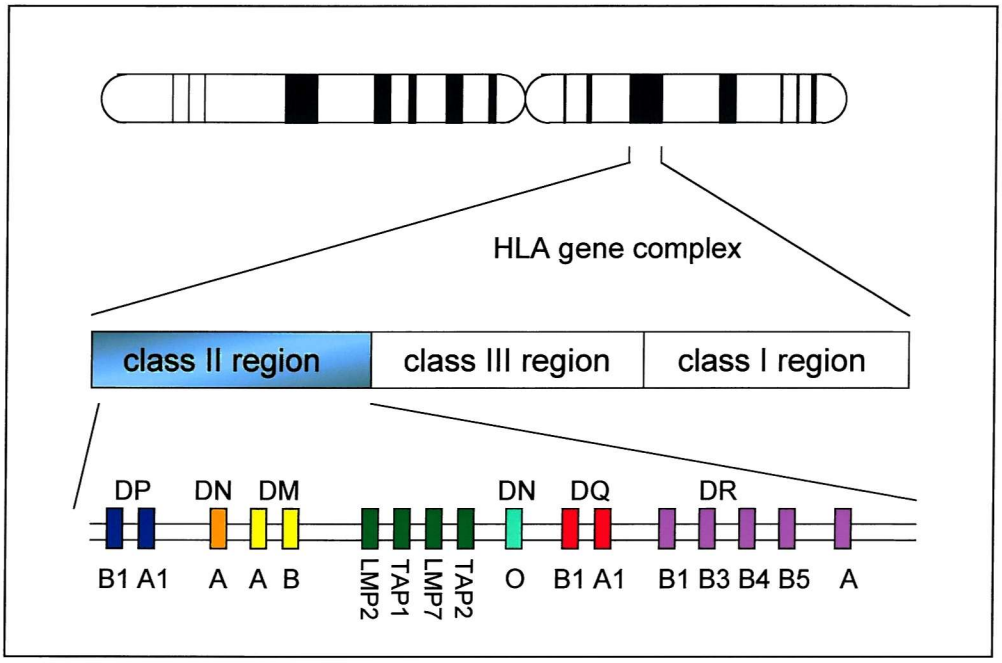

Fig. 1.2.1. The HLA class II gene complex on the short arm of chromosome 6. Only loci with known protein products are shown (adapted from Sollid and Thorsby, 1993).

Class II genes are encoded in the HLA-D region, which can be divided into three major sub-regions termed -DP, -DQ and -DR (Fig. 1.2.1). Each of these sub-regions contains at least one expressed A and B gene encoding, respectively, the α and β chains of an HLA class II molecule. The class II HLA genes are highly polymorphic and there are currently known to be at least 2 DRA, 264 DRB, 20 DQA1, 39 DQB1, 15 DPA1, and 85 DPB1 alleles (Bodmer *et al.*, 1999).

A class II molecule is a membrane-bound glycoprotein that contains external domains, a transmembrane segment, and a cytoplasmic anchor segment. It is a heterodimer that consists of an α chain (MW 31-34 kDa) non-covalently associated with a β chain (MW 26-29 kDa), which together form a peptide-binding groove. This groove is open at both ends and is capable of binding peptides of variable lengths (12-24 amino acid residues), derived from extracellular antigens, and presenting them to T cells (Howell & Jones, 1995; Brown *et al.*, 1993).

1.2.1.2 HLA associations in coeliac disease

Coeliac disease has been found to be preferentially associated with the expression of certain HLA-DQ heterodimers. While the majority of patients (approximately 90 % or more) carry the HLA-DQ (α1*0501, β1*0201) heterodimer, with the DQA1*0501, DQB1*0201 alleles encoding in either *cis* or *trans* configuration (Sollid *et al.*, 1989), a small subset of CD patients has been shown to carry the HLA-DR4 haplotype, which has the DQB1*0302 allele, or HLA-DQ8, which codes for the DQ (α1*0301, β1*0302) molecule. This suggests that the DQB1*0302 allele may confer CD susceptibility on these haplotypes (Sollid and Thorsby, 1993).

Coeliac disease was first reported to be associated with the HLA-class I molecule B8 (Stokes *et al.*, 1972). Later, a stronger association was found with the HLA-class II molecule DR3 (Keuning *et al.*, 1976). The association with HLA-B8 simply appeared to reflect strong linkage disequilibrium between the allele that encodes HLA-B8 and the allele that encodes HLA-DR3 (Kagnoff, 1990).

The proportion of patients carrying the DR3 haplotype varies considerably between different populations, with a higher frequency being found in patients with a northern European ancestry. Patients of Italian or Spanish ancestry have been shown to be either DR3 or DR5/DR7 heterozygous. While DR3 has been shown to be a susceptibility allele together with any other DR allele, DR7 is associated with CD almost only in combination with DR3 or DR5 (Sollid and Thorsby, 1993).

Subsequently, an even stronger association was reported between CD and HLA-DQ2, an HLA class II molecule in linkage disequilibrium with both DR3 and DR7. The DR3-DQ2 haplotype showed the strongest association (Tosi *et al.*, 1983). In order to determine which locus (or loci) of this haplotype confers disease susceptibility the HLA-DQ genes were sequenced (reviewed in Sollid and Thorsby, 1993). The DR3-DQ2 haplotype was shown to carry the DQA1*0501 and DQB1*0201 alleles, the DR5-DQ7 haplotype carries the DQA1*0501 and DQB1*0301 alleles, and the DR7-DQ2 haplotype carries the DQA1*0201 and DQB1*0201 alleles. The DR3-DQ2 and DR5-DQ7 haplotypes have the same DQA1 allele, while the DR3-DQ2 and DR7-DQ2

haplotypes have the same DQB1 alleles. Thus, patients with CD who have DR3 or who are DR5/DR7 heterozygous may express the same DQ molecule, DQ (α1*0501, β1*0201), in either *cis* or *trans* position (see Fig. 1.2.2) (Sollid and Thorsby, 1993). This suggests that this particular heterodimer might be primarily associated with CD (Sollid *et al.*, 1989).

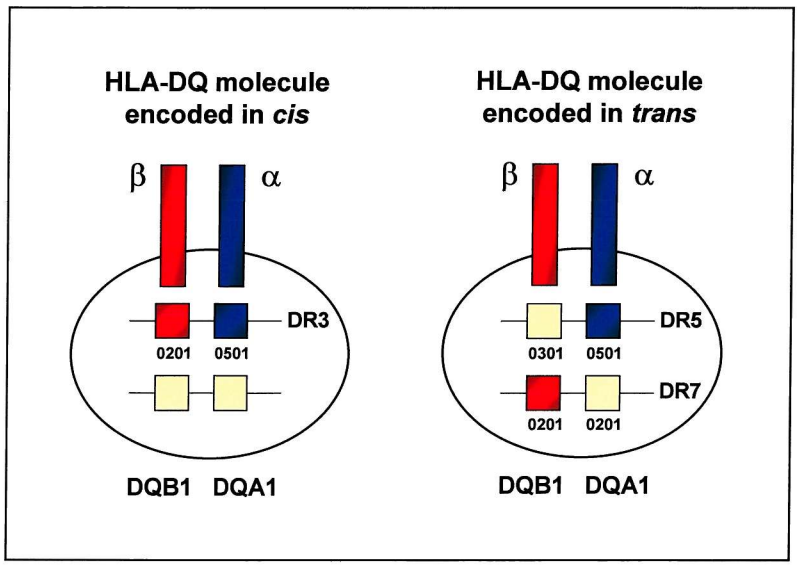

Fig. 1.2.2. Representation of the HLA-DQαβ heterodimer associated with CD. Patients with CD who have DR3 or who are DR5/DR7 heterozygous may express the same DQ molecule, DQ (α1*0501, β1*0201). The DQA1*0501 and DQB1*0201 genes are located in *cis* (on the same chromosome) in DR3 individuals, whereas they are located in *trans* (on different chromosomes) in DR5/DR7 heterozygous individuals. Reproduced from Sollid and Thorsby, 1993.

It has been shown that the DQB1*0201allele may exert a gene dosage effect, as homozygosity for this allele increases susceptibility to CD due to an increased expression of the DQ (α1*0501, β1*0201) heterodimer in such individuals. The presence of a second copy of DQB1*0201 is also associated with earlier onset of the disease (Congia *et al.*, 1994; Ploski *et al.*, 1993).

*1.2.1.3 The binding of gliadin peptides to HLA-DQ (α1*0501, β1*0201)*

The association of CD with certain alleles suggests that a substitution encoded by the allele within the antigen-binding cleft allows efficient binding and presentation of a gliadin antigen to pathogenic T cells (Tighe and Ciclitira, 1995). The importance of

antigen presentation by the HLA-DQ (α1*0501, β1*0201) heterodimer is suggested by a study in which gliadin-reactive T cells isolated from the small intestinal mucosa of 23 CD patients were found to be restricted by this HLA heterodimer (Molberg *et al.*, 1997).

Peptides binding to DQ2 molecules have been demonstrated to have negatively charged residues preferentially located as anchors in positions P4, P6 and P7 (Vartdal *et al.*, 1996; Johansen *et al.*, 1996). Anchor residues are amino acid residues of the bound peptide. The side chains of these amino acid residues insert into pockets in the HLA molecule binding the peptide to it. Peptides that bind HLA class II molecules are variable in length and their anchor residues lie at various distances from the ends of the peptide. By convention the first anchor residue is denoted as residue 1, or P1, and so on. Anchor residues differ for peptides binding different HLA molecules but are similar for all peptides binding to the same HLA molecule (Janeway and Travers, 1997).

Synthetic gliadin peptides de-amidated using an acid/heat treatment (Sjostrom *et al.*, 1998) or de-amidated by tTG (Molberg *et al.*, 1998) at position 148 have been shown to have an increased binding affinity to DQ2 in cell-free binding assays. Alignment of the peptide sequence with the DQ2-binding motif suggests that the Q148 residue could be the P7 residue (Sjostrom *et al.*, 1998; Molberg *et al.*, 1998).

1.2.2 Non-HLA genetic associations

Non-HLA genes and/or environmental factors are also thought to contribute to the development of CD, as only a minor proportion of the individuals who have the HLA-DQ(α1*0501,β1*0201) haplotype develop CD (Sollid and Thorsby, 1993). Although the concordance rate of CD seen in monozygotic twins is around 70%, this incomplete concordance suggests that additional factors are involved. However, not all the twin pairs studied had proven monozygosity and some twin pairs had insufficient long-term follow-up to be certain that the disease would not develop at a later stage (reviewed in Houlston and Ford, 1996). There is now evidence, through autosomal genomic screening, that there is linkage of at least one non-HLA locus to CD. This is located on chromosome 6p about 30 cM telomeric from HLA (Zhong *et al.*, 1996).

Another non-HLA gene thought to be associated with CD is CTLA-4 (cytotoxic T lymphocyte-associated), a likely candidate gene for auto-immune diseases because of its role in controlling the T cell proliferative response (Torinsson *et al.*, 1999; Djilali-Saiah *et al.*, 1998). It is located on chromosome 2q33 and encodes a T lymphocyte surface molecule whose binding to the B7 molecule on antigen presenting cells delivers a negative signal to the T cell and can mediate apoptosis (Harper *et al.*, 1991). A study to investigate an A/G substitution polymorphism at the +49 position in exon 1 of the CTLA-4 gene has found an association of the A allele with predisposition to CD (Djilali-Saiah *et al.*, 1998). The frequency of this allele was not found to be further increased in patients with the classic CD-predisposing HLA alleles, which suggests that the effects of the HLA and CTLA-4 loci are independent. It is unclear, however, whether CTLA-4 contributes to CD susceptibility by itself, or whether it is a marker for another locus with which it is in linkage disequilibrium (Djilali-Saiah *et al.*, 1998).

1.3 COMPLICATIONS OF COELIAC DISEASE

There are well described complications of coeliac disease, which include defective splenic function (hyposplenism) due to splenic atrophy, chronic hepatitis, lung disorders, neurological disorders, chronic ulcerative enteritis and malignancy (Wright, 1995; Howdle and Losowsky, 1987).

1.3.1 Malignancy and coeliac disease

An increased risk of developing malignancy is one of the major complications of CD and is the main factor responsible for the increased mortality rate observed among coeliac patients. In one study, mortality was overall 1.9-fold greater than that of the general population, and greatest within one year of CD diagnosis in adults. The mortality rate for those diagnosed in childhood as having CD, however, was similar to that of the general population (Logan, 1989). Various types of malignancies have been observed in association with CD, particularly malignancies of the gastro-intestinal tract, such as small intestinal lymphoma and adenocarcinoma, and carcinomas of the oesophagus and pharynx (Swinson, 1983b; Harris *et al.*, 1967).

1.3.2 Lymphoma and coeliac disease

High grade non-Hodgkin's lymphoma of the upper small intestine seems to be the most frequent malignant complication of CD and the single most common cause of death (Logan, 1989). The association of malabsorption with lymphoma was first recognised by Fairley and Mackie (1937), who attributed it to lymphatic obstruction. Gough *et al.* (1962) later proposed that lymphoma was a complication of idiopathic steatorrhoea, rather than the cause. Later findings supported this view (Harris *et al.*, 1967) and, more recently, HLA typing studies have suggested that lymphoma arises in the same genetic background as CD (Howell *et al.*, 1995).

Intestinal lymphoma associated with CD was first described as malignant histiocytosis of the intestine (Isaacson and Wright, 1978). However, subsequent studies based on clonal rearrangements of T cell receptor (TcR) genes and immunohistochemical markers have shown the tumour cells to be of T cell lineage (Salter *et al.*, 1986; Isaacson *et al.*,

1985). This tumour has therefore been called enteropathy-associated T cell lymphoma (EATL) (O'Farrelly *et al.*, 1986).

1.3.2.1 Clinical diagnosis

Enteropathy-associated T cell lymphoma usually follows relapse or failure to respond to a gluten-free diet in patients who have previously shown complete remission, in newly diagnosed coeliac patients showing non-responsiveness to gluten withdrawal from the outset ("refractory sprue"), and in patients presenting with persistent pyrexia, abdominal pain and muscle weakness. Weight loss, diarrhoea and skin rashes are also often present, and opportunistic infections may present acutely. Diagnostic laparotomy is often required and sometimes has to be performed as an emergency when intestinal perforation, bleeding or obstruction occur (Mathus-Vliegen, 1996). The most frequent site of tumour is the proximal jejunum, although malignancy may occur elsewhere in the small intestine. The affected bowel is often dilated and oedematous, usually showing multiple circumferential ulcers without formation of tumour masses (Wright, 1997).

1.3.2.2 EATL as a complication of coeliac disease

There is still a controversy as to whether EATL arises against a background of coeliac disease or is actually a malignancy from the outset, developing from low grade lymphoma into high grade lymphoma (Wright *et al.*, 1991). Increasing evidence seems to support EATL arising as a complication of CD. First-degree relatives are at risk of developing CD and/or malignancy; splenic atrophy is present in both diseases; both diseases have the same intra-epithelial lymphocyte populations and, in the case of malignant lymphoma, the non-neoplastic, atrophic mucosa will return to normal, but only after resection or chemotherapeutic treatment of the lymphoma (reviewed in Mathus-Vliegen, 1996). In addition, HLA genotyping studies suggest not only that EATL arises in individuals with the CD-predisposing genotype, but also that there are additional HLA-associated alleles, acting independently or in association with known CD-associated genotypes, that may represent risk factors for EATL (Howell *et al.*, 1995).

1.3.2.3 Histological features

Enteropathy-associated T cell lymphomas are usually pleomorphic, composed of blastic cells with rounded or oval nuclei and one or more nucleoli. The neoplasms usually contain an intense infiltrate of inflammatory cells, including many histiocytes and, in some instances, large numbers of eosinophils (Wright, 1997). The tumour cells of EATL express the T cell lineage markers CD2, CD3, CD7, βF1 and CD45RO (Wright, 1997; Murray *et al.*, 1995). They also express HML-1, an intra-epithelial lymphocyte (IEL) marker (Spencer *et al.*, 1988); further, the expression of CD8 antigen has been shown in 30% of tumours analysed (Murray *et al.*, 1995). A recent study has shown the expression of TIA-1 (cytotoxic granule antigen) and granzyme B (markers for activated cytotoxic T cells) in EATL (de Bruin *et al.*, 1997), which, taken together with their HML-1 expression and the fact that IEL in CD are thought to be activated cytotoxic T cells (Oberhuber *et al.*, 1996), could indicate that the cells in EATL are neoplastic equivalents of activated cytotoxic IEL (de Bruin *et al.*, 1997).

In cases in which the tumour has been resected from the jejunum, the uninvolved mucosa characteristically shows villous atrophy and intraepithelial lymphocytosis (Isaacson, 1999). This is shown in Fig.1.3.1 below.

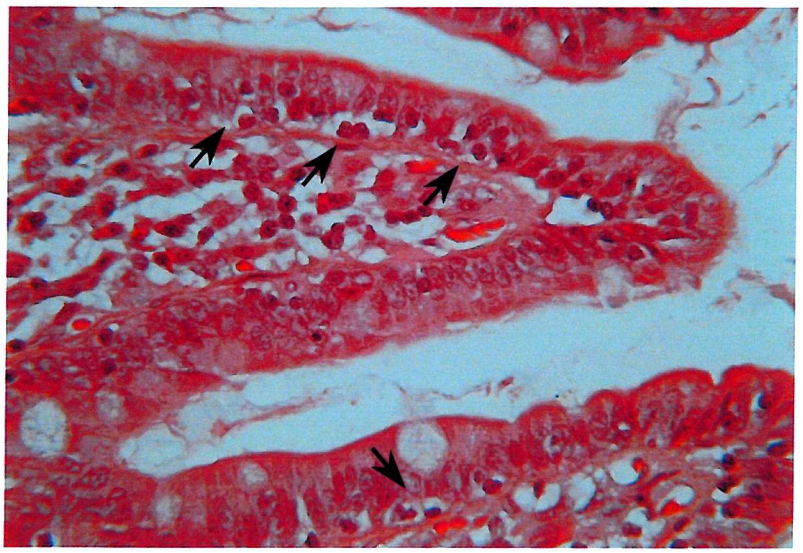

Fig. 1.3.1. Section of enteropathic bowel from an EATL patient. Epitheliotropism is demonstrated in this example (arrows), which may reflect a relationship between neoplastic cells and IEL (H&E, x400).

The fact that infiltrating neoplastic cells can be observed in the uninvolved enteropathic mucosa of EATL, in some cases, further suggests a possible association between IEL and tumour cells (Fig. 1.3.2).

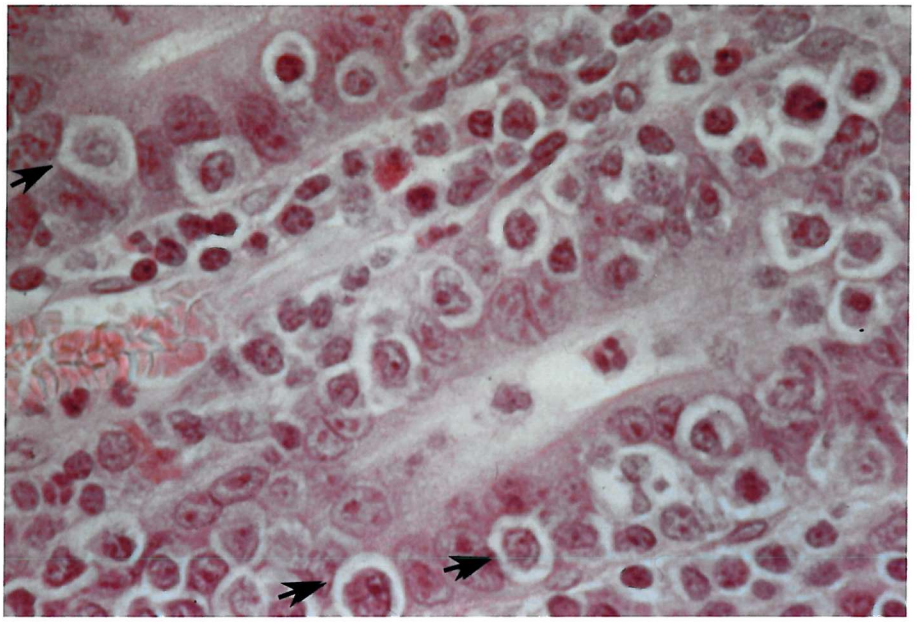

Fig. 1.3.2. Section of EATL showing the presence of large infiltrating neoplastic cells (arrows) in the epithelium (H&E, x630).

1.3.2.4 HLA genes and EATL

In an investigation of the genetic relation between CD and EATL, Howell *et al.* (1995) studied HLA class II DRB1, DQA1 and DQB1 polymorphism in patients with uncomplicated CD and those with EATL, using PCR oligotyping of DNA from paraffin wax biopsy specimens. Their findings suggest that uncomplicated CD and EATL arise in individuals with a similar genetic background (DRB1*03, DQA1*0501/DQB1*0201) as significant increases in the frequencies of these genotypes were found in both the patients with uncomplicated CD and in those with EATL when compared with controls. Also of interest are the differences found between the two patient groups. The increase in DRB1*0304 heterozygosity found in the patients with EATL may indicate a genetic predisposition to the malignancy, while the increase in DRB1*0307 heterozygosity and DQB1*0201 homozygosity in uncomplicated CD patients may indicate a protective effect against the development of EATL.

The results also indicated that the HLA class II genotypes of late onset CD patients are more closely related to those found in EATL patients than are those of patients with early onset CD. This may be significant, as most cases of EATL arise in CD patients with late onset disease. These findings agree with previous studies which have shown that, in CD patients carrying the DQA1*0501/DQB1*0201 genotype, the presence of a second copy of DQB1*0201 increases the susceptibility to CD (Ploski *et al.*, 1993) and may predispose to earlier onset and to more severe disease manifestations (Congia *et al.*, 1994). Thus, in these patients, the earlier onset or more severe symptoms of CD would lead to an earlier diagnosis and treatment, while non-HLA-DQB1*0201 homozygous individuals may have subclinical symptoms, that could go undetected and therefore untreated. The evolution of neoplastic T cell clones from polyclonal T cell populations in the enteropathic bowel could then occur over time, as a result of the continuing antigen drive derived from gliadin. In patients with the genotype predisposing to the more severe form of the disease, however, the early removal of gluten from the diet would protect them against the subsequent development of lymphoma (Howell and Jones, 1995) (Fig. 1.3.3.).

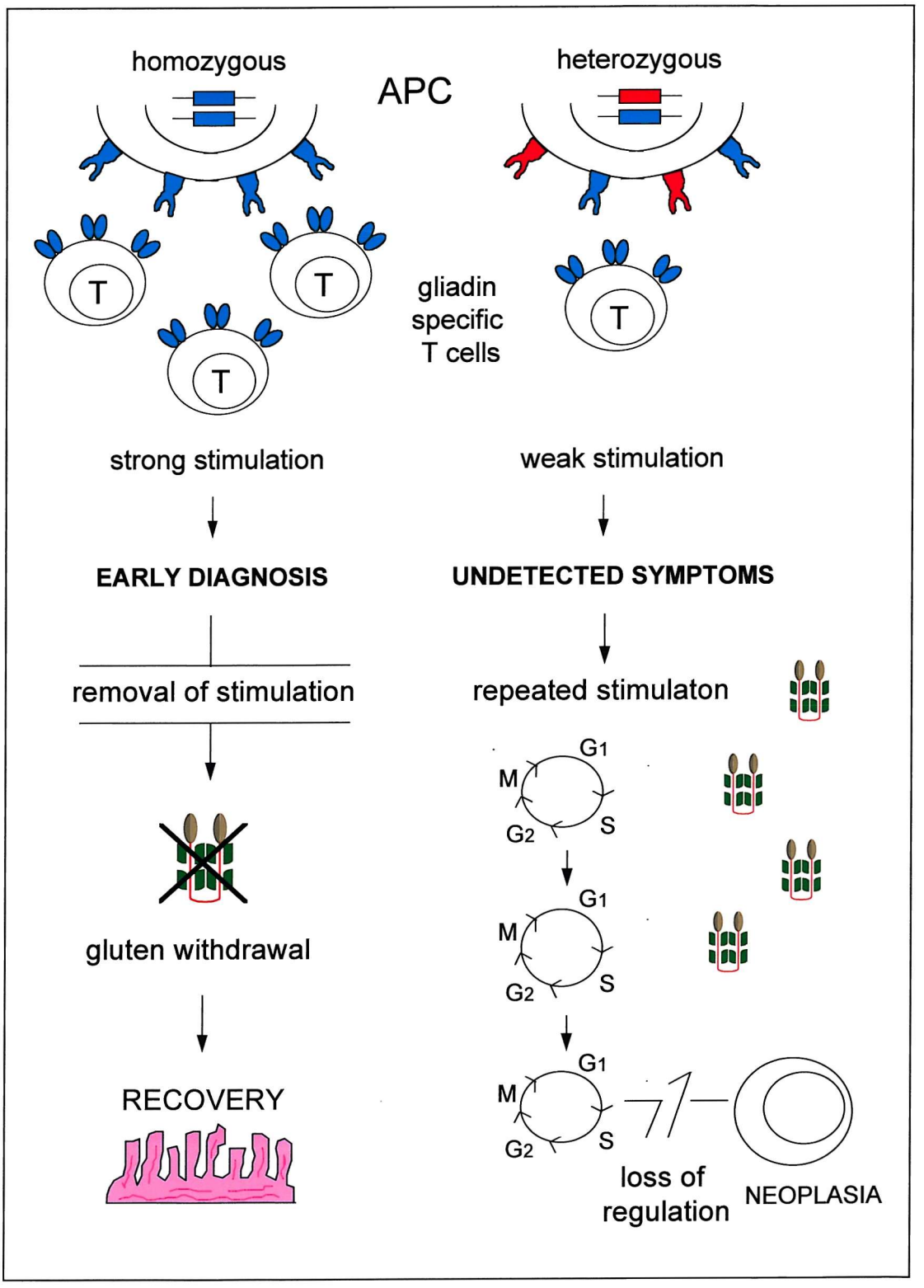

Fig. 1.3.3. Schematic diagram of the possible pathogenesis of EATL in coeliac disease.

1.3.2.5 T cell clonality and EATL

In a study to investigate whether polyclonal or monoclonal T cell receptor gene rearrangements were present in neoplastic and adjacent histologically uninvolved enteropathic bowel, Murray *et al.* (1995) used the polymerase chain reaction with primers for TcR-β and TcR-γ genes in a combination that permitted the identification of approximately 90% of TcR rearrangements. Thirteen out of 14 tumours showed monoclonal TcR rearrangements. Eleven of these 13 cases also showed monoclonal rearrangements in the adjacent enteropathic bowel and, in 10 of these, the amplified DNA was of the same molecular weight in the enteropathic bowel as in the corresponding tumour. These results suggest that there may be occult neoplasia in histologically uninvolved mucosa. However, in order to confirm these findings, DNA sequencing analysis would be necessary to ensure that the sequence of the product amplified from the adjacent enteropathic bowel is the same as that amplified from the corresponding tumour.

1.3.2.6 Gluten free diet and lymphoma

Follow up studies of CD patients on a gluten-free diet (GFD) or a normal diet further support the importance of a GFD in reducing the risk of cancer. Holmes *et al.* (1989) studied 210 patients with CD and their results indicated that, for coeliac patients who had followed a GFD for five years or more, the overall cancer risk was not significantly increased when compared with the general population. However, there was a significantly increased risk among patients on a normal or reduced gluten diet. For coeliac patients on a conventional diet, developing lymphoma had a relative risk of 77.8, while for those on a GFD the relative risk was 16.7. No lymphoma was detected in those adhering to the GFD for more than 10 years.

1.3.2.7 Undiagnosed CD and the importance of screening

It is now believed that CD is an underdiagnosed condition and subclinical or silent CD seems to be more common in the general population than once thought. Catassi *et al.* (1994) have found a prevalence of 3.28 per 1000 in a general school population (aged 11-15 years), suggesting that the number of subclinical cases is five times bigger than that of detected cases (Logan *et al.*, 1986). The number of undetected cases of CD is thought to be smaller in the adult population (Corazza *et al.*, 1997).

Patients with subclinical CD, in spite of being free of major symptoms, have typical damage to the jejunal mucosa on intestinal biopsy and are at risk of developing CD-associated complications in the long term (Logan *et al.*, 1989). Subclinical CD is different from latent CD as the latter refers to patients who have a normal jejunal biopsy while taking a normal diet and, at some other time before or since, have had a flat jejunal biopsy that recovered on a gluten-free diet (Troncone, 1995).

Confirmation of the presence of a large number of undiagnosed subclinical cases of CD in the general population emphasises the importance of screening for CD, as undetected patients are more likely to develop malignancies such as EATL due to long-term exposure to gliadin (Holmes *et al.*, 1989).

1.3.2.8 Screening for CD using anti-gliadin and anti-endomysium antibodies

Although small intestinal biopsies are still the only reliable way to confirm the diagnosis of CD, screening of patients on a larger scale (patients with mild or atypical symptoms, individuals from high risk groups and patients who might have silent or latent CD) requires a less invasive test.

Serum antibodies to gliadin and endomysium have been used as markers for CD and as a means of selecting subjects for small intestinal biopsy (Catassi *et al.*, 1994). Although IgA anti-endomysium antibodies (AEA) are thought to be more specific and sensitive than IgA and IgG anti-gliadin antibodies (AGA) (Cataldo *et al.*, 1995; Ferreira *et al.*, 1992), the reliability of IgA-AEA is compromised in patients with selective IgA deficiency. This is a rare condition but, as CD is ten times more common in patients with selective IgA deficiency than in the general population (Collin *et al.*, 1992), screening tests should also include IgG-AGA (Catassi *et al.*, 1994). It is thought that the combined presence of IgA-AEA and IgA- and IgG-AGA permits an excellent prediction of the state of the jejunal mucosa (Cataldo *et al.*, 1995; Catassi *et al.*, 1994).

1.4 T LYMPHOCYTES AND ANTIGEN RECOGNITION

In CD, the processed gliadin antigen derived from dietary gluten, in association with HLA class II molecules on the surface of antigen presenting cells is recognised by the membrane-bound receptors present on the surface of T lymphocytes. The interaction between T cell receptors and antigen-HLA complexes initiates a cascade of biochemical events that activates the resting T cell, inducing it to enter the cell cycle, causing its proliferation and differentiation into memory and effector cells.

It has been postulated that the repeated stimulation of intestinal T lymphocytes in undiagnosed CD patients, by antigenic gliadin peptides, may eventually lead to a loss of normal cell cycle control, leading, in some cases, to the development of neoplastic T cell clones (Howell and Jones, 1995).

1.4.1 The T cell receptor (TcR)

A T cell has about 30,000 antigen receptor molecules on it surface, each receptor being a glycosylated polymorphic heterodimer composed of either α and β or γ and δ polypeptide chains. Each chain consists of a variable (V) and a constant (C) region (homologous to the variable and the constant regions found in immunoglobulins), a short hinge region which has a cysteine residue that forms the interchain disulfide link, a hydrophobic transmembrane region containing positively charged amino acids involved in interactions with other molecules and a short cytoplasmic domain (Fig. 1.4.1). This heterodimer is associated with a nonpolymorphic membrane-bound complex of proteins known collectively as CD3 (reviewed in Bentley and Mariuzza, 1996; Ashwell and Klausner, 1990).

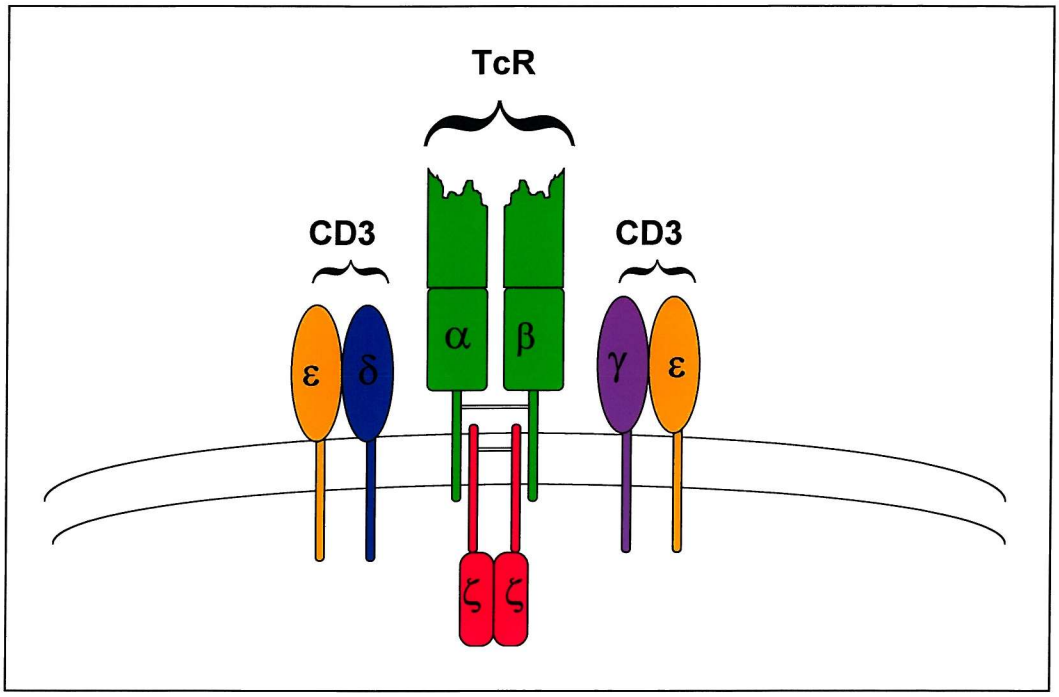

Fig. 1.4.1. The T cell receptor and the associated polypeptide chains that form the CD3 complex (adapted from Janeway and Travers, 1997).

The T cell receptor is classified as a member of the immunoglobulin (Ig) gene superfamily as its domain structure is strikingly similar to that of Ig. As with Ig, TcR are encoded by a family of gene segments that rearrange to generate the diverse TcR repertoire, estimated to contain 10^{14} different sequences (Garboczi *et al.*, 1996). The V-like domains are encoded by V-, D- and J-region gene segments in the β chain, and V- and J-region segments in the α chain. Again, as in Ig molecules, the antigen-binding site of the TcR has been predicted to consist of regions analogous to the three complementarity-determining regions (CDR). The first two variable loops (CDR1 and CDR2) of the human α- and β-chain are encoded by the 42 Vα and 46 Vβ genes, while the third variable loop (CDR3) is encoded following the joining of V genes to one of a number of J-region and, in the case of Vβ, D- and J-region gene segments. The joining reactions also contribute to the generation of further diversity by removing nucleotides and by introducing non-germline ('N') bases at each junction (Garboczi *et al.*, 1996).

The constant region genes of the TcR are relatively simple, encoding only transmembrane polypeptides (not secreted, as in Ig), with only one Cα gene and two Cβ

genes. Even for these two, there is no known functional distinction between their products (Janeway and Travers, 1997).

Some T cells bear an alternative form of TcR consisting of a γ:δ heterodimer, rather than the usual α and β chains. The γ:δ heterodimer is also associated with the CD3 complex on the cell surface. The terminology of these receptor chains should not be confused with that of the CD3 γ and δ chains (Bentley and Mariuzza, 1996).

The organization of TcR γ and δ genes in humans is similar to that of the α and β genes, with a few important differences. The gene complex encoding the δ chain is found entirely within the TcRα chain gene complex, between the Vα and the Jα gene segments, so that any rearrangement of the α chain genes inactivates the genes encoding δ chains. There are three Dδ gene segments, three Jδ gene segments and a single C-region gene. It is thought that there are at least four Vδ gene segments, which are interspersed among the Vα gene segments. The γ chain resembles the β chain, with two C-region gene segments each having its own J gene segments. There are many fewer V gene segments at the γ and δ loci than at either the TcR α or β gene loci. Increased junctional variability in the δ chains may compensate for the small number of possible variable regions (Chien *et al.*, 1996).

1.4.2 TcR antigen recognition

Antigen recognition by the TcR is restricted to peptides bound to molecules of the HLA complex (Bentley and Mariuzza, 1996). This restriction also divides T cells into two major classes, with different effector functions, according to the class of HLA molecule they recognise. Differential recognition of class I or II molecules depends on the surface expression of the T cell proteins CD8 or CD4, respectively. The cell-surface molecule CD8 is expressed on cytotoxic T cells, and binds to invariant parts of the HLA class I molecule, while the CD4 molecule is expressed on both Th1 and Th2 helper cells, binding to invariant parts of the HLA class II molecule (Janeway, 1992).

1.4.3 The interaction between the TcR and the peptide-HLA complex

Most models for the interaction between TcR and peptide-HLA complex have proposed that the relatively less diverse CDR1 and CDR2 loops of both the α and β chains interact with helices of the less diverse HLA molecule, while the highly diverse CDR3 loops contact the (diverse) bound peptides (Bentley and Mariuzza, 1996). A study of the structure of the complex between human TcR, viral peptide and HLA-A2 (Garboczi *et al.*, 1996), however, has shown that the TcR is oriented diagonally over the peptide-HLA complex, with CDR1 and CDR3 from both Vα and Vβ contacting the peptide and CDR2 loops contacting the HLA molecule (Fig. 1.4.2). The diagonal binding observed is thought to result from properties shared by all classical class I and class II HLA molecules and probably all αβ TcR, suggesting that this might represent a general mode of binding (Garboczi *et al.*, 1996).

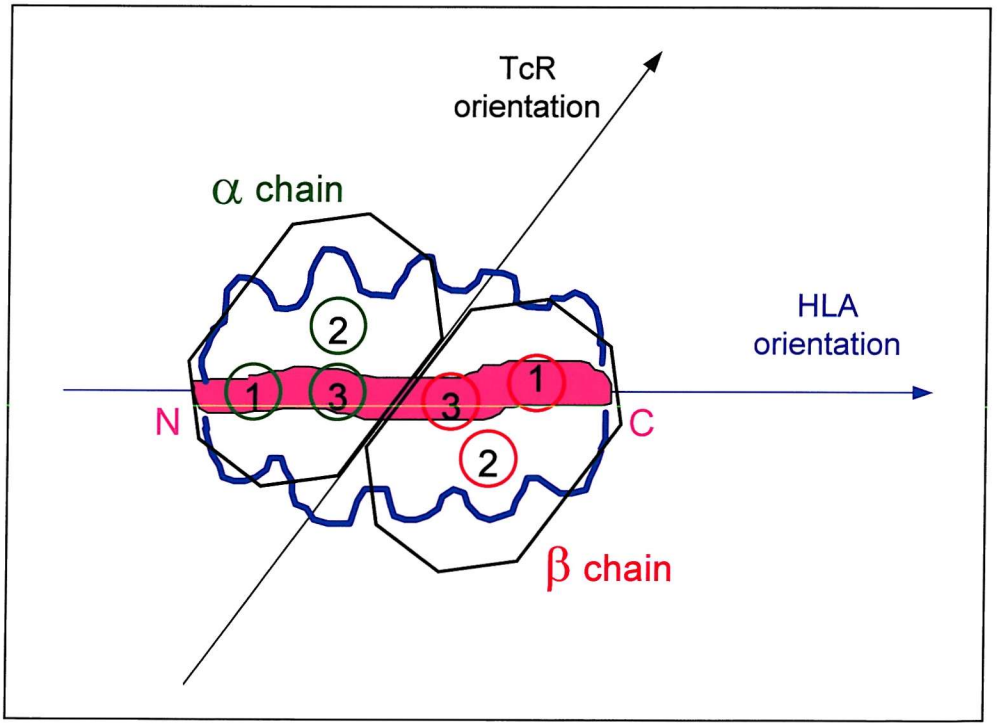

Fig. 1.4.2. Schematic representation of the diagonal binding between the MHC molecules and the TcR, viewed from the top. Green circles represent CDR1-3 from the TcR α chain, and red circles CDR1-3 from the β chain. The MHC molecule is shown presenting a peptide (pink).

After interaction of the TcR with bound peptide-HLA, signal transduction is accomplished through a complex of proteins stably associated with the TcR known as the CD3 complex (Fig. 1.4.1). In man, the three proteins of this complex are called CD3γ, CD3δ and CD3ε and are encoded by linked genes. There is also a fourth molecule, with no sequence or structural homology to either of the other genetic groupings of the receptor complex, composed of the ζ and η chain, associated with the receptor mainly as a ζζ homodimer, but also, to a lesser extent, as a ζη heterodimer. In contrast to the other chains in the TcR-CD3 complex, the ζ and η chains have short (6-9 amino acid residues) extracellular domains, so that most of the polypeptides lie in the cytoplasm (Ashwell and Klausner, 1990).

The cytoplasmic domains of all CD3 proteins contain sequences called immunoreceptor tyrosine-based activation motifs (ITAM) that allow association with cytosolic protein tyrosine kinases following receptor stimulation. Signalling to the interior of the cell occurs through tyrosine kinases, with the cytoplasmic domains of the ζ chain and the CD3ε chain playing particularly important roles (Janeway and Travers, 1997).

1.4.4 Gliadin-specific intestinal T lymphocytes in CD patients

The strong association of CD with HLA-DQ2 or –DQ8 is thought to be due to preferential recognition of gliadin-derived peptides by intestinal T cells when presented by these DQ molecules (Lundin *et al.*, 1994; Lundin *et al.*, 1993). A further study (Molberg *et al.*, 1997), including 23 adult CD patients and 9 non-coeliac controls, demonstrated that gliadin-reactive T cells are commonly found and can be successfully isolated from the intestinal mucosa of CD patients. This study also confirmed that the majority of gliadin-specific T cells are DQ2 restricted. No gliadin-specific T cell responses were found in any of the 9 control patients (Molberg *et al.*, 1997). $CD4^+$ TcR-α/β^+ T cells are preferentially activated when duodenal mucosa from treated CD patients is stimulated with gluten *in vitro*; all gluten responsive T cell lines/clones established in this way carried the $CD3^+$, $CD4^+$, $CD8^-$, TcR-α/β^+ phenotype (Lundin *et al.*, 1994; Lundin *et al.*, 1993). Clones of T cells from two untreated CD patients contained a low percentage of $CD8^+$ T cells (Molberg *et al.*, 1997).

1.4.4.1 Intra-epithelial lymphocyte populations in CD and EATL

The small intestinal mucosa can be considered to have two distinct compartments, the epithelium and the lamina propria. $CD4^+$ T cells dominate the lamina propria. Intra-epithelial lymphocytes (IEL) are phenotypically heterogeneous (Russell *et al.*, 1991) and are present in the intestinal mucosa between enterocytes within the epithelial layer. These IEL are predominantly (80%-90%) cytotoxic T cells that express CD8 and have rearranged TcRβ chain genes (Brandtzaeg *et al.*, 1989).

Approximately 10%-15% of IEL express the variant γδ TcR type, which is similar to the proportion found in peripheral blood T lymphocytes (reviewed in Viney *et al.*, 1990). Cells of IEL type expressing γδ TcR are usually $CD8^+$ (70-90%) and contain the Vδ1 rather than the Vδ2 chain (Trejdosiewicz and Howdle, 1995). In CD there is an increase in abundance and percentage of γδ TcR IEL, which rises to over 30% of the $CD3^+$ IEL. Even in treated CD, after the patient has been on a gluten-free diet and has normal mucosal morphology and IEL levels, the proportion of γδ TcR IEL remains increased. Small intestine from patients with tropical sprue, cow's milk protein intolerance and Crohn's disease have also been studied, but only CD patients have been found to have increased levels of γδ TcR IEL (reviewed in Viney *et al.*, 1990).

It has been shown that 6% of the $CD3^+$ IEL in the normal human jejunum are $CD4^-$, $CD8^-$ and that this percentage increases to 28% in CD (Spencer *et al.*, 1989). In EATL, in which the non-neoplastic mucosa is similar histologically to that of untreated CD, there were no statistically significant differences from the IEL subpopulations found in uncomplicated CD. This observation supports the hypothesis that EATL results as a complication of coeliac disease, and the tendency for EATL patients to become refractory to a gluten-free diet might indicate that the gluten-reactive T cells stimulated persistently in the mucosa have undergone malignant transformation (Spencer *et al.*, 1989).

1.4.5 Mucosal cytokine expression in CD

In order to explain the mucosal damage characteristic of the coeliac lesion, it has been suggested that these changes are caused by increased local production of cytokines, such as interferon (IFN)-γ, that alone or in combination with tumour necrosis factor (TNF)-α, are cytotoxic to epithelial cells (Deem *et al.*, 1991).

In a recent study, cytokine messenger RNA (mRNA) expression was determined in untreated CD, in treated CD after gluten challenge and in normal controls (Nilsen *et al.*, 1998). The results showed that IFN-γ mRNA levels were 10-100 times higher in untreated than in treated mucosal lesions, and more than 1000 times higher in untreated than in histologically normal controls. *In vitro* gluten stimulation of specimens from treated CD patients increased the levels of IFN-γ mRNA to the levels found in untreated CD. In normal controls, mRNA levels were usually below the limit of quantitation. As well as high levels of IFN-γ expression, lower levels of interleukin (IL)-2, IL-4, IL-6 and TNF-α mRNA were also detected after gluten challenge of treated CD specimens (Nilsen *et al.*, 1998).

A previous study (Nilsen *et al.*, 1995), analysing cytokine production by gluten-specific T cell clones isolated from CD mucosa, has shown that $CD4^+$ T cell clones produced cytokines with a Th1-like or Th0-like profile. Naive $CD4^+$ T cells can differentiate upon activation into Th1 cells, which secrete mainly IFN-γ and mediate delayed-type hypersensitivity, or Th2 cells, which secrete mainly IL-4, IL-5 and IL-10 and provide help for certain humoral immune responses, particularly IgE production. Th0 cells are believed to be the progenitors of Th1 and Th2 cells and can produce most cytokines (reviewed in Scott *et al.*, 1997). The relative large amounts of IFN-γ produced by gluten-specific T cells may indicate that intestinal epithelial cells could play an important role in the perpetuation of the disease by continuous activation of gluten-specific T cells in the gut during inflammation (van de Wal *et al.*, 1998a).

1.5 THE CELL CYCLE AND MALIGNANCY

1.5.1 The normal cell cycle

The cell cycle is composed of four stages. In the gap 1 (G1) phase, the cell increases in size and prepares to copy its DNA. This copying occurs in the synthesis (S) stage, and enables the cell to duplicate precisely its complement of chromosomes. After the chromosomes are replicated, gap 2 (G2) follows during which the cell prepares itself for mitosis (M). The parent cell then divides to produce two daughter cells, each of which is endowed with a complete set of chromosomes (Nurse, 1994). The new daughter cells immediately enter G1 and may go through the full cycle again. Alternatively, they may stop cycling either permanently or temporarily, entering the quiescent gap 0 (G0) phase (Weinberg, 1996). The so-called "cell cycle clock" programmes this elaborate succession of events by means of a variety of molecules (Fig.1.5.1).

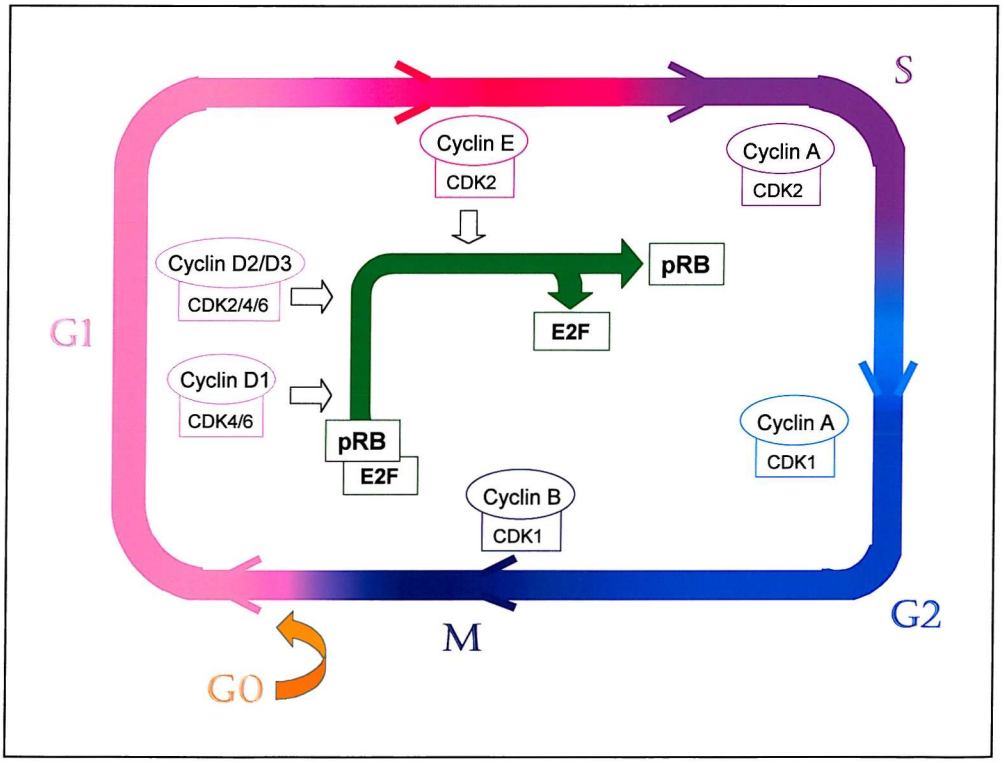

Fig. 1.5.1. Phases of the cell cycle showing predominant cyclin-CDK complexes in each phase. The pRB protein is known as the cell cycle brake and is in its active state when it is hypophosphorylated, binding the transcription factor E2F. Phosphorylation of pRB is performed by cyclins D and E, resulting in the release of bound E2F. E2F can then transactivate its target genes, whose products contribute to S phase entry.

Progression through the four stages of the cycle is largely dependent on the interaction between three main types of proteins: cyclins, cyclin-dependent kinases (CDK), and cyclin-dependent kinase inhibitors (CKI) (Gillett and Barnes, 1998; Nasmyth, 1996; Heichman and Roberts, 1994). There are a number of different cyclins that show a cyclical increase in concentration during the cell cycle. Once a cyclin reaches a critical concentration it can activate its partner CDK, which then phosphorylates other proteins that, in turn, carry out their roles at different phases of the cell cycle. The CKI control activation of the CDK-cyclin complexes by inhibiting their formation (Gillett and Barnes, 1998).

1.5.1.1 Cyclins and CDK

Once a cell has been signalled to progress through the cell cycle, the concentration of cyclin D and cyclin E (known as G1 cyclins) increases. First there is an increase in the expression of D-type cyclins (D1-D3) that form complexes with CDK4 and CDK6. The activation of these CDK initiates the phosphorylation of the retinoblastoma protein (pRB). At the onset of S phase, the concentration of D-type cyclins declines so that they no longer activate CDK4/6; at this stage cyclin E reaches levels at which it can activate CDK2 and this complex takes over the role of phosphorylating pRB. Phosphorylation of pRB causes it to release the bound transcription factor E2F, enabling it to transactivate its target genes, whose products contribute to S phase entry. Once S phase has begun, cyclin E is rapidly degraded and activation of CDK2 is taken over by cyclin A. The cyclin A-CDK2 complex plays an important role in the initiation and maintenance of DNA synthesis. Towards the end of S phase, cyclin A starts to activate CDK1 in preference to CDK2 which signals the completion of S phase and the onset of G2 phase. G2 provides a break in which the cell can ensure that DNA replication is complete and accurate before initiating mitotic division (reviewed in Gillett and Barnes, 1998; Sherr, 1996).

Initiation of mitosis is associated with a group of proteins collectively known as mitosis (M) phase promoting factor (MPF), which actually consists of CDK1 and cyclins A or B. The cyclin A-CDK1 complex is thought to be more important in the completion of S phase, while cyclin B-CDK1 controls the onset, sequence of events and completion of mitosis. Once mitosis is completed and cell division has taken place, cyclin B is

destroyed, CDK1 is inactivated, and the cell enters G1 or G0 (reviewed in Gillett and Barnes, 1998).

1.5.1.2 CDK inhibitors

Cyclin-dependent kinase inhibitors (CKI) control the transition from one phase of the cell cycle to the next by regulating the activation of CDK by their partner cyclins. The two main groups of CKI include the p21 family, and the INK4 (the name being derived from inhibitor of CDK4) family. The p21 family consists of p21 itself, p27 and p57. These proteins tend to have wide-ranging roles and are thought to be negative regulators of cyclin D-, E-, and A-dependent kinases. The INK4 family consists of $p15^{INK4B}$, $p16^{INK4A}$, $p18^{INK4C}$, $p19^{INK4D}$ and the recently identified $p19^{ARF}$ (ARF= alternative reading frame). With the exception of $p19^{ARF}$, the INK4 proteins can block cyclin D-dependent kinase activity directly and cause G1 phase arrest by binding to and inhibiting CDK4 and CDK6 (reviewed in Gillett and Barnes, 1998; Sherr, 1996). The $p19^{ARF}$ protein is encoded by the same gene (INK4A) as $p16^{INK4A}$ but is thought to have a somewhat different function. The $p19^{ARF}$ protein has been shown to associate physically with the murine double minute 2 gene product (MDM2) *in vivo*, blocking MDM2-induced degradation of p53, so that p53-related functions such as transactivation, growth inhibition and, possibly, apoptosis are enhanced (Pomerantz *et al.*, 1998).

1.5.2 Cell cycle checkpoints and p53 protein

Although cell cycle transitions depend on the underlying CDK cycle, superimposed checkpoint controls help ensure that certain processes are completed before others begin. Their role is to brake the cycle in case of stress or damage, allowing repair to take place. By integrating cell cycle progression and DNA repair, cell cycle checkpoints play an important role in maintaining genomic stability (reviewed in Sherr, 1996).

A molecule that plays an important role in the regulation of the G1 DNA damage checkpoint is the p53 protein (Kastan *et al.*, 1991). It is a transcription factor that is activated in response to DNA damage, causing cells to arrest in G1 through the activation of several genes, including the p21 gene (El-Deiry *et al.*, 1994). The p21 gene product binds to CDK2 and CDK4 inhibiting the cyclin-dependent phosphorylation of

their targets, among them pRB. As the cell cannot leave the G1 phase to enter S phase, this allows extra time for DNA to be repaired before it is replicated. If repair fails, p53 may trigger cell suicide by apoptosis (reviewed in Elledge, 1996; Levine, 1995; Lane, 1992). The precise signal transduction pathway that senses DNA damage and recruits p53 has not been elucidated, despite intensive study, but genes like ataxia-telangiectasia mutated (ATM) and Nijmegen Breakage Syndrome 1 (NBS1) (Varon *et al.*, 1998) are likely to be involved (reviewed in Sherr, 1996; Selivanova and Wiman, 1995).

Arrest in G1 of the cell cycle can also be triggered when ribonucleotide pools fall below a critical threshold. However, in contrast to the arrest caused by DNA damage, it is temporary and reversible (Hansen and Oren, 1997). Low oxygen tension is also able to stimulate p53 levels, inducing apoptosis in a p53-dependent manner. This has been suggested as a means by which p53 may protect against tumour formation (Levine, 1997; Graeber *et al.*, 1996).

Any disruption in the normal functioning of cell cycle checkpoints, such as mutations in the p53 gene, can allow DNA replication in the presence of unrepaired lesions and result in an increased risk of cancer (Loeb, 1998; Yin *et al.*, 1992).

1.5.3 Regulation of the p53 protein

In response to signals arising from various forms of cellular stress (e.g. DNA damage) p53 protein levels rise in the cell and p53 becomes activated by conversion from a poorly binding protein to one that binds DNA efficiently. The activated protein can thus elicit adaptive responses, which include cell cycle arrest and apoptosis, according to cell type and tissue-specific modifiers (Prives and Hall, 1999).

The mechanisms thought to be responsible for regulating the levels of active p53 in the cell include a balance between protein synthesis and degradation, protein-protein interactions, and post-translational modifications, such as phosphorylation, acetylation, and glycosylation of various sites of the p53 protein. Such modifications are thought to lead to conformational changes responsible for changing the level of activity and of DNA binding of the protein (reviewed in Prives and Hall, 1999).

1.5.3.1 Upstream interactions of p53

The low level of p53 in normal cells is due to its short half-life (about 20 min) as a result of its rapid turnover rate. The interaction of p53 with MDM2 protein is believed to be the main regulator of p53 stability (Kubbutat *et al.*, 1997).

The MDM2 protein has a molecular mass of 90 kDa. It can form oligomeric complexes with both mutant and wild-type p53 protein and block p53-mediated transactivation of a p53-responsive promoter (Momand *et al.*, 1992). Since MDM2 expression is induced by p53, a p53/MDM2 auto-regulatory feedback loop has been proposed whereby, after an appropriate period of p53 activity, p53 stimulates MDM2 expression so that p53 function is down-regulated by being sequestered in an inactive complex with MDM2 (Wu *et al.*, 1993). Rapid degradation of p53 by MDM2 is thought to ensure the effective termination of the p53 signal. MDM2 is also thought to shuttle p53 from the nucleus into the cytoplasm, where ubiquitin-mediated proteasome-dependent degradation occurs (Haupt *et al.*, 1997).

Modulation of MDM2-mediated inhibition is thought to occur through DNA damage-induced phosphorylation of p53. Shieh *et al.* (1997) have demonstrated that phosphorylation of p53 at serines 15 and 37 impairs the ability of MDM2 to inhibit p53-dependent transactivation probably due to a conformational change in p53. Two candidate kinases, ATM and DNA-dependent protein kinase (DNA-PK), have been identified that can phosphorylate p53 on serine 15 (reviewed in El-Deiry, 1998). According to the proposed model, one of the functions of phosphorylation at N-terminal sites may be to deter the inhibitory effect of MDM2 in the early phase of the p53 response, so that p53 can remain active when it is needed most. In the later phase, the p53/MDM2 auto-regulatory loop may come into play and turn off the p53 response, so that the cell cycle can resume (Shieh *et al.*, 1997).

More recently, it has been shown that, in addition to covalent modifications of the proteins, MDM2's inhibition of p53 can be neutralised by an alternative and independent pathway that involves the induction and action of the $p19^{ARF}$ protein (Pomerantz *et al.*, 1998). This protein is an INK4A gene product like $p16^{INK4A}$, being encoded by a different first exon and an alternative reading frame that resides in a

common second exon. The $p19^{ARF}$ protein has been shown to engage the p53 pathway through physical interactions with MDM2, inhibit the oncogenic actions of MDM2, block MDM2-induced degradation of p53 and enhance p53-dependent transactivation (Pomerantz *et al.*, 1998). It has also been shown that $p19^{ARF}$ binds to MDM2 and promotes its rapid degradation, leading to stabilisation and accumulation of p53 (Zhang *et al.*, 1998). It is interesting to note that p53 is not only regulated by $p19^{ARF}$ and MDM2, but that it also controls these products by transactivating its negative regulator MDM2 and by down-regulating its activator $p19^{ARF}$ (Stott *et al.*, 1998).

The p53 protein also interacts with several other cellular proteins that may play a role in regulating its function. The list continues to increase and includes TATA box binding protein (TBP), dTAFII40 (hTAFII31), dTAFII60, CBF, WT1, Sp1 transcription factor, single-strand binding protein RPA, TFIIH subunits p62, XPB, and XPD, and CSB, a putative helicase involved in transcription-coupled nucleotide excision repair (NER) (reviewed in Prives and Hall, 1999; Gottlieb and Oren, 1996).

The p53 protein has also been found to form tight complexes with several viral proteins, the most well documented interactions being with the simian virus 40 (SV40) large T antigen, the adenovirus E1b protein, and the E6 protein from high cancer risk types of human papillomavirus (HPV) (reviewed in Darnton, 1998; Gottlieb and Oren, 1996). These viruses encode proteins that have anti-apoptosis functions, abrogating p53 function in diverse ways. As p53 is a negative growth regulator, which can arrest cells in late G1, its complexing with viral protein would cause the inactivation of a significant fraction of p53. This could tip the cell into S phase, providing a more amenable environment to the replication of the virus, as it requires an actively dividing cell for maximal replication efficiency (reviewed in Gottlieb and Oren, 1996; Donehower and Bradley, 1993).

1.5.3.2 Downstream interactions of p53

The p53 protein is thought to function primarily as a transcriptional regulator and its activity as such is influenced profoundly by co-activator and co-repressor proteins that associate with it. These associations result in great complexity and subtlety in the regulation of downstream genes (Prives and Hall, 1999).

There is now considerable evidence that the p53-dependent G1 arrest occurs largely through the transactivation of p21 [also known as wild-type p53 activated fragment 1 (WAF1), CDK2 interacting protein 1 (CIP1), senescent derived inhibitor 1 (Sdi1), and melanoma differentiation associated gene (mda-6)], which inhibits G1 cyclin-dependent kinases, preventing entry into S phase. However, p21 is not thought to be entirely responsible for the antiproliferative effect of p53, as cell growth suppression by p53 can happen without p21 induction (Hansen and Oren, 1997; El-Deiry *et al.*, 1994).

The list of genes found to be transcriptional targets of p53 is rapidly increasing in size. The p53 target genes 14-3-3 σ, growth arrest and DNA damage inducible gene 45 (GADD45), and B99 are thought to be potential mediators of p53-dependent G2 arrest. The bcl-2-associated protein X (Bax), Fas/APO1, KILLER/DR5, p53-induced genes (PIG), insulin-like growth factor binding protein 3 (IGF-BP3), and PAG608 are p53 targets involved in mediating p53-dependent apoptosis. Thrombospondin 1 (Tsp1) and brain-specific angiogenesis inhibitor 1 (BAI1) are targets that inhibit angiogenesis. The following list includes genes that are upregulated by p53, but whose functions remain unclear: cyclin G, GPI-anchored molecule-like protein (GML), Wip1, etoposide-induced 24 (EI24), elongation factor-1 alpha (EF-1α), hypermethylated in cancer 1 (HIC-1), reduced in tumour (RTP/rit42), TP53TGI, cathepsin D, and wild type p53-induced gene 1 (wig-1) (reviewed in El-Deiry, 1998; Hansen and Oren, 1997).

The p53 protein is also known to repress expression from serum-inducible promoters including c-fos, and growth inducing promoters such as the IL-6 gene promoter, the c-myc promoter, the insulin receptor promoter, and the IL-2 and IL-4 promoters. It represses the activity of transcription factors such as TBP, SP1, thyroid hormone receptor, estrogen receptor, hypoxia-inducible factor and signal transducer and activator of transcription 5 (STAT5), as well as other genes such as hsp70, multidrug resistance 1 (MDR1), microtubule-associated protein 4 (MAP4) and actin (reviewed in El-Deiry, 1998).

1.5.4 The p53 gene and its product

The p53 gene product is believed to be a multifunctional protein and its importance for genomic stability is reflected by the fact that deletions and mutations occur in the encoding gene at high frequency in a large variety of human tumours (Hollstein *et al.*, 1991; Nigro *et al.*, 1989).

1.5.4.1 The p53 gene

The human p53 gene is located on the short arm of chromosome 17 at position 17p13, spanning 20Kb of DNA. It contains 11 exons, one of which (exon 1) is non-coding and located several kilobases away from the ten coding exons (Donehower and Bradley, 1993; Levine *et al.*, 1991). The gene contains five widely spaced clusters of amino acids, termed domains I to V, that are highly conserved throughout vertebrate evolution, indicating that these protein regions are involved centrally in p53 activity (Gottlieb and Oren, 1996). Full sequence data for exons 5 to 8, corresponding to the evolutionary conserved domains II to V, are presented in Appendix A (Lamb and Crawford, 1986).

1.5.4.2 The p53 protein

The p53 gene product is a 53 kDa nuclear phosphoprotein, 393 amino acids in length, and divided structurally and functionally into four domains (Fig. 1.5.2).

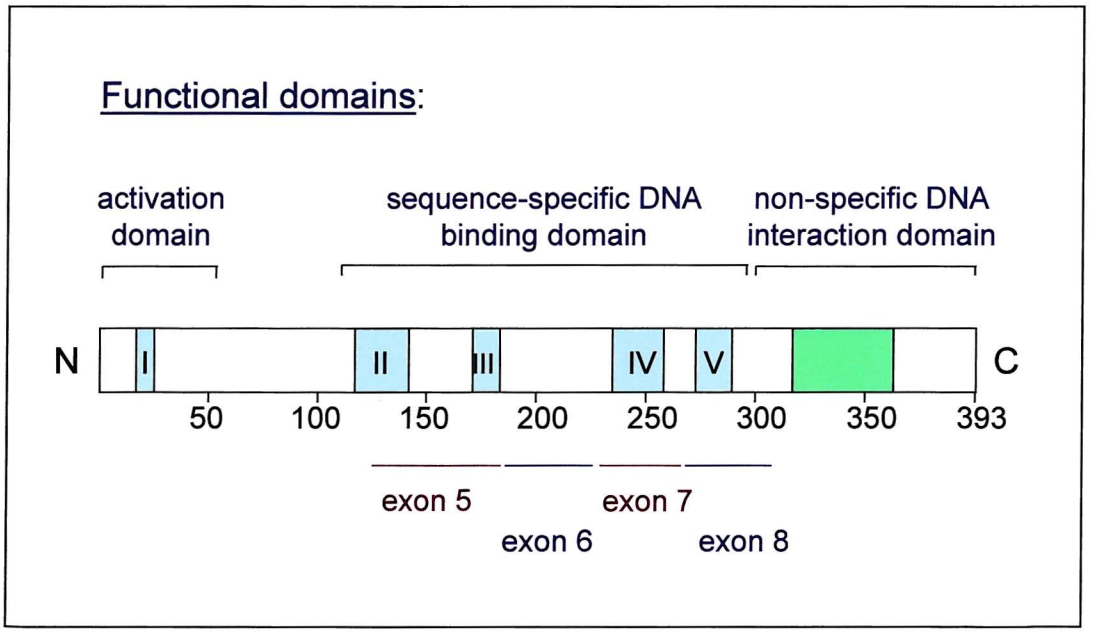

Fig. 1.5.2. Schematic representation of the p53 protein. Blue boxes indicate the 5 evolutionary conserved domains and the green box represents the tetramerisation domain (adapted from Ko and Prives, 1996).

The first 42 amino acids at the acidic amino terminus constitute a transcriptional activation domain that interacts with the basal transcriptional machinery in positive regulation of gene expression. Amino acids 13-23 are identical in a variety of species (Levine, 1997).

The middle region of the p53 protein, localized between amino acid residues 102 and 292, forms the sequence-specific DNA-binding domain and consists of a β sandwich that serves as a scaffold for two large loops and a loop-sheet-helix motif (Fig. 1.5.3). The two loops, which are encoded by conserved domains III and IV, in combination with the loop-sheet-helix motif encoded by conserved domains II and V, form the DNA binding surface of p53. This explains the evolutionary pressure to conserve the amino acid sequence of these domains. The loops are held together partly by a tetrahedrally coordinated zinc atom (Gottlieb and Oren, 1996; Cho *et al.*, 1994). Mutations of the p53 gene associated with human tumours tend to cluster in the conserved domains II to V (Hollstein *et al.*, 1991).

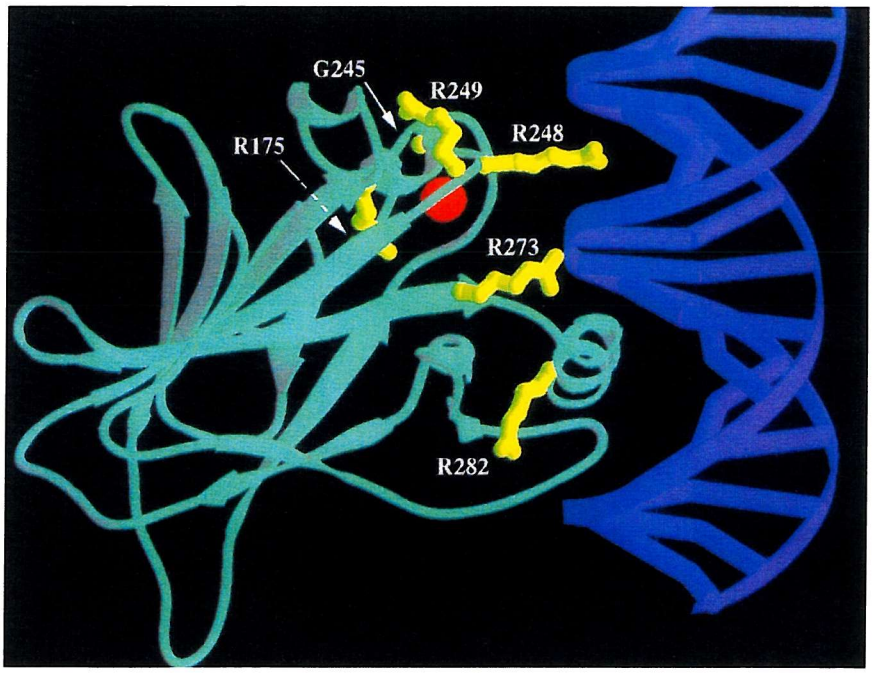

Fig. 1.5.3. Ribbon drawing of the p53 sequence-specific DNA-binding domain in a complex with DNA. The identified amino acid residues represent the 6 most frequently mutated residues of p53. The side-chains of these residues are coloured yellow, the DNA-binding domain is green, DNA is blue, and the red sphere represents a zinc atom. Reprinted with permission from Cho *et al.*, 1994. Copyright 1994 American Association for the Advancement of Science.

The p53 protein exists in oligomeric form and the domain that mediates oligomerisation has been mapped to C-terminal amino acid residues 324 to 355. The predominant form of p53 is tetrameric, and the structure of the domain contains a pair of dimers with two β sheets and two α helices. The two dimers are held together by a large hydrophobic surface of each helix pair, which then forms a four-helix bundle. This tetramerisation domain is linked to the sequence-specific DNA-binding domain by a flexible linker of 37 residues (287-323) (reviewed in Levine, 1997; Gottlieb and Oren, 1996).

The highly basic extreme C-terminus (26 amino acid residues) forms an open (protease-sensitive) domain composed of nine amino acid residues that bind to DNA and RNA readily with some sequence or structural preferences. There is considerable evidence to show that p53 protein derived from several sources requires a structural change to allow sequence-specific binding to DNA. The non-DNA-binding or latent form of p53 can be regulated by the basic C-terminal domain (reviewed in Darnton, 1998; Levine, 1997).

1.5.4.3 The emerging p53 family

Two proteins homologous to p53 have been recently identified; p73 and p51 (also known as p40, p63, Ket, or p73L). The sequence homology between these proteins and p53 is substantial within the most conserved p53 functional domains and they have been shown to be able to activate p53-responsive promoters and induce apoptosis (reviewed in Kaelin, 1999).

The human p73 gene is located at chromosome 1p36.33, a region frequently deleted in neuroblastoma and other tumours (Kaghad *et al.*, 1997). It encodes at least four distinct polypeptides, p73α, p73β p73γ, and p73δ, which arise through alternative splicing of the p73 transcript (reviewed in Chen, 1999).

The p51 gene maps to chromosome 3q27-8, a region that is deleted in some bladder cancers and amplified in some cervical, ovarian and lung cancers (reviewed in Chen, 1999). It also encodes multiple isotypes (at least 6) by 2 transcription initiation sites and extensive alternative splicing. It appears that the p51 gene is not frequently mutated in human cancers but it has been shown that heterozygous germline mutations in the p51

gene are the cause of **e**ctrodactyly, **e**ctodermal dysplasia and **c**left lip with or without cleft palate (EEC) syndrome (Celli *et al.*, 1999).

Both p73 and p51 are transcription factors that can induce cell-cycle arrest and apoptosis. They can both induce p21 synthesis, although the level of p21 induced by p73 is lower than that induced by p53. On the other hand, p73 can induce the14-3-3σ gene product, which is involved in G2 arrest, to levels several times higher than those induced by p53 (reviewed in Chen, 1999).

In contrast to p53, p73 is not induced by DNA damage and is not targeted for inactivation by viral oncoproteins such as SV40 T antigen, adenovirus E1B and HPV E6 (Marin *et al.*, 1998). P51 and p73 seem to be more closely related to one another than either is to p53 (Kaelin, 1999).

1.5.5 p53 and tumorigenesis

The p53 tumour suppressor gene undergoes inactivation with high frequency in a great number of malignancies, with p53 mutations estimated to occur in 50-55% of all human cancers. In addition to point mutations, allelic loss, rearrangements and deletions of the p53 gene have also been detected in human tumours (Hollstein *et al.*, 1994; 1991). Although p53 mutation alone, as a single genetic event, has no oncogenic capacity, in association with other accumulated genetic alterations neoplasia may arise (Piris *et al.*, 1995).

Mechanisms other than mutations are also thought to contribute to inactivation of the p53 protein. These include amplification of the mdm2 gene, localization of p53 in the cell cytoplasm and stabilisation of p53 by DNA tumour virus proteins (Donehower and Bradley, 1993; Momand *et al.*, 1992). The loss of activation of MDM2 mRNA, and therefore of MDM2 protein, so that the MDM2-dependent degradation pathway of p53 (Haupt *et al.*, 1997) does not operate, is also thought to cause the accumulation of an inactive form of p53 in the cell (Prives and Hall, 1999).

Loss of p53 function, as well as contributing to tumour development through dysregulation of the cell cycle, is also thought to be involved in allowing tumour

progression. Wild-type p53 expression is induced in hypoxic conditions, such as those found in a tumour with inadequate blood supply, resulting in apoptosis through the induction of bax. Low oxygen conditions can provide a selective advantage for cells carrying mutations in p53, allowing escape from apoptosis (Graeber *et al.*, 1996). In addition, p53 mutations would be expected to favour expansion of the tumour by loss of expression of anti-angiogenic factors (induced by p53 accumulation), allowing growth of new blood vessels to the tumour (Ko and Prives, 1996).

1.5.5.1 Mutations of the p53 gene

The vast majority of p53 missense mutations are clustered in the central region of the protein, corresponding to the sequence-specific DNA binding domain, and exons 5 to 8 of the gene. Due to the realisation that most mutations occur in this conserved midregion, many mutational studies limit their analysis to this portion of the gene, which could have resulted in a bias against identification of DNA sequence alterations outside this mutation cluster region (Gottlieb and Oren, 1996).

Although mutations involving nucleotides that encode most individual amino acid residues along the centre of the protein have been reported in tumours, there are a number of hotspots that are mutated at an unusual high rate. The most frequently mutated nucleotides lie in codons 175, 245, 248, 249, 273, and 282 (Fig. 1.5.4). Missense mutations of the p53 gene fall into two classes: Class I mutations affect residues of the DNA-binding surface, such as R248 and R273, resulting in defective contacts with the DNA and loss of the ability of p53 to act as a transcription factor; Class II mutations affect residues critical in stabilising the structure of the DNA binding surface of p53, altering the conformation of the p53 protein (Levine, 1997; Gottlieb and Oren, 1996).

Of all the mutational events observed in the p53 gene in human neoplasia, the most commonly observed are transitions (C:G to T:A and G:C to A:T) at CpG dinucleotides (Hollstein *et al.*, 1991).

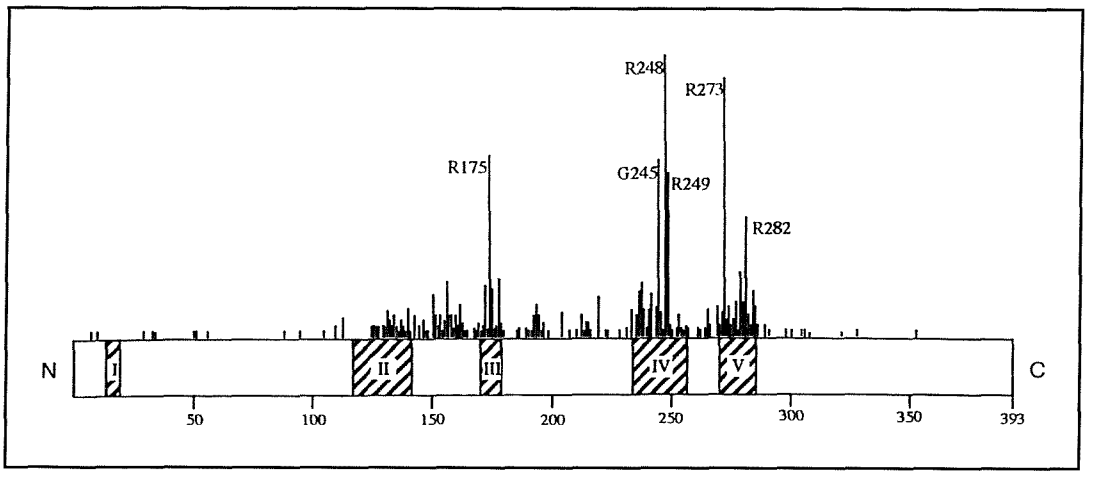

Fig. 1.5.4. Distribution of p53 mutations found in human cancer. Hatched boxes represent evolutionarily conserved regions and vertical lines above represent the frequency at which mutations are found at each particular residue. The most common hotspots are labelled with the corresponding codon numbers. Reproduced with permission from Ko and Prives, 1996.

Examination of many human neoplasms has revealed that frequently both p53 alleles are inactivated, commonly one by point mutation and the other by deletion (Gottlieb and Oren, 1996). In some cases, mutant p53 proteins with altered conformation can self-aggregate and complex with wild-type p53 protein, with the wild-type protein in the complex assuming the mutant conformation (Donehower and Bradley, 1993). This dominant negative effect of mutant p53 proteins results in an inhibition of the ability of wild-type protein to bind DNA and activate transcription. Indeed, p53 wild-type mice carrying a dominant-negative transgene show increased tumour incidence and decreased survival when compared to non-transgenic animals (Harvey *et al.*, 1995).

There are also some types of p53 mutations that are thought to confer increased tumorigenicity, metastatic potential, and/or tissue invasiveness (Dittmer *et al.*, 1993). The gain-of-function properties of these mutant p53 proteins may be related to the ability of mutant, but not wild-type, p53 proteins preferentially to stimulate the transcription of several cellular and viral promoters, to associate with cellular proteins p38 and p42, or to synergise with protein kinase C (PKC) in the induction of the expression of the angiogenic vascular endothelial growth factor (VEGF) gene (Reviewed in Ko and Prives, 1996).

Timing of p53 mutation in tumorigenesis varies with different tumour types and even with different carcinogens. In general, mutations or inactivation of the p53 protein are thought to be early events in cancers of the lung, oesophagus, head and neck, breast, cervix and stomach; and late events in cancers of the brain, thyroid, liver and ovary. Cancers of the colon, bladder, liver and, perhaps, other organs may develop through multiple pathways, with p53 alterations being early events in some tumours, and late events in others (reviewed in Greenblatt *et al.*, 1994).

1.5.5.2 p53 stabilisation due to mutation?

Wild-type p53 protein is present at low levels in the cell due to its relatively short half-life of 15-30 min. The proteases responsible for its breakdown are not known, but some evidence has suggested that ubiquitin-mediated proteolysis plays a role (Levine, 1997). Due to conformational changes resulting from missense point mutations, mutant p53 proteins have a prolonged half-life (4-8 hr), leading to the accumulation of the altered protein in the cell and making detection possible by immunohistochemical techniques (Martinez-Delgado, 1997; Selivanova and Wiman, 1995).

An alternative molecular mechanism by which the stabilisation of the p53 protein may occur in the cell is through its complexing with other cellular proteins, such as MDM2, or with viral oncoproteins, such as the SV40 large T antigen. Studies have shown that in SV40-transformed cells p53 protein complexes to T antigen in large oligomers which are stabilised and this increases the half-life of p53 to such an extent that it is increased by approximately a 100-fold in comparison with corresponding nontransformed cells (reviewed in Donehower and Bradley, 1993).

Over-expression of MDM2 has been reported in human tumours and, in one study, the gene was amplified in over a third of 47 sarcomas studied (Oliner *et al.*, 1992). In 5 of these tumours with mdm2 gene amplification no p53 mutations were observed, suggesting that the over-expression of MDM2 effectively abrogated p53 activity. In another study, sequencing of p53 gene transcripts in patients with mdm2 gene amplification revealed no mutations and restriction fragment length polymorphism analysis showed no losses of alleles on chromosome 17, except in one patient with anaplastic astrocytoma (Reifenberger *et al.*, 1993). Over-expression of MDM2 has

therefore been suggested as an alternative mechanism by which some human tumours may escape p53-regulated growth control (Watanabe *et al.*, 1996). It is important to note, however, that MDM2 overexpression has also been observed in tumours that overexpress p53 (Cordon-Cardo *et al.*, 1994).

1.5.5.3 p53 mutations and lymphoma

Over-expression of p53 has been found to be a common feature in high grade non-Hodgkin's lymphomas (NHL) but it has also been observed in some low-grade NHL. Overexpression of p53 is reported in several different series of NHL and fluctuates between 25% and 35% of cases (reviewed in Piris *et al.*, 1995). In a study of a series of low and high grade NHL, p53 positivity was detected in 31% of cases (Soini *et al.*, 1992) and, in another series studied, 21% of positive cases of different types of NHL were identified, including B and T cell lymphomas, anaplastic large cell lymphomas and B cell mucosa-associated lymphomas (Martinez-Delgado *et al.*, 1997).

The difference in half-life between the mutant and wild-type protein has led to the claim that p53 detection by immunohistochemistry is synonymous with mutation and thus with neoplasia. Indeed, this association was suggested as concentration of p53 positivity was observed in high grade lymphomas, but no p53 positivity was detected in non-neoplastic lesions of the lymph nodes (Soini *et al.*, 1992). Nevertheless, the use of microwave antigen retrieval for immunohistochemical detection of p53 over-expression has been shown to lower detection thresholds of p53 (McKee *et al.*, 1993). The increased sensitivity in p53 immunoreactivity can detect elevated levels of wild-type p53, rendering the assumption that p53 immunopositivity is associated with mutation unreliable (Dowell and Ogden, 1996).

The frequency of p53 mutations in NHL varies between 10% and 25% in different series (reviewed in Piris *et al.*, 1995; Villuendas *et al.*, 1993). In a study in which a panel of diverse NHL and lymphoid leukaemias were screened for mutations in exons 5 to 9 of the p53 locus, the highest frequencies of mutation were found in certain categories of B cell neoplasia; specifically Burkitt's lymphoma (33%), L_3-type B cell acute lymphoblastic leukaemia (55%), B cell chronic lymphocytic leukaemia (15%) and Richter's syndrome (42%). Mutations of the p53 gene were only found in 1 of 36 (2.8%)

T cell neoplasms (Gaidano *et al.*, 1991). One study demonstrated p53 mutations in 3 of 10 (30%) cases of adult T cell leukaemia/lymphoma analysed (Cesarman *et al.*, 1992), but other studies suggest that the incidence of p53 mutations is low in other categories of B and T cell NHL and lymphoid leukaemia, including non-human T cell lymphotropic virus type I (non-HTLV-I) related post-thymic T cell lymphomas (8.8%) (Matsushima *et al.*, 1994a) and anaplastic large cell lymphomas (Cesarman *et al.*, 1993).

The spectrum of mutations in NHL seems to have the same pattern as other types of tumours, with three peaks occurring in codons 175, 248, and 273 (Fig. 1.5.5). Transitions from G to A have been the most frequent finding, methylation-mediated spontaneous de-amination being responsible for this type of mutation (Piris *et al.*, 1995).

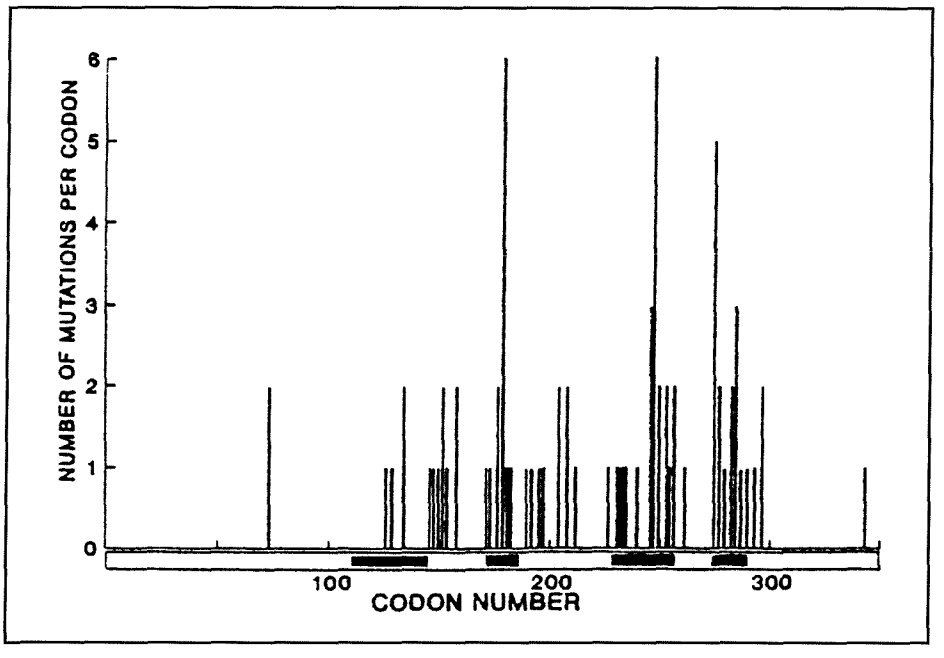

Fig. 1.5.5. Schematic diagram of p53 mutations in NHL. Three hotspots are identified and represent codons 175, 248, and 273. The thick horizontal lines indicate the evolutionarily conserved regions. A total of 76 mutations are shown compiled from 10 different molecular studies in which analysis of exons 5 to 8 was performed. Reproduced from Piris *et al.*, 1995, with permission from Gordon and Breach Publishers. Copyright 1995 Overseas Publishers Association N.V.

Over-expression of the p53 protein in NHL is not always associated with mutations in the gene; in fact, only 37.5% of cases reported with intense p53 expression, as shown by

immunohistochemistry, have an underlying mutation as the cause for the stabilisation of the protein (Piris *et al.*, 1995). As mentioned earlier, most studies only screen for mutations in the classic hotspot regions within exons 5 to 8 (reviewed in Piris *et al.*, 1995). Kocialkowski and colleagues (1995) have detected p53 mutations in exons 4 and 10 in the past, in NHL, suggesting that the number of cases containing underlying p53 mutations may be underestimated. On the other hand, Matsushima and co-workers (1994b) investigated a series of 105 lymphoid tumours, which lacked mutations in the p53 gene exons 5 to 9, for mutations within the coding regions of exons 2, 3, 4, 10 and 11 of the same gene, and failed to detect mutations in any of the cases.

Due to the low correlation between p53 over-expression and mutations, other mechanisms of stabilisation of the protein may be operating in NHL. Stabilisation by the cellular protein MDM2 has been proposed but studies analysing simultaneous expression of p53 and MDM2 show variable results. While some studies have shown a strong correlation between p53 and MDM2 expression in lymphoid cells, and in reactive and neoplastic lymphoid tissue (Martinez *et al.*, 1995), other studies have found that the mdm2 gene was amplified in only a very small proportion of human lymphoid tumours and did not correlate with p53 gene expression in the absence of p53 gene mutations (Cesarman *et al.*, 1994).

1.6 AIMS OF THE STUDY

Enteropathy-associated T cell lymphoma is believed to arise as a complication of coeliac disease in patients who have inherited the predisposing HLA genotype (Howell *et al.*, 1995).

Alterations in the p53 tumour suppressor gene are a common feature of many malignancies (Hollstein *et* al., 1991) and immunohistochemical studies, previously undertaken in the department, have detected p53 over-expression in EATL tumour cell nuclei, as well as in small lymphocytes in areas of enteropathic bowel unaffected by tumour (Murray *et al.*, 1995).

The aim of this study is to examine a series of formalin-fixed, paraffin embedded specimens representing EATL and histologically non-involved small bowel tissue for the presence of mutations in exons 5-8 of the p53 gene using PCR-SSCP analysis and DNA sequencing. This will determine whether the p53 protein detected in EATL and in small lymphocytes in adjacent enteropathic bowel is due to mutation or due to stabilisation of the protein by another molecule, such as MDM2.

If mutations are detected, determining the correlation between mutations found in tumour cell nuclei and small lymphocytes in resection margins should give interesting insights into the molecular evolution of EATL from reactive T cells in enteropathic bowel, i.e., whether mutations arise independently from different clones of reactive cells, or whether they represent the same mutation in cells at different stages of the neoplastic process.

2 - MATERIALS AND METHODS

2.1 TISSUE SAMPLES

Formalin fixed, paraffin-embedded specimens of small intestine were obtained from the files of the Pathology Department, Southampton General Hospital. Additional cases were obtained from the archives of Portsmouth, Isle of Wight, Basingstoke, Exeter and Bristol hospitals.

Tissue blocks containing tumour from EATL cases were analysed, as well as tissue, resected at the same time, from adjacent histologically uninvolved areas, when available. Histological sections from all blocks were examined to confirm these features prior to use.

2.2 IMMUNOHISTOCHEMISTRY - INTRODUCTION

Immunohistochemical staining of sections of formalin-fixed paraffin-embedded tissues is usually a straightforward technique, as many antigens retain their antigenicity indefinitely in paraffin blocks, even in sections stored for many years at room temperature. Formaldehyde fixation, however, is thought to mask tissue antigens by forming hydroxy-methylene bridges between components of amino acid chains of the same molecule or of adjacent proteins (Polak and Norden, 1997a). In order to circumvent this problem, antigen retrieval techniques have been developed to restore immunoreactivity without compromising the structure of the tissues. The method used here involves heat-mediated antigen retrieval with a solution of citrate buffer in a microwave oven (Cattoretti *et al.*, 1993).

After antigen retrieval, sections are incubated with 1% bovine serum albumin (BSA) in order to decrease background staining due to non-specific binding of the primary or second antibodies with endogenous proteins (Rainbow, 1996). After incubation of the sections with the appropriate primary antibody, a streptavidin-biotin peroxidase complex technique is used for detection. As endogenous peroxidases, cytochrome oxidases and catalases can all react with the substrate and become confused with specific labelling, their activity must be suppressed before applying the peroxidase-linked reagent. This is usually done with excess of the enzyme substrate, hydrogen peroxide, in methanol (itself an inhibitor of peroxidase), buffer or water (Polak and Norden, 1997a).

The peroxidase label is demonstrated using hydrogen peroxide as the substrate and diaminobenzidine (DAB) as the chromogen. The reaction between peroxidase and its substrate yields a primary complex, which dissociates in the presence of an electron donor (the chromogen DAB). The reduced state of the enzyme is thus regenerated and the oxidised donor released. Upon oxidation, a polymer forms that is seen as a dark brown, highly insoluble precipitate at the site of reaction (Rainbow, 1996).

The high sensitivity of the streptavidin-biotin peroxidase complex method lies in the fact that it is a three-layer amplification technique and that the third reagent contains large and highly labelled complexes. The second antibody is biotinylated and the third reagent is a complex of streptavidin mixed with biotin conjugated to peroxidase. The proportion of streptavidin to biotinylated peroxidase is such that some binding sites on the streptavidin are left free to attach to biotin on the second antibody (Fig. 2.2.1) (Polak and Norden, 1997b).

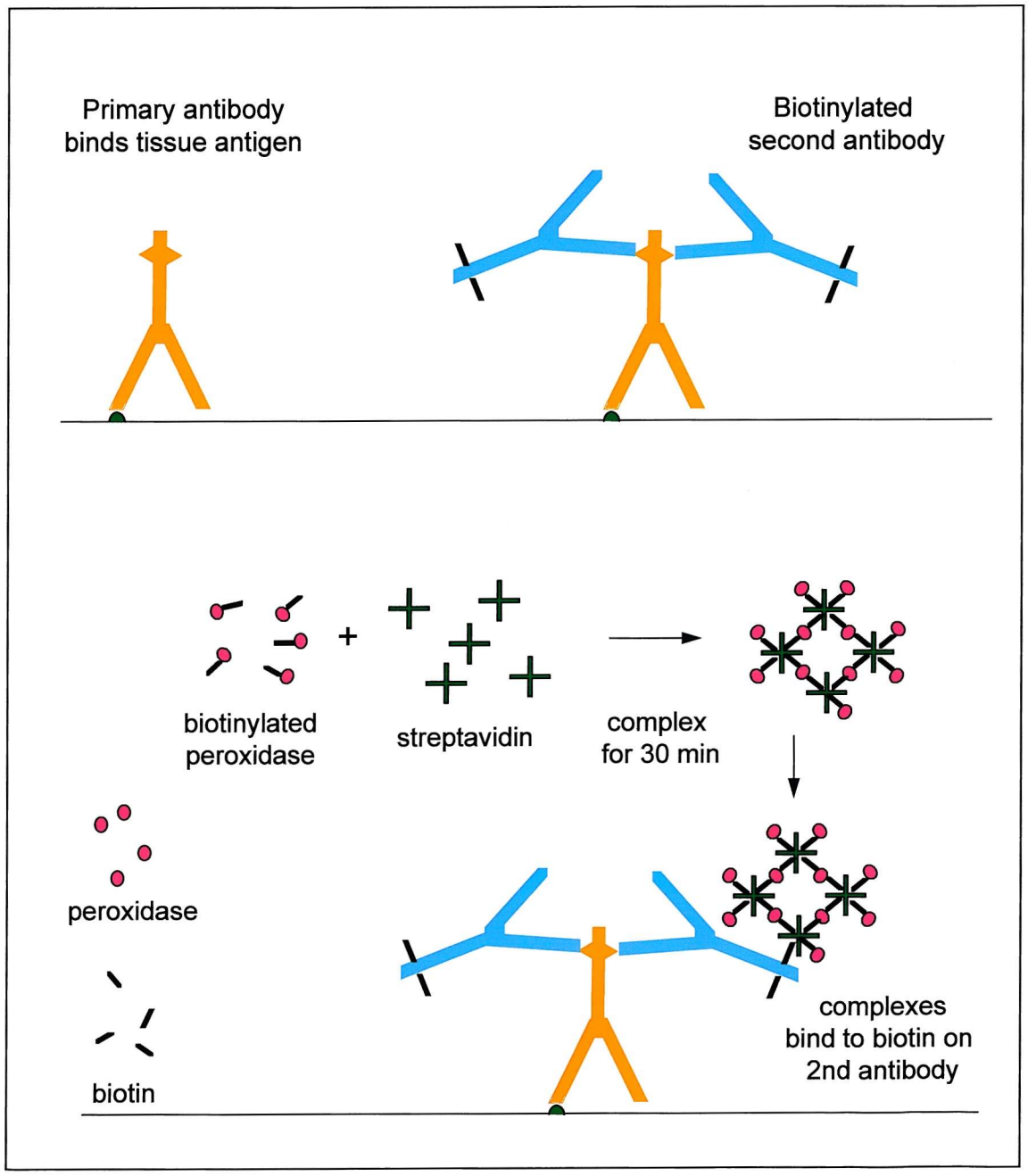

Fig. 2.2.1. The three-layer streptavidin-biotin peroxidase complex technique.

2.3 IMMUNOHISTOCHEMISTRY - METHODS

2.3.1 Sectioning for immunohistochemistry (IHC)

Routinely fixed and processed paraffin-embedded blocks of tissue to be analysed were placed on ice 30 min prior to sectioning. Sections of 4 μm thickness were then cut from the blocks using a microtome, floated on warm water and collected on clean, aminopropyltriethoxysilane (APES)-coated glass slides. Slides were left to dry at 37°C overnight. It is important to note that paraffin sections for immunostaining should not be dried on a hot plate, as this may degrade antigenicity (Polak and Norden, 1997a).

2.3.2 IHC using the streptavidin-biotin peroxidase complex technique

The tissue sections were deparaffinized in xylene and rehydrated in 100% and 70% alcohol. Endogenous peroxidase activity was quenched with 0.5% hydrogen peroxide in methanol for 10 min, followed by a single wash in Tris buffered saline (TBS, Appendix F).

Antigen retrieval was performed in a microwave oven (Panasonic NN-6450, 800 watts) using 10mM citrate buffer (pH6.0). A standardised method was employed in which a constant load of three polythene boxes with perforated lids, each containing a full plastic slide staining rack and 330 ml of citrate buffer, was placed in the microwave oven and run on medium power for 25 min. Each staining rack could hold 24 slides, so, when necessary, blank slides were used to make up the numbers. Slides were rinsed in cold running water for 2 min, then washed in TBS twice for 5 min.

To eliminate any non-specific binding of antibody, sections were incubated with 400 μl of 1% BSA (Sigma) in TBS for 30 min at room temperature. After shaking off the serum, 300 μl of primary antibody diluted in TBS (for dilution see Table 2.3.1) were applied to each section and incubated overnight at 4°C in a humidified chamber. The primary antibodies employed in this study were all mouse monoclonals. Working dilutions were determined by previous titrations (Table 2.3.1). Tissue sections known to show positive staining for each antibody were included in each experiment as controls, and were as follows: colon carcinoma sections for p53 and pRB antibodies, breast carcinoma for MDM2 antibody, and tonsil for CD3 antibody.

Primary antibody	Specificity (staining pattern)	Working dilution	Source of 1° Ab*	Second antibody	Source of 2° Ab
p53 (DO-7)	Human p53 gene protein, wild-type and mutant (nuclear)	1:500	Dako Ltd.	Anti-mouse IgG raised in sheep	Amersham/ Pharmacia
MDM2	MDM2 gene product (nuclear)	1:100	Novocastra Laboratories Ltd.	Anti-mouse IgM raised in goat	Vector Laboratories
pRB	Human retinoblastoma gene protein (nuclear)	1:500	Novocastra Laboratories Ltd.	Anti-mouse IgG raised in sheep	Amersham/ Pharmacia
CD3	Epsilon chain of the human CD3 complex on T cells (membrane)	1:200	Novocastra Laboratories Ltd.	Anti-mouse IgG raised in sheep	Amersham/ Pharmacia

Table 2.3.1. Specificity, working dilution, second antibody, and sources of antibodies.
* Address details of suppliers of reagents and equipment employed in this study are found in Appendix J.

After three 5 min TBS washes, 300 µl of the appropriate biotinylated second antibody, at a 1:200 dilution in TBS, were applied to each section and incubated for 30 min at room temperature. After three 5 min TBS washes, 300 µl of peroxidase-labelled streptavidin-biotin complex reagent (Dako Ltd.), prepared at a 1:200 dilution in TBS and left to complex for 30 min before incubation, were applied to each section and left to incubate for 30 min at room temperature.

After three 5 min TBS washes, 400 µl of 3,3-diaminobenzidine chromogen solution (Vector Laboratories) were applied to each section and left to incubate for 5 min at room temperature. After a quick rinse with TBS, slides were washed in running water for 2 min, then dipped in 70% alcohol and counterstained in Harris' haematoxylin for 1 min. Sections were rinsed in running water for 1 min, immersed in 1% acid alcohol for 5 seconds to eliminate excess haematoxylin stain, then left in running water for 5 min to

blue. Sections were dehydrated in 70% and 100% alcohol solutions and xylene, before being coverslipped using DPX mountant (Surgipath Europe Ltd.).

2.4 PCR-SSCP ANALYSIS - INTRODUCTION

The polymerase chain reaction-single-strand conformation polymorphism (PCR-SSCP) analysis is an efficient method to screen discrete segments of DNA for the presence of mutations, being sensitive enough to detect single base substitutions in the analysed DNA (Orita *et al.*, 1989a). The PCR is used to amplify the target DNA and the resultant products are denatured to form single-stranded DNA (ssDNA) which is then analysed in a non-denaturing polyacrylamide gel according to its conformation rather than its size (Orita *et al.*, 1989b).

2.4.1 Fixed tissue and the polymerase chain reaction

The sensitivity of PCR has allowed great advances in molecular studies and its successful application to fixed paraffin-embedded tissue has opened great opportunities for retrospective molecular genetic studies of human disorders since it gives researchers access to a vast quantity of archival biopsy material.

The successful amplification of DNA extracted from fixed tissue depends on several factors associated with the fixation process, including the fixative used, the duration of the fixation, the age of the paraffin block and the length of the DNA fragment to be amplified (Greer *et al.*, 1994). The type of fixative is one of the most important factors but, since most tissues are routinely fixed in 10% buffered formalin, they are usually good quality PCR substrates, as long as fixation time does not exceed 24 hours. After this time, the ability to amplify large PCR products decreases (Shibata, 1994, Greer *et al.*, 1994).

The length of the DNA fragment to be amplified is also an important factor since it is limited by the partial degradation of DNA inherent of fixed tissues. During fixation formalin cross-links DNA to histone and other associated proteins, making the DNA molecule rigid and susceptible to mechanical shearing (Mies, 1994; Warford, 1988). The action of nucleases during the period between surgical removal of the tissue and formaldehyde fixation is also thought to contribute to DNA degradation (Goelz, 1985).

In general, it is thought that the PCR target should be less than 400 base pairs for successful amplification from formalin-fixed tissues. There is a decrease in the rate of success as the target fragment increases in size, as there are likely to be fewer strands of sufficient length to serve as templates (Shibata, 1994). The age of the specimen also has an effect in the rate of amplification success, which decreases with older specimens (Greer *et al.*, 1994). The presence of inhibitors of *Taq* DNA polymerase is another factor that may affect the amplification of DNA extracted from some fixed specimens, producing false-negative PCR results (Mies, 1994).

2.4.2 DNA preparation

In order to prepare sections of paraffin-embedded tissue for PCR analysis, tissue samples need to be de-waxed first and then the DNA needs to be liberated from the samples. A variety of techniques have been used for this DNA recovery step, including boiling, proteinase K digestion and Chelex 100 treatment (Lo, 1998c), however, proteinase K digestion seems to be the most efficient in extracting longer DNA fragments (Greer *et al.*, 1994; Forsthoefel *et al.*, 1992). A last step before the DNA can be used for PCR amplification is heat inactivation of the proteinase K enzyme, which could otherwise digest the *Taq* polymerase (Greer *et al.*, 1994). Although the extract produced is relatively impure, containing a high proportion of proteins, it is usually adequate for PCR (Pan *et al.*, 1995).

2.4.3 The PCR technique

The PCR is a simple *in vitro* method used for nucleic acid synthesis by which a discrete segment of DNA can be replicated exponentially using synthetic sequence-specific oligonucleotide primers. The reaction takes place in a single tube and consists of three steps: thermal denaturation of the target DNA, primer annealing and extension of the annealed primers by the thermostable *Taq* polymerase (Fig. 2.4.1). This cycle is then repeated 25-40 times, each time approximately doubling the number of product molecules, the size of which is determined by the distance between 5'-ends of the two primers (Lo, 1998a; Loda, 1994).

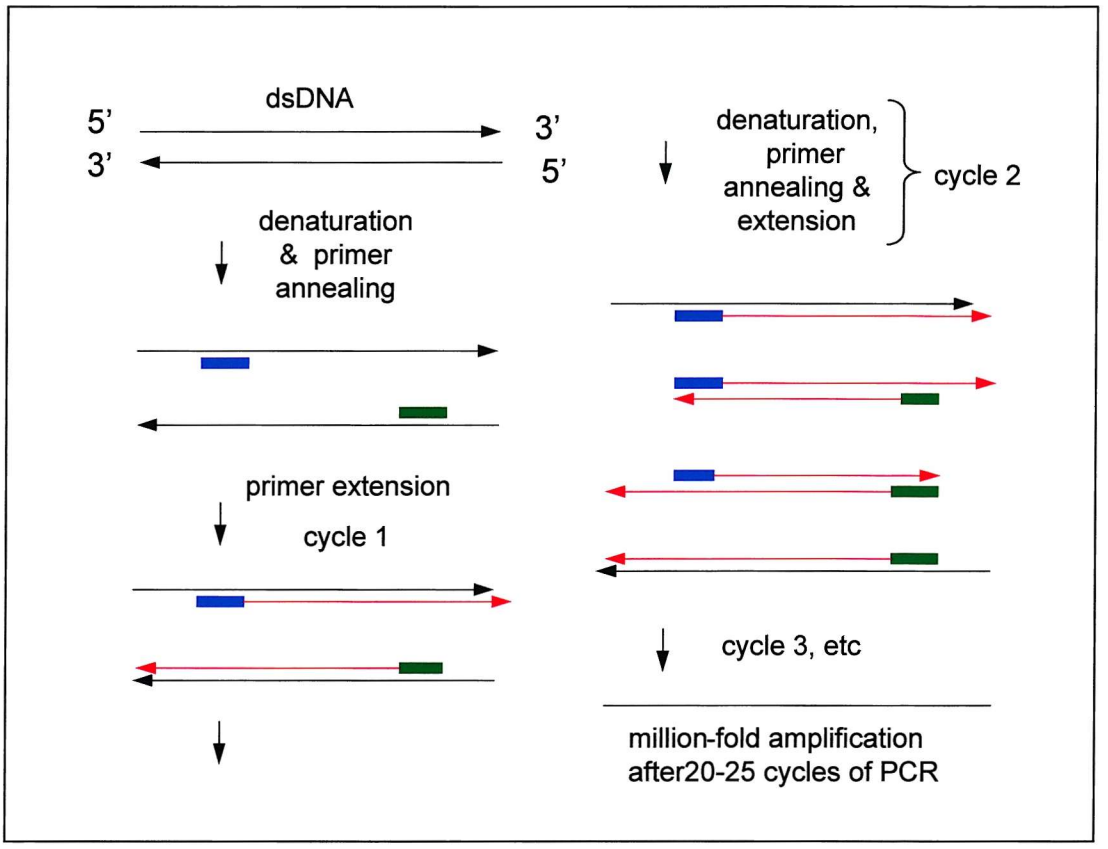

Fig. 2.4.1. Schematic representation of the polymerase chain reaction.

2.4.4 PCR parameters

The reaction mixture consists of a DNA template, two synthetic oligonucleotides, a DNA polymerase, the 4 deoxynucleoside triphosphates (dATP, dCTP, dGTP, and dTTP) and a buffer containing magnesium chloride. In order to maximise the amplification of the target sequence, avoiding the generation of non-specific products, the PCR conditions and cycling parameters must be optimised for each pair of primers used (Harris and Jones, 1997). The magnesium chloride concentration and annealing temperature are critical for achieving specific amplification, but all the other factors also need careful consideration.

2.4.4.1 Target DNA concentration

While the concentration of target DNA extracted from fresh tissues does not seem to be crucial for PCR sensitivity, the concentration of DNA from fixed tissues is far more critical for efficient amplification. A range between 250 ng and 500 ng of template DNA from fixed tissue produces good results (Harris and Jones, 1997). Factors thought to be responsible for the lower and upper limits of template concentration are, respectively, the partially degraded nature of DNA from fixed tissues, containing fewer strands with

intact target areas, and the presence of PCR inhibitors in fixed tissue samples that would increase in concentration with increases in target DNA concentration (Harris and Jones, 1997; An and Fleming, 1991).

2.4.4.2 Primer design

Oligonucleotide primers are designed to be complementary to regions flanking the DNA sequence of interest. They are ideally between 18 and 30 bases long, with a GC content of about 50%. Complementarity at the 3'-ends of the primers is avoided to decrease the likelihood of them forming a primer-dimer artifact. Runs of three or more C or G residues at the 3'-ends of the primers are also avoided to decrease the probability of priming GC-rich sequences nonspecifically (Lo, 1998a).

2.4.4.3 Effect of magnesium chloride concentration

Free magnesium ions are required for *Taq* DNA polymerase activity and are included in the reaction in the form of magnesium chloride. The concentration of magnesium chloride has a great effect on the efficiency and specificity of the PCR. While higher concentrations of magnesium chloride improve the efficiency of amplification, they also reduce its specificity. The opposite is true for lower concentrations of magnesium chloride, i.e. increased specificity, but reduced efficiency. The optimal concentration of magnesium chloride for each pair of primers needs to be determined empirically. It usually lies between 1.5 and 4.0 mM (Harris and Jones, 1997).

2.4.4.4 Taq DNA polymerase

The most commonly used DNA polymerase, *Taq*, has a molecular weight of 94 kDA and was originally isolated from the thermophilic bacterium *Thermus aquaticus* (Chien *et al.*, 1976). An important issue with regard to point mutation analysis is the possibility of nucleotide mis-incorporation by *Taq* polymerase due to its lack of 3'-5' exonuclease ('proof-reading') activity. The mis-incorporation rate varies considerably and ranges from one in 6,000 to one in 200,000 bases. However, in most instances this does not affect interpretation of results as the proportion of altered bases is low and the errors are randomly introduced at different positions (Loda, 1994). To reduce the mis-incorporation rate, especially when the initial copy number of DNA templates is very low, careful optimisation of the amplification conditions is necessary (Lo, 1998a;

Gelfand and White, 1990). Additionally, a DNA polymerase with 3' to 5' exonuclease proof-reading activity, such as the ones isolated from *Thermococcus* litoralis (*Tli*), *Pyrococcus furiosus* (*Pfu*), and *Pyrococcus woesei* (*Pwo*) can be used. The fidelity of DNA synthesis is enhanced as these enzymes excise any incorrectly added, mismatched 3'-terminal nucleotides from the primer extension product, and then incorporate the correct nucleotide. The fidelity of DNA synthesis by such enzymes with proof-reading activity is 10 to 15-fold higher than that of *Taq* DNA polymerase. A disadvantage associated with the 3' to 5' exonuclease activity is that it can also degrade primers or template, therefore it is advisable to add the enzyme last to the reaction or use a hot-start method (reviewed in Newton and Graham, 1997a).

2.4.4.5 Hot start PCR

Amplification by PCR of low copy-number targets can also be affected by nonspecific amplification due to pre-PCR mispriming or primer dimerisation. The development of hot start PCR has allowed greatly increased specificity and yield when amplifying low copy-number targets (Chou *et al.*, 1992). In hot start PCR, at least one of the reagents, usually the DNA polymerase, is withheld from the reaction mixture until the reaction temperature has reached 60-80°C and the template is denatured. This prevents the formation of misprimed products and primer-dimers at low temperatures (Chou *et al.*, 1992).

With the development of modified forms of the *Taq* DNA polymerase, the enzyme is now commercially available in an inactive state with no polymerase activity at room temperature (e.g., HotStar Taq DNA polymerase by Qiagen). The enzyme can thus be added to the reaction mixture as usual and only becomes activated during a 15-min, 95°C incubation step that is incorporated into the thermal cycling programme.

2.4.4.6 Cycling parameters

a) Denaturation

The first step in the PCR is the thermal denaturation of the target DNA in order to expose sequences to which the primers will anneal. This is usually done at 94°C. There is commonly a long initial denaturation step (5 min.) to ensure complete separation of the DNA strands, with subsequent shorter denaturations (30-45 sec) as the targets of later cycles are mainly PCR products. It is best to avoid very high denaturation

temperatures or long incubation times in order to prevent loss of DNA polymerase activity (Harris and Jones, 1997).

b) Annealing temperature

The temperature at which primers anneal to their complementary sequences on the target DNA also plays an important role in the specificity and efficiency of the PCR. While too low a temperature may lead to nonspecific amplification due to mispriming, too high an annealing temperature may lead to failure of amplification as the primers fail to anneal. The annealing temperature is dependent on the melt temperature (T_m) and base sequence of each primer and should be similar for both primers in a pair (Innis and Gelfand, 1990). The annealing temperature (T_a) for a pair of primers needs to be determined empirically. A good starting point is a temperature 5°C below the true T_m of the primers used, for approximately 30 sec (Newton and Graham, 1997a):

$$T_a = T_m - 5°C = 2(A+T) + 4(G+C) - 5°C$$

c) Primer extension

This is typically carried out at 72°C, which is close to the optimal temperature for *Taq* polymerase activity for about 45 sec. At the end of the amplification, when the amount of product exceeds the enzyme concentration, there is usually a final extension step for 5 min to ensure complete extension of all amplified products (Lo, 1998a; Harris and Jones, 1997).

d) Cycle number

The number of cycles employed depends on the copy number of the target DNA, the primers used and the efficiency of each amplification step. As a rule of thumb, to amplify 10^5 template molecules to produce a signal visible in an ethidium bromide-stained agarose gel, requires 25 cycles. Similarly, 10^4, 10^3, and 10^2 target molecules would need 30, 35, and 40 cycles, respectively (Lo, 1998a).

2.4.5 The SSCP technique

In SSCP analysis, the denatured PCR products are run in a non-denaturing gel so that the ssDNA can conserve its three-dimensional folded structure. The conformation that ssDNA assumes depends on its primary structure, i.e. its nucleotide sequence. Consequently, single changes in nucleotide sequence, such as those found in mutated sequences, alter the intramolecular interactions generating different folded structures. Molecules with different conformations migrate at different rates through the gel and can be identified as shifted bands in relation to wild-type alleles (reference DNA) analysed alongside them (Hayashi, 1991) (Fig. 2.4.2).

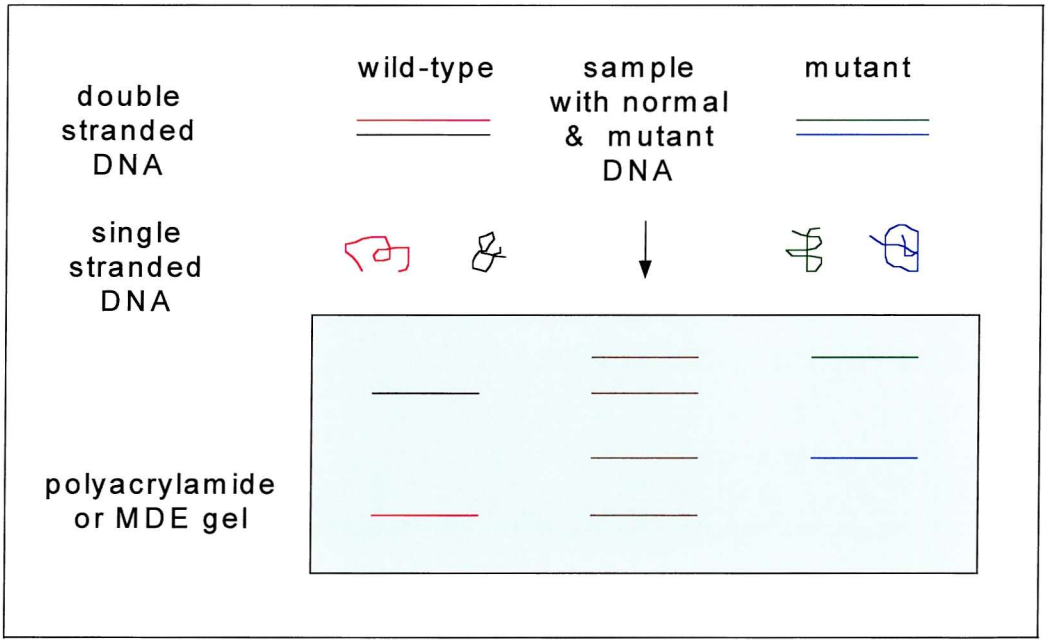

Fig. 2.4.2. The principle of SSCP analysis. Denatured PCR products are run as ssDNA on a non-denaturing gel, showing differential mobility according to changes in conformation determined by their nucleotide sequence.

Analysis by SSCP has become the method of choice when screening for mutations occurring in non-predictable locations, due to its relative simplicity and high sensitivity. The sensitivity of the method, however, is dependent on two main factors: the size of DNA segments analysed and whether two different conditions (e.g. different ambient temperatures, or presence and absence of glycerol in the gel) are used when performing the electrophoresis (Loda, 1994; Hayashi, 1991).

In general, in order to ensure high levels of sensitivity, the DNA segments should not exceed 300 or 400 bp in size. The reported probability of detecting a shift in at least one strand using gels containing 5-10% glycerol is of more than 99% for 100- to 300-bp fragments and 89% for 300- to 450-bp fragments (Hayashi, 1991). Although some workers have reported SSCP to be most sensitive when used to detect sequence variation in DNA molecules approximately 150-bp in length (Sheffield *et al.*, 1993), another sensitivity study using various gel conditions with the majority of PCR products tested ranging between 257- and 322-bp reported an approximately 100% detection sensitivity when combining two gel conditions (with/without glycerol) (Vidalpuig and Moller, 1994).

The electrophoretic mobility of ssDNA in polyacrylamide gels is strongly dependent on environmental conditions such as ambient temperature and the presence of 5-10% glycerol in the gel. It has been reported that mobility shifts caused by base substitutions of most sequences were best resolved when electrophoresis is carried out at room temperature in the presence of 10% glycerol (Orita *et al.*, 1989b).

Another condition that affects the sensitivity of the technique is the use of mutation detection enhancement (MDE) gels instead of normal polyacrylamide gels. An MDE gel (FMC Bioproducts) is a polyacrylamide-based vinyl polymer that produces improved resolution of conformationally different DNA molecules, as well as reproducibility in the detection of ssDNA in SSCP (Soto and Sukumar, 1992). Analysis of SSCP products in MDE gels is very similar to the conventional method using 6% polyacrylamide. Running times need to be extended, since SSCP products move slower through MDE than standard polyacrylamide under comparable running conditions.

Additional factors that could theoretically play a role in the sensitivity of SSCP for detecting single base substitutions include the position of the base substitution within the fragment, the nature of the base substitution (i.e. transition vs. transversion) and the sequence composition of the DNA fragment. All of these factors would be expected to influence the secondary structure of DNA molecules (Sheffield *et al.*, 1993). Sensitivity of mutation detection is often much greater for one strand of a DNA sequence compared

to the complementary strand. This suggests that certain sequences alter their conformation more readily, due to single base substitutions, than do other sequences. Preliminary studies suggest that the strand with the greater purine concentration migrates faster in the gel and shows more dramatic band shifts with base substitutions. However, this observation needs to be confirmed (Sheffield *et al.*, 1993).

Occasionally, misinterpretation of results may occur due to one strand of DNA being separated into two or more bands in the SSCP gel, even though the sequence is the same. This suggests that strands with the same sequence can assume more than one stable conformations (Orita *et al.*, 1989b). Usually, the different conformer bands show variation in signal intensity. Hayashi (1991) reported that these cases can be identified as multiple conformer bands rather than mobility shifts, as the ratio of signal intensity between bands of the same sample is constant and consistent from sample to sample.

2.5 PCR-SSCP ANALYSIS - METHODS

2.5.1 Sectioning for PCR

Two to four 15 μm sections were cut from routinely fixed and processed paraffin-embedded blocks of EATL and adjacent areas. Sterile disposable needles were used to handle the tissue sections, which rolled up when cutting and thus could be placed into 1.5 ml microcentrifuge tubes. The microtome was wiped thoroughly with xylene between cutting different blocks and a different area of the microtome blade was used for different blocks, with a maximum of two blocks per blade, to avoid cross-contamination. The blade was cleaned between blocks using a xylene-soaked tissue and one wipe across from the unused area to the used area of the blade.

2.5.2 DNA extraction from formalin fixed paraffin-embedded tissue

The tissue sections were dewaxed in 1 ml xylene for 5 min, centrifuged for 5 min at 13,000 rpm and then washed twice in 600μl absolute ethanol and twice in 600μl phosphate buffered saline (PBS), centrifuging for 5 min at 13,000 rpm after each wash. Genomic DNA was extracted by incubating the tissue in 200μl to 300μl of digestion buffer (Appendix F) containing 400μg/ml proteinase K at 55°C for 18 to 20 hours. The tubes were briefly microcentrifuged to bring down condensate, then the proteinase K was inactivated by placing the tubes over boiling water for 8 minutes, with a sterile syringe needle inserted through each lid to allow for expansion of air. The samples were centrifuged for 5 min at 13,000 rpm and the supernatant transferred to a clean microcentrifuge tube. The DNA concentration was determined spectrophotometrically and the purity of the sample calculated by determining the ratio of the absorbance at 260nm (absorbance wavelength of DNA) and the absorbance at 280nm (absorbance wavelength of protein). This should be around 1.8 for a pure sample.

2.5.3 PCR

The sequences of the oligonucleotide primers used to amplify exons 5 to 8 of the p53 gene were derived from published sequences (Shi *et al.*, 1996; Milner, 1993) and checked to ensure specificity using the basic local alignment search tool (BLAST), a sequence comparison tool accessible on the world wide web (Altschul *et al.*, 1990). Primers were synthesised by Oswel Research Products Ltd. This set of primers has been

termed Set 1 and the sequences and sizes of the PCR products generated are shown in Table 2.5.1. The full sequence data for exons 5-8, with primer annealing sites, is presented in Appendix A (Lamb and Crawford, 1986).

Exon	Primer sequence	Length of PCR product	Annealing temperature
5	F: 5' TTCCTCTTCCTACAGTACTC 3' R: 5' GCCCCAGCTGCTCACCATCG 3'	214 bp	55°C
6	F: 5' GGCCTCTGATTCCTCACTGATT 3' R: 5' AGAGACCCCAGTTGCAAACC 3'	167 bp	57°C
7	F: 5' AGGCGCACTGGCCTCATCTT 3' R: 5' TGTGCAGGGTGGCAAGTGGC 3'	177 bp	58°C
8	F: 5' TGCTTCTCTTTTCCTATCCTGA 3' R: 5' CGCTTCTTGTCCTGCTTGCT 3'	186 bp	60°C

Table 2.5.1. Set 1 of primers used for the amplification of exons 5-8 of the p53 gene using the PCR method.

Each PCR was carried out in 20µl of reaction buffer (Qiagen PCR buffer, 1.5 mM $MgCl_2$) containing 8 pmol of each primer, 200 µM of each dNTP and 0.5 unit of *Taq* polymerase (for definition of unit of *Taq* polymerase see Appendix I.4). Three hundred to 500 ng of DNA template were added to each reaction. The thermal cycles consisted of an initial cycle of 5 min at 94°C for denaturation of the DNA, followed by 35 cycles of 30 sec at 94°C, 30 sec at the corresponding annealing temperature for each exon, and 45 sec at 72°C, and concluded by 5 min at 72°C for final elongation. A blank control to which no DNA template had been added was included in every PCR run to ensure that no contamination had occurred. A positive control containing DNA that had previously been amplified successfully was also included, so that poor amplification due to an

inadequate template could be differentiated from poor amplification due to problems with reagents or the thermal cycler.

The optimal annealing temperatures and $MgCl_2$ concentrations for the PCR of each exon were determined empirically (see section 3.4.1).

2.5.4 Visualisation of PCR products

Four µl of PCR products were mixed with 1µl of gel loading buffer A (Appendix F) and loaded into a 2.5% agarose gel containing ethidium bromide (0.5µg/ml). A ϕX174 *Hae* III DNA size marker (0.375µg/lane) was loaded alongside the PCR products to confirm the size of the PCR product obtained. Electrophoresis was performed in Tris-acetate-EDTA (TAE) X1 buffer, at 100V, for 60 min at room temperature. The amplified products were viewed with an ultraviolet light transilluminator (TM-36E, Ultra-Violet Products Ltd.), as the ethidium bromide used to stain the products fluoresces under ultraviolet light. Results were recorded on photographic film (Polaroid, type 55).

2.5.5 SSCP Analysis

Five µl of the PCR products were mixed with 4µl of stop solution (Appendix F), denatured for 8 min at 94°C, rapidly chilled on ice and immediately loaded into a 0.35 mm thick SSCP gel [MDE gel, prepared according to manufacturer's instructions with slight modifications (Appendix G.2), FMC Bioproducts]. Prior to mounting, one plate was coated with silane to increase adherence, while the other one was coated with Sigmacote (Sigma) to prevent it. This ensured that the gel adhered to only one of the glass plates. The DNA size marker ϕX174 *Hae* III (0.375µg/lane) was diluted in gel loading buffer B (Appendix F) and loaded alongside the denatured PCR products. Electrophoresis was performed in 0.6X Tris-borate-EDTA (TBE), at 120V for 5.5 to 6 h using SE600 vertical electrophoresis equipment (Hoefer Scientific Instruments). A water-jacketed apparatus was used to keep the temperature of the gel constant (usually between 10°C and 18°C).

After electrophoresis, the glass plates holding the gel were carefully separated, so that the gel remained on one of the plates that acted as a support during fixation and staining.

Bands of ssDNA were detected by silver staining (Bosari *et al.*, 1995) using the PlusOne DNA silver staining kit (Pharmacia Biotech), according to manufacturer's instructions. Band patterns on gels were recorded on photographic film (Polaroid, type 55).

2.6 MICRODISSECTION OF IMMUNOSTAINED TISSUE SECTIONS

The molecular genetic analysis of tissue sections containing small numbers of scattered target cells using PCR is a difficult task due to their low abundance in a background of irrelevant cells. This is the case in tissue sections of uninvolved bowel resected from areas adjacent to tumour (A samples), showing p53 protein accumulation only in a few scattered lymphocytes.

In an attempt to enrich the p53 immunostain-positive cells of A samples and T samples with scattered stained cells, so that a higher proportion of target cells would be present for SSCP analysis or sequencing, a microdissection technique has been employed.

Sections 10μm thick were immunostained for p53 protein, incubated with PCR buffer containing 2.5% glycerol for 2 min to reduce brittleness of the tissue (Moskaluk and Kern, 1997) and left to air dry. From each tissue block, an additional 4μm section, immediately adjacent to the previous sections, was also immunostained and coverslipped to serve as a 'guide slide'. After inspection of the guide slides, areas rich in stained cells were encircled using a fine-tip permanent marker pen and then the equivalent areas were marked on the underside of the slides carrying sections to be microdissected.

Slides for microdissection were placed on the stage of a Leitz inverted microscope fitted with 10X eyepiece lenses and 5, 10, and 20X objective lenses. Manually-pulled glass pipettes were used to drop PCR buffer onto the marked areas of the section. Microdissection was performed under X100 magnification using a hand-held, sharpened tungsten wire needle (diameter 0.5 mm) mounted into a microdissection tool-holder (see Appendix H for method used to sharpen needles). The tissue of interest was separated from adjacent tissue, scraped off the slide, picked up and transferred into a microcentrifuge tube containing digestion buffer (Appendix F) using the wire needle. DNA extraction then proceeded as in Section 2.5.2. The volume of digestion buffer used varied according to the microdissected area; approximately 10μl of digestion buffer were used per 100 cells (Moskaluk and Kern, 1997). The smallest microdissected area was estimated to have approximately 150 cells and the largest area about 600 cells.

Although PCR amplification of the microdissected tissue was successful, the minimum size of microdissected areas achieved with the facilities available was not believed to be small enough for sufficient enrichment of target cells in all samples. An alternative method to achieve this aim was therefore sought.

2.7 IMMUNOHISTOSELECTIVE ANALYSIS (IHSA) - INTRODUCTION

In order to ensure that failure to detect mobility shifts in tissue sections containing scattered p53 immunostain-positive cells was due to lack of mutation and not due to the low abundance of cells containing a mutation, an alternative method to enrich the p53 positive cells for PCR-SSCP analysis and sequencing was used, adapted from the technique of immunohistoselective sequencing (Shi *et al.*, 1996).

The principle of the method is first to protect DNA in the target cells selectively and then to use ultraviolet (UV) light irradiation to inactivate DNA in the undesired, unprotected cells (Shibata *et al.*, 1992). Shi and colleagues (1996) refined the technique, using the immunostain itself as a protective barrier from the UV light, by darkening its coloration. The protected DNA from selected cells can subsequently be amplified to detectable amounts using the PCR (Fig. 2.7.1). Potentially, this method can be used for any cells that can be immunoselected on the basis of expression of a nuclear antigen.

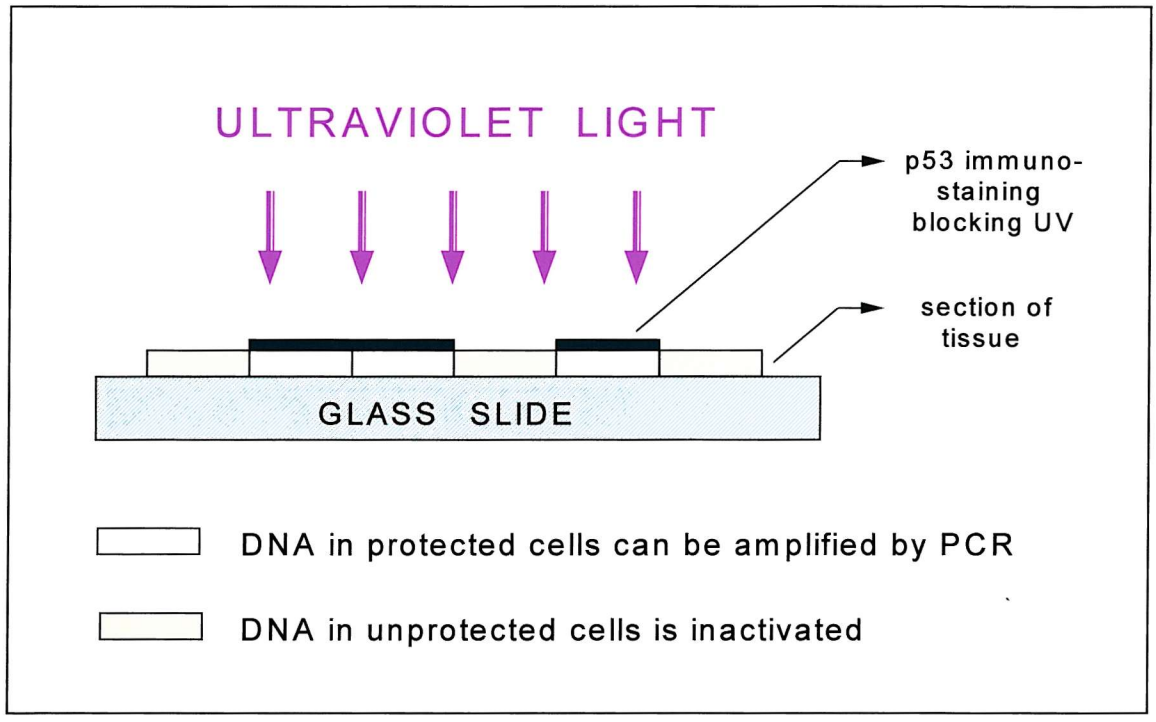

Fig. 2.7.1. The principle of immunohistoselective analysis. The enhanced immunostaining offers the cells over-expressing p53 protein a protective shield during UV irradiation. As the DNA in the unstained (unprotected) cells is inactivated by the UV light, only DNA in the positively selected cells will be amplified during PCR.

2.7.1 Effect of UV light on DNA

When DNA is exposed to UV irradiation at wavelengths approaching its absorption maximum (approximately 260 nm), adjacent pyrimidines (most often thymines) in the same polynucleotide chain become covalently linked by the formation of a 4-membered ring structure resulting from the saturation of their respective 5,6 double bonds (Friedberg, 1985). The structure formed by this photochemical cyclo-addition is referred to as a cyclobutyl dipyrimidine, or pyrimidine dimer (Fig. 2.7.2).

Pyrimidine dimers are thought to contribute to UV-induced DNA inactivation by functioning as termination sites during the extension reactions of the PCR procedure. Dimerisation draws the thymine residues together and distorts the helix in such a way that replicative polymerisation is blocked at this site (Shi *et al.*, 1996). Non-dimer photodamage, such as interstrand and intrastrand DNA-DNA crosslinks and DNA

strand breaks, can also be termination sites for *Taq* DNA polymerase (Cimino *et al.*, 1990).

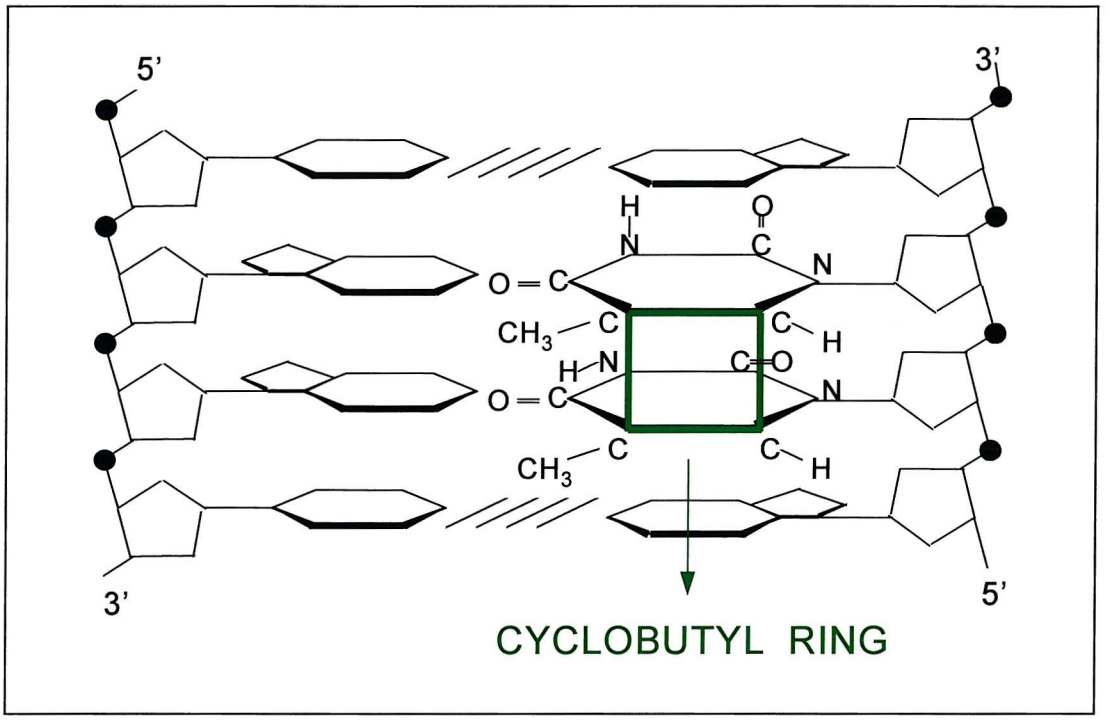

Fig. 2.7.2. The cyclobutyl pyrimidine dimer is formed in DNA by the covalent interaction of two adjacent pyrimidines in the same polynucleotide chain. The green square represents the cyclobutyl ring that links the two pyrimidines.

2.7.2 Factors affecting UV inactivation of DNA segments

The rate of inactivation of DNA by UV irradiation is thought to be influenced mainly by the relative abundance of adjacent thymine residues in the segment of DNA to be treated. Shi and co-workers (1996) have found a rough correlation between susceptibility to UV inactivation and number of T-T units per DNA segment, with segments containing fewer T-T units requiring longer UV exposure times for complete DNA inactivation than segments containing more adjacent thymine residues.

The size of the target sequence (Shibata *et al.*, 1992; Sarkar and Sommer, 1990) has also been reported to influence sensitivity to UV irradiation, with larger fragments being more susceptible to UV inactivation than smaller fragments (< 120 bp) (Shibata, 1994).

2.7.3 Enhancement of the immunostaining

In order to increase the protection that immunostaining provided during the UV irradiation of tissue sections, enhancement of the diaminobenzidine (DAB) chromogenic product was achieved by adding a nickel solution.

The addition of nickel chloride to DAB prior to incubation causes the colour of the reaction to change from brown to a purplish blue/black (Hsu and Soban, 1982), increasing the intensity of the stain and making it more opaque to UV light. The intensity of the stain was increased even further by adding twice the amount of nickel solution suggested by the manufacturer of the kit used (see Section 2.8.2.).

2.7.4 Nested PCR

In some instances, when the DNA template is of poor quality or present at low copy numbers, the sensitivity of PCR can be affected. To improve the sensitivity and specificity of the reaction, nested PCR methods can be employed.

In nested PCR, two separate amplifications are carried out and the product obtained from the first round is used as the template for the second amplification. For the second round of PCR, a set of primers that anneals to sequences within the initial product is used, so that a second, smaller product is produced (Baumforth *et al.*, 1999) (see Fig. 2.7.3).

The use of nested PCR enhances the amplification sensitivity from 100 to 1000-fold (Lo, 1998b). The specificity of DNA amplification is also dramatically increased as nonspecific amplification products are almost always eliminated. This happens because any nonspecific products produced after the first round of PCR are unlikely to be sufficiently complementary to the nested primers to be able to serve as a template for further amplification (Newton and Graham, 1997b). The specificity and sensitivity enhancement is also observed when the second round PCR is carried out using one internal primer and one of the original external primers, in a strategy termed 'semi-nesting' (Lo, 1998b).

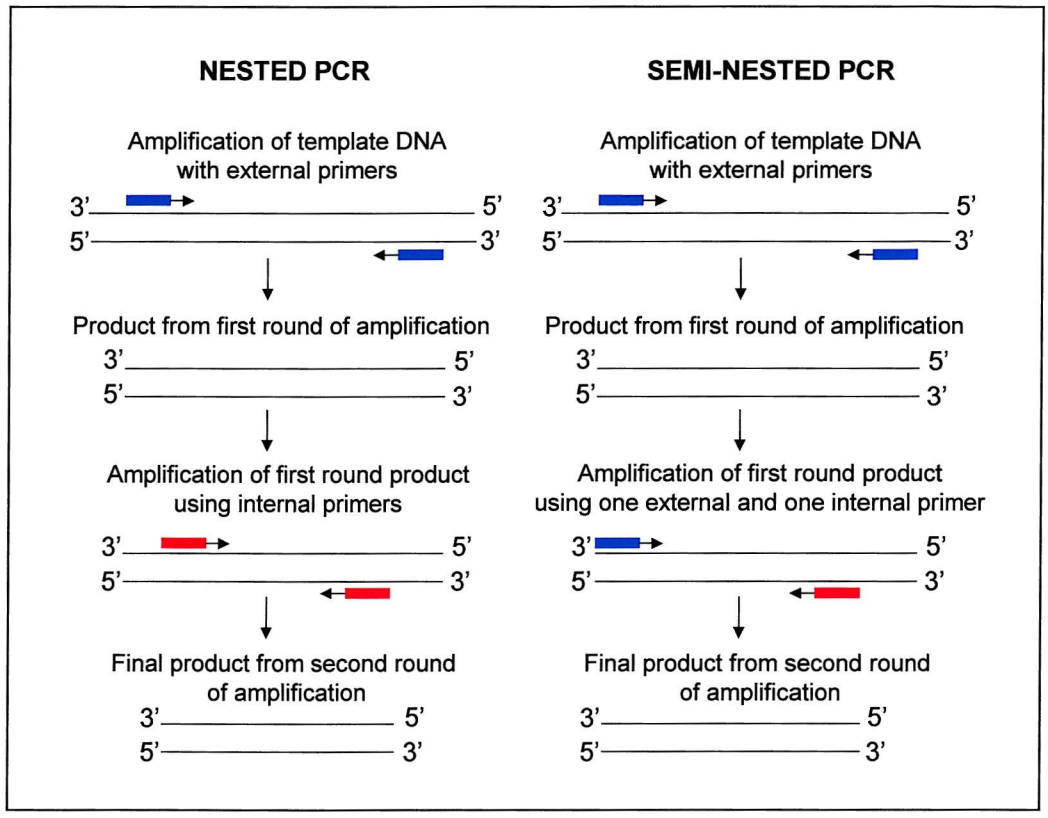

Fig. 2.7.3. Principle of nested and semi-nested PCR. Two separate amplifications are performed in nested or semi-nested PCR. The first one employs a pair of primers that yield a large product, which is then used as template for the second amplification. In nested PCR, a second pair of primers, which anneal to sequences within the initial product, is used. In semi-nested PCR, one of the original external primers is used in conjunction with an internal primer.

2.8 IMMUNOHISTOSELECTIVE ANALYSIS - METHODS

2.8.1 Sectioning for IHSA

Sections of 6μm thickness were cut from the blocks to be analysed, using all precautions as for PCR sectioning (Section 2.5.1) to avoid contamination. However, instead of rolled sections, flat sections were cut that were floated into a container containing warm water, and picked up onto APES-coated glass slides. The water in the container was exposed to UV light before use, to inactivate any contaminating DNA present. The slides were placed into metal racks and left to dry overnight at 37°C.

2.8.2 Immunostaining for IHSA

Sections to be stained for IHSA were deparaffinized and rehydrated as for IHC, using fresh xylene and graded alcohols. Immunostaining of the sections proceeded as for normal IHC up to the DAB incubation. Instead of the normal DAB solution, a DAB solution containing nickel chloride (Vector Laboratories) was used and incubated for 5 min. Twice the suggested amount of nickel solution was added to the DAB solution to further enhance the staining, as determined in a preliminary experiment (see Section 3.7.1.2). Slides were washed in TBS twice and then rinsed in sterilised water. The sections were then incubated in 2.5% glycerol in water for 3 min to reduce brittleness of the tissue (Moskaluk and Kern, 1997) and allowed to air dry.

2.8.3 Ultraviolet irradiation and DNA preparation

The p53-immunostained slides were placed, tissue side up, into a UV crosslinker (Model CL-1000, Ultra-Violet Products Ltd.) for varying lengths of time. The UV wavelength used was 254 nm and the UV energy was 8000 $\mu W/cm^2$.

UV exposure times needed for complete inactivation of DNA from p53-negative cells were determined for each exon by irradiating unstained sections for increasing lengths of time. For the cases analysed, the range of optimal UV exposure times for inactivation for each exon varied between 60 and 120 min for exon 5, 50 and 150 min for exon 6, 60 and 210 min for exon 7, and 30 and 120 min for exon 8.

After irradiation, 10-15 µl of digestion buffer (Appendix F) were applied to each section, which was then gently scraped off the slide with a sterile scalpel blade. The tissue was then picked up with a sterile pipette tip and placed into a microcentrifuge tube containing digestion buffer. Two sections of UV-treated p53-immunostained tissue were placed into each tube containing 70 µl of digestion buffer and incubated at 55°C for 18 to 20 hours. One section of p53-immunostained cells without UV treatment was digested in 40 µl of buffer and included as a positive control. As a negative control, 2 sections of immunostained cells, not exposed to primary antibody, were UV irradiated and digested in 50 µl of buffer. This was used to confirm that all background DNA had been inactivated by the UV irradiation. The tubes were microcentrifuged briefly to bring down any condensate, then placed on a PCR thermal cycler at 94°C for 8 min to inactivate the proteinase K. The samples were centrifuged for 5 min at 13,000 rpm and the supernatant transferred to a clean microcentrifuge tube. Five µl of supernatant were used as the substrate for PCR.

2.8.4 Nested PCR

PCR amplification of exons 5-8 of the p53 gene was carried out in 20µl reactions containing 8 pmol of each primer, 200 µM of each dNTP, 1.5mM $MgCl_2$, 0.5 unit of HotStar Taq polymerase (Qiagen Ltd.), and the DNA template. Primers used are shown in Tables 2.5.1 and 2.8.1, and were derived from published sequences (Shi *et al.*, 1996; Milner *et al.*, 1993; Gaidano *et al.*, 1991). For the first round PCR, set 2 primers (external primers, Table 2.8.1) were used. Amplification consisted of an initial step at 95°C for 15 min for enzyme activation and DNA denaturation, followed by 35 cycles at 94°C for 30 sec, annealing at the appropriate temperature (Table 2.8.1) for 30 sec, and extension at 72°C for 45 sec. A final elongation step at 72°C for 5 min completed the PCR. For the second round PCR, set 1 primers (internal primers, Table 2.5.1) were used and 1 µl of a 1/10 dilution of the product obtained from the first round PCR was used as the substrate; otherwise conditions were as above. It is important to note the need for diluting the first round PCR product; otherwise, multiple bands were produced during the second round of reactions (see Fig. 3.7.8). This has also been observed by another group (Wang *et al.*, 1996).

Exon	Primer sequence	Length of PCR product	Annealing temperature
5	F: 5' GTTTCTTTGCTGCCGTGTTC 3' R: 5' ACCCTGGGCAACCAGCCCTGT 3'	313 bp	64°C
6	F: 5' TGGTTGCCCAGGGTCCCCAG 3' R: 5' GGAGGGCCACTGACAACCA 3'	223 bp	64°C
7	F: 5' CTTGCCACAGGTCTCCCCAA 3' R: 5' AGGGGTCAGCGGCAAGCAGA 3'	237 bp	64°C
8	F: 5' TTGGGAGTAGATGGAGCCT 3' R: 5' AGGCATAACTGCACCCTTGG 3'	281 bp	62°C

Table 2.8.1. Set 2 of primers used for the amplification of exons 5-8 of the p53 gene using the PCR method (external primers).

2.9 PRIMER-EXTENSION PRE-AMPLIFICATION (PEP) - INTRODUCTION

Amplification by PCR from initial IHSA-produced samples did not show detectable products by agarose gel electrophoresis. The technique of primer-extension pre-amplification (PEP) (Zhang *et al.*, 1992) was therefore used for universal amplification of the minority population of intact DNA strands present in the UV-irradiated samples.

Primer-extension pre-amplification is a PCR-based method that has been developed to achieve whole genome amplification of a single haploid cell using a mixture of 15-base random oligonucleotides. These oligonucleotides are also known as totally degenerate primers as any of the four possible bases could be present at each position, so that, in theory, they contain a mixture of 4^{15} (1×10^9) sequences. By using such primers and lowering the annealing temperature to 37°C, it has been estimated that at least 78% of the genomic sequences in a single human haploid cell can be copied at least 30 times (Zhang *et al.*, 1992).

Degenerate oligonucleotide-primed (DOP)-PCR (Telenius *et al.*, 1992) is another type of random PCR that uses a partially degenerate primer (e.g. 5'-CCGACTCGAGNNNNNNATGTGG-3') for whole genome amplification. However, when using this method, there is a likelihood that a given locus might not be represented in the product obtained when genomic DNA amounts are below 640 pg (Cheung and Nelson, 1996). Primer-extension pre-amplification is thought to offer a more complete coverage at lower genomic DNA copy numbers (Sun *et al.*, 1995).

2.10 PRIMER-EXTENSION PRE-AMPLIFICATION (PEP) – METHODS

Primer-extension pre-amplification was performed in 50µl of reaction buffer (Qiagen PCR buffer, 1.5 mM $MgCl_2$) containing 15µg of a 15-mer random primer (3'-NNNNNNNNNNNNNNN-5', synthesised by MWG Biotech UK Ltd.), 200 µM of each dNTP and 5 units of *Taq* DNA polymerase. Fifteen µl of DNA samples extracted from UV irradiated tissue sections were added to each reaction. Amplification consisted of 50 cycles of 1 min at 92°C, 2 min at 37°C, a programmed ramping of 1 sec/0.1°C to 55°C, and 4 min at 55°C for polymerase extension (Zhang *et al.*, 1992). A 1 µl aliquot of the PEP product was used subsequently as the template for specific amplification.

2.11 SELECTIVE ULTRAVIOLET RADIATION FRACTIONATION - INTRODUCTION

When immunohistoselective analysis (IHSA) is used for isolating DNA from p53-positive cells, the intensity of the immunostain is an important factor for successful application of the technique. In some instances, the amount of p53 protein accumulated in the nucleus is not enough to provide sufficient protection from UV light upon staining.

The method of selective ultraviolet radiation fractionation (SURF) follows the same principles as IHSA. The protection of target cells against UV irradiation, however, is provided by ink dots placed directly on the tissue section, with each ink dot typically covering 50 to 300 cells (Shibata, 1994). This method cannot be as specific as IHSA when protecting the target cells, as a manually-applied ink dot covers a minimum of approximately 50 cells. However, it can provide better protection from UV light as the ink can fully block the passage of light. This method can be especially useful in cases in which direct comparison between microscopic phenotype and genotype is needed (Shibata, 1998).

2.12. SELECTIVE ULTRAVIOLET RADIATION FRACTIONATION - METHODS

Tissue sections for SURF were prepared in the same way as for IHSA (Section 2.8). Sectioning and immunostaining procedures were the same, with the exception that no enhancement was required during immunostaining for SURF.

Once sections were dry, 20 to 30 ink dots were applied to areas containing target cells on each section using a black, fine point, permanent marker. A "Sharpie" pen (Sanford Corporation) has been recommended (Shibata, 1998) as the ink is opaque enough to fully block the UV light, without inhibiting PCR amplification.

Ultraviolet irradiation of the sections, DNA preparation and PCR amplification were carried out as for IHSA (Section 2.8).

2.13 SEQUENCING - INTRODUCTION

Sequencing of DNA segments that showed mobility shifts during SSCP analysis was undertaken in order to confirm the presence of a mutation and determine the nucleotide change in the sequence of the DNA fragment analysed.

The sequencing method used was the thermal cycle dideoxy DNA sequencing technique based on the enzymatic chain termination method (Sanger *et al.*, 1977). As with the PCR method, thermal cycle sequencing involves the extension of a synthetic primer, annealed to the template to be sequenced by a DNA polymerase until a dideoxynucleotide (ddNTP) is incorporated. The chain-terminating ddNTPs (ddATP, ddGTP, ddCTP or ddTTP) are nucleotides that lack the 3'-OH group and therefore cannot form a phosphodiester bond with the next nucleotide. As incorporation of ddNTP is random, at the end of the reaction the mixture contains a collection of fragments of different sizes, each ending with the ddNTP present in each particular reaction (Sanger *et al.*, 1977). The amount of product DNA increases in a linear manner with the number of cycles, as the process only uses a single primer (Newton and Graham, 1997c).

Conventionally, primers or nucleotides labelled with radioactive isotopes (commonly ^{32}P, ^{33}P, or ^{35}S) are used in 4 different reactions, each containing only one of the 4 ddNTPs. The 4 sequencing reactions are run in separate but adjacent lanes in a denaturing polyacrylamide gel and bands each representing a different size fragment terminated at a different point in the sequence can be visualised by autoradiography (Slatko, 1996).

2.13.1 Automated fluorescent DNA sequencing

In fluorescent DNA sequencing, the DNA fragments produced during cycle sequencing are labelled with fluorescent dyes rather than radioactive isotopes. This has allowed automation of the DNA sequence analysis, based on automated detection of fluorescence emitted from dye-labelled DNA fragments. The fluorescent dyes are excited by an argon-ion laser scanned across a line near the bottom of the gel during electrophoretic separation in polyacrylamide gels. The emitted light is filtered, collected

and transformed into digital signals that are automatically analysed by a computer to interpret the DNA sequences (Connell *et al.*, 1987).

Fluorescent label can be incorporated into DNA fragments through dye-labelled primers or labelled ddNTP.

a)Dye-labelled primers

When using dye-labelled primers, four reactions each containing primers labelled with one of four different fluorescent dyes and one type of ddNTP are performed. A different fluorophore is paired with each ddNTP chain terminator so that the fragments produced in the separate A (green), C (blue), G (yellow), and T (red) reactions can be combined, electrophoresed in a single lane, and distinguished during electrophoresis by the colour of their fluorescence (Connell *et al.*, 1987).

b)Dye terminators

When using dye terminators, each different ddNTP is labelled with a different colour dye, so that termination and labelling occur simultaneously during cycle sequencing in a single-tube reaction (Fig. 2.13.1).

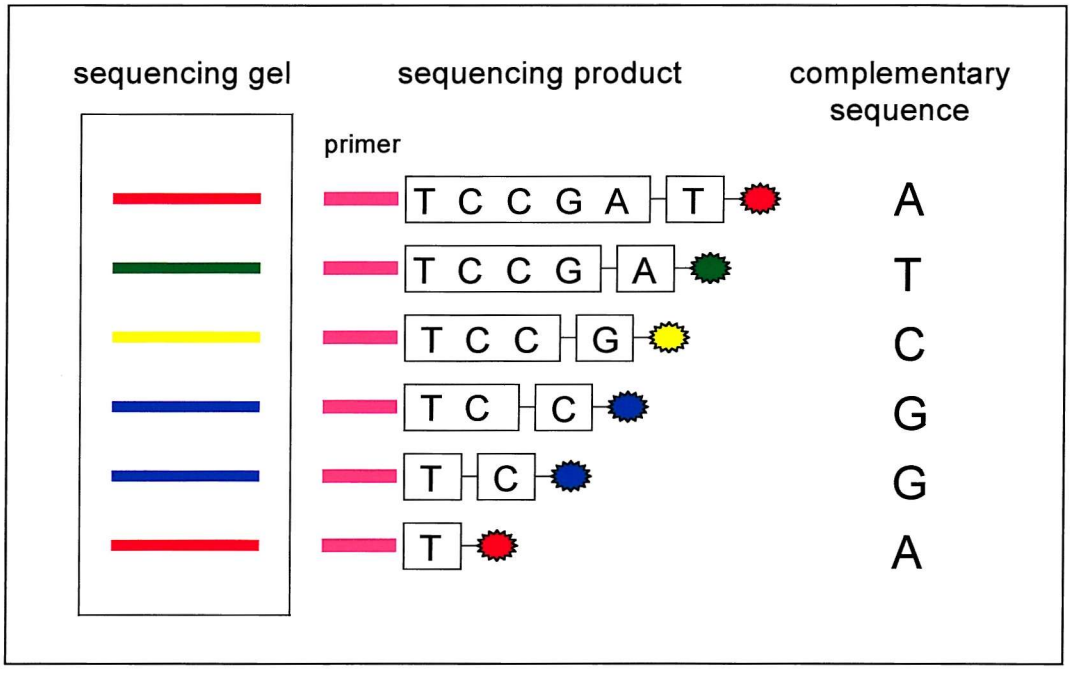

Fig. 2.13.1. Dye terminator sequencing. Unlabelled primer is used in conjunction with labelled ddNTPs so that DNA fragments randomly terminated at G, A, T, or C will be labelled with different colour dyes.

2.14 SEQUENCING - METHODS

2.14.1 Sample preparation

When sequencing of nested PCR products was required, the relevant PCR reactions were repeated using semi-nested, instead of nested primers, to ensure clear sequencing results for the whole exon, especially the beginning of the sequence. One of the problems associated with the use of dye terminator reactions is the presence of residual unincorporated dye, known as 'dye blobs', which can obscure the first 40 bases of the sequence. The method of DNA sequencing using dye terminator reactions was chosen so that the same primers used for PCR amplification could be employed, avoiding the need to have dye-labelled primers prepared especially.

The primers employed for sequencing each exon were the external F primer (Set 2, Table 2.8.1) in conjunction with the internal R primer (Set 1, Table 2.5.1) for a forward strand sequencing reaction, and the internal F primer (Set 1, Table 2.5.1) in conjunction with the external R primer (Set 2, Table 2.8.1) for a reverse strand sequencing reaction. Annealing temperatures were the same as for Set 1 primers. Table 2.14.1 shows the size of semi-nested PCR products for each exon for forward and reverse strand reactions.

Exon	Forward strand	Reverse strand
5	282	245
6	186	204
7	196	218
8	251	216

Table 2.14.1. Size of semi-nested PCR products used as template for sequencing reactions.

In order to remove any remaining primers or non-specific amplification products that could contaminate the cycle sequencing reaction, the PCR products were run in an agarose or MDE gel and then purified from the gels as described below.

2.14.1.1 DNA extraction from agarose gels

Bands containing the PCR products of interest were excised from agarose gels with a sterile scalpel blade and PCR products were purified using the Qiaquick gel extraction kit (Qiagen Ltd.) according to the manufacturer's instructions.

2.14.1.2 DNA extraction from MDE gels

Single-stranded PCR products were isolated from MDE gels using an adapted version of the 'crush and soak' method described by Sambrook *et al.* (1989). Segments containing the bands of interest were excised from the gel, transferred to microcentrifuge tubes and crushed against the wall of the tube with a sterile disposable pipette tip. The approximate volume of the excised segment was estimated and distilled water of twice that volume was added for elution. Tubes were incubated at 37°C overnight.

Samples were centrifuged at 13,000 rpm for 1 min at 4°C, then transferred carefully to a clean microcentrifuge tube, ensuring that all fragments of MDE gel were left behind. An additional 0.5 volume of distilled water was added to the MDE gel pellet, vortexed briefly and centrifuged (13,000 rpm for 1 min at 4°C). Both supernatants were then combined.

Fifty µl of 3M sodium acetate, pH5.2, and 2 volumes of ice cold 100% ethanol were added to each sample, then kept on ice for 30 min to precipitate the DNA. Tubes were then centrifuged at 15,000 rpm for 20 min at 4°C, the supernatant removed and the pellet rinsed in 400 µl ice cold 70% ethanol by carefully adding the 70% ethanol, centrifuging at 15,000 rpm for 2 min at 4°C and aspirating the supernatant.

The pellet was left to dry in air and resuspended in 6-8 µl of elution buffer (see Appendix F), depending on the number of gel segments used per tube.

2.14.2 Cycle sequencing

Cycle sequencing was performed using the Thermo Sequenase dye terminator pre-mix kit (Amersham Life Science Inc.). Each 20µl reaction contained about 200ng of dsDNA template, 20pmol of the relevant primer and 8µl of the sequencing reagent pre-mix

containing the Thermo Sequenase DNA polymerase, 1.25mM dITP, 0.25mM each dATP, dCTP, dTTP, and dye labelled ddATP, ddCTP, ddGTP, and ddTTP (see Appendix F for complete contents of sequencing pre-mix). The cycling parameters included 30 cycles of denaturation at 96°C for 30 sec, annealing of primer at 45°C for 15 sec, and extension of products at 60°C for 4 min. Cycling was performed in a Hybaid thermal cycler (Hybaid Limited).

2.14.3 DNA precipitation and preparation for gel loading

Seven µl of 7.5M ammonium acetate and 68µl of 100% ethanol at -20°C were added to each reaction tube, vortexed and placed on ice for 20 min to precipitate the DNA. The microcentrifuge tubes were then centrifuged for 15 min at 13,000 rpm at room temperature. The supernatant was drawn off carefully and 400µl of 70% ethanol at -20°C were added to wash the pellet. After brief centrifugation, the supernatant was drawn off and the pellet left to dry in air for 10-15 min.

The pellet was then resuspended in 3µl of formamide loading dye (Amersham/ Pharmacia), heated to 70°C for 3 min to denature and placed immediately on ice until loading into the sequencing gel. The samples were loaded into a denaturing polyacrylamide gel (see Appendix G.4) and electrophoresed using an Applied Biosystems DNA sequencer (Model 373A) equipped with sequence analysis software.

2.15 LOSS OF HETEROZYGOSITY - INTRODUCTION

Studies of many human tumours have shown that frequently both alleles of the p53 gene are inactivated. Usually, one allele is inactivated by point mutation and the other one by deletion (reviewed in Gottlieb and Oren, 1996). The deletion of an allele, also known as loss of heterozygosity (LOH), can be demonstrated by using Southern analysis and restriction fragment length polymorphisms (RFLP) or by using PCR (Merlo *et al.*, 1991). As Southern analysis is limited by the small amounts of normal or tumour DNA available, the use of PCR for the detection of LOH has become a popular choice (Yamaguchi *et al.*, 1997; Jones and Nakamura, 1992).

The polymerase chain reaction can detect LOH by identifying single base polymorphisms with the use of restriction enzyme digestion of the PCR product (Foulkes et al., 1993) or, more easily, by amplifying microsatellite markers from germline and tumour DNA (Koreth *et al.*, 1998). Microsatellite markers consist of mono-, di-, tri-, or tetranucleotide repeat stretches of DNA flanked by unique sequences (Thomas *et al.*, 1995). The stretches of nucleotide sequences are typically (dA-dC/dT-dG)$_n$ where n is between 15 and 30 (Koreth *et al.*, 1998).

Dinucleotide repeat sequences are very abundant and highly polymorphic (Thomas *et al.*, 1995). One such dinucleotide repeat polymorphism has been identified at the human *TP53* locus and has been used to detect LOH on chromosome 17p in a variety of cancer types (Jones and Nakamura, 1992).

Following PCR amplification of the microsatellite marker from both germline and tumour DNA, the products are electrophoresed in a polyacrylamide gel. In patients who are heterozygous (i.e. informative) for the marker used, LOH is detected when a band corresponding to one of the two tumour alleles is absent or its intensity reduced relative to the normal DNA (Jones and Nakamura, 1992). Loss of heterozygosity is very often indicated by the diminished signal of one of the two alleles rather than its complete loss, due to the presence of variable amounts of contaminating, normal cells, such as stromal and inflammatory cells, in the tumour tissue or due to cellular heterogeneity with respect to the mutation (Merlo *et al.*, 1991).

Although contamination with normal DNA may be a problem, titration experiments in different studies have shown that LOH remains detectable in the presence of 60% to 80% contaminating DNA (Thomas *et al.*, 1995; Gruis *et al.*, 1993). Nevertheless, to reduce the chance of missing LOH, samples with a minimum of 60% tumour cells should be used (Gruis *et al.*, 1993).

2.16 LOSS OF HETEROZYGOSITY - METHODS

A dinucleotide repeat polymorphism is only useful as a tool for the evaluation of LOH if that locus shows a high frequency of constitutional heterozygosity. In order to perform LOH analysis on EATL samples, primers flanking a $(CA)_{25}$ repeat at the *TP53* locus (chromosome 17p13.1), estimated to have 70% of constitutional heterozygosity (Gen Bank accession ID: GDB,191095) were used for PCR giving a 118 bp product. The sequences of the primers were derived from published sequences (Jones and Nakamura, 1992) and are shown in Table 2.16.1. For the full sequence data of the amplified PCR product with primer annealing sites see Appendix C.

2.16.1 PCR

Each PCR was carried out in 25µl of reaction buffer (Qiagen PCR buffer, 1.5 mM $MgCl_2$) containing 10 pmol of each primer (synthesised by MWG Biotech UK Ltd., see Table 2.16.1), 200 µM of each dNTP and 0.75 unit of HotStar Taq polymerase. Three hundred to 500 ng of DNA template were added to each reaction. Amplification consisted of an initial step at 95°C for 15 min for enzyme activation and DNA denaturation, followed by 35 cycles at 94°C for 30 sec, annealing at 55°C for 30 sec and extension at 72°C for 45 sec. A final elongation step at 72°C for 5 min completed the PCR. A blank control to which no DNA template had been added was included in every PCR run to ensure that no contamination had occurred.

Primer	Sequence
LOHp53 – F	5' –ACT GCC ACT CCT TGC CCC ATT C- 3'
LOHp53 – R	5' –AGG GAT ACT ATT CAG CCC GAG GTG- 3'

Table 2.16.1. Sequence of primers used for LOH analysis.

2.16.2 LOH analysis

Prior to LOH analysis, PCR products were electrophoresed in a 2.5% agarose gel (see Section 2.5.4) to ensure the presence of specific product. Amplified products were analysed by mixing 4μl of stop solution (see Appendix F) to 5μl of PCR products, denaturing for 8 min at 94°C, rapidly chilling on ice and immediately loading the samples into an MDE gel as described in Section 2.5.5. Bands were detected by silver staining as described in Section 2.5.5.

3 - RESULTS

3.1 CASES STUDIED

In total 31 cases of enteropathy-associated T cell lymphoma (EATL) were analysed. Where possible, sections of histologically uninvolved adjacent tissue (A) were analysed, as well as the tumour tissue (T). This was possible in 19 cases for which A and T paraffin blocks were available. In 10 cases only the T blocks were available and in 2 cases only the A blocks were available. In several cases, more than one T block was analysed from the same case and, in total, 68 biopsy blocks were included in the study.

3.2 IMMUNOHISTOCHEMISTRY

3.2.1 Staining for p53 protein

Immunostaining to detect p53 protein accumulation in tumour cell nuclei was performed in 31 cases. In 19 cases both T and respective A sections were analysed. In 10 cases only T sections were available for analysis. In 2 cases it was not possible to trace the blocks containing tumour tissue therefore only A sections were analysed.

Positive staining for p53 protein was detected in 24/29 (82.8%) T sections and in 5/21 (23.8%) A sections. In cases where T and respective A sections were available, 16/19 T sections (84.2%) and 5/19 (26.3%) A sections showed p53 positivity (Fig. 3.2.1).

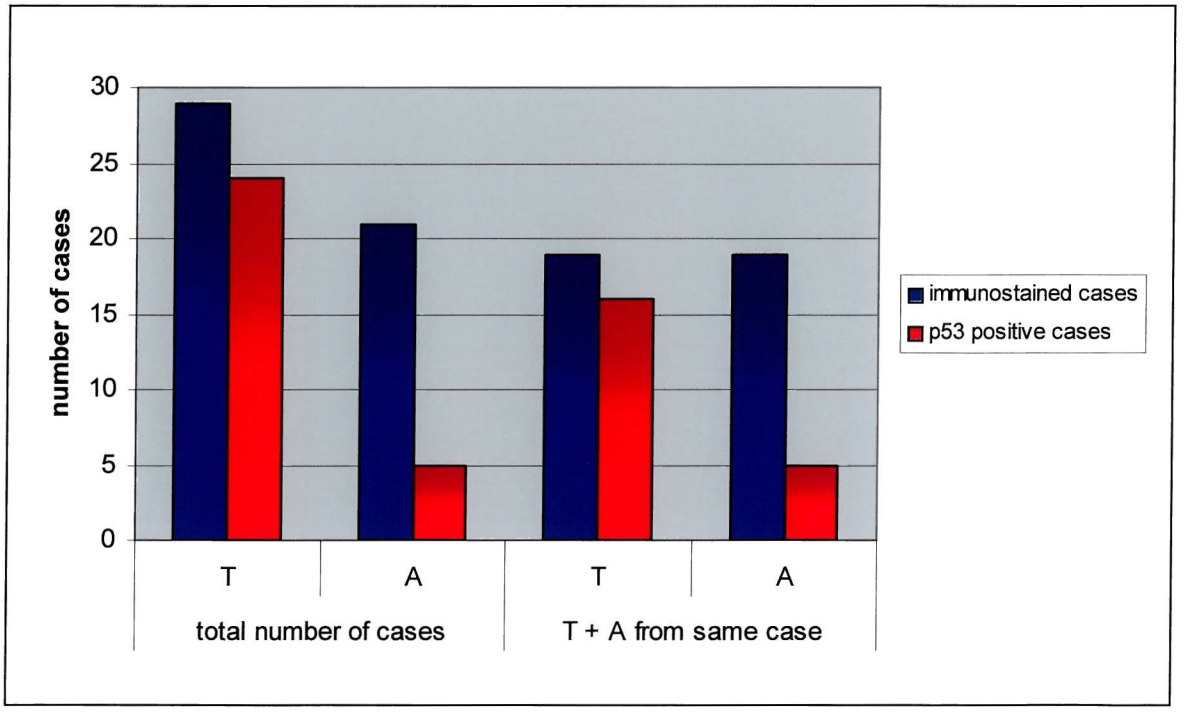

Fig. 3.2.1. p53 positivity detected in total number of T (tumour) and A (adjacent) sections, and in the subgroup of cases (n=19) where T and A sections from the same case were stained.

Positivity for p53 protein detected in different cases showed various patterns of staining. Generally p53 positive ($p53^+$) cells comprised only a proportion of cells in the tumour (Fig. 3.2.2). The proportion of $CD3^+$ tumour cells that over-expressed p53 protein varied between 2.4% and 99% and is shown later in Fig. 3.2.8.

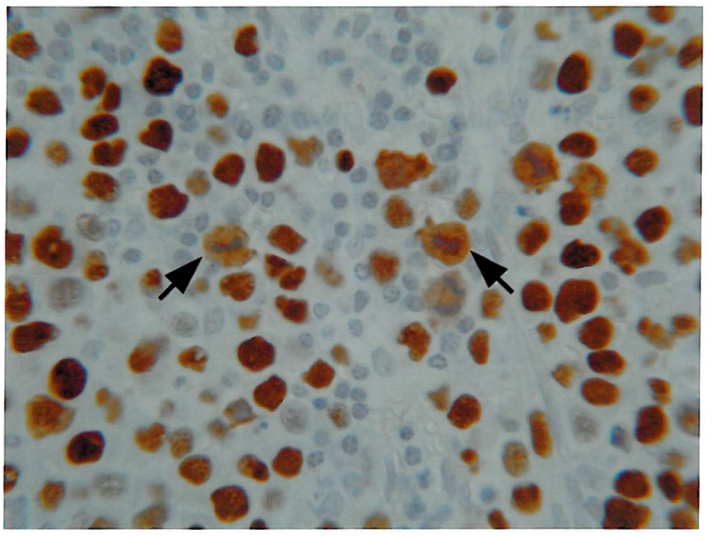

Fig. 3.2.2. Immunostaining of p53 protein in tumour. The large tumour cells show dark p53 immunostain. Dividing cells can also be seen, as indicated by the arrows (x400).

Some T sections (7/30) showed nuclear p53 staining in 70% to 99% of $CD3^+$ cells forming the tumour mass (Fig. 3.2.3, a). Tumour cells with large nuclei scattered throughout the tumour area were also observed in cases showing p53 positivity only in a proportion of cells (Fig. 3.2.3, b).

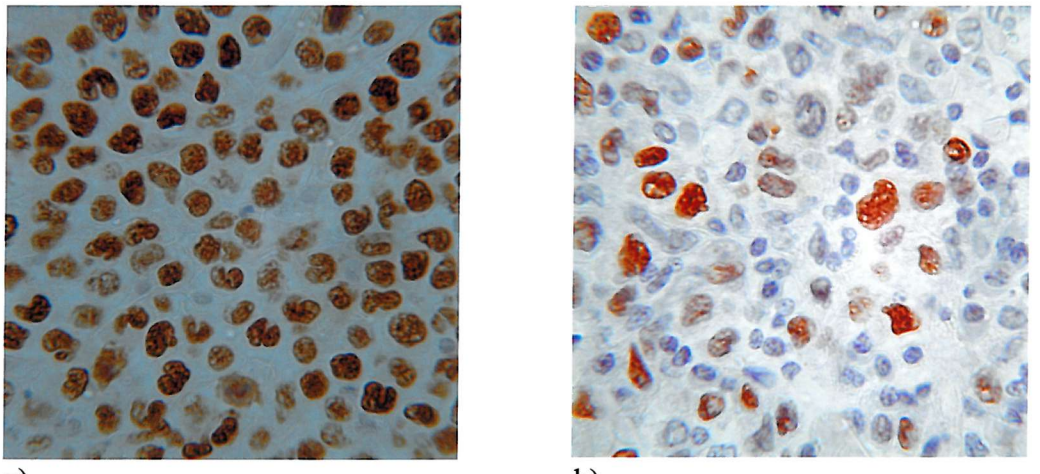

a) b)

Fig. 3.2.3. Different patterns of staining were observed in different tumour samples. (a) In some samples over 90% of tumour cells were $p53^+$ (x630); (b) in other samples only large tumour cells showed p53 positivity (x630).

In 2 cases, sections described as tumour showed an abnormal mucosa with high infiltration of IEL rather than a distinct tumour mass. These sections may represent an intermediate phase in the evolution of the disease progressing from ulcerative jejunitis to lymphoma.

In these sections, p53 positive small lymphocytes were found interspersed in the epithelial layer and in the lamina propria (Fig. 3.2.4).

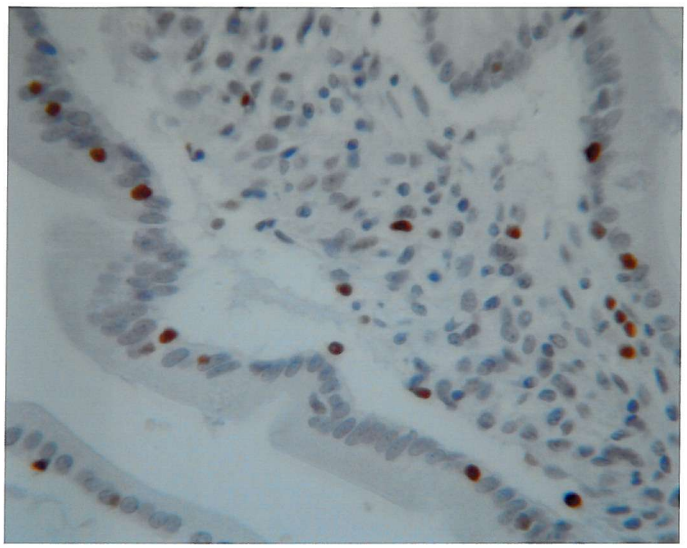

Fig. 3.2.4. Tumour section (Case 2, Sample 10) showing large number of $p53^+$ IEL as well as $p53^+$ cells in the lamina propria (x400).

The intensity of the staining also varied between cases, from dark to pale brown (Fig. 3.2.5).

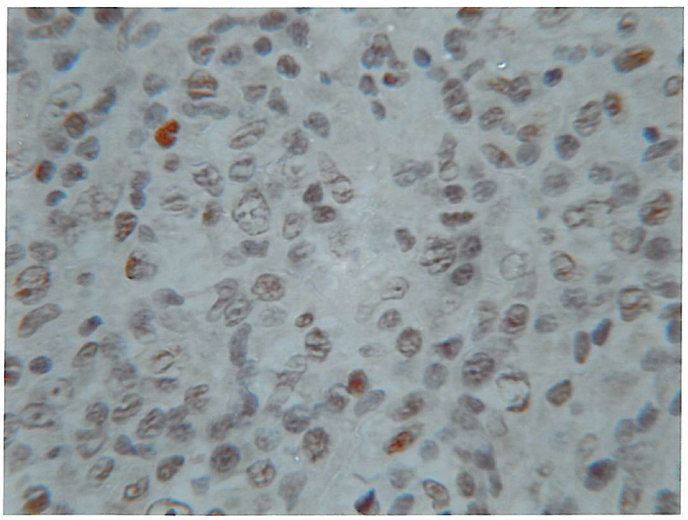

Fig.3.2.5. Large tumour cells showing pale p53 immunostaining (x630).

In A sections, p53 positive cells were usually intra-epithelial lymphocytes or lymphocytes dispersed throughout the lamina propria (Fig. 3.2.6 a, b).

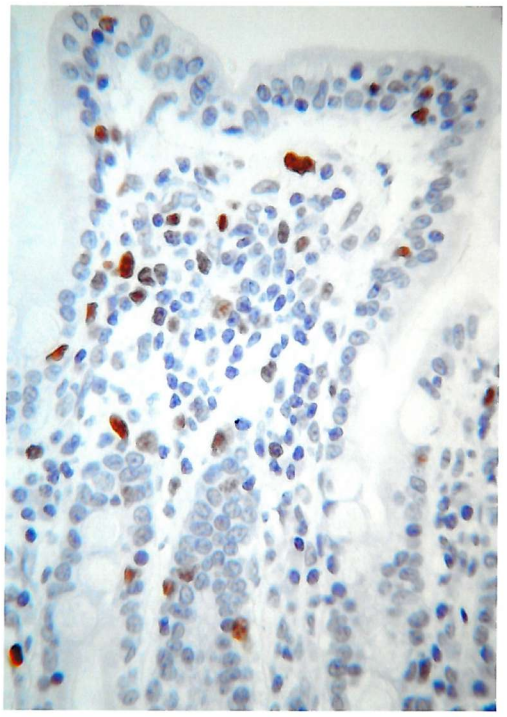

a)

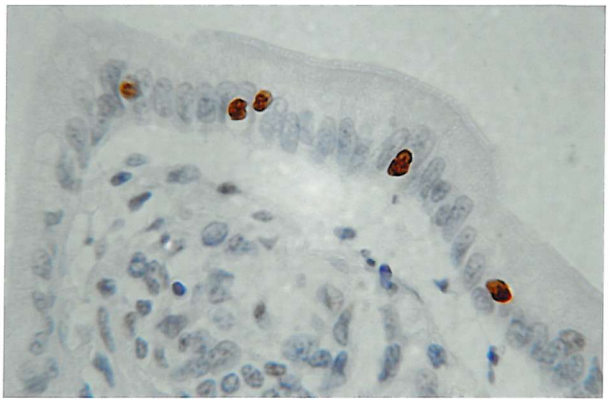

b)

Fig. 3.2.6. (a) Immunostaining of p53 protein in adjacent tissue (x400). (b) Cells showing clear IEL morphology and p53 positivity (x630).

Weak positive p53 staining was also observed in epithelial cells at the bottom of crypts of Lieberkuhn (Fig. 3.2.7). This is likely to be due to normal p53 expression in proliferating cells, which can be detected as a result of increased sensitivity of p53 immunoreactivity following microwave antigen retrieval (Dowell and Ogden, 1996).

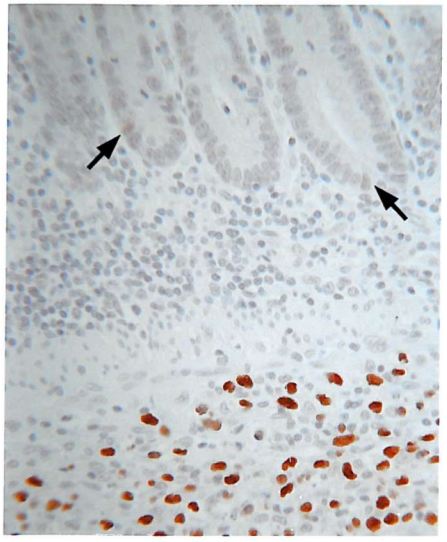

Fig. 3.2.7. Weak p53 immunostaining in intestinal crypts was frequently observed (arrows). Positivity due to p53 over-expression was usually stronger, as seen in the tumour mass below (x250).

The graphs below show the proportion of $CD3^+$ cells that showed p53 positivity in the cases studied, in T sections (Fig. 3.2.8) and in the epithelium (Fig. 3.2.9 a) and lamina propria (Fig. 3.2.9 b) in A sections. Calculations are based on cell counts done on separate serial sections immunostained for p53 and CD3. The method used for cell counting is described in Appendix I.1. The mean values (±S.E.) of cell counts can be found in Appendix D, Tables D.1, D.3 and D.4.

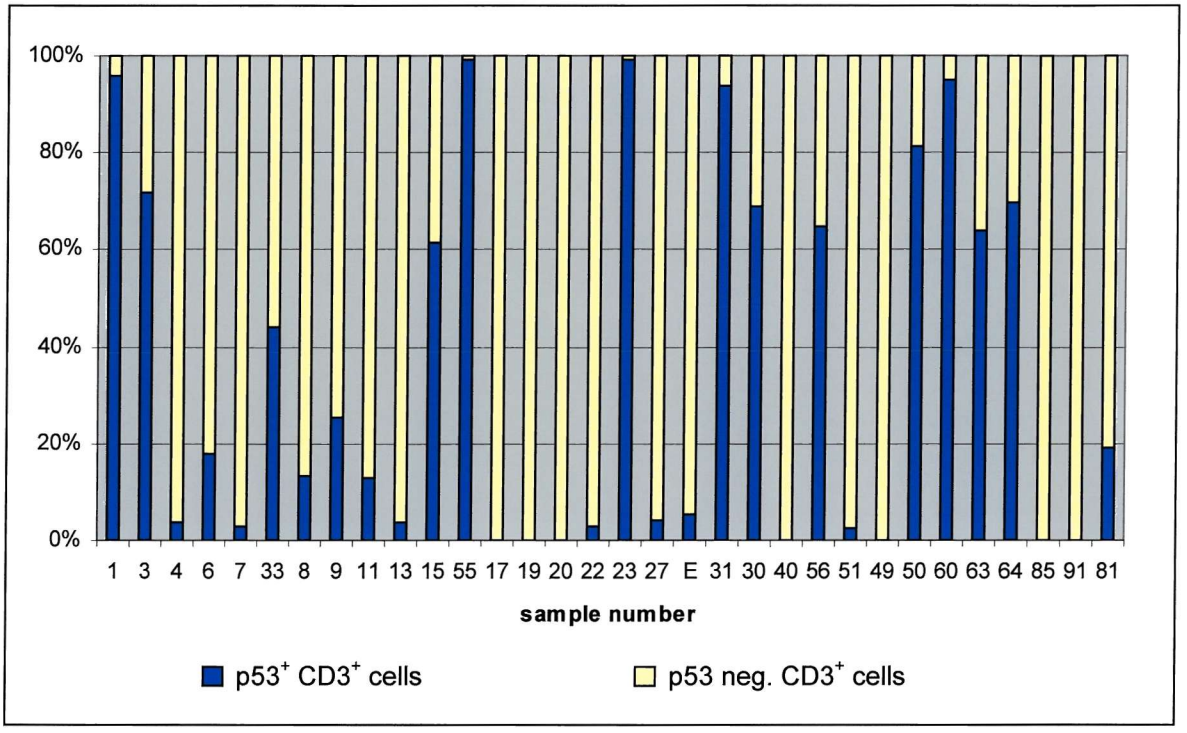

Fig. 3.2.8. Proportion of CD3+ tumour cells that are also positive for p53.

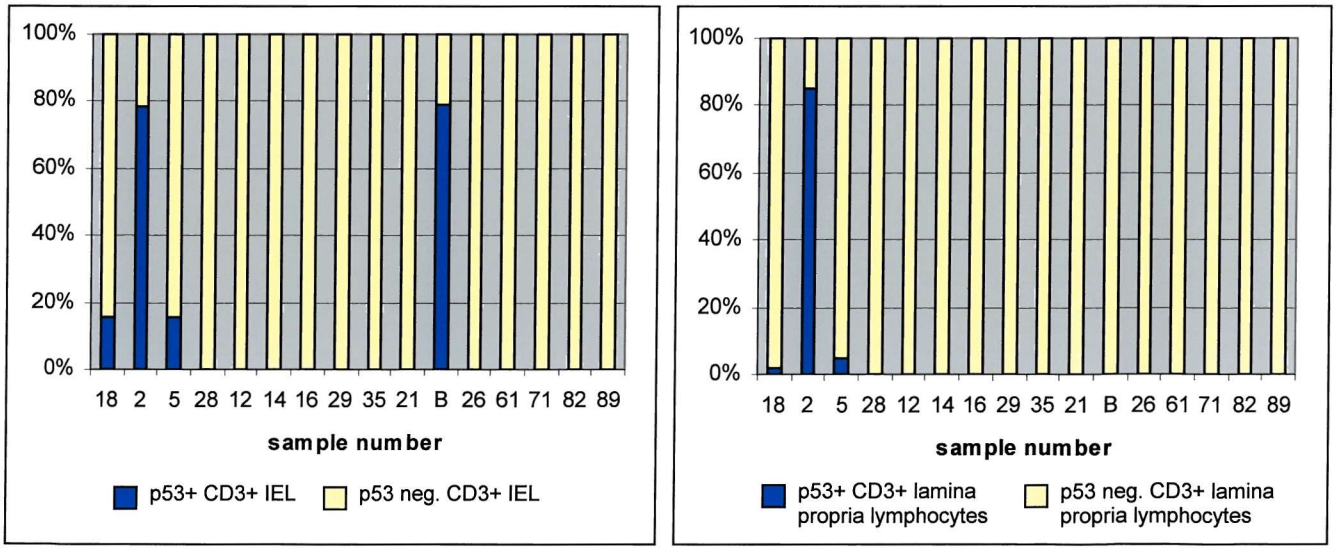

a) b)

Fig. 3.2.9. Proportion of (a) $CD3^+$ IEL and (b) $CD3^+$ lamina propria cells that are also p53 immunopositive in A sections.

Although in 7 T sections p53 positivity was only observed in 2.4% to 5.6% of tumour cells, these sections were scored as positive as the stain was strong and clearly associated with large tumour cells.

Positive staining for p53 was observed in A sections in 5 cases (only 4 are represented on Figures 3.2.9 a and 3.2.9 b, as the CD3 immunostained section for the fifth case could not be evaluated). Positivity for p53 in A sections did not seem to be associated with the proportion of p53 positive cells in T sections. While for 2 A sections (samples 18 and 2), p53 positivity in the respective T sections (samples 1 and 3) was greater than 70%, for the remaining p53 positive A sections [samples 5, 'B' and 80 (not shown)], T sections (samples 6, 'E' and 81, respectively) showed less than 20% p53 positive cells.

Biopsy tissue sections from normal intestine and uncomplicated coeliac disease were immunostained for p53 as controls (n=6). No p53 staining was observed in any of the controls (Fig. 3.2.10 a, b), confirming previous results obtained in the department (Murray *et al.*, 1995).

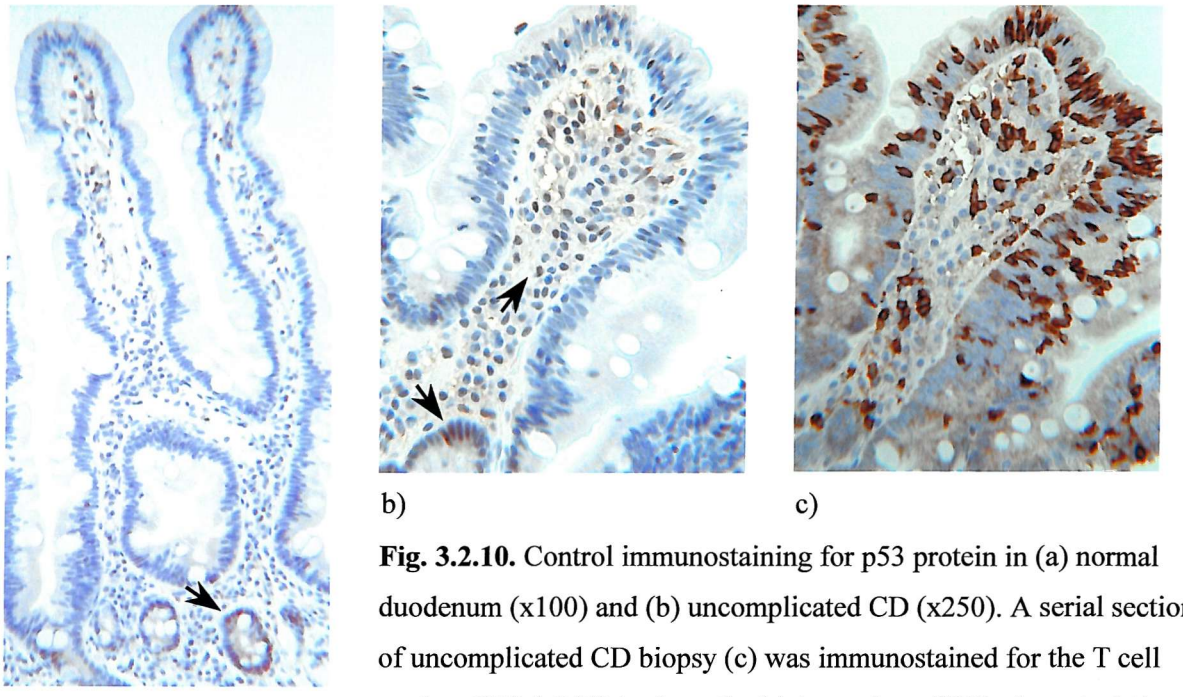

a) b) c)

Fig. 3.2.10. Control immunostaining for p53 protein in (a) normal duodenum (x100) and (b) uncomplicated CD (x250). A serial section of uncomplicated CD biopsy (c) was immunostained for the T cell marker CD3 (x250) to show the high number of IEL characteristic of CD. Despite the increased number of IEL, no p53 overexpression was detected in uncomplicated CD. Background levels of p53 expression were observed in stromal and crypt cells in both normal duodenum and uncomplicated CD (arrows).

3.2.2 Staining for retinoblastoma protein (pRB)

Immunostaining to detect pRB accumulation in tumour cell nuclei was performed in 30 EATL cases using NCL-RB antibody (clone 1F8, Novocastra Laboratories Ltd.). In 19 cases both T and respective A sections were analysed. In 10 cases only T sections were available for analysis and in 2 cases only blocks containing uninvolved resection margin tissue could be traced.

The retinoblastoma protein is involved in cell-cycle control, negatively regulating cell growth through gene transcription regulation. It is generally accepted that it is ubiquitously expressed in human normal tissues (Cordon-Cardo and Richon, 1994) and normal and stimulated peripheral blood lymphocytes analysed on cytospin preparations show a gradual increase of pRB during progression through the cell cycle with a peak in the mitosis phase (Martinez *et al.*, 1993).

Nuclear pRB staining was observed in tumour cells and in epithelial and lamina propria cells. Epithelial cells showed pale staining, decreasing in intensity towards the tip of the villi. All cases showed pRB positivity in T sections with the proportion of pRB^+ $CD3^+$ cells varying between 10% and 99% (Fig. 3.2.13). The data used to generate Fig. 3.2.13, including mean values ±S.E., can be found in Appendix D, Tables D.1 and D.3. The intensity of staining also varied between sections analysed with 39% of T sections showing medium to strong immunostain (Fig. 3.2.11) and 61% showing weak immunostain in tumour cell nuclei (Fig. 3.2.12).

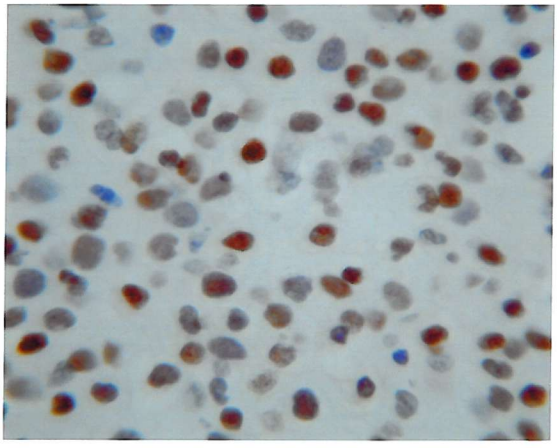

Fig. 3.2.11. Strong pRB positivity in tumour cells (x630).

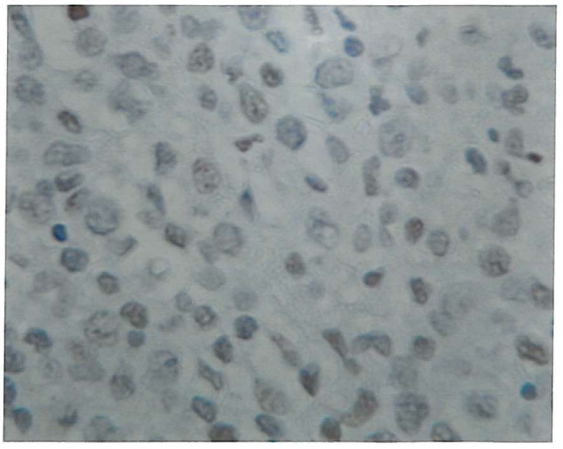

Fig. 3.2.12. Weak pRB positivity in tumour cells (x630).

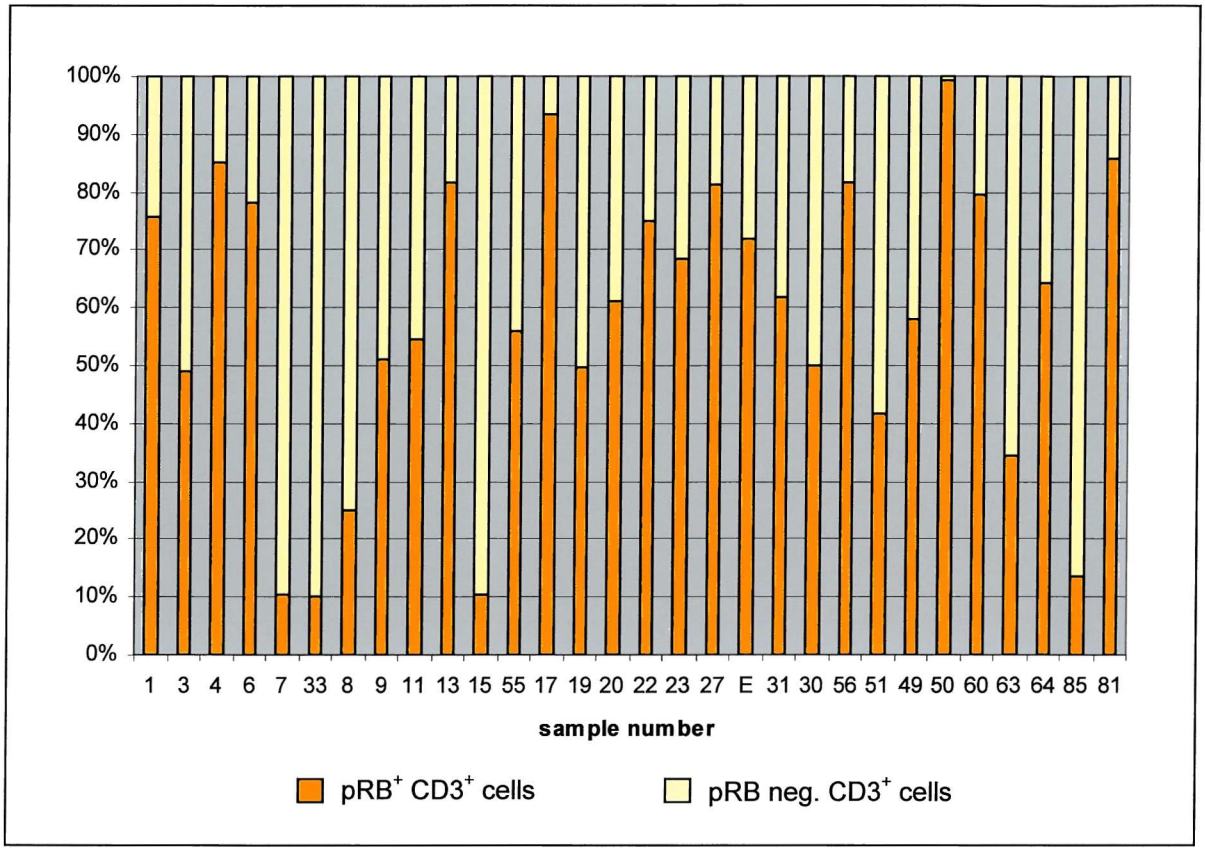

Fig. 3.2.13. Proportion of $CD3^+$ cells in T samples that showed pRB protein expression.

Positivity for pRB was more difficult to assess in A sections. Out of 20 A sections, 45% showed pRB^+ IEL (Fig. 3.2.14). In 55% of A sections the intensity of the immunostain over the whole section was too weak to allow accurate counting of positive IEL. As IEL nuclei usually counterstain in a darker shade of blue than enterocyte nuclei, very pale pRB^+ immunostain was difficult to identify in IEL nuclei, even though enterocyte nuclei were pRB^+. Positivity for pRB could not be assessed in lamina propria cells either, due to the general weakness of the staining.

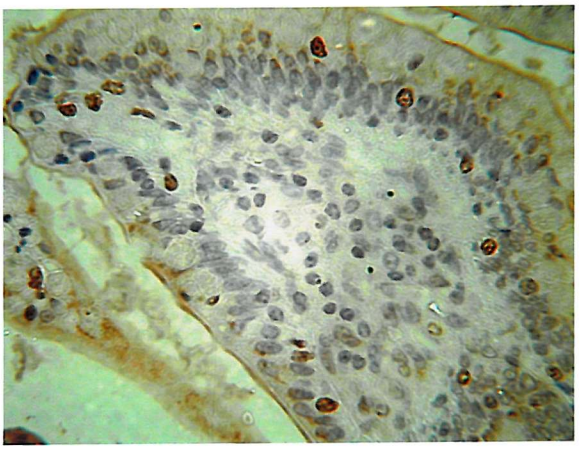

Fig. 3.2.14. pRB positive IEL in A section (x400).

The proportion of $CD3^+$ IEL that were also pRB^+ in A sections is shown in Fig. 3.2.15. Only samples showing pRB positivity were included in this graph. One A section containing pRB^+ IEL was not included, as the CD3 immunostained section for this case could not be evaluated. The data used for this graph, including mean values ±S.E., can be found in Appendix D, Tables D.1 and D.4.

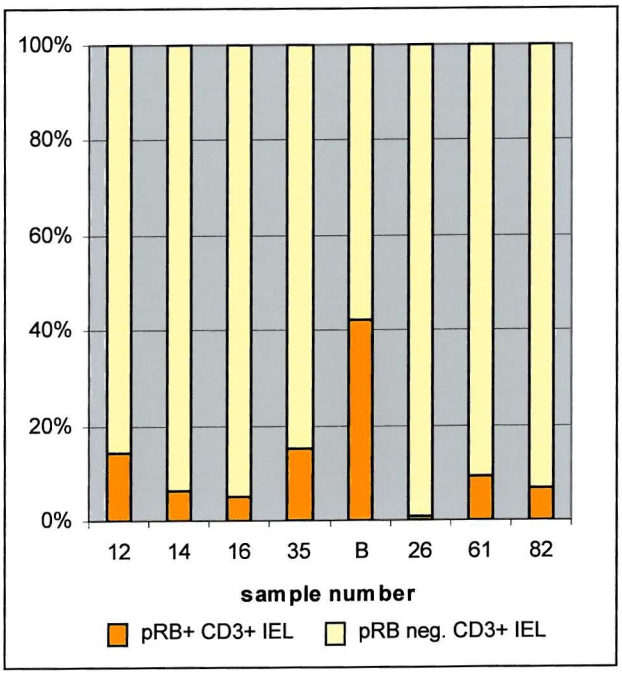

Fig. 3.2.15. Proportion of $CD3^+$ IEL in A samples that showed pRB positivity.

In order to correlate the staining results obtained for p53 and pRB proteins, the proportion of $p53^+$ cells was plotted against the proportion of pRB^+ cells recorded for each T section and is shown in Fig. 3.2.16. The data used for this scattergram can be found in Appendix D, Table D.1.

Figure 3.2.16 seems to show a very slight increase in the proportion of pRB^+ cells with an increase in $p53^+$ cells. However, the very low correlation coefficient (R^2=0.065) indicates that this correlation is very weak. It is also possible to see that low p53 expression or lack of it has no effect on pRB expression, which showed a range of expression between 5% and 67% in T sections expressing less than 3% of $p53^+$ cells.

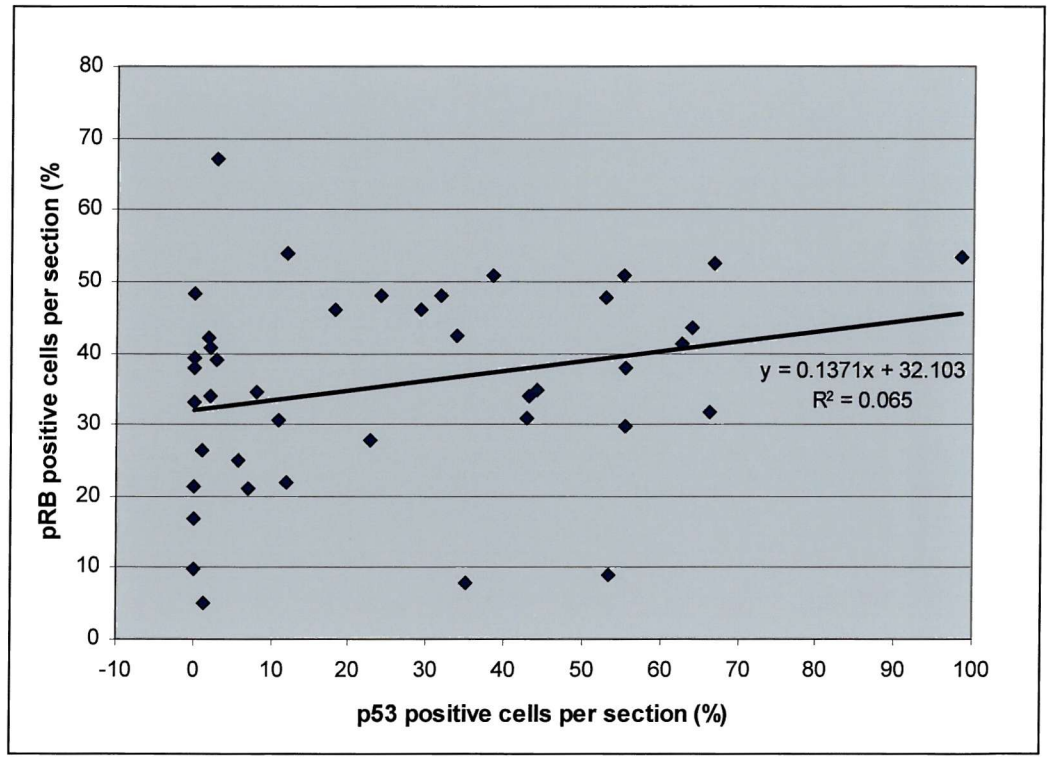

Fig. 3.2.16. Scattergram derived from plots of percentages of $p53^+$ cells in each T section against the respective proportion of pRB^+ cells.

3.2.3 Staining for MDM2 protein

The antibody (clone 1B10, Novocastra Laboratories Ltd.) reactive with MDM2 protein shows a nuclear pattern of staining. The MDM2 protein is constitutively expressed by normal cells, albeit at a level that is not normally detectable by standard immunohistochemical techniques such as the one used in this study. Repeated immunohistochemical staining of EATL sections showed specific immunopositive cells in the epithelium, in the lamina propria and in the tumour mass (Fig. 3.2.17) in 46/47 sections analysed from 27 cases. The proportion of MDM2 positive cells observed is demonstrated in Fig. 3.2.18. MDM2 positivity was observed as pale nuclear stain in 80%-100% of epithelial cells. Lamina propria MDM2 positive cells generally showed a darker nuclear stain than epithelial cells (Fig. 3.2.19).

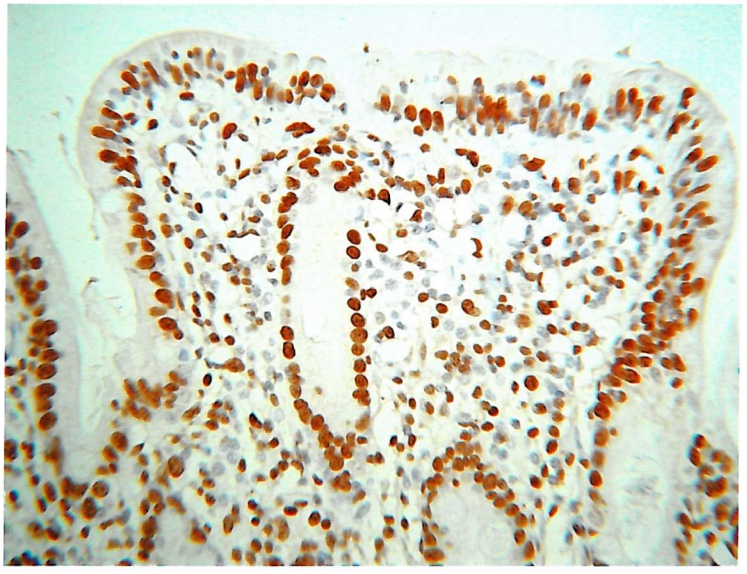

Fig. 3.2.17. Immunostaining for MDM2 protein on EATL (x250).

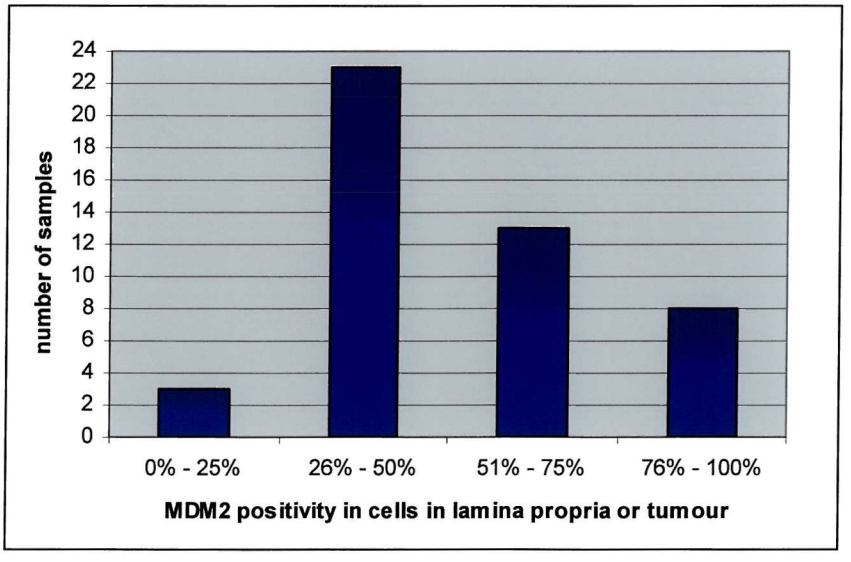

Fig. 3.2.18. MDM2 positivity observed in samples analysed.

As positive staining for MDM2 protein indicates over-expression of the protein, MDM2 immunopositivity would not be expected in enterocytes of the intestinal epithelium. In order to ensure that no non-specific reactivity was occurring with endogenous molecules at any stage of the immunohistochemical method used, the following experiment was performed.

The immunohistochemical method was applied to 6 sets of tissue sections (as in Section 2.3.2) with the modifications described below. Each set consisted of 4 sections: one section of breast carcinoma tissue as a positive control, 2 sections of intestinal mucosa that had previously been shown to have MDM2 positive staining and one section of human tonsil as a negative control. For each set of sections a different stage of the method was omitted, as follows:

1- No pre-incubation with 1% BSA (blocking agent for non-specific protein binding).
2- No primary antibody.
3- No secondary antibody.
4- No streptavidin-biotin complex solution.
5- Serum control, i.e. 1% BSA was added instead of primary and secondary antibody.
6- Normal control, i.e. no alteration to the original method.

The results of this experiment showed no positive immunostaining in sets 2 to 5 in any of the tissues tested. Positive staining was observed in all tissues tested in sets 1 and 6, including the negative control (Figures 3.2.19 and 3.2.20).

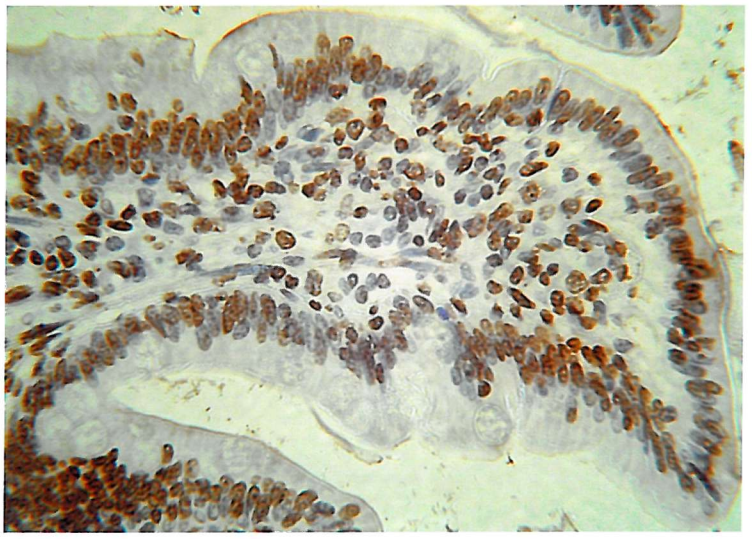

Fig. 3.2.19. Reactivity of antibody against MDM2 protein in EATL (x400). Epithelial and lamina propria cells still showed positive staining after incubation with 1% BSA to block non-specific protein binding.

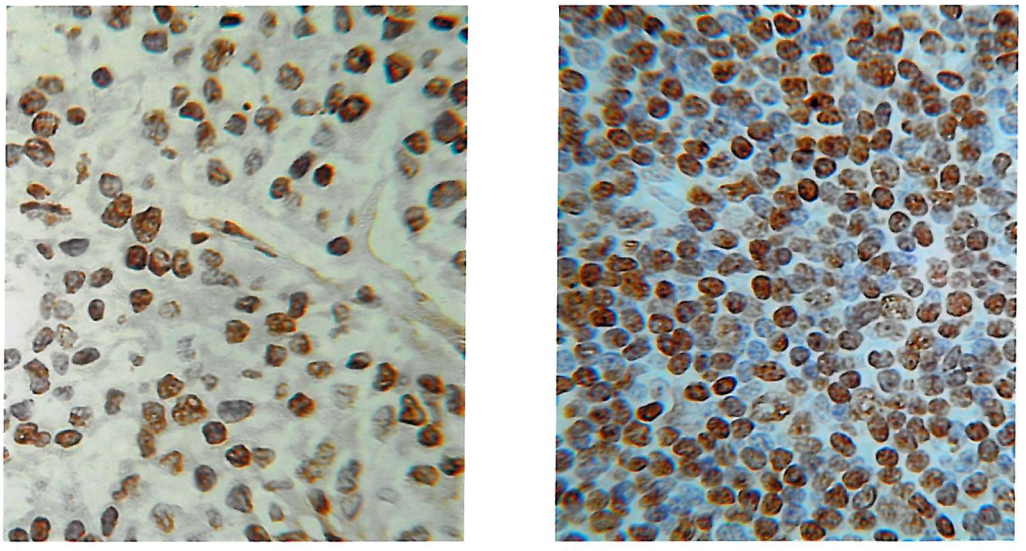

a) b)

Fig. 3.2.20. MDM2 immunostaining of test tissues. (a) Positive staining was obtained in the positive control tissue (breast carcinoma, x400), but also in (b) the negative control tissue (normal human tonsil, x630).

It can be seen that the pattern of staining obtained with this antibody would not allow the detection of genuine nuclear over-expression of the MDM2 protein, since normal, constitutive expression was demonstrated. Therefore, immunohistochemistry did not provide a method for correlating potential MDM2 over-expression with the accumulation of the p53 and pRB proteins in the nuclei of cells. Consequently no further analysis was undertaken using MDM2 immunostaining.

3.2.4 Staining for CD3

The CD3 antibody (clone PS1, Novocastra Laboratories Ltd.) binds the epsilon chain of human CD3 that is associated with the T cell antigen receptor complex present on T cell membranes.

Intra-epithelial T lymphocytes expressing CD3 were observed in all sections analysed. CD3 positive T cells were also observed in the tumour mass in all T sections analysed. Fig. 3.2.21 shows the distribution of CD3 positive IEL and lamina propria T cells of the intestinal mucosa in an A sample. It is possible to observe the membrane staining obtained with this antibody at the higher magnification shown in Fig. 3.2.21 b (arrows).

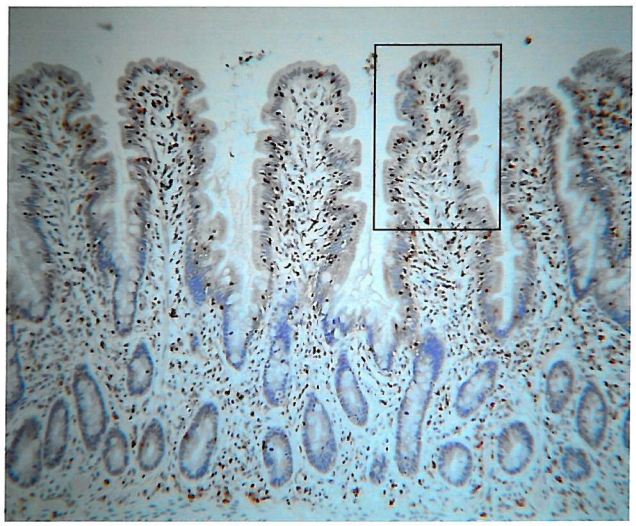

a)

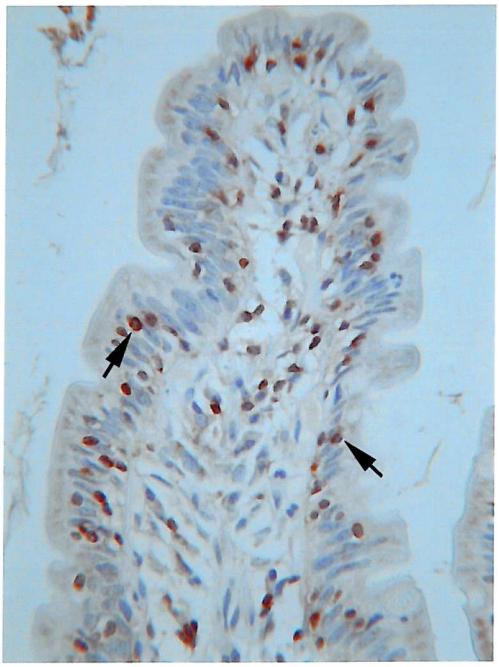

b)

Fig. 3.2.21. (a) Distribution of CD3 positive T lymphocytes in the epithelium and lamina propria in the intestinal mucosa of an A sample (x100). (b) Highlighted area is shown at higher magnification (x400). Arrows indicate lymphocytes showing clear membrane stain.

A comparison between immunostaining for CD3 and for p53 protein, using sections from the same block (A sample), indicates that only a proportion of IEL and lamina propria T lymphocytes are p53 positive (Fig. 3.2.22). This has been demonstrated graphically in Figures 3.2.8 to 3.2.10 for T and A sections analysed.

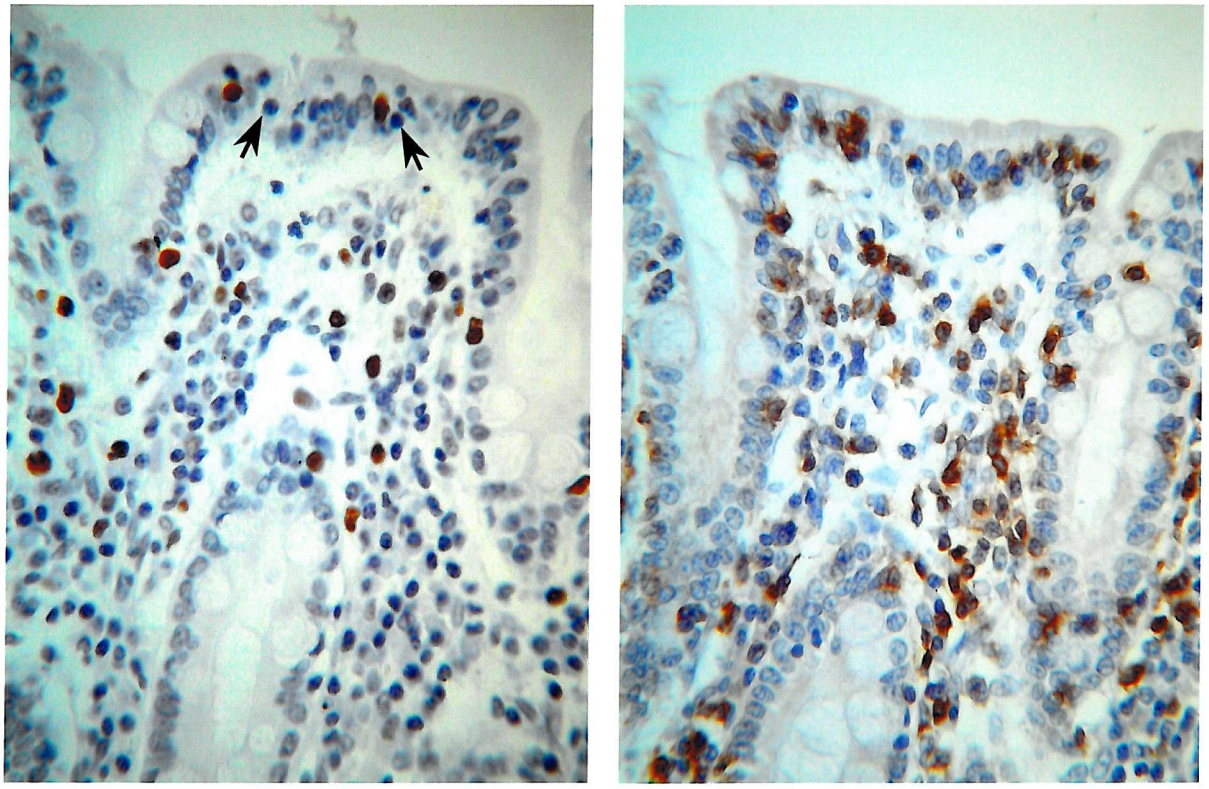

a) b)

Fig. 3.2.22. Comparison between immunopositivity for p53 (a) and CD3 (b) in the same area of an A section of EATL (x400). Arrows indicate p53-negative IEL.

3.2.4.1 Comparison between CD3 and CD8 positivity in EATL cases

It has been shown recently that simple comparative immunohistochemical studies using anti-CD3 and anti-CD8 antibodies on paraffin sections can distinguish active CD from refractory sprue (Patey-Mariaud de Serre *et al.*, 2000). Refractory sprue (RS), like CD, is characterised by severe malabsorption and total or severe duodenal villous atrophy, without evidence of lymphoma. However, unlike CD, it fails to improve after 6 months on strict gluten-free diet (Patey-Mariaud de Serre *et al.*, 2000, Trier *et al.*, 1978). In normal intestine and untreated coeliac disease most IEL are $CD3^+$ $CD8^+$. However, in RS abnormal intra-epithelial T lymphocytes were reported to express cytoplasmic CD3 (CD3c), lacking surface CD3 and CD8 expression (Patey-Mariaud de Serre *et al.*, 2000).

In order to assess if any of the EATL cases analysed showed phenotypically abnormal T lymphocytes that could be associated with origin from a background of refractory sprue, slides immunostained with anti-CD8 antibodies were retrieved from archival stores to compare with the respective CD3 stained slides (Fig. 3.2.23). Both CD3 and CD8 immunostained A sections were available for 17 cases and the results are shown in Figures 3.2.24 and 3.2.25. The percentage of IEL positive with either antibody was determined by counting the number of positive lymphocytes per 100 epithelial cells. Four hundred enterocytes were counted on the surface epithelium in each case.

The mean number of $CD3^+$ and $CD8^+$ IEL recorded was similar in 65% of cases (n=17). A marked reduction in IEL expressing CD8 in comparison to CD3-expressing IEL was observed in 3 cases (Case 5, 22 and 27). Case 22 showed not only a discrepancy between CD3 and CD8 expressing IEL, but also a very high number of $CD3^+$ IEL (178±11 IEL per 100 epithelial cells) in comparison to the other cases (between 8±1 IEL per 100 epithelial cells and 63±19 IEL per 100 epithelial cells). A reduced number of CD8 expressing IEL was also recorded in 2 additional cases (Cases 4 and 6). The decrease observed, however, was not as great as for cases 5, 22 and 27. The data used to generate Figures 3.2.24 and 3.2.25 is presented in Appendix D, Table D.2.

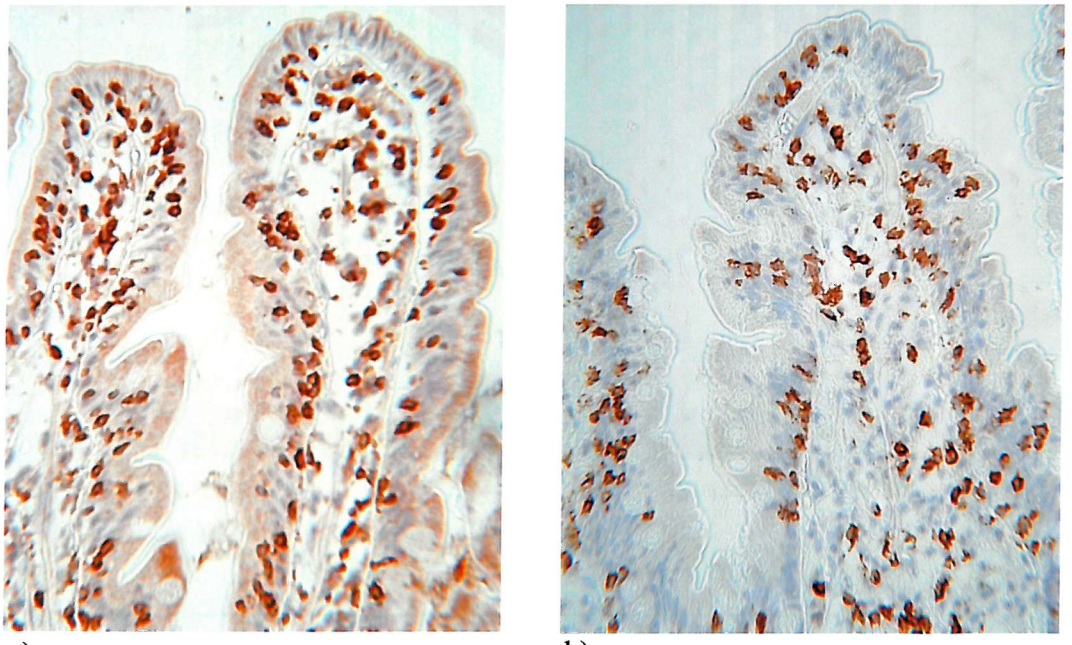

a) b)

Fig. 3.2.23 . Immunostaining for (a) CD3 and (b) CD8 of A sections from the same case (Case 7) (x250). A similar proportion of positive cells (approximately 30 positive IEL per 100 epithelial cells) was observed in both sections for this case.

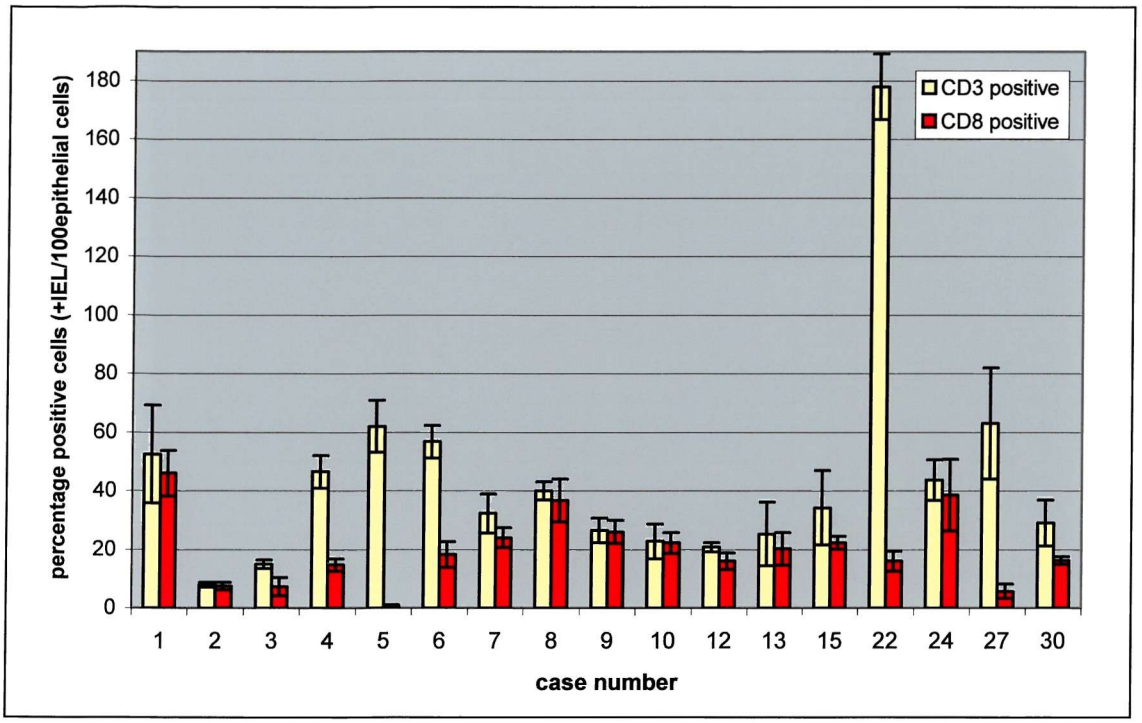

Fig. 3.2.24. Mean number (± SD) of $CD3^+$ and $CD8^+$ IEL in intestinal mucosa of EATL cases.

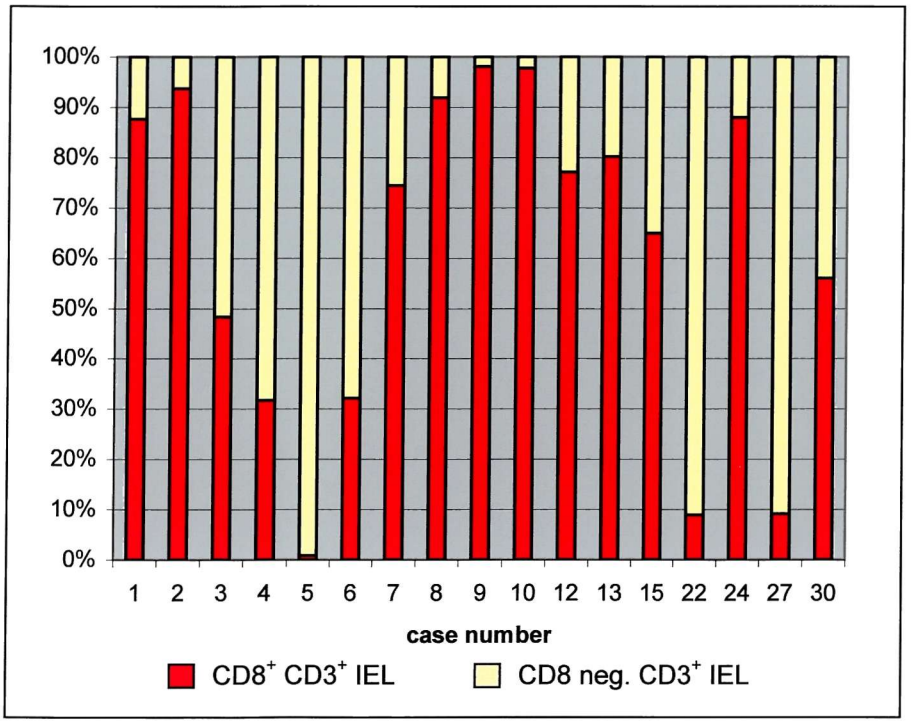

Fig. 3.2.25. Proportion of $CD3^+$ IEL that also express CD8 in EATL cases studied.

3.2.5 Summary

Immunohistochemical analysis of EATL cases detected p53 over-expression in a large proportion (83%) of tumour sections, but only in 24% of adjacent tissue sections.

The retinoblastoma gene that encodes the pRB protein is referred to as a tumour suppressor gene since its inactivation appears to be causally related to cancer. Loss or functional inactivation of the gene product due to alterations in the pRB gene structure have been observed in human tumours, such as small cell lung carcinomas, breast cancers, osteogenic sarcomas, leukemias, prostate and bladder carcinomas and malignant gliomas (reviewed in Paggi *et al.*, 1996).

Immunohistochemical and molecular studies on retinoblastoma gene expression in high-grade nodal peripheral T cell lymphomas (Pescarmona *et al.*, 1999) have detected loss of pRB expression in 10/45 (22%) of cases analysed, indicating the presence of abnormalities of pRB gene expression at either the transcriptional or post-transcriptional level. The expression of p53 was also investigated by immunohistochemical analysis in the same cases and the results showed that p53-positive cases (9/45) were also pRB-positive, and all pRB-negative cases were also p53-negative. These results suggest that there may be two different and mutually exclusive pathways of possible pathogenetic significance in high-grade nodal peripheral T cell lymphomas, involving abnormalities associated with either the p53 protein or the pRB protein (Pescarmona *et al.*, 1999).

The detection of pRB expression in tumour cells of all EATL sections analysed indicated the presence of functional pRB protein. This increased pRB expression is consistent with a growth inhibitory cellular response to neoplastic growth (Martinez *et al.*, 1993). The results obtained suggest that pRB gene alterations are not involved in tumour formation in the EATL cases studied.

Weak positivity for pRB was observed in 61% of T sections. In A sections, pRB positivity could not be assessed in IEL in 55% of sections, or in the lamina propria in 100% of sections, due to the weakness of the staining of lymphocytes as well as of epithelial cells. The manufacturers (Novocastra Laboratories Ltd.) of the antibody (NCL-RB) used have since acknowledged the poor performance of this antibody and have brought out a new, more effective antibody (NCL-RB-358) reactive with pRB protein. Immunohistochemical

analysis of the same series of cases using the new antibody could provide important results to compare with the data presented here.

The antibody against MDM2 protein could not be included in the analysis, as it seemed to recognise and bind to other molecules besides MDM2. MDM2 over-expression could therefore not be assessed and correlated with p53 immunostain results.

In order to confirm whether the pattern of staining obtained with this antibody is specific or not, additional analyses are necessary. The use of an alternative antibody of proven specificity against MDM2 and comparison with MDM2 staining results obtained previously may provide an indication of how specific the original antibody is. Additionally, molecular analyses, such as Western blotting, could be used to verify the specificity of the MDM2 antibody used in this study. Further discussion is presented in Section 4.2.

It has been suggested that refractory sprue (RS), a disorder believed to be related to CD, is a form of cryptic T cell lymphoma (Cellier *et al.*, 2000; Carbonnel *et al.*, 1998) and that RS is associated with an abnormal subset of IEL (Cellier *et al.*, 1998). Immunophenotypically aberrant clonal intraepithelial T cell populations, similar to that of most cases of EATL ($CD3c^+$, $CD8^-$, $CD4^-$; Bagdi *et al.*, 1999), were found in up to 75% of patients (n=17) with RS. In addition, the aberrant IEL population was shown to precede the onset of overt T cell lymphoma in 3 patients (Cellier *et al.*, 2000).

Out of the cases for which sections stained with anti-CD8 antibodies were available, it was observed that at least 3 cases (Case 5, Case 22 and Case 27) showed the presence of phenotypically abnormal T lymphocytes virtually lacking CD8 expression. These results indicate that, in the 3 cases above, EATL may have originated from a background of RS, in keeping with the suggestion that monoclonal IEL populations observed in patients with complications of CD, such as RS and ulcerative jejunitis, are neoplastic, even though they are not cytologically abnormal and do not form tumour masses (Bagdi *et al.*, 1999).

3.3 DNA EXTRACTION

The extraction of DNA was performed successfully using tissue sections cut from nearly all paraffin blocks used. An extraction was considered unsuccessful when PCR amplification of the p53 gene exons generated undetectable or barely detectable amounts of product after electrophoresis in an agarose gel subsequently stained with ethidium bromide. DNA extraction was successful for 97% of the blocks used (n=68). DNA extraction failed with tissues from 2 blocks, one 14 years old and the other 7 years old at the time of extraction.

The DNA concentration of the samples was determined by spectrophotometry and ranged between 0.18 μg/μl and 0.96 μg/μl, with about 66.2% of samples having values between 0.32 μg/μl and 0.67 μg/μl. In general, concentration of DNA from analysed samples was within a range that did not compromise the efficiency of PCR amplification, i.e., there was enough template of sufficient length for successful amplification, without the undesired effect of PCR inhibitors. Samples containing high DNA concentration may fail PCR amplification due to PCR inhibitors, also present at a higher concentration.

Samples showed purity values ranging between 0.90 and 1.50, with 79.4% of samples between 1.10 and 1.39. The calculation to obtain purity values is described in Appendix I.2. Although 1.8 is the value for a pure sample, the lower purity values obtained in the samples analysed did not seem to be a problem since PCR amplification was successful in most cases.

Only one sample (no. 27) showed a low purity value of 0.90 and was one of the two that failed DNA extraction. The other sample (no. 25) was 14 years old and prolonged storage could have been responsible for a higher degree of DNA degradation. Table 3.3.1 below shows the DNA concentration and purity of all the samples analysed.

Sample	DNA (μg/μl)	Purity A_{260}/A_{280}	Sample	DNA (μg/μl)	Purity A_{260}/A_{280}	Sample	DNA (μg/μl)	Purity A_{260}/A_{280}
1	0.60	1.43	29	0.56	1.24	39	0.50	1.16
18	0.90	1.29	35	0.38	1.15	47	0.32	1.14
2	0.33	1.18	19	0.66	1.25	49	0.18	1.00
3	0.50	1.06	20	0.67	1.18	50	0.93	1.45
10	0.49	1.20	41	0.44	1.13	25	0.28	1.08
4	0.36	1.06	42	0.33	1.00	60	0.72	1.36
5	0.38	1.09	21	0.61	1.15	61	0.44	1.13
6	0.42	1.17	22	0.55	1.22	63	0.55	1.20
7	0.87	1.07	23	0.61	1.11	64	0.71	1.39
24	0.46	1.15	27	0.28	0.90	65	0.48	1.33
33	0.28	1.17	B	0.33	1.50	66	0.44	1.25
28	0.54	1.26	E	0.43	1.26	68	0.19	1.04
8	0.96	1.32	I	0.55	1.31	70	0.41	1.40
54	0.85	1.24	26	0.79	1.18	71	0.70	1.36
9	0.82	1.24	32	0.65	1.14	84	0.30	1.14
11	0.67	1.20	34	0.75	1.25	85	0.44	1.13
12	0.88	1.20	36	0.42	1.17	80	0.31	1.16
13	0.75	1.34	30	0.36	1.12	81	0.39	1.21
14	0.36	1.13	56	0.37	1.06	82	0.53	1.19
15	0.73	1.33	37	0.55	1.28	83	0.43	1.13
55	0.76	1.22	51	0.62	1.32	89	0.50	1.37
16	0.47	1.12	38A	0.58	1.23	91	0.85	1.35
17	0.34	1.10	40	0.32	1.10			

Table 3.3.1. DNA concentration and purity of samples analysed.

3.4 PCR

Polymerase chain reaction amplification of exons 5-8 of the p53 gene was performed using samples of DNA extracted from all 68 tissue blocks used. However, before specific and efficient amplification of the desired segments could be achieved, optimisation of the PCR was required for each pair of primers used.

3.4.1 Preliminary work

Specific amplification of target DNA is a crucial factor in PCR-SSCP analysis, as a non-specific PCR product present in the sample could be misinterpreted as a mobility shift of the analysed sample in a SSCP gel.

3.4.1.1 Optimisation of the PCR (I)

The standard from which optimisation of PCR amplification of fixed tissue started was the optimised set of conditions used in our department for amplification of DNA extracted from fresh tissue using the same set of primers (Set 1). The starting conditions were as follows: 300-600 ng DNA, 10 pmol of each primer, 200 μM of each dNTP and 2.0 units of *Taq* DNA polymerase in 50μl reactions. Magnesium chloride concentration was 2.0 mM for exons 5, 6, and 7, and 4.0 mM for exon 8, and the annealing temperature was 55°C for all exons.

By performing PCR amplification of DNA extracted from blocks of formalin-fixed paraffin embedded human tonsil tissue, using primer annealing temperatures ranging between 55°C and 60°C, optimal temperatures for specific amplification with Set 1 primers, were found to be as follows: 55°C for exon 5, 57°C for exon 6, 58°C for exon 7 and 60°C for exon 8. Magnesium chloride concentration was not changed for any of the exons, as amplification was efficient and specific with the new annealing temperatures. During the course of the study a new *Taq* DNA polymerase (Qiagen instead of Promega) was adopted, which improved the specificity of the PCR reactions due to the use of a buffer of a different formulation. The new enzyme was used at a concentration of 1.5 units (rather than 2.0 units) per reaction and magnesium chloride concentration was 1.5 mM for all four exons.

3.4.1.2 Optimisation of the PCR (II)

During development of the IHSA technique it became apparent that the sensitivity of the PCR method employed was not enough to amplify the minority population of intact DNA strands present in the UV irradiated samples to detectable levels. In order to overcome this problem, a nested PCR method was developed utilising a new set of primers (Set 2, Table 2.8.1), as described in section 2.8.4.

Optimisation of the PCR for the second set of primers used the optimised conditions established for Set 1 as a starting point. As non-specific products were generated for all exons, new annealing temperatures (58°C, 60°C, 62°C, and 64°C) and a range of magnesium chloride concentrations between 1.5 mM and 4.0 mM were attempted. Efficient and specific amplification was achieved employing annealing temperatures of 64°C for exons 5, 6, and 7, and 62°C for exon 8, combined with a magnesium chloride concentration of 1.5 mM for all exons (Fig. 3.4.1).

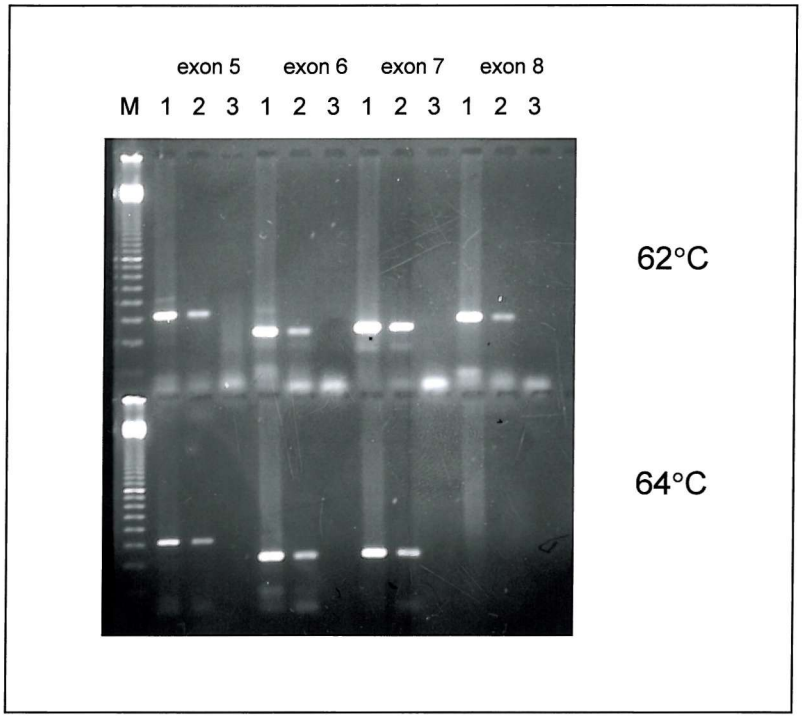

Fig. 3.4.1. Agarose gel showing final stage of annealing temperature optimisation of exons 5-8. While at 62°C there were still non-specific products present in reactions for exons 5-7, at 64°C amplification products were specific for those exons. For exon 8, specific products were generated at 62°C, but 64°C seemed unfavourable for primer annealing.

Key: M, 100 bp molecular weight marker. 1,2 represent two different samples of DNA, 3 represents the negative control to which no DNA was added.

3.4.2 PCR amplification of samples – Round I

Amplification using PCR was successful for all 4 exons in 49 out of 52 samples (94% success rate). Amplification failed for exon 8 in one sample (sample 47), for exons 5, 7 and 8 in another (sample 27) and for all 4 exons in a third sample (sample 25). For the first two samples where PCR failed, other blocks containing equivalent tissue resected at the same time were available as replacements. Only in one case (sample 25) was there no available replacement and, therefore, this case was not included in the SSCP analysis. PCR amplification was performed twice for each sample analysed.

3.4.3 PCR amplification of samples – Round II

With the development of nested PCR, a second round of PCR amplifications for subsequent SSCP analysis was undertaken using the more sensitive and specific technique. As this second round was performed at a later date, additional cases were available for analysis. Using nested PCR, amplification was successful for all 4 exons in 66 out of 68 samples (97% success rate). The samples for which PCR failed (samples 25 and 27) had also failed to amplify in round I. As described above, a replacement block was utilised for sample 27 and sample 25 was excluded from SSCP analysis. PCR amplification was performed twice for each sample analysed.

3.5 SSCP ANALYSIS

3.5.1 Preliminary work – Round I

Before SSCP analysis of the amplified exons from each case was initiated, two different gel conditions were tried in order to select the condition that produced the most efficient separation of the ssDNA bands on the gel, as well as the best resolution.

A set of PCR products containing exons 5, 6, 7, and 8 was run in 6% polyacrylamide gels containing 5% glycerol (Appendix G.3) and in MDE gels with no glycerol (Appendix G.2). In general, better separation of bands and resolution was achieved using the MDE gel, which was then adopted for subsequent SSCP analyses.

3.5.2 SSCP analysis results – Round I

The first round of SSCP analysis was performed on 21 cases, including 49 samples, available at the time. In 14 cases both T (tumour) and A (adjacent) tissue samples were available, in 6 cases only T samples were available and, in one case, only the A sample was available. Each sample was amplified twice and analysed in two different SSCP gels.

Mobility shifts were identified in 13 (65.0%) of the 20 T samples, and in 5 (33.3%) of the 15 A samples. Out of the 14 cases where both T and A samples were available, mobility shifts were detected in 10 (71.4%) T samples and in 5 (35.7%) A samples. This is represented in Fig. 3.5.1.

Three examples of mobility shifts in different exons are shown in Fig. 3.5.2.

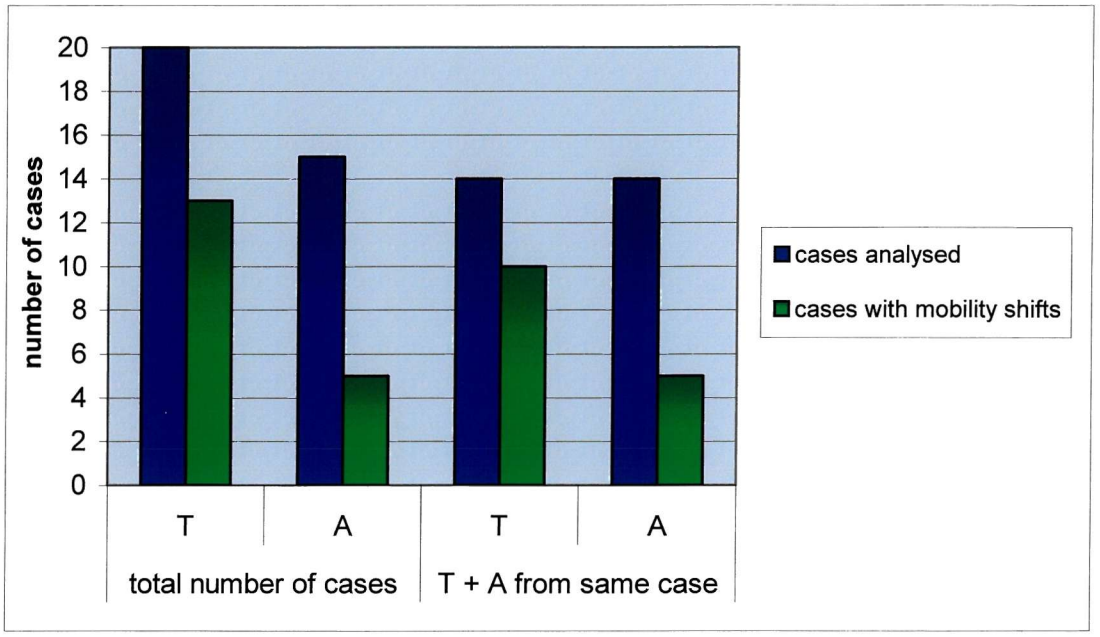

Fig. 3.5.1. Summary of mobility shifts identified in the cases analysed in round I.

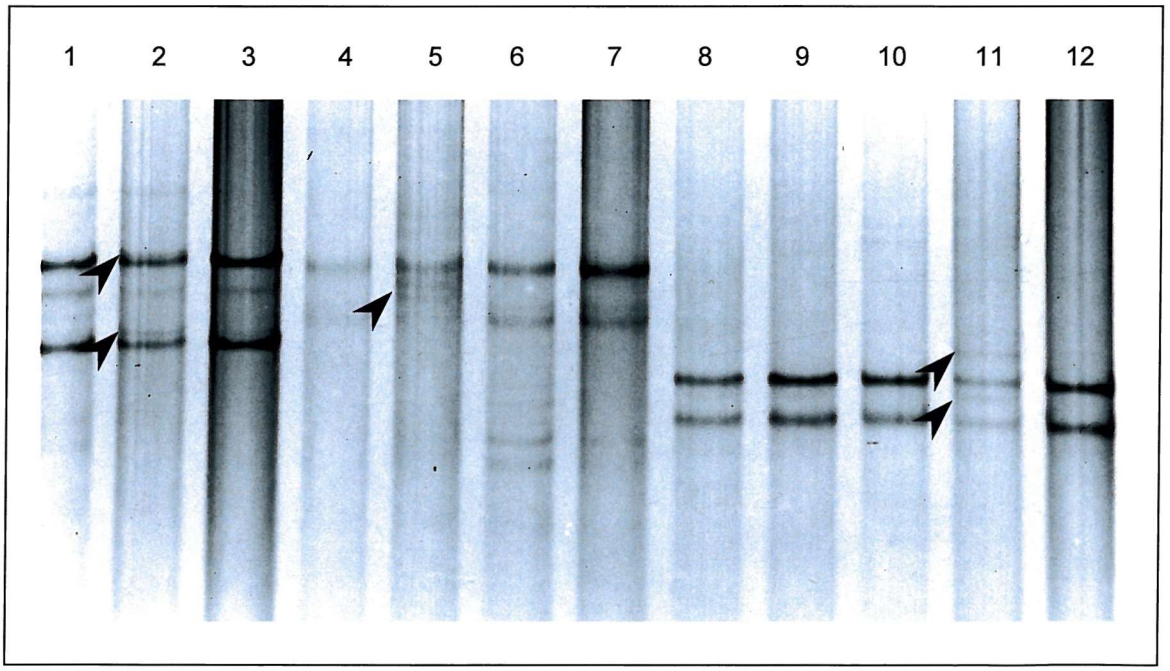

Fig. 3.5.2. SSCP analysis showing mobility shifts in PCR products amplified from different cases. Lanes 1-3, exon 5; Lanes 4-7, exon 7; Lanes 8-12, exon 8. Mobility shifts (arrowheads) are seen in lanes 2, 5 and 11. Lanes 3, 7 and 12, wild-type DNA extracted from human tonsil.

Most mobility shifts detected (65%) were present in exons 7 or 8, with the lowest number of shifts in exon 6 (15.4%) (Fig. 3.5.3).

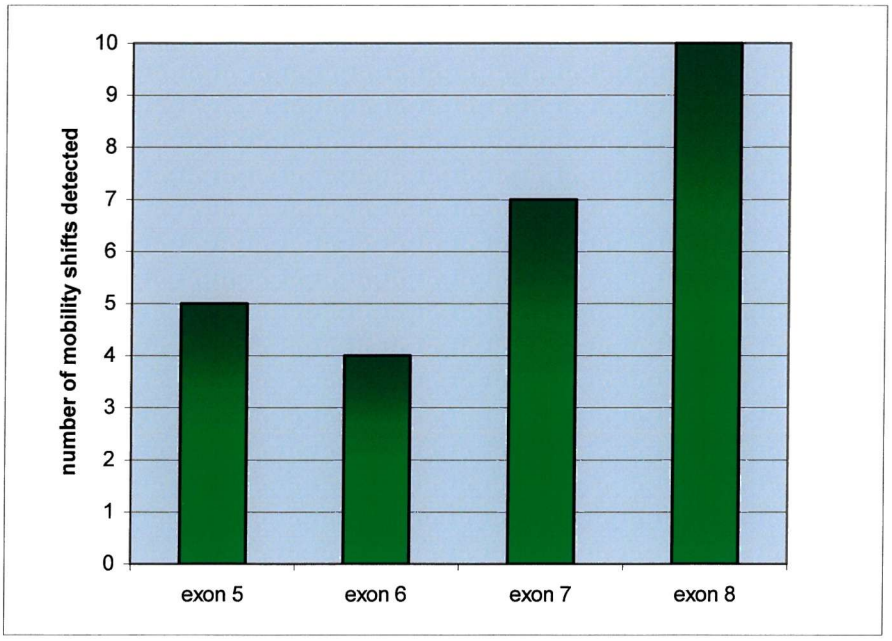

Fig. 3.5.3. Number of mobility shifts detected in the four different exons during round I.

In 4 cases the T sample showed a mobility shift in the same exon as in the corresponding A sample (Table 3.5.1). In 3 of these cases the shift was the same in both T and A samples (Fig. 3.5.4) while in the fourth case, the relative position of the shifted band was slightly different. However, in this case, T and A samples were run on different gels and slight changes in electrophoretic conditions such as changes in ambient temperature, could have affected the relative mobility of the shifted band.

It was interesting to note that in 7 cases (5 T and 2 A samples belonging to different cases), mobility shifts were detected in more than one exon (Fig. 3.5.4).

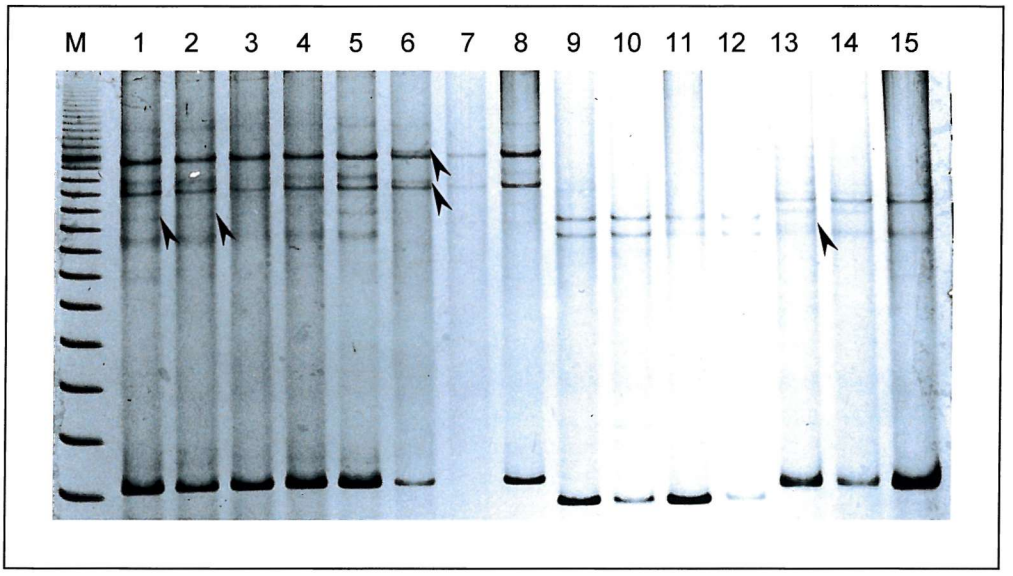

Fig. 3.5.4. SSCP analysis showing mobility shifts (arrows) in multiple exons. Lanes 1-8, exon 5; Lanes 9-12, exon 6; Lanes13-15, exon 8. Lanes 6 and 13 show mobility shifts in exons 5 and 8, respectively, in PCR products amplified from the same DNA sample. Lanes 1 and 2 represent, respectively, A and T samples from the same case, and show the same mobility shift. Lanes 3-5 represent products amplified from lymph node tissue from the same case as in Lanes 1 and 2. Lanes 8, 11, and 15, wild-type DNA extracted from human tonsil. M, 100bp molecular weight marker.

A phenomenon observed during SSCP analysis was the presence of multiple conformers. These are single stranded DNA fragments assuming two or more conformations, which are detected on the gel as multiple bands but which originate from the same specific PCR product (Hayashi, 1991). Multiple conformers were more often present in exons 5, 7, and 8, and more frequently observed in samples of analysed cases than in the control samples of p53 exons amplified from normal human tonsil, making interpretation of results difficult in some cases.

In one instance, a band showing mobility shift was excised from the gel and the ssDNA extracted was re-amplified using the same primers and cycling conditions employed in the original PCR amplification. The product of this reaction was run alongside the original sample and showed similar mobility to the excised shifted band (Fig. 3.5.5), suggesting that the re-amplified product is more likely to have an altered sequence rather than being a multiple conformer.

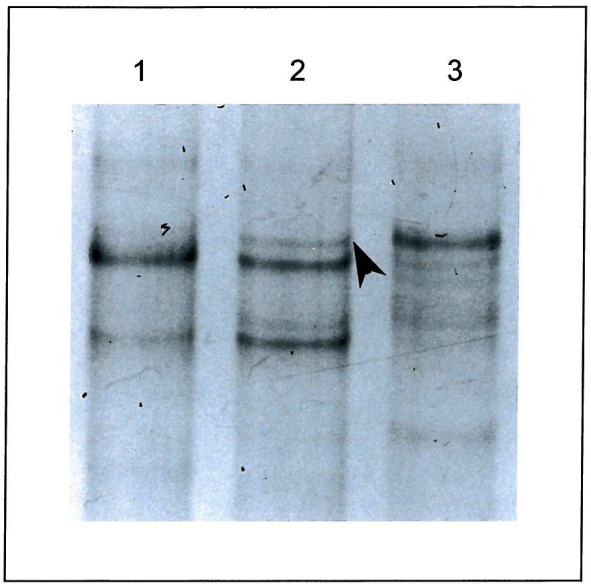

Fig. 3.5.5. Comparison between original T sample showing mobility shift in exon 5 (Lane 2) and product of PCR re-amplification of shifted band (Lane 3). The excised and re-amplified band is identified with an arrowhead. Lane 1 shows the product of re-amplification of normal double stranded exon 5 excised from the original gel for comparison.

3.5.3 SSCP analysis results – Round II

Single stranded conformation polymorphism analysis of PCR products amplified in round II was performed using MDE gels as before, with the exception of the analysis of PCR products of exon 6. During the development of the IHSA technique, electrophoresis of a PCR product, known to contain a mutation in exon 6, showed a mobility shift in a 6% polyacrylamide gel containing 5% glycerol, but not in an MDE gel. Amplified products of exon 6 were therefore analysed using polyacrylamide rather than MDE gels, in spite of the poorer band resolution. Amplified products of exons 5, 7 and 8 were analysed using MDE gels. Each sample was amplified twice and analysed in two different SSCP gels.

During the second round of SSCP analysis, a decrease in the relative number of mobility shifts has been observed, when compared to the mobility shifts detected in the same 21 cases that were available for the first round. The number of mobility shifts detected in T samples dropped from 65% to 45%, and in A samples the number fell from 33.3% to 20%. For the 14 cases where both T and A samples were available, mobility shifts detected fell from 71.4% to 50% for T samples and, for A samples, the number of shifts observed dropped from 35.7% to 21.4%.

In total, SSCP analysis was performed on 30 cases in round II. In 19 cases both T and A tissue samples were available, in 10 cases only T samples were available and in 1 case only the A tissue sample was available for analysis.

Mobility shifts were detected in 10 (34.5%) of the 29 T samples and in 3 (15%) of the 20 A samples. Where both T and A samples were available (19 cases), mobility shifts were identified in 7 (36.8%) T samples and in 3 (15.8%) A samples. These results are shown in Fig. 3.5.6. With exception of Cases 10 and 11, all samples in which mobility shifts were detected also showed p53 protein accumulation in a proportion of cells. A summary of the mobility shifts detected in both rounds I and II and the percentage of p53 expression in each sample is shown in Table 3.5.1.

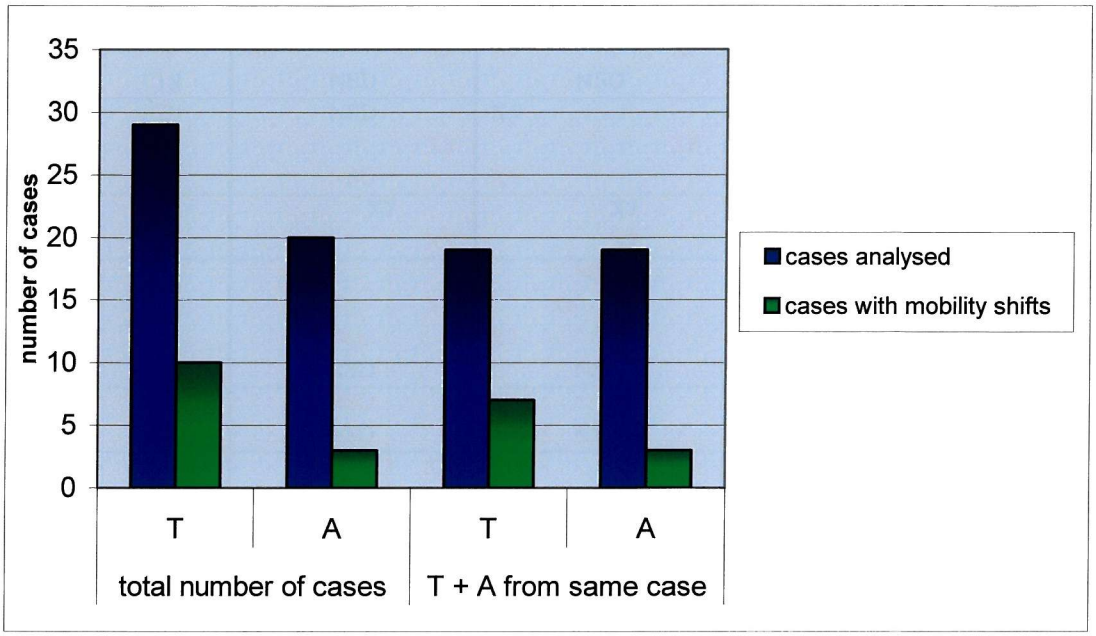

Fig. 3.5.6. Summary of mobility shifts identified in the cases analysed in round II.

Case no.	Sample no.	Round I PCR-SSCP	Round II PCR-SSCP	p53 positivity
1	1	X5 X8	X5 X8	43.1%
	18	NSD	NSD	8/100* (1%)
2	2	NSD	X5	11/100* (23%)
	3	X8	X8	64%
	10	NSD	X5	7/100* (2%)
3	5	X7	X7	2/100* (2.9%)
	6	X8	X7	5.7%
5	8	X6	NSD	11.8%
	9	X8	X6	23.9%
	54	NA	X5	31.8%
	28	NSD	NSD	-
7	13	NSD	X5 X7	3%
	14	NSD	NSD	-
8	15	X7 X8	X7 X8	53.3%
	16	X7	NSD	-
9	17	X8	NSD	-
	29	X7 X8	NSD	-
	35	X6	NSD	-
10	20	X6	X6	-
	NA	NA	NA	-
11	41	X5 X7	X6	-
	42	X5	NSD	18.1%
13	23	NSD	X8	55.5%
	NA	NA	NA	-
14	B	X5	NSD	15/100*
	E	X5 X8	NSD	3%
16	34	X7	X7	10.9%
	32	NSD	NSD	-
17	36	X7 X8	NSD	38.4%
	30	X7	NSD	42.8%
	56	X7	NSD	33.7%
	NA	NA	NA	-
18	37	X8	NSD	29.1%
	NA	NA	NA	-
21	49	X6	NSD	-
	39	NSD	NSD	-
25	63	NA	X8	55.5%
	NA	NA	NA	-

Table 3.5.1. Summary of mobility shifts detected in exons 5-8 in both rounds of SSCP analysis and percentage of cells showing p53 expression in each sample. Sample numbers refer to different tissue samples from the same case.

Key: Numbers in red represent tumour samples; histologically uninvolved adjacent tissue samples are shown in blue; NA, tissue sample not available; NSD, no shifts detected.

* denotes number of $p53^+$ IEL per 100 epithelial cells. Percentages in brackets refer to $p53^+$ cells in the lamina propria.

For this set of results the distribution of mobility shifts identified were as shown in Fig. 3.5.7.

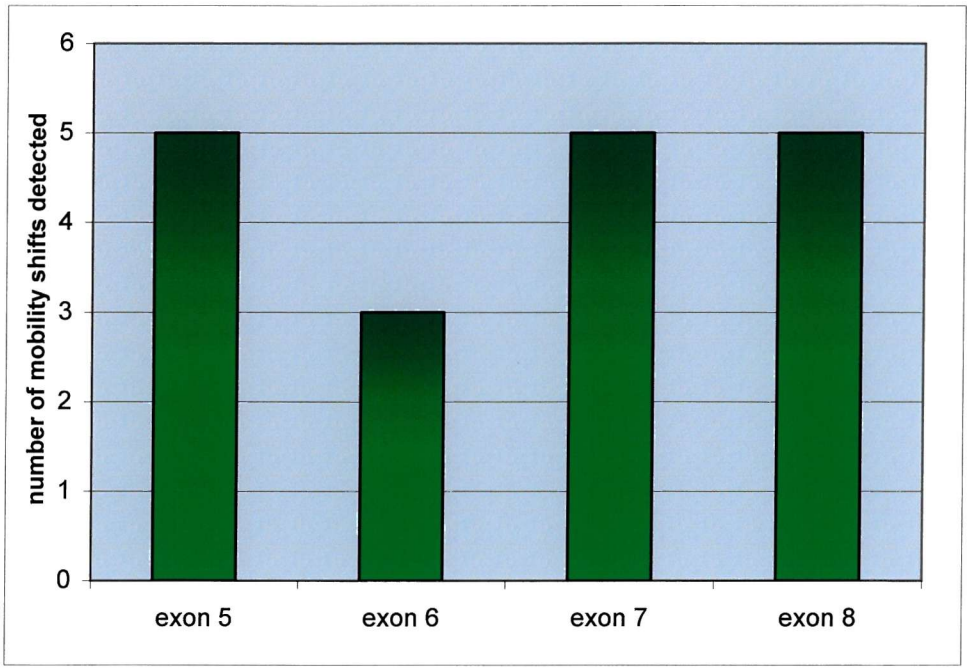

Fig. 3.5.7. Number of mobility shifts detected in the four different exons during round II of SSCP analysis.

In 2 cases (cases 2 and 3, Table 3.5.1) in which mobility shifts were detected in paired T and A samples, the shift was present in the same exon. Examples of mobility shifts detected in an A sample (sample 2) and a T sample (sample 10) of the same case (case 2) are shown in Figs. 3.5.8 and 3.5.9, respectively.

Cases 10 and 11 are samples from the same patient who had 2 tumours resected with a two-year interval between the 2 resections. A mobility shift in exon 6 was detected in the T sample in case 10 and also in the A sample of case 11. The mobility shifts did not appear to be the same, however the samples were analysed in different gels and differences in electrophoretic conditions could account for differences in mobility shift. These 2 samples were the only ones to show mobility shifts in the absence of p53 over-expression.

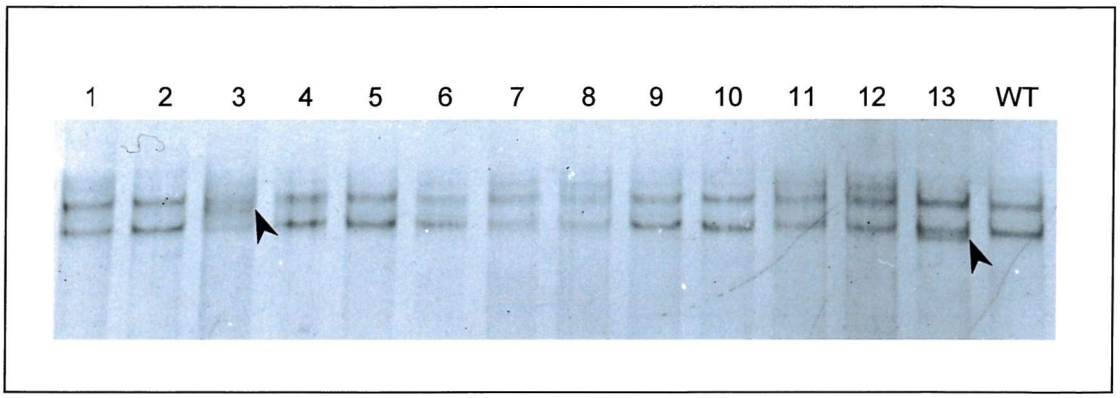

Fig. 3.5.8. SSCP analysis of PCR products of exon 5 showing mobility shifts in samples 2 (lane 3) and 13 (lane13). Arrowheads point to shifted bands. WT, wild-type DNA extracted from human tonsil.

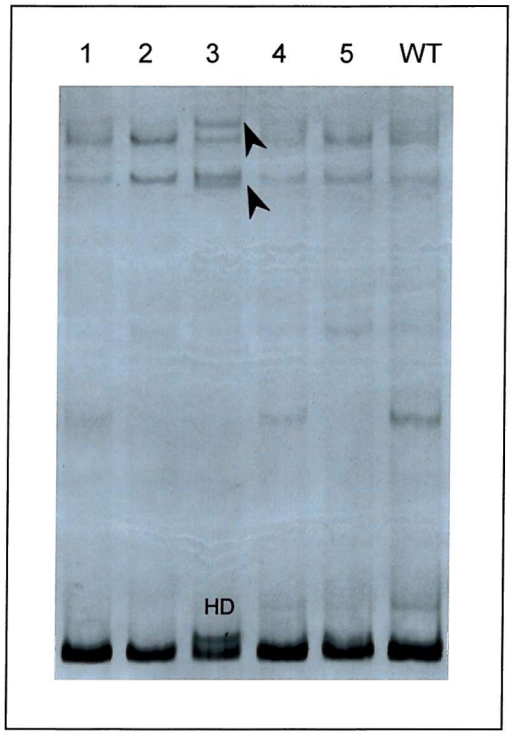

Fig. 3.5.9. SSCP analysis of PCR products of exon 5 showing mobility shift and heteroduplex band.
Lanes 1-5 represent different samples. Arrowheads point to shifted bands present in sample 10 in lane 3. Sometimes a double band can be seen at the level of the double-stranded DNA. This is termed a heteroduplex (HD) and results from the re-annealing of mutant with wild-type DNA. WT, wild-type DNA extracted from human tonsil.

In order to confirm that a mobility shift was genuine, PCR amplification was repeated and reanalysed in an SSCP gel. Figures 3.5.10 and 3.5.11 both show mobility shifts in sample 5. The fact that the shift is not the same in both cases could be due to changes in electrophoretic conditions or due to different alterations to the sequence.

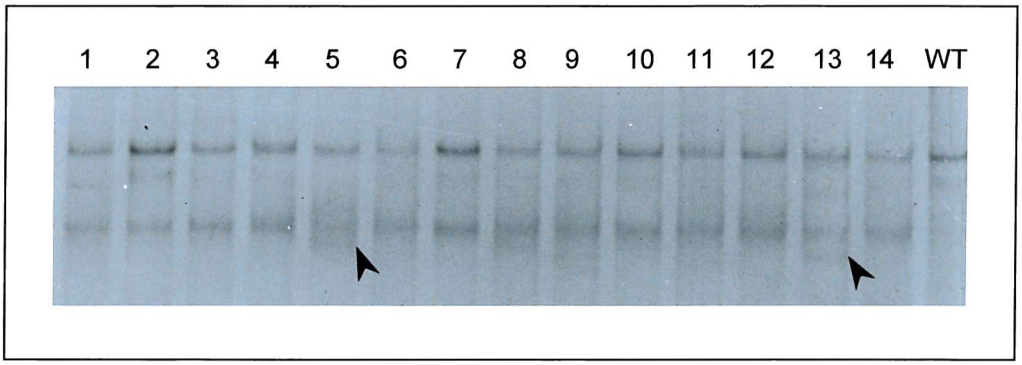

Fig. 3.5.10. SSCP analysis of PCR products of exon 7. Lanes 1-14 represent different samples. Arrowheads point to mobility shifts in sample 5 (lane 5) and in sample 13 (lane 13). WT, wild-type DNA.

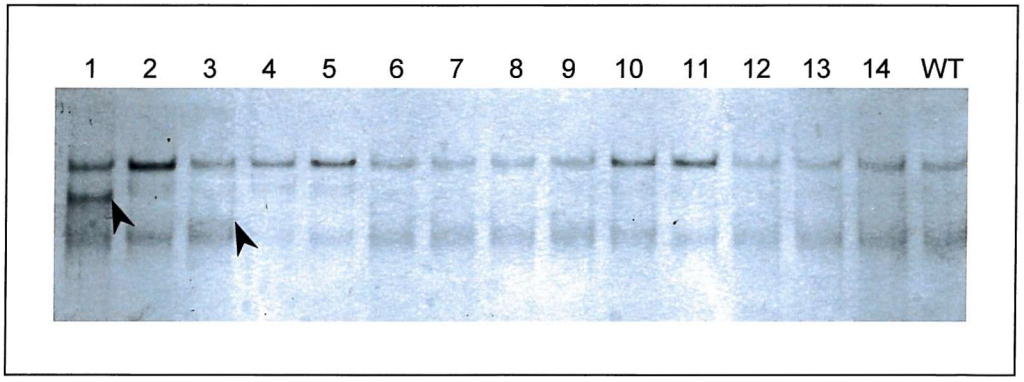

Fig. 3.5.11. SSCP analysis of PCR products of exon 7. Arrowheads point to mobility shifts in sample 5 (lane 1) and sample 15 (lane 3). WT, wild-type DNA.

In 3 cases, mobility shifts were detected in 2 exons amplified from the same sample. Fig. 3.5.8 (lane 13) and Fig. 3.5.10 (lane 13) show mobility shifts detected in sample 13 in exons 5 and 7, respectively.

Figure 3.5.12 below shows a second example of such a case. A mobility shift was observed in sample 15 in exon 7 (Fig. 3.5.11, lane 3) and in exon 8 (Fig. 3.5.12, lane 5).

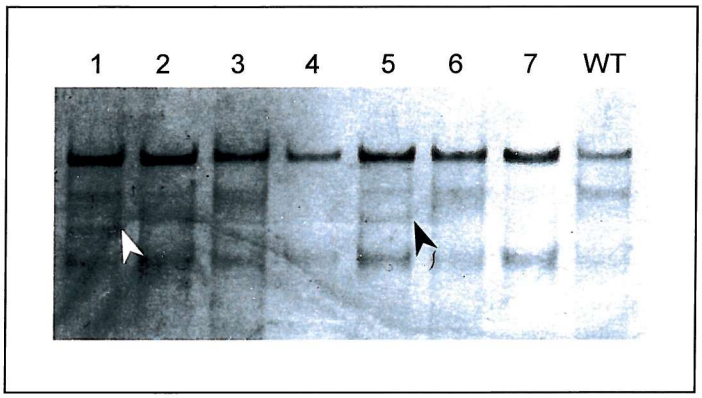

Fig. 3.5.12. SSCP analysis of PCR products of exon 8. Lanes 1- 7 represent different samples. Arrowheads point to mobility shifts in sample 1 (lane 1) and sample 15 (lane 5). WT, wild-type DNA.

3.5.4 Summary

The second round of PCR-SSCP analysis detected a smaller number of mobility shifts than the first round. Samples in which mobility shifts were detected in the same exon during both rounds of analyses showed similar shifts in some cases but not in others. It is difficult to tell, however, whether they are the same or not since separation of the bands can show different patterns in different SSCP analyses.

Optimisation of the PCR-SSCP for the second round of amplifications ensured that the results obtained were more accurate than for the first round, i.e. mobility shifts were easier to detect and to distinguish from multiple conformers. The PCR products that showed mobility shifts during the second round of amplification were therefore selected for sequence analysis.

3.6 SEQUENCING

Direct sequencing of PCR products in which SSCP analysis had detected mobility shifts was attempted, as sometimes the proportion of mutated sequences in the sample can be sufficient to be detected by automated DNA sequencing. Somatic point mutations can be identified as two electropherogram peaks at the same base position, with the ratio of peak intensities dependent on the proportion of mutated sequences in relation to the wild-type sequence.

3.6.1 Sequencing of mobility shifts detected during SSCP analysis – Round I

Sequencing was performed on 15 samples of PCR products, with both the forward and the reverse DNA strands being sequenced. None of the reactions showed a definite double peak to confirm the presence of two different sequences in the sample. In some samples, peaks of different intensities were observed at the same position, which could have indicated either the presence of a small proportion of sequences with a mutation, or background artefact. Sequencing of the reverse strands had a lower success rate and the reactions that were successful did not confirm the double peaks observed in the sequencing of the forward strands. An example is shown in Fig. 3.6.1.

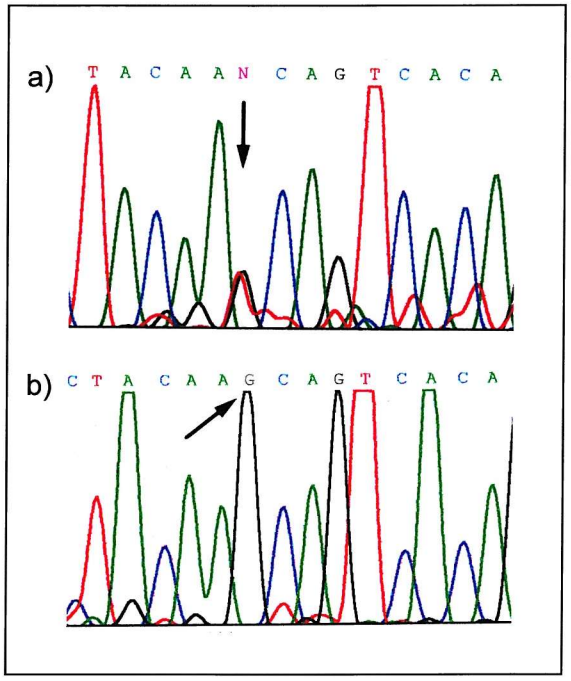

Fig. 3.6.1. Electropherograms showing sequencing results for one sample. Forward sequencing of exon 5 is shown in (a). The double peak is identified by the arrow. Reverse sequencing of the same sample (b) showed a single peak at the corresponding base (arrow). The reverse sequence has been changed into its complementary sequence for comparison.

3.6.2 - Sequencing of mobility shifts detected during SSCP analysis – Round II

Forward sequencing was performed on 18 samples from 11 cases that showed a mobility shift in either the T or the A sample. Alterations to the sequence in comparison to the wild-type sequence or double peaks were detected in 7 samples belonging to 6 different cases. A list presenting all the mutations detected is shown below (Table 3.6.1).

Case No.	Sample No.	Sample type	Exon	Codon	Sequence change	Amino acid change	Nucleotide change
1	1	T	8	280	AGA→ATA	Arg→Ile	G:C→T:A
2	10 (a)	T	5	184	GAT→AAT	Asp→Asn	G:C→A:T
2	10 (b)*	T	5	128	CCT→CTT	Pro→Leu	C:G→T:A
2	2	A	5	183	TCA→TTA	Ser→Leu	C:G→T:A
3	5	A	7	256	ACA→ATA	Thr→Ile	C:G→T:A
5	54	T	5	159	GCC→GCT	Ala→Ala	C:G→T:A
7	13	T	5	155	ACC→ACT	Thr→Thr	C:G→T:A
13	23(a)	T	8	275	TGT→TAT	Cys→Tyr	G:C→A:T
13	23(a)	T	8	280	AGA→GGA	Arg→Gly	A:T→G:C
13	23(b)	T	8	306	CGA→CAA	Arg→Gln	G:C→A:T

Table 3.6.1. List of p53 gene mutations detected in EATL cases. Letters next to sample numbers refer to sequencing of different PCR products amplified from the same sample. * IHSA was applied to this sample, UV irradiation for 15 min.

In samples 1, 2 and 5, the mutated sequence shows up as a smaller peak in relation to the wild-type one (Fig. 3.6.2). In sample 10 (a) only one peak representing the new sequence was detected (Fig. 3.6.3).

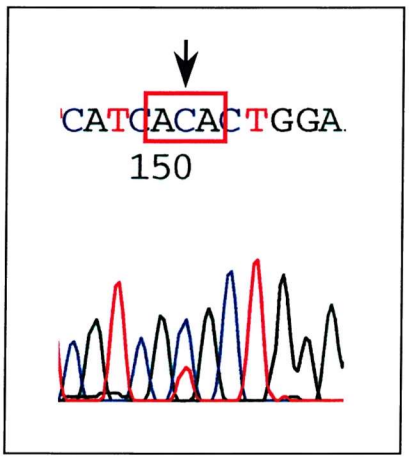

Fig. 3.6.2. Electropherogram showing an additional peak in the sequence of sample 5. The red peak (arrow) indicates a small population of PCR products containing a thymine base rather than the cytosine base at that position.

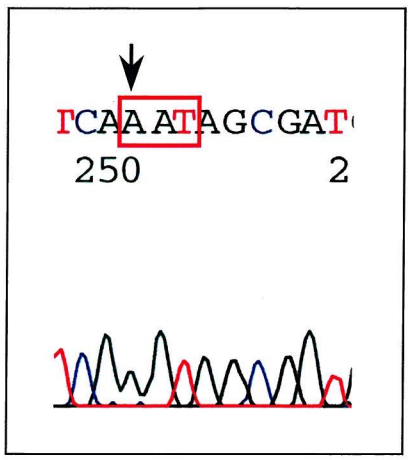

Fig. 3.6.3. Electropherogram showing the change in sequence in sample 10 (a). The mutated base (G→A) is indicated by the arrow.

It is interesting to note that sequencing of different PCR products amplified from the same sample showed different changes in the sequence for samples 10 and 23. The altered sequence in sample 10 (b) is different from the one in sample 10 (a) and appears as a large peak superimposed on a small peak representing the wild-type base (Fig. 3.6.4). As IHSA had been applied to this sample, the smaller peak may represent the wild-type DNA that was not completely inactivated by UV irradiation.

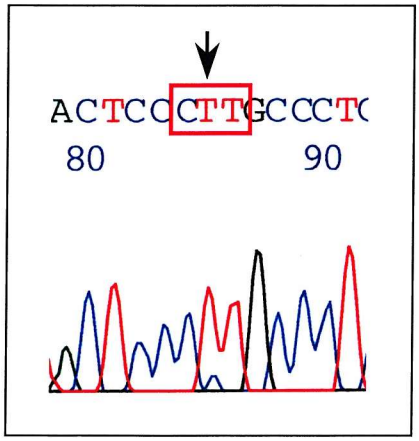

Fig. 3.6.4. Electropherogram showing altered sequence of sample 10 (b). The small blue peak (arrow) indicates a small proportion of wild-type DNA present in the sample.

Samples 54 and 13 contained silent mutations. These are detected through SSCP analysis, due to the change of sequence, but have no effect on the protein since the new codon codes for the same amino acid. The equal size peaks seen at the altered base of the sequence for sample 13 suggests that both sequences are present in equal numbers (Fig. 3.6.5).

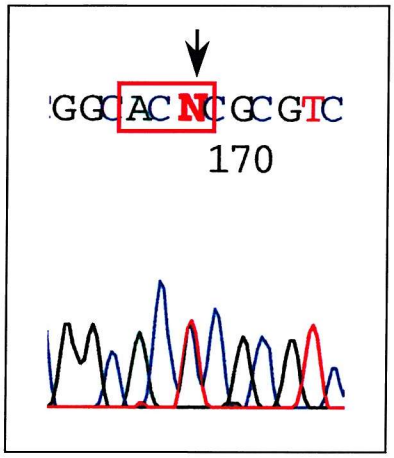

Fig. 3.6.5. Electropherogram showing peaks of equal size at the same position in the sequence of sample 13.

Sequencing of the reverse strand was performed on samples 2, 5 and 23(a) to confirm that the mutation was genuine, as the change of sequence was represented by a peak smaller than that for the wild-type base. Reverse strand sequencing was also performed on sample 54 to confirm the presence of the silent mutation.

The new sequencing data confirmed that the detected mutations were genuine in samples 2 (Fig. 3.6.6) and 23(a).

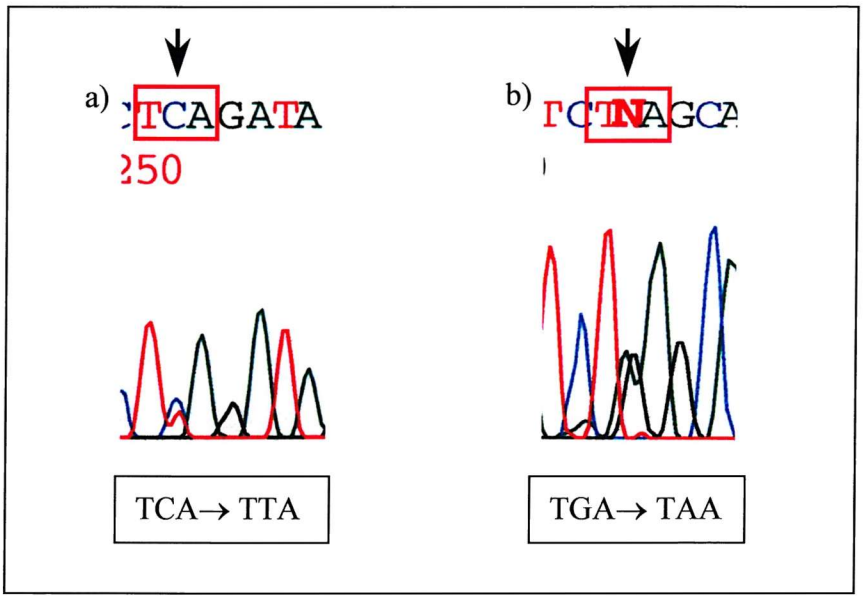

Fig. 3.6.6. Forward (a) and reverse (b) sequencing data for Sample 2. The red boxes indicate the mutated codon. The change in sequence in (b) is shown to be complementary to the mutation detected in (a).

The data for sample 5 were inconclusive due to excess background noise in the form of additional smaller peaks below the main peaks on the electropherogram. These masked the possible presence of a genuine extra peak that would confirm the previously detected mutation.

Reverse sequencing of sample 54 confirmed the presence of the first silent mutation and also detected an additional silent mutation (codon 131). This had been overlooked in the forward sequencing data, as the additional peak was very small and had been dismissed as data "noise" (Fig. 3.6.7).

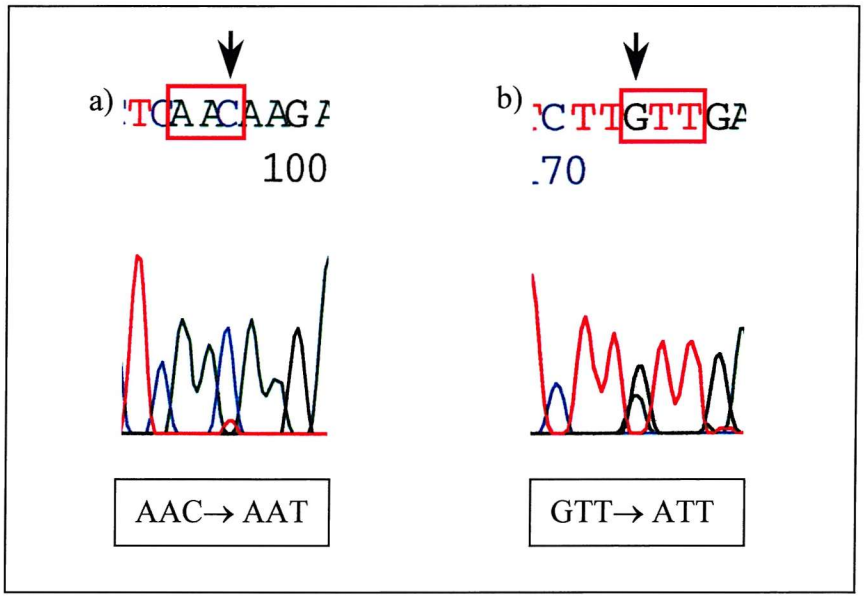

Fig. 3.6.7. Forward (a) and reverse (b) sequencing data for additional silent mutation in Sample 54 (codon 131). The red boxes indicate the mutated codon. The change in sequence in (b) is shown to be complementary to the mutation detected in (a).

The sequence analysis described in Section 3.6.2 was performed by Oswel Research Products Ltd.

3.6.3 Summary

Sequencing analysis of samples showing mobility shifts detected sequence alterations in 7 samples from 6 different cases. In 2 cases the changes in sequence represented silent mutations. Genuine mutations were identified in 4 cases, which represent 13.3% of the 30 cases included in this study.

In case 2, mutations were detected in both the tumour and the adjacent tissue sample. Although they were not the same mutation, they were present in adjacent codons.

Two separate cases showed different mutations in the same codon (codon 280). Sample 23 showed the presence of 2 mutations in the same PCR product. These were confirmed to be genuine by sequencing of the reverse strand.

All 5 samples for which mutations were detected were also positive for p53 protein.

3.7 IMMUNOHISTOSELECTIVE ANALYSIS

In order to use UV irradiation to inactivate DNA in p53 immunostain-negative cells, optimal conditions for inactivation needed to be determined.

3.7.1 Preliminary work

A series of sections cut from blocks containing tumour from colon adenocarcinoma cases were stained for p53 protein and a suitable block was chosen to be used in the preliminary work. The chosen block contained an area of immunostained tumour tissue next to an area of unstained cells, clearly separate from each other. Because of this, the tissue section itself would contain a control for complete inactivation of unstained background DNA (Fig. 3.7.1).

3.7.1.1 Determination of optimal UV irradiation using a transilluminator

During the first set of experiments, UV irradiation was performed using a UV transilluminator (302nm, Model TM36-E, 8000$\mu W/cm^2$, Ultra Violet Products Ltd.).

Sections immunostained for p53 were placed tissue side down on the UV transilluminator, with their edges resting on blank slides. Slides were exposed to UV for different lengths of time, with 3 slides allocated for each time. Three extra slides were also immunostained, but not exposed to UV, to be used as positive controls. Exposure times were 30 min, 60 min, 90 min, 120 min, 180 min, and 240 min. For each exposure time, 3 samples were prepared for DNA extraction: 1 containing the whole section of one slide (W sample), 1 containing only the p53 immunostain-positive areas of two slides (p53+ sample), and 1 containing only the unstained areas of two slides (p53-neg. sample) (Fig. 3.7.1).

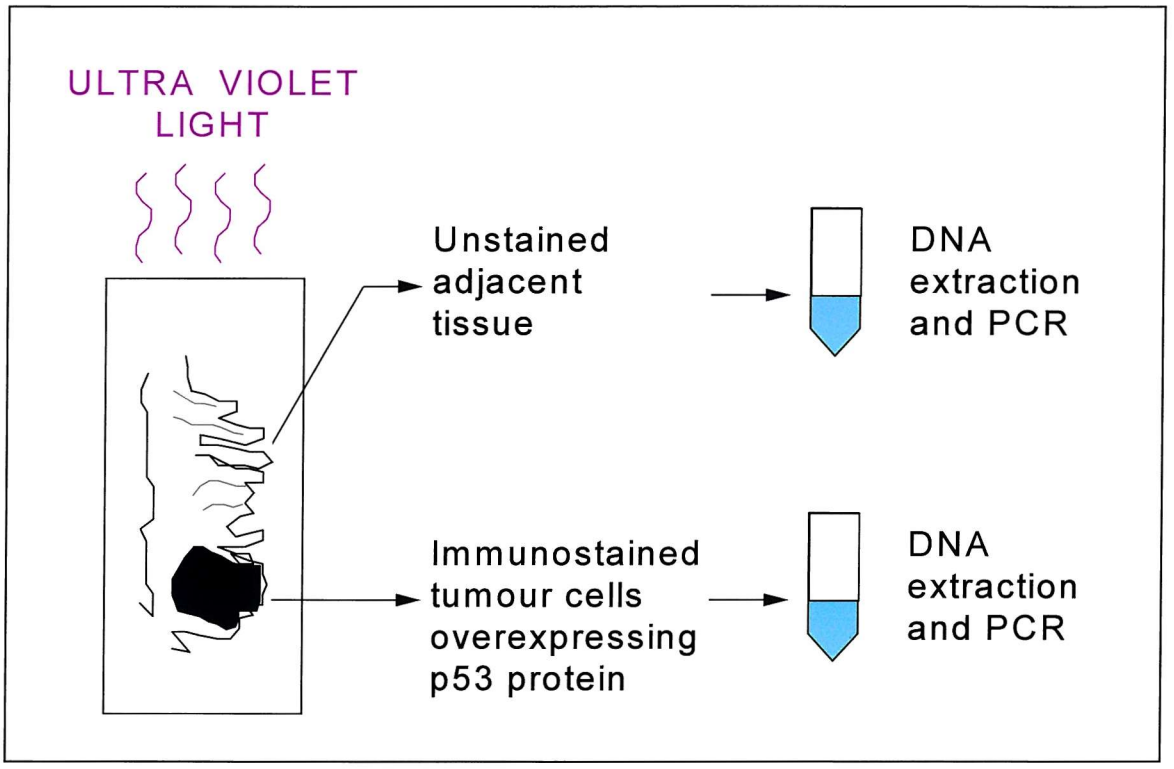

Fig. 3.7.1. Preparation of sample for DNA extraction during optimisation of UV exposure times for immunohistoselective analysis.

After DNA extraction, PCR amplification was performed and results analysed by agarose gel electrophoresis. The time-dependent inactivation of DNA by UV is shown in Fig. 3.7.2 using the PCR products of exon 8 as an example.

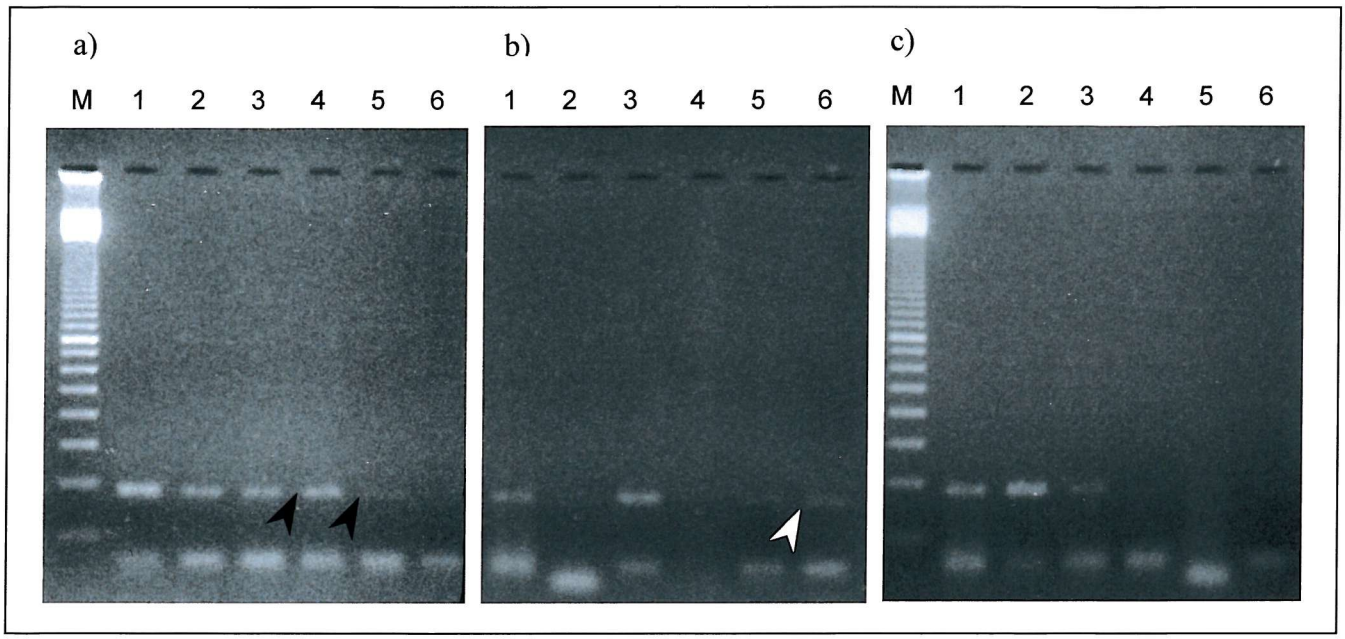

Fig. 3.7.2. Time-dependent inactivation of DNA by UV irradiation. PCR amplification of exon 8 of the p53 gene from W samples (a), p53+ samples (b), and p53-neg. samples (c). Lane M, 100bp molecular weight marker; Lane 1, 30 min; Lane 2, 60 min; Lane 3, 90 min; Lane 4, 120 min; Lane 5, 180 min; Lane 6, 240 min of irradiation. Arrowheads indicate PCR product; see text for details.

Both W and p53-neg. samples [shown in Fig. 3.7.2 (a) and (c), respectively] showed a clear decrease in the intensity of the PCR product as the UV irradiation time lengthened. In the W sample, the PCR product present in lanes 4 and 5 (black arrowheads) was likely to have been amplified from the protected p53 immunostain-positive cells of the section. PCR amplification of the p53-positive sample showed products with varying intensities, however even after 240 min of UV irradiation, the DNA could still be amplified (Fig. 3.7.2 (b), white arrowhead).

After analysis of PCR amplifications of exons 5, 6, 7, and 8, the optimal exposure times to UV irradiation that inactivated DNA in the p53 immunostain-negative cells, but still allowed amplification of the protected p53 immunostain-positive cells, were found to be 120 min for exon 5, and 180 min for exons 6, 7, and 8. However, inactivation of DNA could be inconsistent between different experiments in some tissue sections.

3.7.1.2 Maximizing p53 immunostain enhancement

In order to produce the darkest immunostain possible, so that p53-positive cells could have maximum protection from UV irradiation, the following experiment was performed. Immunostaining of known p53-positive sections was carried out and, during the chromogen enhancement step, slides were incubated with either the normal amount of nickel solution recommended by the manufacturer, twice the amount or three times the amount of nickel solution.

Immunostained sections were inspected by light microscopy and showed a darker stain when using twice the recommended amount of nickel solution than when using the recommended amount. The latter only produced a grey-black stain. Using three times the recommended amount of nickel solution did not increase the intensity of the stain any further. Using twice the recommended amount of nickel solution in the enhancement of the staining was therefore adopted as the method of choice for subsequent IHSA.

3.7.1.3 Determination of optimal UV irradiation using a UV crosslinker

A UV crosslinker should provide a more even and constant output of UV irradiation, as it is fitted with a sensor that measures the UV irradiation emitted and compensates for any wear of the UV tubes over time. Internal reflective surfaces also ensure that UV exposure is even over the surface of all tissue sections.

In an attempt to produce more consistent and reproducible DNA inactivation a crosslinker was used (254nm, Model CL 1000, Ultra Violet Products Ltd.) set at $8000\mu W/cm^2$. An experiment similar to the one in section 3.7.1.1 was performed, with a few added changes, to determine the optimal UV exposure times using the crosslinker.

Only one p53 immunostained tissue section (8μm in thickness) was used per exposure time. As before, the p53 immunostain-positive area (p53+ sample) and the unstained area (p53-neg. sample) were removed subsequently and placed into separate microcentrifuge tubes containing digestion buffer. The volume of digestion buffer used was reduced accordingly. Exposure times to UV irradiation were 1h, 1.5h, 2h, 2.5h, 3h, 3.5h, 4h, 4.5h, 5h, and 6h.

After DNA extraction, PCR amplification of all four exons was performed and results analysed by agarose gel electrophoresis. PCR amplification of exon 7 of the p53 gene is shown in Fig.3.7.3 as an example.

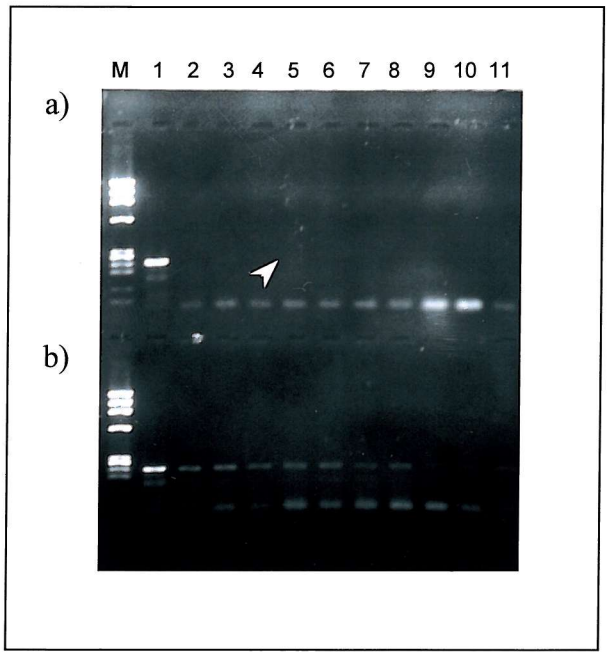

Fig. 3.7.3. Time-dependent inactivation of DNA by UV irradiation using a crosslinker. PCR amplification of exon 7 of the p53 gene from p53 immunostain-negative (p53-neg.) (a), and p53 immunostain-positive (p53+) (b) samples. Lane M, ΦX174 molecular weight marker; Lane 1, no UV irradiation; Lane 2, 1h; Lane 3, 1.5 h; Lane 4, 2h; Lane 5, 2.5h; Lane 6, 3h; Lane 7, 3.5h; Lane 8, 4h; Lane 9, 4.5h; Lane 10, 5h; and Lane 11, 6h of UV irradiation. Optimal UV exposure time for exon 7 was determined as 3h as a weak PCR signal was still present after 2.5h of UV irradiation (arrowhead).

The inactivation of DNA by UV irradiation using the crosslinker seemed to be more efficient than when using the transilluminator, as a general decrease in optimal UV exposure time was observed. The new determined optimal exposure times were 1.5h for exon 5, 2h for exons 6 and 8, and 3h for exon 7. The nuclear immunostaining of p53+ cells provided efficient protection from UV irradiation as detectable PCR product was obtained even after 6h of irradiation (b, Lane 11).

3.7.1.4 Determination of optimal tissue section thickness for IHSA

Tissue sections used for IHSA should not be too thick, otherwise p53-negative cells on a second layer of cells could be protected from UV irradiation by p53 immunostain-positive cells above them and their DNA might be amplified during PCR. On the other hand, if the tissue section is too thin, this could give rise to variations in the amount of DNA extracted from different sections, as a variable and lower proportion of cells is likely to have enough DNA to contain the relevant p53 gene templates present.

Three sets of tissue sections were cut at the different thicknesses of 4μm, 6μm, and 8μm. All sections were p53 immunostained; one from each set was kept for coverslipping and light microscopy inspection and the others were used for IHSA. This experiment was similar to that described in section 3.7.1.3, with the modification that different tissue section thicknesses were used and UV exposure times were only up to 60 min. With these conditions a gradual decrease in the intensity of the PCR products could be observed and the variation between sections of different thickness assessed.

PCR amplification of all exons of the p53 gene showed good consistent amplification of DNA extracted from sections 6μm and 8μm thick, while amplification of DNA from 4μm sections was variable. Only results from 4μm and 6μm sections are shown in Fig. 3.7.4.

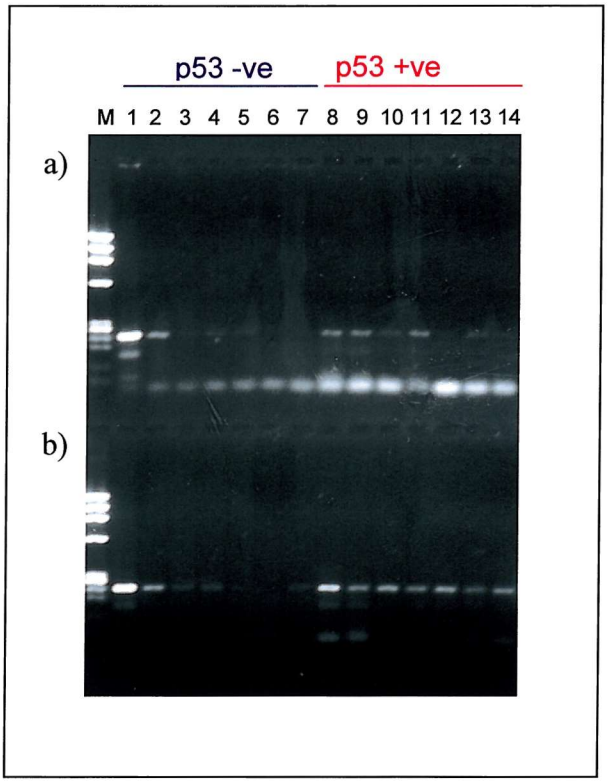

Fig. 3.7.4. Determination of optimal tissue section thickness for IHSA. PCR amplification of exon 7 of the p53 gene from DNA extracted from 4μm thick (a) and 6μm thick (b) sections after UV irradiation for different lengths of time. For both sets: Lane M, ΦX174 molecular weight marker; Lane 1, no UV irradiation; Lane 2, 10 min; Lane 3, 20 min; Lane 4, 30 min; Lane 5, 40 min; Lane 6, 50 min; Lane 7, 60 min of UV irradiation of p53 immunostain-negative cells; Lane 8, no UV irradiation; Lane 9, 10 min; Lane 10, 20 min; Lane 11, 30 min; Lane 12, 40 min; Lane 13, 50 min; and Lane 14, 60 min of UV irradiation of p53 immunostain-positive cells. PCR amplification of p53 positive cells was less variable for 6μm sections (b) than it was for 4 μm sections (a).

Inspection of the different sections by light microscopy showed that, while 4μm and 6μm sections contained cells in a clear single layer, the 8μm section looked less clear, with cells present from more than one layer. Based on these results, tissue section thickness of 6μm was chosen for subsequent IHSA experiments.

3.7.2 Initial IHSA results

Positive results obtained during the optimisation steps of the IHSA technique demonstrated that this strategy could be applied successfully to immunostained tissue sections. Therefore, sections from four EATL blocks were prepared for IHSA and an experiment was performed as described in section 2.8.3. Based on results obtained in section 3.7.1.4, a UV irradiation time of 50 min was selected for this initial experiment.

PCR amplification of the four exons of the p53 gene from the DNA extracted from the UV irradiated sections showed no detectable product on agarose gels. PCR amplification of non-irradiated DNA was positive.

The PCR method employed might not have been sensitive enough to amplify the minority population of intact DNA strands present in the sample to detectable levels, therefore methods to increase the sensitivity of PCR amplification were investigated.

3.7.3 Increasing PCR sensitivity

In order to increase the sensitivity of PCR amplification of samples that had been exposed to UV irradiation, methods such as degenerate oligonucleotide-primed (DOP)-PCR, primer-extension pre-amplification (PEP) and nested PCR were applied.

A series of samples containing DNA extracted from p53-positive, UV-irradiated tissue sections was prepared as in section 2.8, so that DOP-PCR and PEP could be applied and results compared. Fifteen UV exposure times were used as follows: no UV exposure, 2 min, 5 min, 10 min, 15 min, 20 min, 25 min, 30 min, 35 min, 40 min, 45 min, 50 min, 55 min, 60 min and 65 min. A control containing DNA extracted from a section that had not been immunostained or UV irradiated was included to ensure that DNA extraction was successful.

3.7.3.1 Degenerate oligonucleotide-primed (DOP)-PCR

Degenerate oligonucleotide-primed PCR amplification was performed according to conditions described in Appendix E.3. Only a selection of time-points was chosen for amplification, including samples irradiated for 2 min, 10 min, 30 min, 60 min and 65 min. Specific PCR amplification was performed using DOP-PCR products as templates (2μl aliquots from each reaction) and external primers for exon 8 (see Appendix E.1).

Although DOP-PCR amplification was successful, as can be seen by the amplification of the control sample (Fig. 3.7.5, Lane 6) and the sample irradiated for 2 min (arrowhead), it was not sensitive enough to amplify the DNA from samples UV irradiated for longer times. Fig. 3.7.5 (a) shows the result of specific PCR amplification of the respective DOP-PCR products shown in (b).

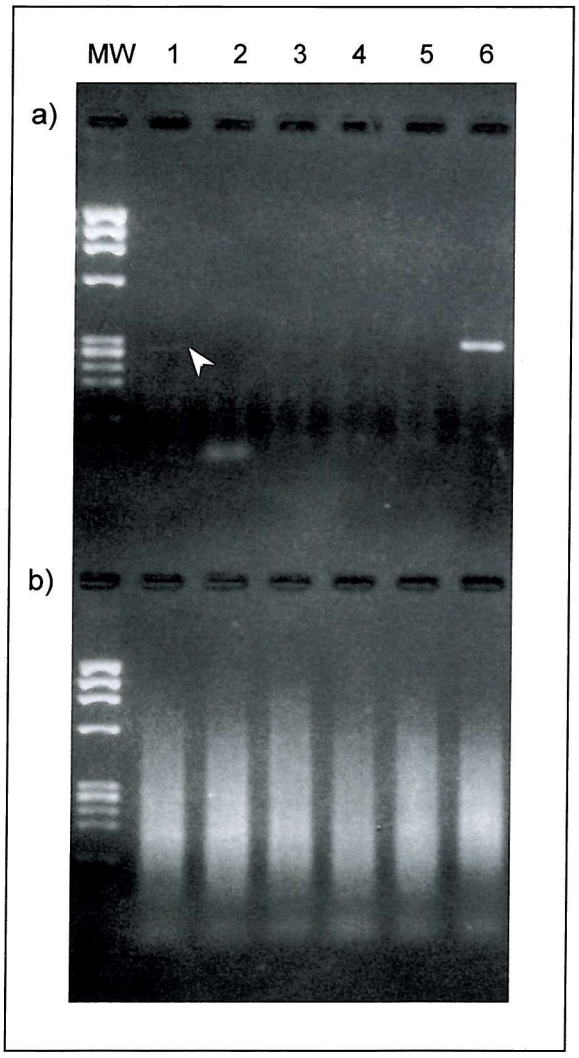

Fig. 3.7.5. Specific PCR amplification of exon 8, following DOP-PCR amplification of UV irradiated samples. (a) Specific PCR products. MW, ΦX174 molecular weight marker; Lane 1, 2 min; Lane 2, 10 min; Lane 3, 30 min; Lane 4, 60 min; Lane 5, 65 min of UV irradiation. Lane 6, no UV irradiation, no immunostaining. (b) DOP-PCR products. Lanes as for (a). Arrowhead indicates weak specific PCR product in Lane 1.

3.7.3.2 Primer-extension pre-amplification (PEP)

The PEP method was applied to the same series of UV-irradiated samples, followed by specific amplification of exon 8, as described in section 2.10.

Successful PCR amplification of exon 8 was achieved using PEP products as templates and is shown in Fig. 3.7.6.

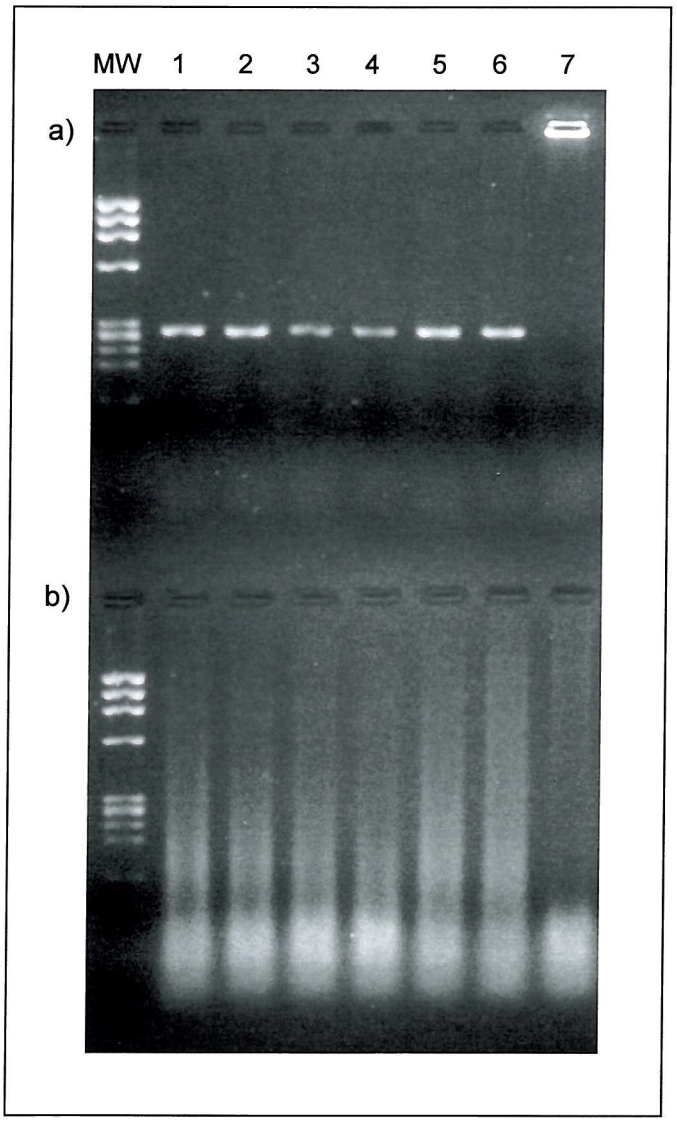

Fig. 3.7.6. Specific PCR amplification of exon 8, following PEP of UV irradiated samples. (a) Specific PCR products. MW, ΦX174 molecular weight marker; Lane 1, no UV irradiation; Lane 2, 2 min; Lane 3, 25 min; Lane 4, 55 min of UV irradiation; Lane 5, positive control using amplifiable DNA from a different sample; Lane 6, no UV irradiation, no immunostaining; Lane 7, negative control to which no DNA had been added during PEP. (b) PEP products. Lanes as for (a).

3.7.3.3 Nested PCR

Despite the successful results described in section 3.7.3.2, PEP failed to amplify UV-irradiated DNA in a subsequent IHSA experiment. This experiment was similar to that described above, the only differences being the use of a different tissue sample and UV exposure times as follows: no UV irradiation, 2 min, 5 min, 10 min, 20 min, 30 min, 40 min, 50 min, 60 min, 70 min and 90 min of UV irradiation.

Amplification of the UV-irradiated DNA samples using the standard PCR technique (Section 2.5.3) produced only weak products (Fig. 3.7.7 a). However, when PEP was performed prior to specific amplification, no great improvement in the intensity of the PCR products was achieved (Fig. 3.7.7 b).

The nested PCR method (Section 2.8.4) was then carried out using the same samples with markedly improved results (Fig.3.7.7 c). Bright bands can be seen, even in lanes 9 and 10 in which no PCR product could be detected using the PEP method (Fig. 3.7.7 b).

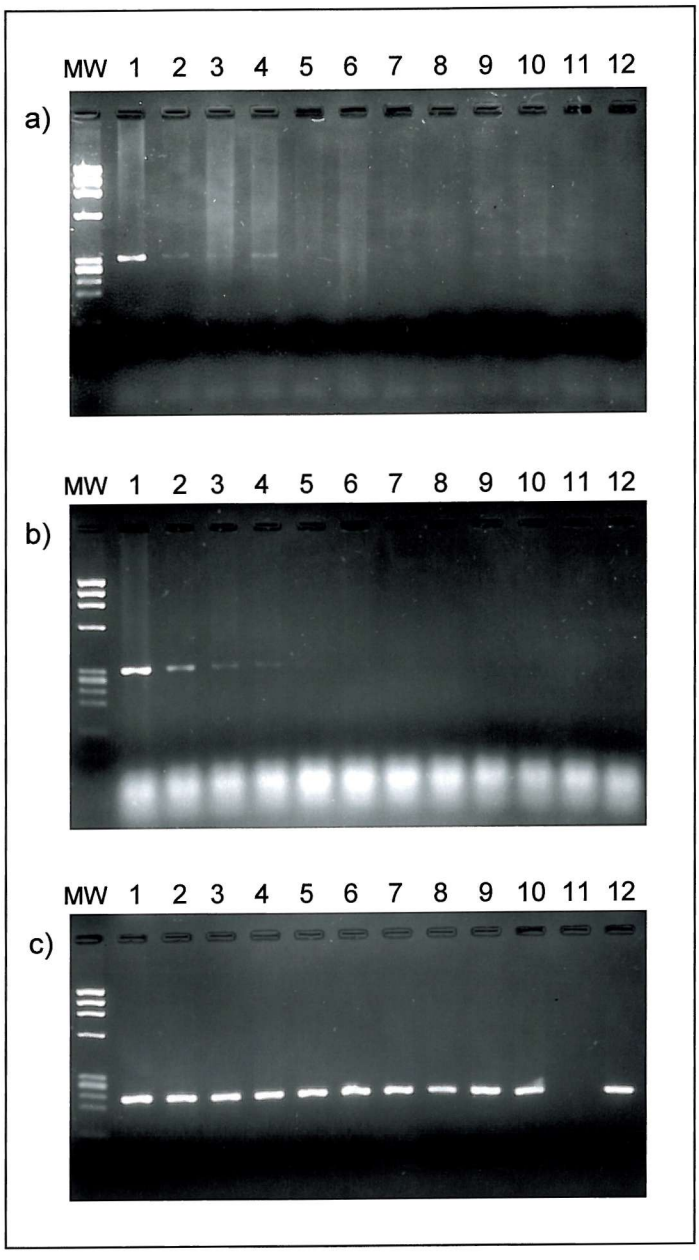

Fig. 3.7.7. Comparison between amplification using standard PCR (a), standard PCR following PEP amplification (b) and nested PCR (c). MW, ΦX174 molecular weight marker; Lane 1, no immunostaining and no UV irradiation; Lane 2, no UV irradiation; Lane 3, 2 min; Lane 4, 5 min; Lane 5, 10 min; Lane 6, 20 min; Lane 7, 30 min; Lane 8, 40 min; Lane 9, 50 min; Lane 10, 60 min; Lane 11, 70 min and Lane 12, 90 min of UV irradiation of sections.

Due to the superior sensitivity of nested PCR, this method was chosen for amplification of UV irradiated DNA samples in subsequent experiments. The increased sensitivity of nested PCR is also illustrated in Fig. 3.7.14 in Section 3.7.4.3.

Optimisation of the nested PCR technique was required before successful specific amplification was achieved. This optimisation is described in Section 3.7.3.4 below.

3.7.3.4 Optimisation of nested PCR

Initial nested PCR results were obtained by amplifying DNA samples with primers external to the ones originally used. A 1µl aliquot of PCR product from the first round reactions was used as template for the second round of PCR, in which primers internal to the first set were employed. Electrophoresis of these products showed the presence of multiple weaker bands, as well as the expected specific product.

A titration of the amount of first round PCR product to be used as template for the second round PCR was performed. Aliquots from a first round PCR product were diluted 1:2, 1:5 and 1:10, and 1µl used as template for the second round PCR. A specific band was obtained when using a 1:10 dilution of the first round PCR product and is shown in Fig. 3.7.8, lane 4.

In order to increase the sensitivity and specificity of PCR amplification, the DNA polymerase employed was changed to a 'hot start' DNA polymerase (HotStar *Taq* DNA polymerase, Qiagen Ltd.).

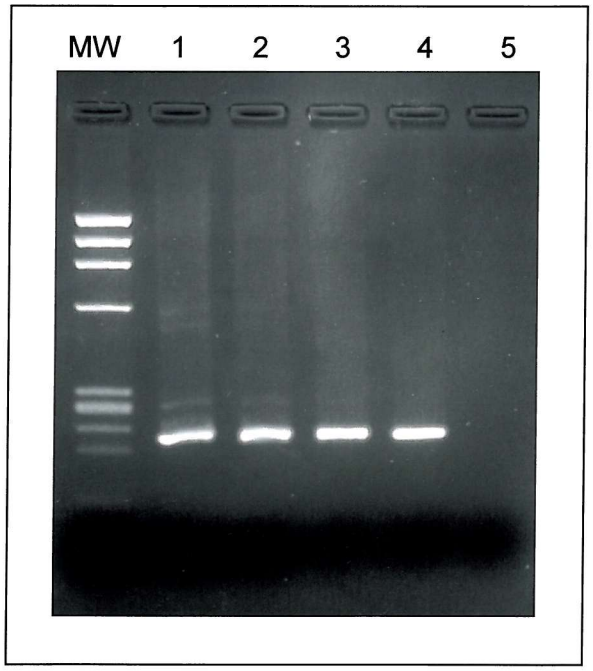

Fig. 3.7.8. Titration of first round PCR product for specific nested PCR. MW, ΦX174 molecular weight marker; Lane 1, neat; Lane 2, 1:2 dilution; Lane 3, 1:5 dilution; Lane 4, 1:10 dilution of first round PCR product. Lane 5, negative control.

3.7.4 Experiment to confirm that UV light selectively inactivates background DNA

Preliminary IHSA results obtained from PCR amplification of p53 immunostain-positive and –negative cells after UV irradiation suggested that background DNA from immunostain-negative cells had been inactivated, while DNA from positive cells was protected from UV irradiation and could be amplified selectively by PCR (Fig. 3.7.3).

In order to confirm these results, a p53 immunostain-positive tissue sample of ovarian carcinoma containing a known p53 mutation was employed. A series of sections was immunostained for p53, irradiated for increasing lengths of time (no UV irradiation, 2 min, 5 min, 10 min, 20 min, 30 min, 40 min, 50 min, 60 min and 90 min of UV irradiation) and prepared for PCR amplification as described in Section 2.8.

After nested PCR amplification, SSCP analysis was performed on the amplified products and the result can be seen in Fig. 3.7.9. The inactivation of wild-type DNA (exon 5) can be seen from 10 min (lane 4) of UV irradiation onwards, as bands representing normal DNA disappear while the mutated DNA (identified by the shifted bands) can still be amplified. This result confirmed that the background (wild-type) DNA can be inactivated so that only PCR products containing the mutated sequence will be obtained. These data have now been published (Phelps *et al.*, 2000).

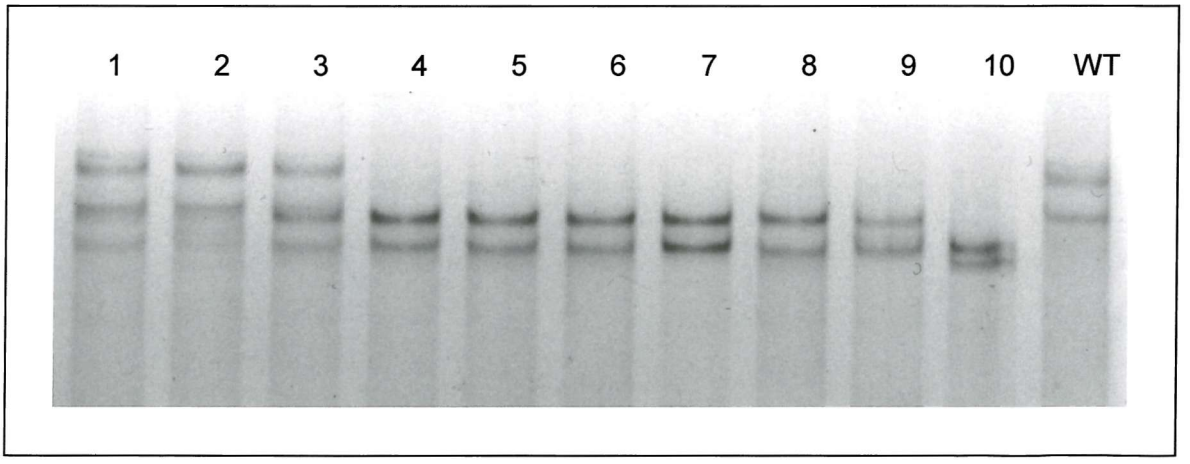

Fig. 3.7.9. SSCP analysis of PCR amplification of exon 5 of the p53 gene after UV irradiation of tissue sections containing p53 immunostain-positive cells. UV irradiation times were as follows: Lane 1, no UV irradiation; Lane 2, 2 min; Lane 3, 5 min; Lane 4, 10 min; Lane 5, 20 min; Lane 6, 30 min; Lane 7, 40 min; Lane 8, 50 min; Lane 9, 60 min; and Lane 10, 90 min of UV irradiation. WT, wild-type DNA.

3.7.4.1 Sequencing of PCR products

Direct sequencing of the PCR product in lane 8 (Fig. 3.7.10) confirmed that it contained the same mutation as previously identified by Dr. Ian Campbell's research team (Princess Anne Hospital, Southampton).

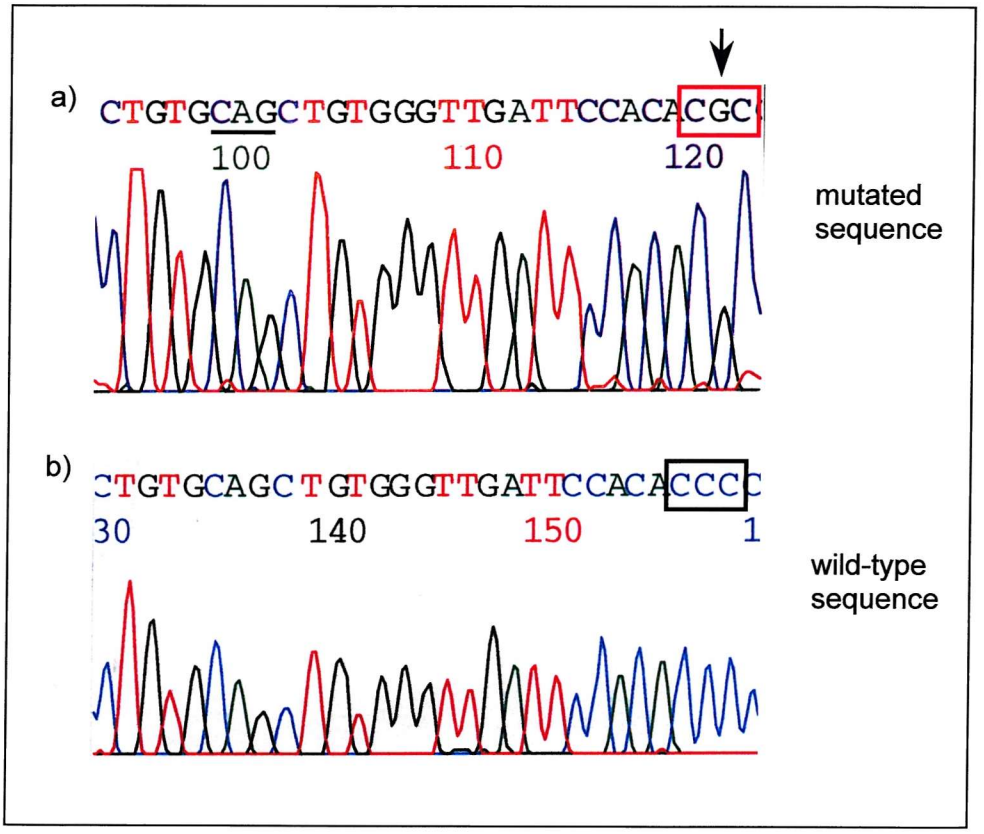

Fig. 3.7.10. Electropherogram showing a point mutation in exon 5. Sequencing of the PCR product shown in Fig. 3.7.9, lane 8, confirmed it to contain a previously identified mutation (a). The arrow indicates the mutated base. The wild-type sequence of exon 5 is shown for comparison (b). The underlined codon is highlighted for comparison with Fig. 3.7.11.

A mobility shift different from the one present in the remaining samples was observed in the sample in lane 10. Direct sequencing of this PCR product was also performed and showed that the change in mobility shift was due to an alteration in the sequence, additional to the original mutation (Fig. 3.7.11). Sequencing of the PCR products was performed by Oswel Research Products Ltd.

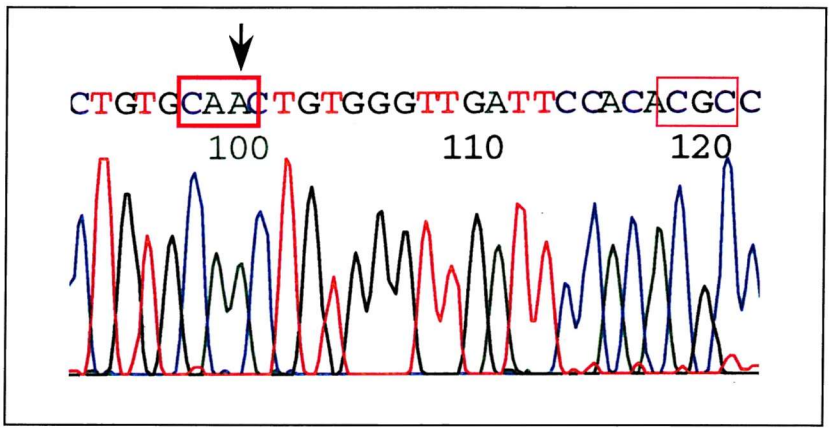

Fig. 3.7.11. Electropherogram showing the additional mutation in the sample with altered mobility shift. Arrow indicates the mutated base.

Nested PCR was repeated for the sample in lane 10 (Fig. 3.7.9), and new products showed the original mobility shift rather than the altered one (Fig. 3.7.12).

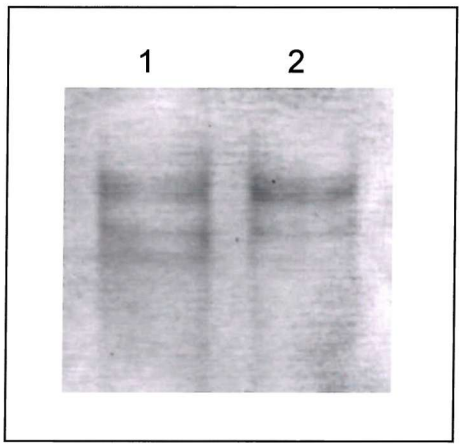

Fig. 3.7.12. Re-amplification of sample from lane 10 in Fig.3.7.9 using nested PCR. Lane 1, sample from lane 10 (90 min UV irradiation); Lane 2, sample from lane 8 (50 min UV irradiation).

3.7.4.2 Use of a proof-reading enzyme to increase amplification fidelity

A potential problem associated with amplification of samples containing low copy number targets is misincorporation of nucleotides by the DNA polymerase. A mis-incorporation that occurs early in the cycling programme can be amplified exponentially and come to be present in a significant proportion of the final PCR product.

In order to decrease the probability of possible misincorporations when amplifying UV irradiated samples a proof-reading DNA polymerase isolated from *Pyrococcus woesei (Pwo)* was employed (Hybaid Ltd.). The composition of PCR reactions and cycling parameters are described in Appendix E.5. Nested PCR was performed using *Pwo* DNA polymerase for the first round PCR and HotStar *Taq* DNA polymerase (Qiagen Ltd.) for the second round of amplification.

The samples chosen for amplification included DNA from p53 immunostain-positive tissue sections UV irradiated for 40 min, 60 min and 90 min, as well as PEP products pre-amplified from the same three samples of DNA. All samples selected had been previously successfully amplified using HotStar *Taq* DNA polymerase. A control sample containing DNA from sections that had not been immunostained or exposed to UV irradiation was included.

Amplification using the *Pwo* DNA polymerase was only successful for the control sample and no bands were detected for any of the other samples following agarose gel electrophoresis (Fig. 3.7.13). As the sensitivity of this enzyme did not seem sufficient to amplify UV-irradiated samples, HotStar *Taq* DNA polymerase remained the enzyme of choice for subsequent IHSA experiments.

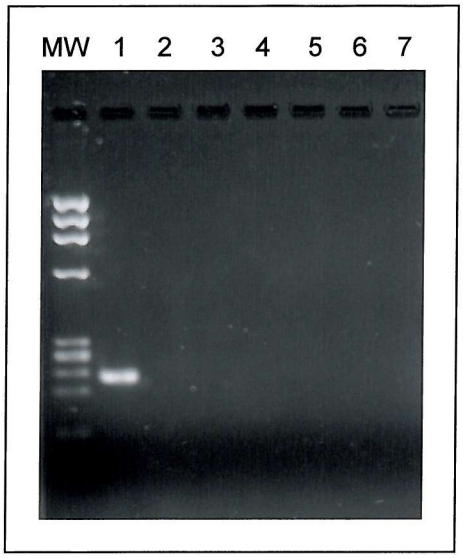

Fig. 3.7.13. Nested PCR amplification of UV irradiated samples using *Pwo* DNA polymerase in the first round PCR. MW, ΦX174 molecular weight marker; Lane 1, control containing intact DNA; Lane 2-4, DNA from tissue samples irradiated for 40 min (Lane 2), 60 min (Lane 3) and 90 min (Lane 4); Lane 5-7, PEP products pre-amplified from DNA from tissue samples irradiated for 40 min (Lane 5), 60 min (Lane 6) and 90 min (Lane 7).

3.7.4.3 Determining UV exposure times necessary for each exon for complete DNA inactivation

Unstained tissue sections were irradiated for increasing lengths of time in order to determine UV exposure times required for complete inactivation of DNA present in p53 immunostain-negative cells.

Nested PCR amplification for each exon was performed using these samples and results are shown in Fig. 3.7.14.

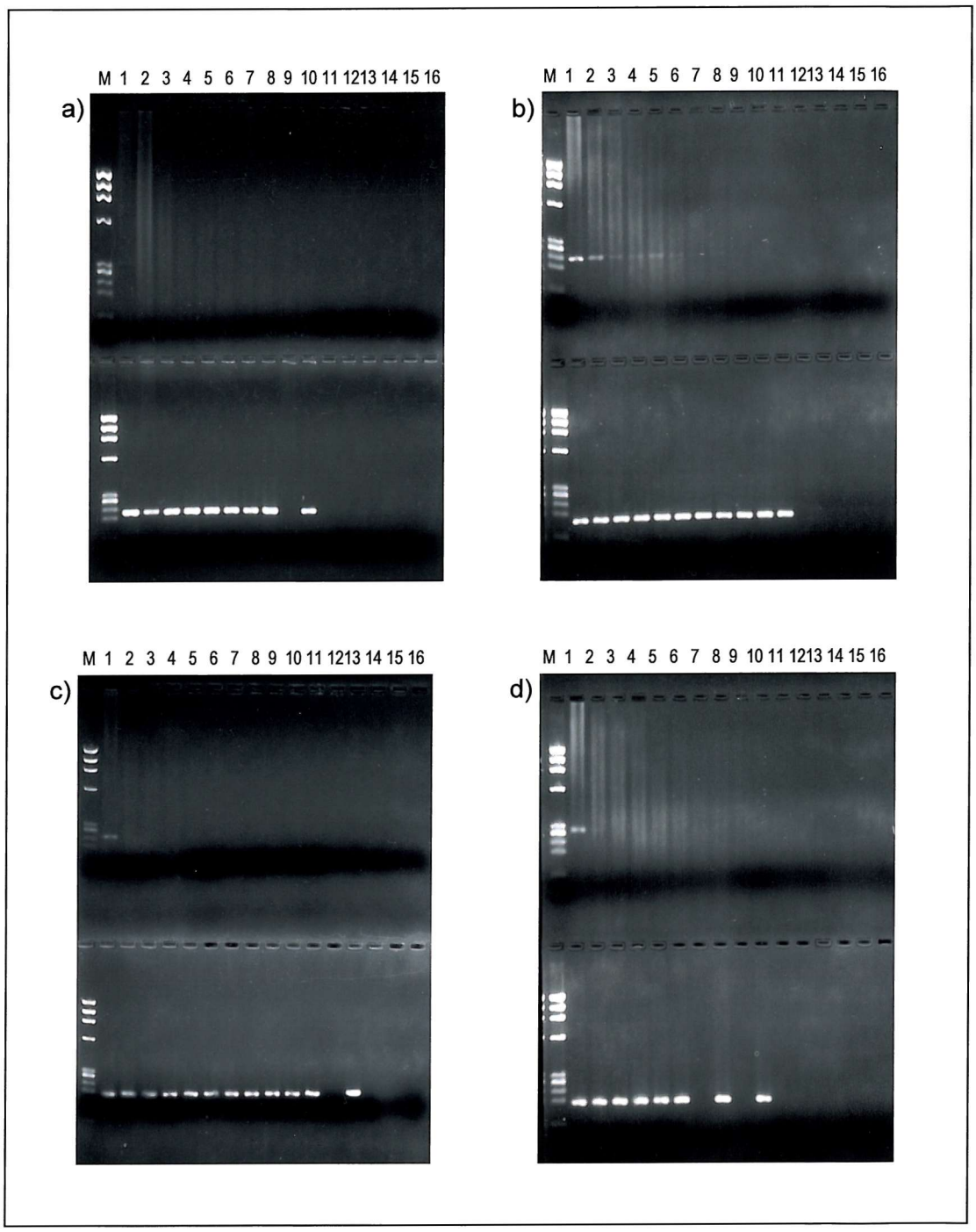

Fig. 3.7.14. Inactivation of unprotected DNA from unstained cells. Amplification of exons 5, 6, 7 and 8 are shown in (a), (b), (c) and (d), respectively. For each exon amplification of UV irradiated samples is shown after first round PCR (top half) and after nested PCR (bottom half). M, ΦX174 molecular weight marker; Lane 1, no UV irradiation; Lane 2, 5 min; Lane 3, 10 min; Lane 4, 15 min; Lane 5, 20 min; Lane 6, 30 min; Lane 7, 40 min; Lane 8, 50 min; Lane 9, 60 min; Lane 10, 90 min; Lane 11, 120 min; Lane 12, 150 min; Lane 13, 180 min; Lane 14, 210 min; Lane 15, 240 min; Lane 16, 300 min of UV irradiation.

For this experiment, optimal UV exposure times for DNA inactivation for each exon were 120 min for exon 5, 150 min for exon 6, 210 min for exon 7, and 120 min for exon 8 (Fig. 3.7.14). Different UV exposure times for DNA inactivation were observed for different blocks of tissue; the mean values (±S.E.) obtained after 4 experiments were 83 min ± 14 min for exon 5, 95 min ± 24 min for exon 6, 113 min ± 35 min for exon 7, and 75 min ± 26 min for exon 8.

It is interesting to note that, when unstained sections were used, UV exposure times for complete DNA inactivation were longer than the times established when protected cells were present. Fig. 3.7.9 shows an example in which background DNA was inactivated after only 10 min of UV irradiation for exon 5.

3.7.4.4 Application of IHSA to EATL cases

Five blocks of tissue from EATL cases (3 T and 2 A samples) were selected for IHSA. Positivity for p53 protein was present in 43% and 64% of cells in 2 T samples, the third T sample showed p53-positive cells in IEL (7 IEL per 100 epithelial cells) and in the lamina propria (2%). The A sections also showed p53 positivity in IEL (8 and 11 IEL per 100 epithelial cells) and in the lamina propria (1% and 23%, respectively). After three unsuccessful attempts at PCR amplification following UV irradiation, a weak PCR product was obtained for one of the samples (Sample 10) after 15 min UV irradiation. This sample showed a mobility shift upon SSCP analysis and was selected for sequencing analysis. A mutation was identified and the results obtained are described in Section 3.6.2.

3.7.5 Selective ultraviolet radiation fractionation

In order to apply selective ultraviolet radiation fractionation (SURF) to cases in which the amount of p53 protein accumulated in the nuclei of cells is not enough to provide adequate protection from UV light upon immunostaining, the following experiment was performed.

A case that showed p53-positive staining was selected and a series of sections was cut and immunostained. Two sets of tissue sections were prepared to be UV-irradiated for different lengths of time. One set was prepared for IHSA, as in Section 2.8, and one set

was prepared for SURF, as in Section 2.12. A separate set of unstained tissue sections was also included to ensure inactivation of DNA from p53-negative cells.

Photocopies of sections used for IHSA and SURF were enlarged to show the ink dots placed on the p53-positive areas of tissue sections used in SURF (Fig.3.7.15).

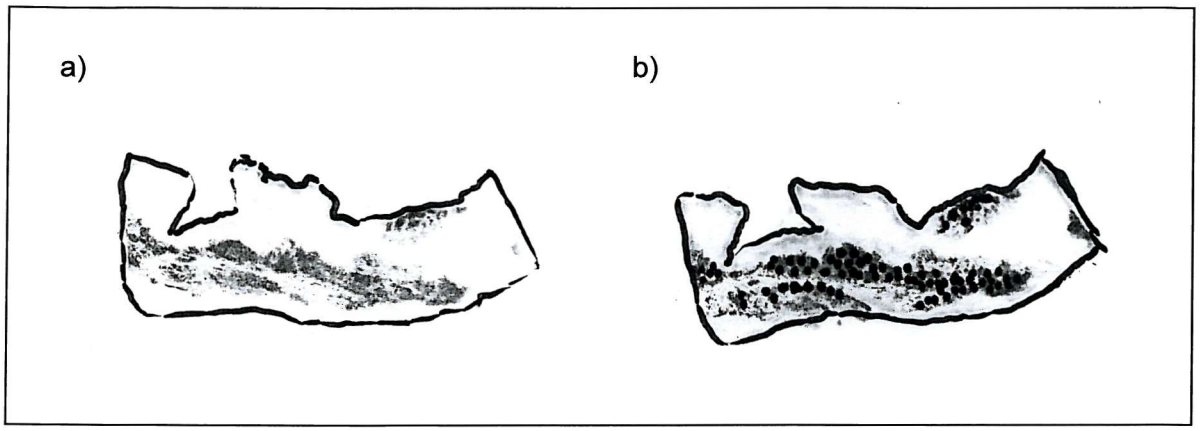

Fig. 3.7.15. Tissue sections prepared for IHSA and SURF. The outline of the section has been drawn onto the glass slide for reference. (a) The dark areas represent the enhanced immunostaining used for IHSA. (b) Sections for SURF are prepared by applying approximately 70-80 ink dots on p53-positive areas.

Tissue sections from each set were UV irradiated as follows: no UV irradiation, 2 min, 5 min, 10 min, 20 min, 40 min, 90 min and 150 min. After DNA extraction, nested PCR for exon 8 was performed on the samples.

The results only showed successful amplification of the samples that had not been irradiated in the IHSA set and in the unstained set of sections. No product, however, was amplified from the corresponding section from the SURF set. This strongly suggested that the ink used was inhibiting PCR amplification.

A titration of the number of ink dots applied to each section was performed in order to confirm a possible inhibitory effect of the ink used. An increasing number of dots was applied to each tissue section as follows: no dots, 10 dots, 20 dots, 40 dots and 80 dots. Three such sets of sections were prepared and exposed to UV irradiation for 0 min, 5 min and 60 min.

The results obtained after nested PCR amplification of exon 5 indicate that higher concentration of ink dots exert an inhibitory effect on PCR that seems to be enhanced by prolonged exposure to UV light (Fig.3.7.16). A decrease in PCR product intensity is observed with the increase in number of ink dots for all three sets. A decrease in band intensity is also seen for the '80 dots' samples as UV irradiation time increases. The absence of a band in lane 11 indicates the inactivation of unprotected background DNA after 60 min of irradiation.

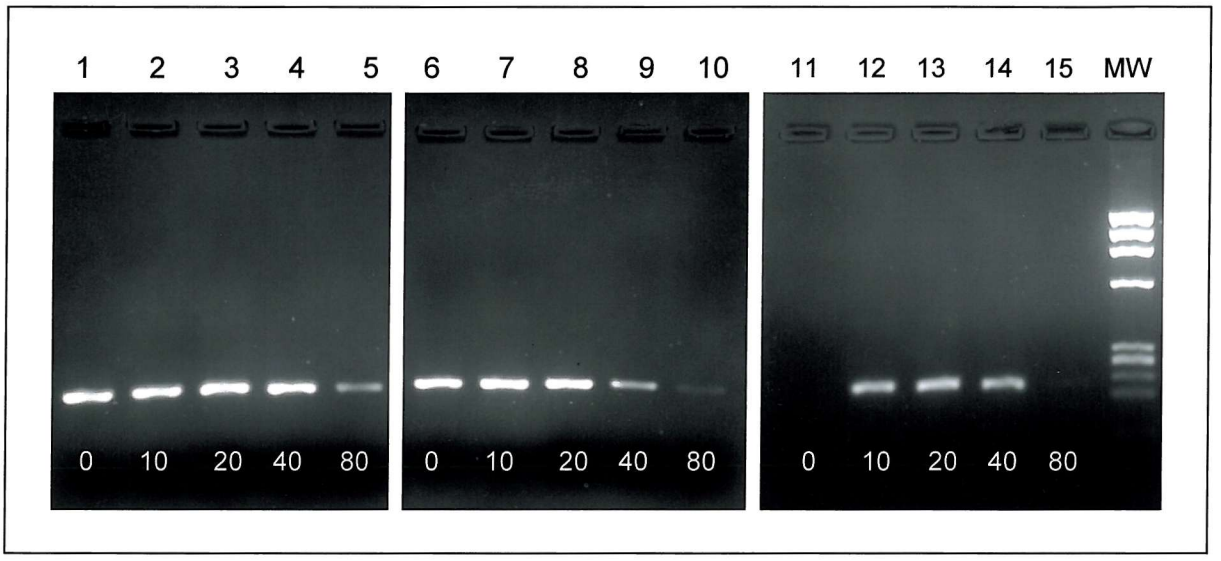

Fig. 3.7.16. Titration of number of ink dots applied to SURF tissue sections. Lanes 1-5, no UV irradiation; Lanes 6-10, 5 min UV irradiation; Lanes 11-15, 60 min UV irradiation. MW, ΦX174 molecular weight marker. White numbers below the bands show the number of ink dots applied to the sections.

The results above indicate that, to ensure successful PCR amplification of UV-irradiated samples, ink dot numbers should be kept below 20. The results also show that sufficient cells are protected from irradiation even when only 10 ink dots are applied. The strong intensity of the band for 10 dots indicates that a smaller number of ink dots should still protect enough DNA to produce detectable PCR products.

3.7.6 Summary

All steps involved in the IHSA method were optimised so that it could be applied successfully to formalin-fixed, paraffin-embedded tissue sections. Although it was possible to apply IHSA to 4 cases of ovarian and colon carcinoma, attempts to apply the technique to EATL cases were less successful. Only one sample (Sample 10, Case 2) produced a detectable PCR product after UV irradiation of the section. A mutation was identified in the amplified product upon sequencing analysis.

The SURF technique was also optimised and shown to produce PCR amplimers with strong signal in an agarose gel. This suggests that, for cases which fail PCR amplification during IHSA, the immunostaining is not offering enough protection from UV irradiation, as insufficient p53 protein is accumulated in the cell nuclei to provide a dense coloured product. The use of SURF for cases with weak p53 staining is indicated.

3.8 LOSS OF HETEROZYGOSITY ANALYSIS

3.8.1 Preliminary results

Ideal conditions for LOH analysis were determined through the experiments described below.

3.8.1.1 Determination of ideal conditions for electrophoresis

To ensure that optimal band resolution was achieved, two different gel conditions were attempted, as well as two different treatments to the samples prior to loading. The samples chosen for this experiment were EATL cases for which T and A samples were available. Cases for which T samples showed a high percentage of p53 immunopositive cells were selected in order to decrease the possibility of contaminating DNA from normal cells obscuring initial LOH analysis results. The selected samples are shown in Table 3.8.1 below.

Case	1		16		14		
Sample	1	18	31	32	B	E	H
T/A	T	A	T	A	A	T	lymph node
p53 % positivity	43%	< 1%	63%	negative	< 1%	< 1%	negative

Table 3.8.1. Samples selected for LOH analysis and percentage of p53 positive cells present. T and A refer to tumour and adjacent tissue samples, respectively.

Amplification of DNA samples was performed as described in Section 2.16.1. Samples were analysed in a nondenaturing 6% polyacrylamide gel containing 5% glycerol (see Appendix G.3) and in an MDE gel (see Appendix G.2). Samples 31 and 32 were not analysed in an MDE gel, as analysis in a 6% polyacrylamide gel had shown that samples from Cases 1 and 14 would provide sufficient information to determine ideal gel conditions for LOH analysis. Results obtained are shown in Figures 3.8.1 and 3.8.2.

Samples were prepared in the following ways before loading into the gels. One set of samples was prepared by mixing an aliquot of the sample with a TBE-based loading buffer (gel loading buffer B; see Appendix F), and the second set was prepared by

mixing an aliquot of the sample with stop solution (see Appendix F), then denaturing the samples for 8 min at 94°C and rapidly chilling them on ice before loading into the gel. In an attempt to improve resolution of samples that were not denatured prior to loading, samples analysed in MDE gels were mixed with gel loading buffer C, containing glycerol (see Appendix F), rather than gel loading buffer B.

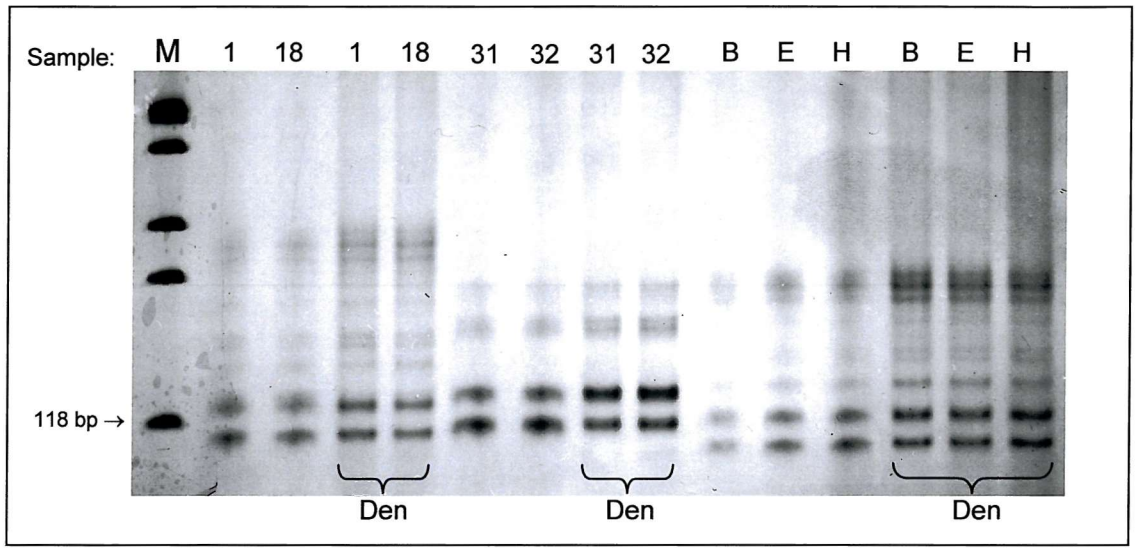

Fig. 3.8.1. LOH analysis of samples in a 6% polyacrylamide gel containing 5% glycerol. Key: M, ΦX174 molecular weight marker; Numbers/letters above each lane refer to samples used (see Table 3.8.1); *Den* refers to denatured samples.

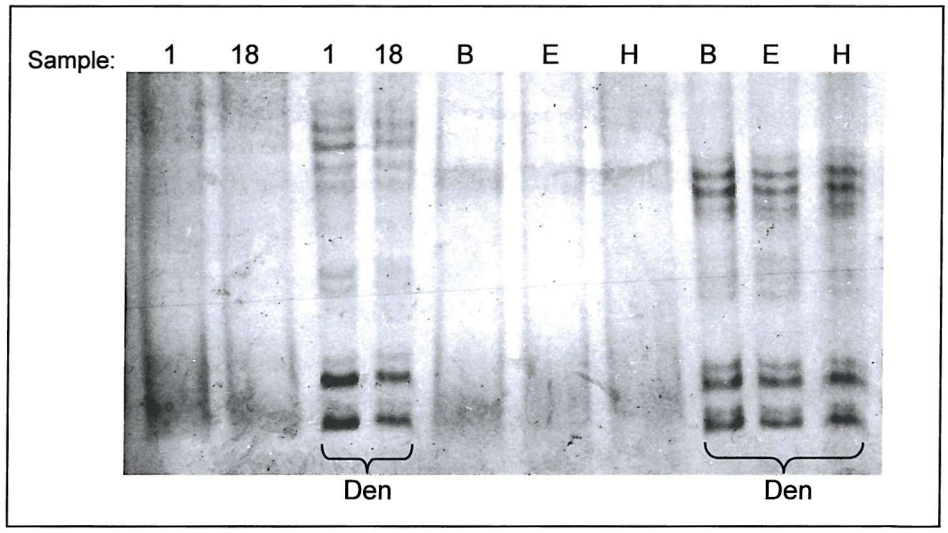

Fig. 3.8.2. LOH analysis of samples in an MDE gel.
Key: Numbers/letters above each lane refer to samples used (see Table 3.8.1); *Den* refers to denatured samples.

Samples electrophoresed in MDE gels showed bands with better separation. Samples prepared by mixing them with gel loading buffer B (Lane 1) showed poor resolution under both sets of gel conditions. Gel loading buffer C (Lane 2) was only tested with MDE but produced the worst results, with very faint bands visible. Fig. 3.8.3 shows the superior band resolution obtained by using stop solution and sample denaturation (Lane 3) in comparison to mixing the samples with gel loading buffers B or C.

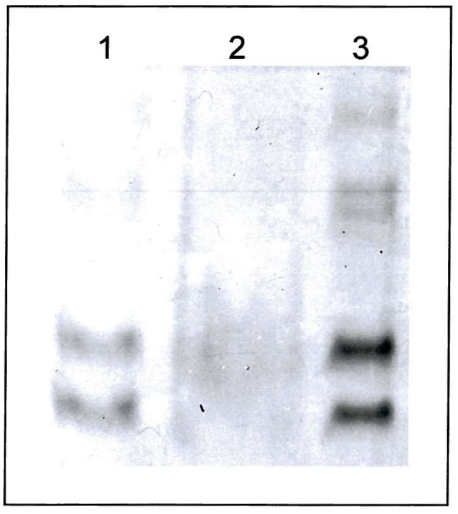

Fig. 3.8.3. Comparison between different types of sample preparation prior to loading into an MDE gel. Aliquots used were taken from the same sample. Lane 1, sample mixed with gel loading buffer B; Lane 2, sample mixed with gel loading buffer C; and Lane 3, sample mixed with stop solution then denatured and chilled on ice.

3.8.1.2 Determination of ideal number of PCR cycles

The interpretation of LOH analysis results when utilising microsatellite PCR can be complicated by the presence of "stutter bands". These are artefacts of amplification that vary in length around the major fragments by either 1 bp, 2 bp, or multiples thereof (Koreth *et al.*, 1998). They are believed to be produced by "slipped strand mispairing", a process in which the *Taq* polymerase and the DNA strand it is synthesizing slip forward or backward to the next dinucleotide repeat (Koreth *et al.*, 1998).

Another hypothesis to explain stutter bands is that their presence is a secondary phenomenon resulting from improper reannealing of fully-extended PCR products that undergo denaturation and reassociation after PCR efficiency reaches the amplification plateau. Because reassociation of repetitive sequences is much faster than that for the flanking non-repetitive sequences, misalignment of double stranded DNA by one or more units of repeat might occur during reannealing. This would appear as high

molecular weight products in non-denaturing gel electrophoresis, because of overhanging sequences at the 5' and 3' ends of the PCR fragments (Bovo *et al.*, 1999).

Whether the presence of multiple bands is due to slippage of the DNA polymerase or due to improper reannealing of the DNA strands, decreasing the number of cycles during PCR amplification is believed to eliminate or significantly reduce the problem (Bovo *et al.*, 1999; Koreth *et al.*, 1998).

In order to eliminate the presence of larger fragments observed during LOH analysis in non-denaturing conditions, two sets of DNA samples from ovarian carcinoma cases were amplified by PCR for different number of cycles. One set was amplified for 35 cycles, while for the second set the amplification programme was reduced to 28 cycles.

The reduction of cycle number produced a decrease in signal for both specific and non-specific products (Fig. 3.8.4). For case 2, the intensity of the signal obtained for the specific product using a 28-cycle programme was too weak to allow analysis, therefore cycle number for subsequent PCR-LOH analyses was kept at 35.

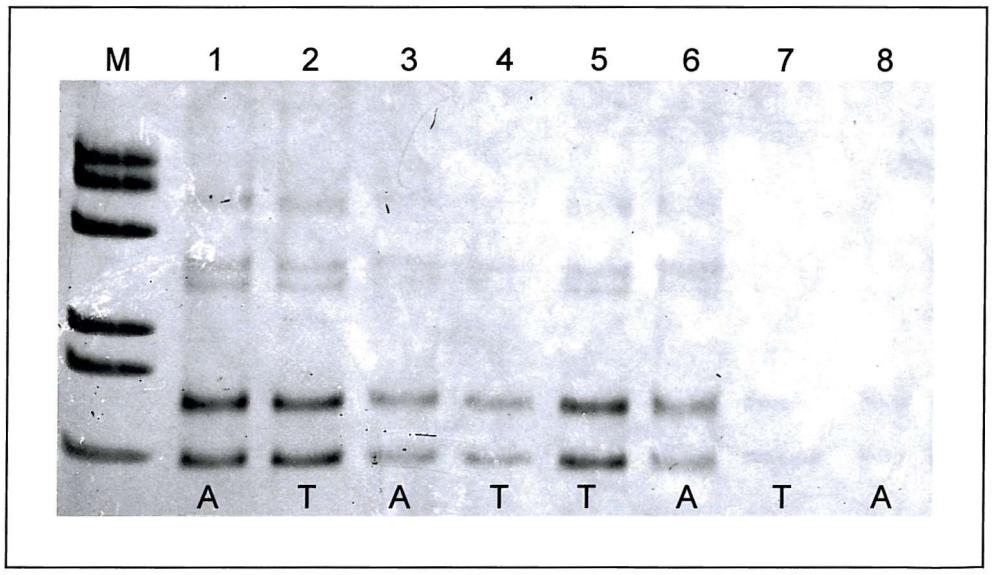

Fig. 3.8.4. Effect of reduction of PCR cycles on the presence of multiple bands during LOH analysis. M, ΦX174 molecular weight marker; Lanes 1-4, case 1; Lanes 5-8, case 2. *A* refers to p53-immunonegative tissue adjacent to tumour; *T* refers to p53-immunopositive tumour tissue.

3.8.2 Analysis of cases with known LOH

Paraffin blocks of cases of ovarian carcinoma known to show LOH for the *TP53* locus were selected for analysis to ensure that the sensitivity of the technique allowed detection of LOH (data obtained from Dr. Ian Campbell, personal communication).

As normal DNA from different tissue blocks from these selected cases was not available at the time, tissue sections were prepared and different areas were microdissected out as described in Section 2.6. In this way, tissue containing p53-positive cells could be analysed separately from tissue containing p53-negative cells.

Despite microdissection, no difference was observed between PCR products amplified from tumour DNA and from DNA from p53-negative cells (Fig. 3.8.5).

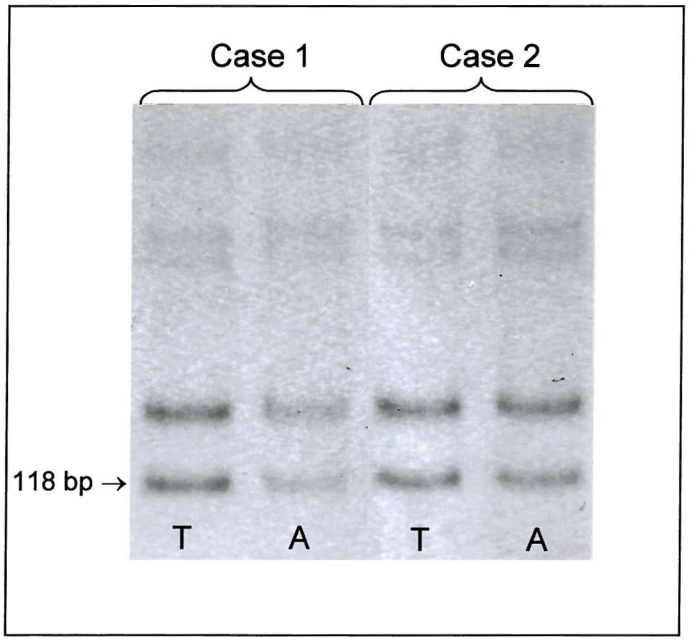

Fig. 3.8.5. LOH analysis of microdissected tissue from cases of ovarian carcinoma with known LOH. *T* refers to DNA from tumour tissue; *A* refers to DNA tissue containing p53-negative cells.

The negative results obtained in the previous experiment could be due to the presence of cells showing LOH for the *TP53* locus in the microdissected tissue, in spite of p53 negativity. Normal DNA extracted from peripheral blood from the same patients was obtained subsequently and analysed alongside DNA from tumour tissue (Fig. 3.8.6).

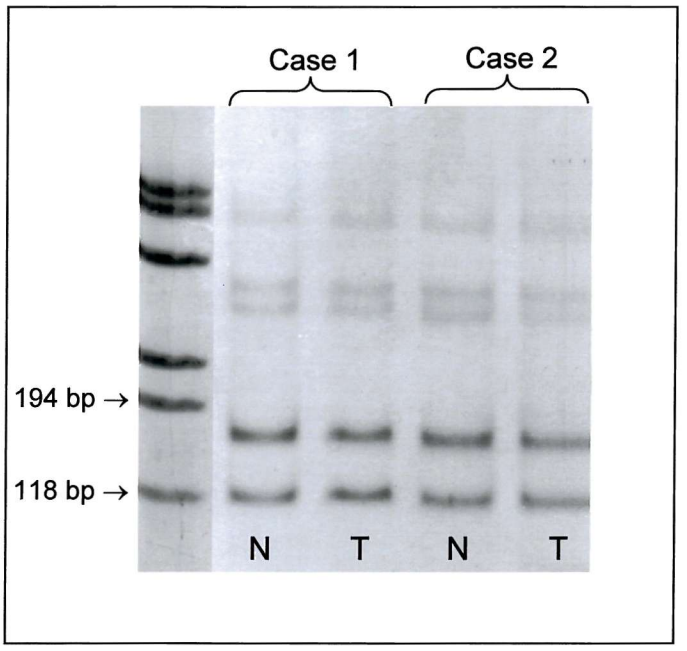

Fig. 3.8.6. LOH analysis of cases of ovarian carcinoma known to show LOH. *N* refers to normal DNA; *T* refers to DNA from tumour.

As still no difference was observed in the pattern of bands between DNA from tumour and normal DNA, IHSA was applied to sections of the ovarian tumour tissue in an attempt to eliminate contaminating normal DNA that could be masking LOH.

3.8.3 Applying IHSA to samples for LOH analysis

A case of ovarian carcinoma with known LOH for the *TP53* locus was selected for IHSA. Tissue sections were cut, immunostained and exposed to UV irradiation as in Section 3.8. UV irradiation times were 10 min, 20 min and no irradiation.

After DNA extraction, PCR amplification of the microsatellite marker was performed in two rounds, as in nested PCR. However, as no internal set of primers was available, the second round of amplification was performed with the same primers and using the same annealing temperature. A 1 μL aliquot from a 1:10 dilution from the first round PCR products was used as template for the second round of amplification. The results are shown in Fig. 3.8.7 below.

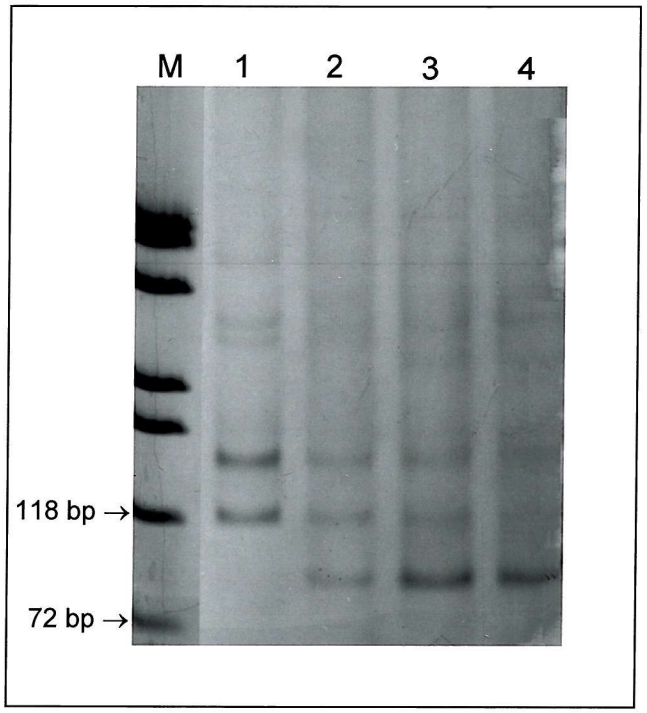

Fig. 3.8.7. LOH analysis of ovarian carcinoma case after IHSA. M, ΦX174 molecular weight marker; Lane 1, normal DNA; Lane 2, DNA from tumour section (no UV); Lane 3, DNA from tumour after 10 min UV irradiation; and Lane 4, DNA from tumour after 20 min UV irradiation.

When comparing the DNA from tumour with normal DNA, there is an extra band in the tumour DNA, indicating the presence of an additional, smaller product. While the product from the non-irradiated sample shows three bands of equal intensity, the samples that were UV irradiated show a stronger signal for the additional band, with a decrease in signal for the bands representing products from normal DNA.

A possible explanation for this result is that the tumour DNA shows a different size product due to microsatellite instability, as well as the loss of one of the bands. The decrease in signal for the normal bands seen in samples in Lanes 3 and 4 is probably due to the inactivation of contaminating DNA from normal cells in the tumour.

3.8.4 Summary

Preliminary experiments determined the ideal conditions for LOH analysis to be PCR amplification for 35 cycles, sample preparation by mixing with stop solution followed by sample denaturation and electrophoresis in an MDE gel.

Initial LOH analysis experiments were performed on paired T and A samples of EATL cases. As LOH could not be detected in the EATL cases initially tested (n=3), it was

necessary to determine whether the negative results were due to lack of LOH or due to a sensitivity problem. Cases of ovarian carcinoma with known LOH were therefore used in optimisation experiments and showed that contaminating DNA from normal cells was masking LOH. The result obtained after applying IHSA to one of the ovarian carcinoma cases has shown that it is possible to increase sensitivity of LOH analysis using UV irradiation of p53 immunostained sections. Even if sections were only irradiated for short periods of time, the resultant partial inactivation of background DNA was enough to allow detection of LOH.

4 - DISCUSSION

4.1 INTRODUCTION

Coeliac disease patients are at an increased risk of developing enteropathy-associated T cell lymphoma (EATL). Previous immunohistochemical studies in this department have shown that a large proportion (96%) of EATL cases analysed (n=23) showed p53 protein accumulation in tumour cell nuclei. Nuclei positive for p53 were also detected in lymphocytes in resection margins of enteropathic bowel unaffected by tumour (Murray *et al.*, 1995).

Accumulation of p53 in cell nuclei may occur as a result of diverse molecular mechanisms. Alterations of the p53 gene have been reported in many malignancies (Hollstein *et al.*, 1991) and, in some cases, they are responsible for increasing the gene product's half-life, so that p53 can be detected by immunohistochemistry (Adamson *et al.*, 1995; Villuendas *et al.*, 1993). The aim of this study was to determine whether p53 over-expression observed in EATL is due to mutations in the gene and, if so, whether the mutations identified in the tumour are also present in p53-immunopositive lymphocytes detected in resection margins of enteropathic bowel unaffected by tumour. Molecular genetic analysis of tumour and uninvolved adjacent tissue was used to advance understanding of the evolution of EATL from reactive T cell clones in enteropathic bowel.

The present study has confirmed that p53 protein over-expression in tumour cell nuclei is a common occurrence in EATL. Positivity for p53 was recorded in 82.8% of cases in tumour sections and in 23.8% of cases in small lymphocytes of the adjacent, uninvolved enteropathic bowel. These results are lower than the ones obtained by Murray and colleagues (1995), in which p53-positive cells were observed in 96% and 47% of cases, in tumour and uninvolved enteropathic bowel. The molecular genetic analysis revealed mobility shifts, indicative of p53 gene alterations, in 34% of tumour samples and in 15% of adjacent bowel samples. However, DNA sequencing analysis only confirmed the presence of p53 gene mutations in 10% of tumour samples and 10% of adjacent tissue

samples. Two additional cases showed p53 gene alterations but the base changes were silent, i.e. they encoded the same amino acid residue as the wild-type one.

The technique of immunohistoselective analysis (IHSA) was developed from a published method for immunohistoselective sequencing (IHSS) so that it can now be applied to formalin-fixed paraffin-embedded tissue and used to study a wide range of archival biopsy material.

4.2 IMMUNOHISTOCHEMISTRY

Accumulation of p53 protein, either caused by mutation or stabilisation by complexing with cellular or viral proteins, is a common feature in high grade non-Hodgkin's lymphomas (NHL) (Piris *et al.*, 1995). The percentage of p53 positive cases has varied in different series studied: 21% in a series of different types of NHL (including B and T cell lymphomas, anaplastic large cell lymphomas, and B cell mucosa-associated lymphomas (Martinez-Delgado *et al.*, 1997), 24% in a series of low and high grade B and T cell NHL (Adamson *et al.*, 1995), approximately 24% in high grade B cell NHL (Villuendas *et al.*, 1992), 29% in follicular lymphomas (Sander *et al.*, 1993), 31% in a series containing a variety of low and high grade NHL (48% in the high grade NHL) (Soini *et al.*, 1992), 69% in high grade NHL and 8.6% in low grade NHL (Tzardi *et al.*, 1996), 50% in non-human T cell lymphotropic virus type I (HTLV-I) related post-thymic T cell lymphomas (Matsushima *et al.*, 1994a), 30% of B cell immunoblastic lymphomas and 40% of T cell immunoblastic lymphomas (Said *et al.*, 1992), and 80% in anaplastic large cell lymphomas (Cesarman *et al.*, 1993).

Over-expression of p53 has also been demonstrated in the cutaneous T cell lymphoma (CTCL) mycosis fungoides, a disease in which neoplastic and reactive T cells, as in EATL, show epitheliotropism (MacLennan, 1996). Lauritzen and co-workers (1995) have detected p53 over-expression in 8/25 (32 %) cases of CTCL analysed. All positive cases corresponded to high grade lymphomas (8/17). In another study, over-expression of p53 protein was reported in 11/37 (29.7 %) CTCL cases, including 10/15 (67 %) cases with large cell transformation (Li *et al.*, 1998).

Recently, Camozzi and co-workers (2000) detected p53 expression in 4/9 (44%) EATL cases analysed. In the present study, 82.8% of EATL cases investigated (n=29) were positive when immunostained for p53. This figure is higher than that previously reported for other types of lymphoma, with the exception of one series of anaplastic large cell lymphomas that were shown to have p53 positivity in 80% of cases (Cesarman *et al.*, 1993).

The results suggest that p53 dysregulation, through mutation or stabilisation by another molecule, is a common event in the development of EATL. The observation that 23.8% of uninvolved adjacent (A) tissue sections also contained p53 positive cells suggests that p53 dysregulation could represent either an early event in the development of neoplastic T cell clones or that cell cycle dysregulation is also a feature of putatively non-neoplastic adjacent lymphoid cells which are undergoing antigen drive.

In 2 A biopsies, p53 positivity was observed in very few intra-epithelial lymphocytes (IEL); 1 per 100 epithelial cells or less was found. Detection of p53 in occasional cells within lymphoid tissue has been seen in non-neoplastic conditions, suggesting that p53 positivity might be a normal phenomenon, probably related to lymphocyte differentiation; Villuendas and co-workers (1992) have described occasional p53 positive cells in cases of reactive lymphadenitis whilst Mercer and Baserga (1985) showed that p53 positive nuclei were present in cultures of mitogen-stimulated lymphocytes.

It has been shown that, in some cases, the use of antigen retrieval for immunohistochemical detection of p53 over-expression may reduce p53 detection thresholds. This could lead to the detection of low levels of wild-type p53 protein that might be misinterpreted as indicating abnormality in the p53 functional pathway (Dowell and Ogden, 1996; McKee *et al.*, 1993). Indeed, in some of the cases analysed, weak p53 staining was observed in some non-lymphoid cells, especially at the base of crypts of Lieberkühn. However, this staining could easily be differentiated from the intense staining observed in tumour cells, especially when present in the same section. The weaker staining was, therefore, interpreted as representing slightly elevated cellular levels of wild-type p53 protein under conditions of active cellular proliferation, as found in cells at the base of intestinal crypts. Immunostained cells in A sections were only scored as positive when they clearly showed stronger staining than other, weakly stained, cells in the same section, such as those in the base of crypts.

Correlation of genetic analysis data with p53 immunoreactivity is discussed later in Section 4.3.

Stabilisation of the p53 protein is believed to occur in some cases as a result of the formation of complexes with other nuclear proteins such as MDM2 (Momand *et al.*, 1992). In normal cells MDM2 is part of a p53/MDM2 auto-regulatory feedback loop, in which its level in the cell is controlled by the levels of wild-type p53 protein. The p53 protein can stimulate MDM2 expression and this can then downregulate p53 function by sequestering it in an inactive complex (Gottlieb and Oren, 1996; Wu *et al.*, 1993).

Over-expression of MDM2 has been shown to inhibit p53-mediated transactivation (Momand *et al.*, 1992) and has been identified in certain tumours, particularly sarcomas (Oliner *et al.*, 1992). Watanabe and co-workers (1996) examined the expression of the mdm2 gene in 60 cases of B cell chronic lymphocytic leukaemia (B-CLL) and B cell non-Hodgkin's lymphoma (B-NHL). They found that 28.3% of cases showed over-expression at levels more than 10-fold higher than that observed in control splenic B cells. Another study investigated the pattern of expression of p53 and MDM2 protein in 87 cases of nodal NHL (Tzardi *et al.*, 1996), finding p53 positivity in approximately 45% of cases and MDM2 positivity in 26.4% of cases. All cases over-expressing MDM2 were also positive for p53. Although some studies have reported that tumours with mdm2 gene amplification showed no evidence of mutated p53 (Oliner *et al.*, 1992), some patients in whom both a mutation of the p53 gene and MDM2 over-expression are present have also been described (Watanabe *et al.*, 1996).

In order to determine whether MDM2 might play a role in the stabilisation of p53 protein in positively stained cells, immunostaining of EATL sections to detect over-expression of MDM2 protein in tumour cell nuclei was performed. Despite repeated attempts, immunohistochemical analysis using a mouse monoclonal antibody against MDM2 protein (clone 1B10, Novocastra Laboratories Ltd.) was not informative. Immunostaining of sections showed immunopositive nuclei in epithelial and stromal cells, where normal expression of MDM2 protein would be expected. Due to the pattern of staining obtained with this antibody, detection of genuine nuclear over-expression of MDM2, that could be correlated with the accumulation of p53 and pRB proteins, was not possible.

As p53 mutations were only identified in 4/24 (16.7%) cases that showed p53 accumulation in T or A sections, another mechanism is likely to be contributing to p53 stabilisation in the cell. It is therefore important that future work should include immunohistochemical analysis using an alternative MDM2 antibody to determine whether MDM2 protein accumulation has occurred in EATL cases. It may also be fruitful to investigate whether other p53 regulatory molecules are associated with the stabilisation of p53 in EATL.

4.3 PCR-SSCP ANALYSIS AND SEQUENCING

4.3.1 DNA template quality

In general, DNA suitable for PCR can be extracted from most tissue samples whether fresh, fixed, or stained. Two important factors that affect the size of target DNA which can be amplified successfully from formalin-fixed paraffin-embedded specimens are tissue fixation and the length of time for which the tissue has been stored (Greer *et al.*, 1994). Different fixatives and fixation times result in different yields and levels of degradation of DNA, which in turn affect the size of fragment which can be consistently amplified. This is generally up to 400 base pairs for paraffin-processed material (Shibata, 1994). The size of fragments that it was necessary to amplify did not pose a problem in this study, as the largest fragment analysed was 313 base pairs long.

The DNA extraction technique used most frequently with archival tissue samples involves removal of wax, overnight digestion with a proteinase enzyme to release the DNA and heat treatment to inactivate the enzyme. This produces a relatively impure extract containing a high proportion of protein but is usually adequate for PCR. Nevertheless, a failure rate of up to 10% can be expected when routine preparations are examined (Pan *et al.*, 1995).

Out of 68 paraffin blocks containing tissue samples, DNA extraction failed in only 2. This represents a 2.9 % failure rate, which is well within the range expected from routinely prepared fixed tissue samples. The seemingly low purity (ratio of absorbance at 260 nm to 280 nm) of DNA samples, averaging 1.2 (in comparison to 1.8 for a pure sample) is due to the high proportion of protein present in the extracts, as these are not further purified. Satisfactory PCR amplification was achieved in most cases; therefore, a purification step was unnecessary. In fact, if amplification is successful, further purification of the sample is generally considered undesirable because the additional steps may increase the risk of contamination (Lo, 1998c) and could further degrade the DNA as a result of mechanical shearing during handling.

DNA amplified from some samples, however, provided only a suboptimal PCR product. This usually occurred in samples in which low purity (around 1.0) was combined with a

low DNA concentration (< 0.2μg/μl). As suboptimal PCR products can affect interpretation of SSCP analysis results, this sensitivity problem was addressed by use of nested PCR. As well as increasing the sensitivity of the reaction from 100 to 1000-fold (Lo, 1998b), use of nested PCR dramatically enhances the specificity of DNA amplification since spurious, nonspecific amplification products are eliminated.

4.3.2 Frequency of p53 mutations in lymphoma

Mutations of the p53 gene have been identified in different types of NHL by PCR-SSCP analysis and sequencing. The frequency of p53 mutations detected has varied between different studies and alterations of the gene are only believed to be commonly associated with certain subtypes of lymphoma. Gaidano and co-workers (1991) have found p53 mutations associated with 9/27 (33%) cases of Burkitt lymphoma and with 5/9 (55.5%) of its leukemic counterpart L_3-type B cell acute lymphoblastic leukemia. Mutations of the p53 gene have also been identified in 9/34 (26.5%) cases of follicular lymphoma (Sander *et al.*, 1993), in 10/22 (45.5%) cases of high grade NHL (Kocialkowski *et al.*, 1995), in 9/48 (18.8%) cases of B cell lymphoma (Ichikawa *et al.*, 1992), in 1/17 (5.8%) cases of anaplastic large cell lymphoma (Cesarman *et al.*, 1993), and in 3/34 (8.8%) cases of non-HTLV-I related post-thymic T cell lymphoma (Matsushima *et al.*, 1994a). Martinez-Delgado and co-workers (1997) analysed a series of different types of lymphomas and described p53 mutations in 4/12 (33%) cases of high grade B-NHL, in 1/5 (20%) cases of high grade mucosa-associated lymphoid tissue (MALT) lymphomas, in 1/22 (4.5%) cases of anaplastic large cell lymphoma, and in 1/24 (4%) cases of T cell NHL. Mutations in the p53 gene have also been reported in 2/21 (9.5%) cases of low grade B cell NHL and 1/7 (14.3%) cases of high grade B cell NHL (Adamson *et al.*, 1995).

The frequent association of p53 mutations with high grade rather than low grade tumours suggests that p53 dysregulation may play a role in the progression of lymphomas rather than acting during the initiation phase. Du and co-workers (1995) examined 75 cases of MALT lymphoma for p53 allele loss and mutation; their results suggest that p53 partial inactivation may be involved in the development of low grade MALT lymphomas, whereas complete inactivation of the gene may be associated with high grade transformation. They found p53 mutations in 3/44 (6.8%) cases and loss of

heterozygosity (LOH) in 9/48 (18.8%) cases of low grade MALT lymphomas; in high grade MALT lymphoma, LOH was detected in 6/21 (28.6%) cases and p53 mutations were found in 9/27 (33.3%) cases. While only 1/11 (9%) low grade tumours with p53 abnormalities showed both p53 mutation and allele loss, in high grade tumours this was the finding in 6/9 (66.7%) tumours with p53 abnormalities (Du *et al.*, 1995). Recently, another study by the same group has detected mobility shifts indicative of p53mutations in 5/25 (20%) EATL cases (Camozzi *et al.*, 2000).

4.3.3 Mutation analysis of EATL cases

The detection of mobility shifts in 10/29 (34.5%) tumour (T) samples and in 3/20 (15%) adjacent histologically uninvolved tissue (A) samples in the current study suggests that p53 over-expression is associated with p53 mutation in some cases of enteropathy-associated T cell lymphoma.

Mobility shifts were identified in 7/19 (36.8%) T samples, where T and A sections were available from the same case. In 2 cases, mobility shifts were identified in the same exon in paired T and A samples. For one of the cases (Case 2), sequence analysis revealed the presence of mutations in both T and A samples. Although the mutations detected in T and A samples were present on different codons, it was interesting to note that they were adjacent to each other (codons 183 and 184). For the other case (Case 3), sequence analysis confirmed the presence of a mutation in the A sample, but not in the T sample. Although p53 immunopositivity was low in both T and A samples (5.7% and 3%, respectively), it is possible that p53 mutation in the T sample was missed due to variable sensitivity of the DNA sequencing technique when detection of DNA from relatively small populations of p53-positive cells is involved. If the same mutation had been identified in cells from both T and A samples, this would have supported the hypothesis that EATL arises by expansion and migration of a single neoplastic T cell clone developing in the enteropathic bowel.

Mobility shifts in exon 6 were detected in 2 samples from the same subject, removed with a 2-year interval between the 2 resection procedures. One sample was a T sample (from the first resection) that showed no p53 expression. The second one was an A sample (from the second resection) that did not show p53 expression by

immunohistochemistry either, although tumour resected in the same specimen did. The mobility shifts, despite involving a single exon, did not appear to be the same and sequence analysis of the samples did not confirm the presence of mutation. It is possible that no p53 expression was detected in the first T sample due to the presence of a nonsense mutation. Such an observation has been reported in a case of Burkitt's lymphoma (Villuendas *et al.*, 1993). The p53 positivity detected in the second tumour could be associated with the neoplastic growth of a different T cell clone.

In 2 cases (Cases 2 and 13), 2 PCR products from the same exon and the same T sample, but generated in separate PCR amplifications, showed different mobility shifts and, upon sequencing, different mutations. In Case 13, sequence analysis showed 2 mutations in one product and a third one in the other PCR product. The 2 mutations detected in the same product may represent p53 genes from the same cells or may have originated from 2 different populations of cells.

It is possible that the detection of more than one mutation in different PCR products from the same T sample indicates that p53 mutations arise in different reactive T cell clones, causing partial loss of p53 function. The instability caused by the initial mutation(s) may then give rise to a deletion of the remaining wild-type allele in some clones. The detection of silent mutations in 2 T samples from different cases (Cases 5 and 7) is in keeping with a scenario in which p53 mutations may arise through continuous stimulation of T cells in the enteropathic bowel, some producing abnormal protein and some not.

When performing PCR, it would be expected that different amplifications, using aliquots from the same DNA sample as template, should produce fragments with the same sequence. However, if the DNA extract contains DNA from a mixed population of cells, i.e. cells from different reactive T cell clones with different alterations of the p53 gene sequence, it is possible that different sequences may be amplified during separate reactions depending on chance. When using nested PCR, the chance that the end-product might not be a result of equal amplification of the DNA from all of the different cell populations present in the sample is increased. During nested PCR, a small aliquot (1 μl) of the first round product was diluted 1:10, then one tenth of that product was

used as template for the second round. It is possible that, by chance, the diluted aliquot did not always contain sufficient template strands from all cell clones present in the original sample to allow detection during sequence analysis.

In 3 cases, mobility shifts were detected in 2 exons amplified from the same T sample and, in 2 additional cases, mobility shifts were demonstrated in different exons amplified from different T samples of the same case. Although sequence analysis did not confirm the presence of mutations in all samples, the possibility that they are genuine cannot be ruled out, as the sensitivity of sequence analysis might not always be sufficient to pick up the altered sequence of mutated DNA of a minority population of cells.

Different T samples, or T and A samples, from an individual case showing discordant mobility shifts, could indicate the onset of transformation occurring in more than one reactive T cell clone. Indeed, Lundin and co-workers (1997) suggest that, in coeliac disease, stimulation of a large number of different gliadin-specific T cells in the small intestinal mucosa may take place. In a study to identify the nature of the stimulating gliadin antigens, a panel of HLA-DQ-restricted small intestinal T cell clones from patients with coeliac disease was tested for recognition of different pools of mixed and purified gliadin preparations (Lundin *et al.*, 1997). The results showed heterogeneous patterns of T cell reactivity when these were tested against group-fractionated gliadin antigens and purified gliadins, with no evidence for a single dominant T cell reactivity pattern. This is in keeping with the proposition that EATL may arise as a result of the continuous stimulation of diverse reactive T cells in the enteropathic bowel by antigenic fractions of gliadin. The occurrence of a heterogeneous pattern of T cell reactivity in coeliac disease is consistent with the identification of EATL cases in which mobility shifts were detected in more than one exon. The multiple shifts identified, in tissue from the same block or in different blocks from the same case, possibly represent mutations arising in different reactive T cell clones in the enteropathic bowel.

The presence of different p53 mutations in different tissue samples (precancerous and neoplastic) from the same subjects has been previously reported in cases of oesophageal neoplasia (Shi *et al.*, 1996; Bennett *et al.*, 1992). Shi and co-workers reported a

mutation in exon 5 in tissue with basal cell hyperplasia and an exon 5 mutation at a different codon as well, as an additional mutation in exon 8, in squamous cell carcinoma tissue from the same subject. Their results suggest that lesions may occur independently at different sites in the oesophageal epithelium, due to exposure to carcinogens, with some of the lesions eventually progressing to cancer (Shi *et al.*, 1996).

It is possible that a similar model of tumorigenesis is responsible for the development of EATL in some patients with CD. In patients with subclinical symptoms, the disease may go undetected and therefore untreated for many years. As a result of the continuing antigen drive derived from intestinal exposure to gliadin, over time, mutations may arise independently in different T cell populations within the enteropathic bowel. Accumulation of further genetic alterations in some T cell clones could then give rise to neoplasia.

4.3.4 Technical considerations on SSCP analysis

Orita and co-workers (1989b) identified the presence of multiple conformers, observed as minor faint bands in lanes in which denatured DNA samples were loaded, but not in lanes in which samples were electrophoresed without denaturation. The relative intensities and the mobilities of these bands varied depending on the conditions of electrophoresis, such as ambient temperature. The conformation of ssDNA is thought to be determined by the balance between thermal fluctuation and weak local stabilising forces such as short intrastrand base pairings and base stackings. It is thought that more than one metastable conformation is sometimes allowed in a given environmental condition and that the additional bands are different conformers of the same sequence (Orita *et al.*, 1989b).

Difficulties have been encountered with occurrence of multiple conformers in this study. In some cases they could have been responsible for the presence of artifacts leading to the misinterpretation of the SSCP gel results and an over-estimation of the number of mobility shifts. The detection of multiple conformers showed variability between different samples electrophoresed in the same gel (amplified during the same PCR) and when aliquots of the same samples were electrophoresed on different days. This contradicts the observation by Hayashi (1991) that, in spite of the intensity of the

conformer bands being different, the ratio of the intensity between them is constant and consistent from sample to sample.

The variation observed between samples electrophoresed on different days can probably be attributed to variations in temperature, as a water-jacketed electrophoresis apparatus was used and changes in ambient temperature would have affected the temperature of running water used to cool the system. Indeed, it has been reported that PCR products which showed multiple conformers in a polyacrylamide gel with 5% glycerol electrophoresed at room temperature, when electrophoresed at 4°C without glycerol only showed a single conformer for the analysed strands. However, use of these conditions also decreased the ability to differentiate mutant from wild-type products, as the separation between the bands was decreased (Sheffield *et al.*, 1993).

Variations between conformer bands present in different samples run on the same gel are more difficult to explain. Comparison of study DNA samples with wild-type DNA control samples that were run alongside them was not always helpful as, on more than one occasion, multiple conformers were present in a series of samples from different cases but not in the wild-type DNA control.

It is generally suggested (Vidalpuig and Moller, 1994; Orita *et al.*, 1989b) that two gel conditions (i.e. running the gel with and without glycerol) should be used in SSCP analysis to increase the sensitivity of the technique, as conformational variations are subtle and one condition might not allow detection of a mobility shift while the other one will, and vice-versa.

A preliminary experiment was performed using 6% polyacrylamide gels with 5% glycerol and MDE gels without glycerol, after which MDE gels were chosen for giving a marginally better separation and resolution of the bands. However, only a limited number of samples was tested. During the development of the IHSA technique, electrophoresis of a PCR product, known to contain a mutation in exon 6, showed a mobility shift in a 6% polyacrylamide gel containing 5% glycerol but not in an MDE gel. Amplified products of exon 6 were therefore analysed using polyacrylamide rather than MDE gels during the second round of SSCP analysis.

During both rounds of SSCP analysis, mobility shifts were detected at a lower frequency in exon 6 than in the other exons. A compilation showing the combined frequency of 76 p53 mutations from 10 different molecular studies on NHL cases (Piris *et al.*, 1995) indicates that mutations in exon 6 occur at a lower frequency than in exons 5, 7 and 8 (see Fig.1.5.5). This is in keeping with the fact that the DNA region encoding exon 6 does not correspond to any of the evolutionary conserved regions, which contain the most frequently mutated amino acid residues (Ko and Prives, 1996).

Although other studies do not refer to problems with multiple conformers during molecular analysis of the p53 gene, over-estimation of mutations can occur during PCR-SSCP analysis. Milner and co-workers (1993) analysed 66 cases of ovarian carcinoma and found that 4 out of the 34 SSCP shifts identified did not represent genuine DNA mutations when sequencing was performed (3 in exon 8 and one in exon 7).

In this study, the use of nested PCR for the second round of PCR-SSCP analysis increased the sensitivity of amplification, so that electrophoresed products showed less variability in band intensity. This helped reduce misinterpretation of SSCP analysis results, decreasing the number of mobility shifts detected during the second round.

4.3.5 Technical considerations on DNA sequence analysis

Initially, DNA sequence analysis was to be performed on products showing mobility shifts in an MDE or polyacrylamide gel, after excision and re-amplification of the band showing the altered mobility. Although the use of small gels (14x16 cm) allowed enough band separation for detection of mobility shifts, the band separation was not sufficient to permit band excision in most cases. The use of large sequencing gels would have been more appropriate, as the samples could have been electrophoresed for longer, so that fragments with different mobilities would have separated further from wild-type fragments. However, the equipment that was available in the department for electrophoresis of larger gels did not have a cooling system associated with it. Such a system is needed to maintain the temperature of the gel below 20°C and constant, as variations in temperature affect the mobility of ssDNA fragments.

Direct sequence analysis was performed on DNA samples in cases for which mobility shifts were detected. This situation was far from ideal as the sensitivity of this technique is limited when applied to DNA from whole tumour sections, which is contaminated with large amounts of DNA from non-tumour cells. Although the success rate for this analysis was compromised, it was still used in an attempt to detect mutations in cases with high enough ratios of mutated DNA.

Mutation detection can be performed using fluorescent automated DNA sequencing as the relative proportions of DNA fragments with different sequences is translated in the resulting electropherogram into two peaks of different intensities at the same base position. Generally, DNA sequencing can detect a mutation if the minority population of DNA containing the mutation comprises at least 20% of the total DNA population (Loda, 1994). Approximately half of the EATL cases (15/29) in this study showed p53 over-expression in 20% of cells or more, in T sections.

DNA sequence analysis performed on samples that showed mobility shifts during the second round of SSCP analysis was more successful than that carried out on samples from the first round. However, it still only permitted detection of mutations in 5/15 mobility shifts identified in T samples from 10 cases, and 2/3 mobility shifts in A samples from 3 cases. The greater success of the second round of sequence analysis could be linked to the use of a more sensitive DNA sequencing chemistry. The Big Dye^{TM} terminator sequencing chemistry (PE Applied Biosystems) used produces more even electropherogram peak heights and the signal is 2-3 times brighter than with the rhodamine dye terminators used previously. These improved characteristics increase the sensitivity and the rate of success when using dye-labelled terminators for heterozygote and mutation detection in samples containing DNA from mixed populations of cells (Rosenblum *et al.*, 1997).

Out of the 11 mutations detected (including the 3 silent mutations), 10 showed transitions (9 G:C to A:T transitions and 1 A:T to G:C transition) and 1 showed a G:C to T:A transversion. This is in keeping with the pattern of mutations found generally in lymphomas and leukemias, in which G:C to A:T transitions (especially at CpG dinucleotides) constitute a major fraction of point mutations. In addition, A:T to G:C

transitions predominate among substitutions at A:T pairs and G:C to T:A transversions are uncommon (Hollstein *et al.*, 1991).

4.4 IMMUNOHISTOSELECTIVE ANALYSIS

As results obtained from sequencing of products from the first round of SSCP analysis were ambiguous, and the microdissection technique did not enrich the p53 immunopositive cells of A and T samples sufficiently, the technique of immunohistoselective analysis (IHSA) was developed.

Immunohistoselective analysis was based on the immunohistoselective sequencing (IHSS) method published by Shi and co-workers (1996). This technique provides an alternative approach to isolating the desired cells from a section, which involves inactivating the DNA from contaminating cells rather than retrieving target cells. This technique is particularly useful when analysing tumour cells, as these tend to be surrounded by non-neoplastic cells and the DNA present in the latter may obscure the results of molecular assays depending on the relative proportion of neoplastic cells present and the sensitivity of the technique used.

The successful application of this technique depends on the strong nuclear expression of proteins, such as p53 protein, which can be targeted by immunostaining. Once the target cells have been protected by immunostaining and the background cells have been inactivated through exposure to UV irradiation, subsequent PCR performed on DNA extracted from the section should selectively amplify intact DNA from the immunostained cells.

Thorough optimisation of each step was necessary due to difficulties associated with the partially degraded DNA present in formalin-fixed tissue. The original IHSS technique (Shi *et al.*, 1996) was applied to tissue samples that had been obtained fresh and then fixed in 80% ethanol before embedding in paraffin wax blocks. As tissue samples for histology are routinely fixed in formalin, this was the main reason why modifications to their method were needed for this study. Fixation in formalin masks tissue antigens and an antigen retrieval step was required for successful immunohistochemistry (Cuevas *et al.*, 1994). Glass slides were used instead of plastic film as support for the tissue sections, which were then scraped off the slides for DNA extraction, rather than cut into small pieces as performed by Shi and colleagues (1996).

Positive results obtained during the early optimisation steps of the technique showed that it was possible to apply IHSA successfully to routinely fixed and processed tissue samples. However, the initial experiment, using IHSA on a T section from an EATL case, failed to produce PCR fragments detectable by agarose gel electrophoresis. This problem was addressed by investigating different ways of increasing the sensitivity of PCR and was solved with the use of nested PCR.

Shi and co-workers (1996) described a control experiment performed in order to ensure that UV irradiation was not introducing mutations to the analysed DNA. A tumour sample with p53 immunostain-positive cells, containing a known mutation at codon 273 in exon 8, was subjected to UV irradiation. PCR amplification was performed and the expected mutation in exon 8 was detected with no obvious additional UV-induced mutations. Furthermore, when tumour cells were enriched by microdissection only, the same mutations were obtained as when the analysis was carried out with UV irradiation. This control experiment showed that UV irradiation did not introduce any artefacts into the mutation analysis of the p53 gene in their study, this being an essential requirement for the validity of the method.

During the current study, however, in contrast to results obtained by Shi and co-workers (1996), when applying IHSA to a sample of ovarian carcinoma containing a known p53 mutation, an additional mutation was demonstrated in a sample exposed to UV irradiation for 90 min. Nested PCR was repeated for this sample and the new products showed the original mobility shift, rather than the altered one. It is not possible to determine whether the introduced artefact was caused by prolonged UV irradiation or was a result of mis-incorporation of a nucleotide by DNA polymerase during early cycles of the first round PCR. As for any method in which low copy number targets are amplified, mis-incorporation by DNA polymerase is a potential source of artefacts (Lo, 1998a). In either case, the change in sequence would be introduced at a random place and repeat experiments should confirm whether the identified mutation is genuine. It is possible that Shi and colleagues (1996) did not encounter this problem as the DNA in their samples was less degraded than that used here and therefore greater quantities of amplifiable DNA were present even after UV irradiation of tissue sections.

In order to increase PCR amplification fidelity, a proof-reading DNA polymerase *Pwo* (Hybaid Ltd.) was employed. This enzyme has 3' to 5' exonuclease activity, which means it enhances the fidelity of DNA synthesis by excising any incorrectly added, mismatched 3'-terminal nucleotides from the primer extension product and then incorporates the correct nucleotide. However, amplification of UV-irradiated samples was not successful using this enzyme, probably due to its decreased sensitivity.

Although there seems to be an unfortunate trade-off, by which an increase in fidelity means lower sensitivity in PCR amplifications, manufacturers of the hot start DNA polymerase (Qiagen Ltd.) used in this study affirm that it may be possible to increase fidelity of a non-proof-reading enzyme by spiking it with small amounts of proof-reading enzyme, so that amplification sensitivity is not lost and fidelity increased (personal communication). However, it has not been possible to test this in the present study.

The most important factor associated with success in the IHSA technique is efficient protection of the target cells. Immunostaining can only be used successfully as a protective barrier if levels of p53 over-expression are high enough to produce a dark stain.

In some sections in this study, p53 immunostaining, although positive, was weak and therefore did not provide sufficient protection from UV irradiation. In such cases, reduced UV exposure times could, in theory, be applied. Although this would not inactivate the DNA in p53 immunostain-negative cells completely, it would enrich the sample with partly-protected DNA. The technique of selective ultraviolet radiation fractionation (SURF) (Shibata *et al.*, 1992), which is similar to IHSA, also uses UV irradiation to inactivate the DNA of background cells. However, the protective shield in SURF is provided by ink dots placed on the target cells. Although not as specific as IHSA, since each dot can cover between 50 and 300 cells (Shibata, 1994), this technique could be used in conjunction with IHSA for cases in which low nuclear protein expression results in weak immunostaining.

When applying IHSA to tissue sections, UV exposure times needed for complete inactivation of DNA from p53-negative cells were determined for each exon by irradiating unstained sections for increasing lengths of time, then selecting the first time-point that showed no PCR product on an agarose gel. Possibly due to variation in fixation conditions, UV exposure times needed to be determined for each block analysed. It was interesting to note that, when unstained sections were used, UV exposure times needed for complete DNA inactivation were longer than the times established when protected cells were present. It is possible that, in a sample containing both intact and partly-damaged DNA, the polymerase enzyme preferentially amplifies the intact sequences. Possible reasons for this include greater affinity of primers for intact sequences than for UV-damaged DNA, or greater efficiency of the enzyme when amplifying intact DNA. In a sample in which all cells have been exposed to UV irradiation and intact template sequences are absent, primers are likely to anneal to some sequences, even if they are partly damaged, and thus allow amplification.

The IHSA technique worked well when applied to the sections of ovarian carcinoma used to develop the method, which contained approximately 60%-65% p53-positive cells. Results obtained when applying IHSA to EATL cases, however, were inconsistent. Five tissue samples (3 T and 2 A samples) were tested but successful amplification was only obtained from one T sample, showing p53 over-expression in intra-epithelial lymphocytes (7 p53-positive IEL per 100 epithelial cells) and 2% of lamina propria cells, even though T sections with 43% and 64% p53 positivity were also included. Sequence analysis demonstrated the presence of a mutation in the IHSA-positive sample, represented by two peaks of different intensities at the same base position in the electropherogram (Fig. 3.6.4). The higher peak represented the mutated base, whereas the lower peak represented the wild-type base that was also present because of incomplete inactivation of DNA from unstained cells.

Shi and colleagues (1996) reported that their method effectively enriched oesophageal pre-cancerous tissue samples that contained as few as 30 p53 immunostain-positive cells per section, or less than 1% of the total epithelial cells. In the present study, despite careful optimisation of the technique, such high sensitivity could not be reproduced when applying it to formalin fixed tissues.

It is possible that, due to its degraded nature, DNA from formalin-fixed tissues may be more susceptible to UV-induced inactivation and therefore, in some cases, it needs better protection than that offered by enhanced immunostaining. For those cases, use of the SURF technique may be a more successful alternative, in spite of its offering a lower degree of enrichment. The use of heat-mediated antigen retrieval during immunostaining (not necessary for the original IHSS method performed using ethanol-fixed tissue) might also contribute to further degradation of DNA and limit the effectiveness of IHSA in formalin-fixed tissue sections.

As with any technique in which analysis of formalin-fixed tissue is involved, a variable success rate is to be expected, due to minor variations in fixation conditions that cannot easily be controlled. Nevertheless, despite some limitations, the IHSA technique potentially allows genetic analysis of specific populations of cells in a wide range of tissues from archival stores that would otherwise be inaccessible using standard PCR methods.

4.5 CONCLUSIONS AND FUTURE PROSPECTS

This study has shown that p53 protein over-expression, commonly detected in EATL tumour cell nuclei, is associated with mutations in the p53 gene in a minority of cases. It has also shown that the number of cases with p53 protein accumulation in small lymphocytes in areas of enteropathic bowel unaffected by tumour is smaller (5 out of 21) than previously reported (Murray *et al.*, 1995). Nevertheless, out of 5 p53-positive samples of non-tumoral enteropathic bowel, 2 samples were found to contain mutations in the p53 gene. This suggests that p53 dysregulation could represent an early event in the development of neoplastic T cell clones, with individual mutations arising independently in different T cell populations that are undergoing antigen drive in the enteropathic bowel.

The fact that different mutations were identified in different samples from individual patients is in keeping with a model of tumorigenesis in which mutations arise independently from different clones of reactive T cells within the enteropathic bowel. Genetic instability caused by the initial mutation(s) could then contribute to causing deletion of the second allele and dysregulation of the p53 gene in some clones.

The detection of mutations in only 4 out of 24 cases showing p53 over-expression indicates that another mechanism must be causing p53 protein stabilisation in the cells in most cases of EATL. Immunohistochemical detection of MDM2 protein accumulation that could be stabilising p53 was hampered by problems with antibody specificity and therefore did not provide any conclusive data.

In order to enrich samples with cells over-expressing p53 protein, the technique of immunohistoselective analysis (IHSA) was developed. Only one other group (Shi *et al.*, 1996) has reported the use of UV inactivation of DNA in association with enhanced immunohistochemistry, which was applied in that study to tissue samples fixed in ethanol, rather than to formalin-fixed tissues. It has been demonstrated in the present study that IHSA can produce samples enriched with DNA from cells targeted by nuclear immunostaining. This approach potentially allows a range of molecular genetic analyses

to be carried out on samples that would otherwise be contaminated by DNA from abundant background cells, which would mask the results of molecular assays.

Future work to investigate the genetic mechanisms involved in the development of EATL should include loss of heterozygosity (LOH) analysis of chromosome 17p. This is where the p53 gene is found and LOH detection of this locus would determine whether the gene is completely inactivated in cases showing p53 point mutations. It would also be of interest to determine through LOH whether any EATL cases show partial inactivation of p53.

Immunohistochemistry, to detect possible accumulation of MDM2 protein, as well as of other regulatory molecules, in tumour cell nuclei, should also be investigated further. The use of an alternative MDM2 antibody to the one used in this study could allow the putative relationship of MDM2 expression with p53 over-expression to be defined and correlated with the presence or absence of p53 mutations.

Due to time constraints, IHSA was only applied to a limited number of EATL cases in this study. The use of this technique results in an enrichment of DNA derived from p53-positive cells, making the DNA more suitable for sequence analysis and perhaps allowing detection of mutations in additional cases.

APPENDICES

A. DNA SEQUENCE OF THE HUMAN p53 GENE AND THE PREDICTED AMINO ACID SEQUENCE OF THE PROTEIN - EXONS 5 - 8

... - Intron 4 - GGTGTAGACG CCAACTCTCT CTAGCTCGCT AGTGGGTTGC

AGGAGGTGCT TACACATGTT TGTTTCTTTG CTGCCGTGTT CCAGTTGCTT

TATCTGTTCA CTTGTGCCCT GACTTTCAAC TCTGTCTCCT TCCTCTTCCT ACAG

Exon 5

TAC TCC CCT GCC CTC AAC AAG ATG TTT TGC CAA CTG GCC AAG
Y S P A L N K M F C Q L A K
126 130

ACC TGC CCT GTG CAG CTG TGG GTT GAT TCC ACA CCC CCG CCC
T C P V Q L W V D S T P P P
140 150

GGC ACC CGC GTC CGC GCC ATG GCC ATC TAC AAG CAG TCA CAG
G T R V R A M A I Y K Q S Q
160

CAC ATG ACG GAG GTT GTG AGG CGC TGC CCC CAC CAT GAG CGC
H M T E V V R R C P H H E R
170 180

TGC TCA GAT AGC GAT G GT GAGCAGCTGG GGCTGGAGAG ACGACAGGGC
C S D S D - Intron 5 -
186

TGGTTGCCCA GGGTCCCCAG GCCTCTGATT CCTCACTGAT TGCTCTTAG

Exon 6

GT CTG GCC CCT CCT CAG CAT CTT ATC CGA GTG GAA GGA AAT
G L A P P Q H L I R V E G N
187 190 200

TTG CGT GTG GAG TAT TTG GAT GAC AGA AAC ACT TTT CGA CAT
L R V E Y L D D R N T F R H
210

AGT GTG GTG GTG CCC TAT GAG CCG CCT GAG GTCTGGTT
S V V V P Y E P P E - Intron 6 -
220 224

TGCAACTGGG GTCTCTGGGA GGAGGGGTTA AGGGTGGTTG TCAGTGGCCC

TCCGGGTGAG CAGTAGGGGG GCTTTCTCCT GCTGCTTATT TGACCTCCCT

ATAACCCCAT GAGATGTGCA AAGTAAATGG GTTTAACTAT TGCACAGTTG

AAAAAACTGA AGCTTACGAG GCTAAGGGCC TCCCCTGCTT GGCTGGGCGC

AGTGGCTCAT GCCTGTAATC CCAGCACTTT GGGAGGCCAA GGCAGGCGGA

TCACGAGGTT GGGAGATCGA GACCATCCTG GCTAACGGTG AAACCCCGTC

TCTACTGAAA AATACAAAAA AAAATTAGCC GGGCGTGGTG CTGGGCACCT

GTAGTCCCAG CTACTCGGGA GGCTGAGGAA GGAGAATGGC GTGAACCTGG

GCGGTGGAGC TTGCAGTGAG CTGAGATCAC GCCACTGCAC TCCAGCCTGG

GCGACAGAGC GAGATTCCAT CTCAAAAAAA AAAAAAAAAG GCCTCCCCTG

CTTGCCACAG GTCTCCCCAA GGCGCACTGG CCTCATCTTG GGCCTGTGTT

Exon 7

ATCTCCTAG **GTT GGC TCT GAC TGT ACC ACC ATC CAC TAC AAC TAC**

V G S D C T T I H Y N Y

230

ATG TGT AAC AGT TCC TGC ATG GGC GGC ATG AAC CGG AGG CCC

M C N S S C M G G M N R R P

240 250

ATC CTC ACC ATC ATC ACA CTG GAA GAC TCC AG G TCAGGAGCCA

I L T I I T L E D S S - Intron 7 -

260 261

CTTGCCACCC TGCACACTGG CCTGCTGTGC CCCAGCCTCT GCTTGCCGCT

GACCCCTGGG CCCACCTCTT ACCGATTTCT TCCATACTAC TACCCATCCA

CCTCTCATCA CATTTCCGGC GGGAATCTCC TTACTGCTCC CACTCAGTTT

CCTTTTCTCT GGCTTTGGGA CCTCTTAACC TGTGGCTTCT CCTCCCACCT

CCTGGAGCTG GAGCTTAGGC TCCAGAAAGG ACAAGGGTGG TTGGGAGTAG

ATGGAGCCTG GTTTTTTAAA TGGGACAGGT AGGACCTGAT TTCCTTACTG

Exon 8

CCTCTTGCTT CTCTTTTCCT ATCCTGAGTA G **T GGT AAT CTA CTG GGA**
G N L L G
262

CGG AAC AGC TTT GAG GTG CGT GTT TGT GCC TGT CCT GGG AGA
R N S F E V R V C A C P G R
270 280

GAC CGG CGC ACA GAG GAA GAG AAT CTC CGC AAG AAA GGG GAG
D R R T E E E N L R K K G E
290

CCT CAC CAC GAG CTG CCC CCA GGG AGC ACT AAG CGA G
P H H E L P P G S T K R
300 306

GT AAGCAAGCAG GACAAGAAGC GGTGGAGGAG ACCAAGGGTG CAGTTATGCC

TCAGATTCAC TTTTATCACC TTTCCTTGCC TCTTTCCTAG
- Intron 8 -

(From Lamb and Crawford, 1986)

OBS.: Coloured lines indicate regions where oligonucleotide primers anneal.

Single lines for internal and double lines for external primers.

Exon 5

Exon 6

Exon 7

Exon 8

B. AMINO ACIDS, THEIR SYMBOLS AND CODONS FROM WHICH THEY ARE TRANSLATED

Amino acids			Codons
A	Ala	Alanine	GCA GCC GCG GCU
C	Cys	Cysteine	UGC UGU
D	Asp	Aspartic acid	GAC GAU
E	Glu	Glutamic acid	GAA GAG
F	Phe	Phenylalanine	UUC UUU
G	Gly	Glycine	GGA GGC GGG GGU
H	His	Histidine	CAC CAU
I	Ile	Isoleucine	AUA AUC AUU
K	Lys	Lysine	AAA AAG
L	Leu	Leucine	UUA UUG CUA CUC CUG CUU
M	Met	Methionine	AUG
N	Asn	Asparagine	AAC AAU
P	Pro	Proline	CCA CCC CCG CCU
Q	Gln	Glutamine	CAA CAG
R	Arg	Arginine	AGA AGG CGA CGC CGG CGU
S	Ser	Serine	AGC AGU UCA UCC UCG UCU
T	Thr	Threonine	ACA ACC ACG ACU
V	Val	Valine	GUA GUC GUG GUU
W	Trp	Tryptophan	UGG
Y	Tyr	Tyrosine	UAC UAU

C. Sequence of DNA containing a dinucleotide repeat polymorphism at the human TP53 locus (chromosome 17p13.1)

GGTACCCCCA CAGAGCGAGA CTGTCTCAAA AAAAAAAAAA

AAGAAAAGAA AAAGAAAAGA AATTCCC**ACT** **GCCACTCCTT**

GCCCCATTCC **CCTTTCCCTA** **AAAACCCCCA** **ACACACACAC**

ACACACACAC **ACACACACAC** **ACACACACAC** **ACACACACAC**

GCACCTCGGG **CTGAATAGTA** **TCCCT**CAGGG GATCCTCTAG

AGTCGACCTG CAGGCATGCA AG

Key:

—— Annealing sites of oligonucleotide primers used

D. IMMUNOHISTOCHEMICAL RESULTS USED TO GENERATE GRAPHS IN SECTION 3.2

Case	Sample	p53 (%)	pRB (%)	Case	Sample	p53 (%)	pRB (%)	Case	Sample	p53 (%)	pRB (%)
1	1-T	43.1±3.8	34±3	**9**	29-A	0	0	**20**	40-T	0	39.3±3.9
	18-A	8±0.6 * 1±0.4 ^{LP}	0 0		35-A	0	12±0.9 *	**21**	39-A	0	0
2	2-A	11±1.4 * 23±3.5 ^{LP}	0 0	**10**	19-T	0	33.2±4.2		47-T	0	ND
	3-T	64±8.4	43.6±5		20-T	0	37.8±5.5		49-T	0	21.4±3.5
	10-T	7±0.4 * 2±0.5 ^{LP}	0 0	**11**	41-A	0	0	**22**	50-T	22.8±2.6	27.8±2.3
3	4-T	1.8±0.8	42±3.2		42-T	18.1±2.7	46.1±8.1	**23**	25-A	0	0
	5-A	2±0.7 * 2.9±1.3 ^{LP}	ND	**12**	21-A	0	0	**24**	60-T	62.7±6.7	52.5±5.9
	6-T	5.7±2.8	25±2.7		22-T	1±0.4	26.3±3.5		61-A	0	3±0.4 *
4	7-T	1.3±0.6	5±1.1	**13**	23-T	55±9.1	37.9±4.1	**25**	63-T	55.5±6.6	29.8±3.1
	24-A	0	0		27-T	2±0.7	40.7±7.4	**26**	64-T	55.2±1.4	50.7±1.1
	33-T	35.2±3.1	8±1.1	**14**	B - A	15±0.6 *	8±1.1 *		65-T	66.3±1.6	31.7±3.8
5	28-A	0	0		E - T	3±0.9	38.9±2.9		66-T	0	0
	8-T	11.8±3.1	22±2.6		I(ln)	0	ND	**27**	68-T	42.2±4.4	ND
	54-T	31.8±4	48±2.9	**15**	26-A	0	0.4±0.2 *		70(ln)	0	ND
	9-T	23.9±6.2	48±3.2	**16**	31-T	62.7±7.9	41.4±4.1		71-A	0	ND
6	11-T	8±1.1	34.4±1.2		32-A	0	0	**28**	84-T	7±0.9	21±1.7
	12-A	0	8±1.1 *		34-T	10.9±1.1	30.7±2		85-T	0	9.7±3.7
7	13-T	3±0.7	67±4.8	**17**	36-T	38.4±4.3	50.7±8.8	**29**	80-A	1±0.2 * 2±0.6 ^{LP}	16±2.1 * 0
	14-A	0	2±0.2 *		30-T	42.8±6.3	31±3.3		81-T	12±1.6	54±5.4
8	15-T	53.3±3.7	9±1.4		56-T	33.7±7.9	42.5±5.3	**30**	82-A	0	2±0.7 *
	55-T	94.2±1.7	53.2±3.9	**18**	37-T	29.1±6.2	45.9±3.8		83-T	44±3	34.7±5.9
	16-A	0	2±0.8 *		51-T	2±0.8	34.1±7.7	**31**	89-A	0	0
9	17-T	0	16.8±2.1	**19**	38-T	52.8±3.9	47.7±4.6		91-T	0	48.4±3.1

Table D.1. Immunohistochemistry results obtained for p53 and pRB antibodies on EATL.

Key: T, tumour sample; A, adjacent tissue sample; ln, lymph node; ND, not done.

Unless otherwise indicated, values represent mean percentages (±SE) of positive cells.

Values marked by (*) represent number of immunopositive IEL per 100 epithelial cells.

Values followed by (^{LP}) indicate percentage of positive cells in the lamina propria.

Case	CD3+ IEL	CD8+ IEL
1	52.5±16.7	46±7.7
2	8±0.8	7.5±1.3
3	15±1.4	7.25±3.1
4	46.5±5.5	14.75±2.1
5	62±8.8	0.5±0.6
6	56.75±5.6	18.25±4.3
7	32.25±6.6	24±3.4
8	40±3.2	36.75±7.3
9	26.5±4.2	26±3.9
10	22.75±5.9	22.25±3.6
12	20.75±1.5	16±2.8
13	25.25±10.9	20.25±5.6
15	34.25±12.8	22.25±2.2
22	178±11.2	16±3.4
24	43.75±6.9	38.5±12.3
27	63±19	5.75±2.5
30	29±7.9	16.25±1.3

Table D.2. CD3/CD8 positivity recorded in IEL from small intestinal mucosa sections of patients with EATL. Results represent numbers of positive IEL per 100 epithelial cells. Figures shown are mean values taken after counting 400 epithelial cells on each section (±SD).

Case	Sample	CD3+ (%)	Case	Sample	CD3+ (%)
1	**1**	45±3.6	**12**	**22**	35±3.1
2	**3**	89±7.8	**13**	**23**	56±6.2
3	**4**	49±8.4	**13**	**27**	50±3.8
3	**6**	32±6.1	**14**	**E**	54±3.6
4	**7**	48±2.9	**16**	**31**	67±5.8
4	**33**	80±6.7	**17**	**30**	62±7.4
5	**8**	88±6.9	**17**	**56**	52±5.0
5	**9**	94±2.3	**18**	**51**	82±7.6
6	**11**	63±7.2	**21**	**49**	37±4.1
7	**13**	82±7.8	**22**	**50**	28±3.2
8	**15**	87±7.7	**24**	**60**	66±4.2
8	**55**	95±1.8	**25**	**63**	87±8.3
9	**17**	18±2.6	**26**	**64**	79±3.6
10	**19**	67±5.7	**28**	**85**	71±6.5
10	**20**	62±5.5	**29**	**81**	63±6.1

Table D.3. Immunohistochemistry results showing mean percentage (±SE) of CD3+ cells in tumour sections from EATL cases.

Case	Sample	CD3+ IEL (cells/100 epithelial cells)	CD3+ Lamina Propria cells (%)
1	**18**	53±8.3	49±8.1
2	**2**	14±2.6	27±1.9
3	**5**	13±2.3	64±3.9
5	**28**	62±4.4	92±4.3
6	**12**	57±2.8	14±1.5
7	**14**	32±3.3	72±5.2
8	**16**	40±1.6	51±6.6
9	**29**	26±2.1	47±3.2
9	**35**	80±9.2	21±2.8
12	**21**	21±0.8	53±3.1
14	**B**	19±0.9	46±3.3
15	**26**	61±4.8	19±0.8
24	**61**	32±2.6	24±2.6
27	**71**	63±9.5	42±6.2
30	**82**	29±4.0	18±3.2
31	**89**	72±3.5	65±7.8

Table D.4. Immunohistochemistry results showing CD3+ IEL and lamina propria cells in histologically uninvolved adjacent tissue sections from EATL cases. Figures represent mean values (±SE).

E. PCR PROTOCOLS

1. STANDARD PCR

Master mix for 50µl reactions:

	Vol. per reaction	**Final conc. per reaction**
PCR buffer (x10)	5µl	x1
15 mM $MgCl_2$ (in PCR buffer)	-	1.5 mM
dNTP mix (10mM each)	1µl	200 µM of each dNTP
Primer A	1µl	20 pmol
Primer B	1µl	20 pmol
Taq DNA polymerase (5 units/µl)	0.3µl	1.5 units
Distilled water	40.7µl	-
Template DNA	1µl	300ng-500ng

Cycling profile:

Initial denaturation:	5 min	94°C	
3-step cycling:			
Denaturation:	30 sec	94°C	35 cycles
Annealing:	30 sec	varies	
Extension:	45 sec	72°C	
Final extension:	5 min	72°C	

2. HOT START PCR

Master mix for 50µl reactions:

	Vol. per reaction	**Final conc. per reaction**
PCR buffer (x10)	5µl	x1
15 mM $MgCl_2$ (in PCR buffer)	-	1.5 mM
dNTP mix (10mM each)	1µl	200 µM of each dNTP
Primer A	1µl	20 pmol
Primer B	1µl	20 pmol
HotStar Taq DNA polymerase (5 units/µl)	0.3µl	1.5 units
Distilled water	40.7µl	-
Template DNA	1µl	300ng-500ng

Cycling profile:

Initial denaturation and enzyme activation:	15 min	95°C	
3-step cycling:			
Denaturation:	30 sec	94°C	35 cycles
Annealing:	30 sec	varies	
Extension:	45 sec	72°C	
Final extension:	5 min	72°C	

3. DEGENERATE OLIGONUCLEOTIDE-PRIMED (DOP)-PCR

Master mix for 50µl reactions:

	Vol. per reaction	**Final conc. per reaction**
PCR buffer (x10)	5µl	x1
15 mM $MgCl_2$ (in PCR buffer)	-	1.5 mM
dNTP mix (10mM each)	1µl	200 µM of each dNTP
Primer (3µg/µl)	5µl	15µg
Taq DNA polymerase (5 units/µl)	0.5µl	2.5 units
Distilled water	33.5µl	-
Template DNA (low copy number)	5µl	variable

Cycling profile:

Initial denaturation:	8 min	96°C	
Denaturation:	1 min	94°C	8 cycles
Annealing:	1 min	30°C	
Extension:	3 min	72°C	
Denaturation:	1 min	94°C	28 cycles
Annealing:	1 min	60°C	
Extension:	3 min	72°C	

4. PRIMER-EXTENSION PRE-AMPLIFICATION (PEP)

Master mix for 50µl reactions:

	Vol. per reaction	**Final conc. per reaction**
PCR buffer (x10)	5µl	x1
15 mM $MgCl_2$ (in PCR buffer)	-	1.5 mM
dNTP mix (10mM each)	1µl	200 µM of each dNTP
Primer (3µg/µl)	5µl	15µg
Taq DNA polymerase (5 units/µl)	1µl	5 units
Distilled water	23µl	-
Template DNA (low copy number)	15µl	variable

Cycling profile:

Denaturation:	1 min	92°C	50 cycles
Annealing:	2 min	37°C	
Programmed ramping of	1 sec/0.1°C to 55°C		
Extension:	4 min	55°C	

5. PCR USING PROOFREADING DNA POLYMERASE (Pwo)

Master mix for 50µl reactions:

	Vol. per reaction	**Final conc. per reaction**
PCR buffer (x10)	5µl	x1
20 mM $MgSO_4$ (in PCR buffer)	-	2.0 mM
dNTP mix (10mM each)	1µl	200 µM of each dNTP
Primer A	1µl	20 pmol
Primer B	1µl	20 pmol
Pwo DNA polymerase (2.5 units/µl)	0.4µl	1 unit
Distilled water	40.6µl	-
Template DNA	1µl	300ng-500ng

Cycling profile:

Initial denaturation:	2 min	94°C	
3-step cycling:			
Denaturation:	30 sec	94°C	30 cycles
Annealing:	30 sec	60°C	
Extension:	45 sec	68°C	
Final extension:	5 min	68°C	

F. COMPOSITION OF BUFFERS

Digestion buffer

PCR buffer x1 (Promega)

5 mM $MgCl_2$

400 µg/mL proteinase K (stored at -20°C)

Prepare fresh each time.

Elution buffer (Qiagen)

10mM Tris-HCl (pH 8.5)

Store at room temperature.

Gel loading buffer A (x6)

TAE x6

30 % (v/v) glycerol

0.25 % (w/v) bromophenol blue

Store at 4°C.

Gel loading buffer B (x1)

TBE x1

0.05 % (w/v) bromophenol blue

0.05 % (w/v) xylene cyanol

Store at 4°C.

Gel loading buffer C (x 2.5)

TBE x 2.5

50% (v/v) glycerol

0.25% (w/v) bromophenol blue

Store at 4°C.

PCR buffer x10 (Promega)

500 mM KCl

100 mM Tris-HCl (pH 9.0)

1 % Triton X-100

Store at -20°C.

PCR buffer x10 (Qiagen)

Tris-HCl

KCl

$(NH_4)_2SO_4$

15 mM $MgCl_2$

pH 8.7

(molarities not available for all components)

Store at -20°C.

Phosphate buffered saline (PBS) buffer

0.14 M NaCl

1.5 mM KH_2PO_4

8.1 mM Na_2HPO_4

2.7 mM KCl

pH 7.3

Autoclave and store at 4°C.

Stop solution

95 % (v/v) formamide

10 mM NaOH

0.25 % (w/v) bromophenol blue

0.25 % (w/v) xylene cyanol

Store at room temperature.

Thermo Sequenase sequencing reagent pre-mix

125 mM Tris-HCl, pH 9.5

5 mM $MgCl_2$

1.25 mM dITP

0.25 mM each dATP, dCTP, dTTP, ddATP (dye-labelled), ddCTP (dye-labelled), ddGTP (dye-labelled), ddTTP (dye-labelled)

Thermo Sequenase DNA polymerase

Thermoplasma acidophilum thermostable inorganic pyrophosphatase (TAP)

Nonidet™ P40

Tween™ 20

6.25 % glycerol

Store at -20°C.

Tris acetate EDTA (TAE) x10 buffer

0.4 M Tris base

11.22 mL/L Glacial acetic acid

0.01 M EDTA (pH 8.0)

Autoclave and store at room temperature.

Tris borate EDTA (TBE) x10 buffer

0.89 M Tris base

0.89 M Boric acid

0.02 M EDTA (pH 8.0)

Autoclave and store at room temperature.

Tris buffered saline (TBS)

0.05 M Tris base

0.14 M NaCl

pH 7.6 (with HCl)

Store at room temperature.

G. COMPOSITION OF GELS

1. AGAROSE GEL (2.5%)

To prepare 80 ml:

Agarose (Sigma)	2 g
Distilled water	72 ml
TAE x10	8 ml
ethidium bromide (10mg/ml)	4µl

2. MUTATION DETECTION ENHANCEMENT (MDE) GEL

To prepare 20 ml:

MDE x2 (FMC Bioproducts)	5.0 ml
Distilled water	13.8 ml
TBE x10	1.2 ml
TEMED	16 µl
Ammonium persulfate (20% w/v)	120µl

3. 6% POLYACRYLAMIDE GEL WITH 5% GLYCEROL FOR SSCP ANALYSIS

To prepare 20 ml:

Polyacrylamide, 40%	
(29:1, acrylamide: bisacrylamide)	3.0 ml
Distilled water	15.0 ml
Glycerol	1.0 ml
TBE x10	1.0 ml
TEMED	18 µl
Ammonium persulfate (20% w/v)	120 µl

4. 6% POLYACRYLAMIDE SEQUENCING GEL

To prepare 50 ml:

Sequagel 6 (National Diagnostics)	40.0 ml
Distilled water	3.4 ml
TBE x10 (National Diagnostics)	6.6 ml
TEMED	25 µl
APS (10% w/v)	250 µl

H. METHOD FOR SHARPENING MICRODISSECTION NEEDLES

Needles employed for microdissection were 76mm tungsten wire needles, 0.5 mm in diameter (Clark Electromedical Instruments).

A rough point was first produced with the use of a bench grinder. A sharper point was then obtained by holding the tip of the needle over the hottest part of a Bunsen burner flame until red, then quickly quenching in a beaker of distilled water. This was repeated 15 to 20 times until a suitable sharp point was obtained when observed under the microscope at 100X magnification.

I. MISCELLANEOUS

1. COUNTING OF IMMUNOPOSITIVE CELLS

In order to estimate the percentage of positively stained cells on EATL sections, a graticule containing 15 evenly distributed short lines was used. At x400 magnification, 5 fields of view were randomly selected and, for both ends of each line, it was recorded whether the tip of the line touched a positive cell, a negative cell or a blank space. The proportion of positive cells over the total number of cells recorded (i.e. excluding counts of blank spaces) was calculated for each field of view. A mean value for all 5 fields of view was produced. An additional 5 fields of view were counted and a mean of all 10 fields of view was calculated and compared with the first mean. If the difference between means was below 5%, the mean of 10 fields of view was recorded as the proportion of immunopositive cells for the section. If the difference was greater than 5%, 5 additional fields were counted and the mean of positive cells counted in 15 fields of view compared with the mean of 10 fields of view. This was done until the difference between means was below 5%.

2. CALCULATION TO OBTAIN DNA CONCENTRATION AND PURITY

The concentration of DNA in solution is calculated by measuring the absorbance of light at 260nm of the DNA solution using a spectrophotometer, and substituting in the following equation:

Concentration (μg/ml) = Absorbance at 260nm x C x Path length x Dilution factor
C = constant (50 for chromosomal DNA)
Path length = 1 for 1 cm, 2 for 0.5 cm

The purity of the DNA solution is calculated by determining the ratio of the absorbance at 260nm and the absorbance at 280nm. For a pure DNA sample without protein contamination this value should be between 1.7 and 1.9.

3. MOLECULAR WEIGHT OF ΦX174 HAE III DNA SIZE MARKER FRAGMENTS (BP)

1.	1353	7.	271
2.	1078	8.	234
3.	872	9.	194
4.	603	10.	118
5.	310	11.	72
6.	281		

4. DEFINITION OF ONE UNIT OF TAQ/HOTSTAR TAQ DNA POLYMERASE

It is the amount of enzyme that will incorporate 10 nmol of dNTPs into acid-insoluble material within 30 min at 72°C, under the assay conditions described in the Quality Control section of the Qiagen Taq/HotStar Taq PCR Handbook (February, 1999).

J. DETAILS OF SUPPLIERS OF REAGENTS AND EQUIPMENT

Amersham/Pharmacia Biotech UK Ltd.
Little Chalfont
Buckinghamshire
http://www.apbiotech.com

Clark Electromedical Instruments
Pangbourne
Reading
tel.: 01734 843888
fax: 01734 845374

Dako Ltd.
High Wycombe
Buckinghamshire
http://www.dakoltd.co.uk

Flowgen
Lichfield
Staffordshire
http://www.flowgen.co.uk

FMC Bioproducts
Distributed by: Flowgen

GRI - Genetic Research Instruments Ltd.
Essex
http://www.gri.co.uk/gri

Hoefer Scientific Instruments

Distributed by: Amersham/Pharmacia

Hybaid Limited

Ashford

Middlesex

http://www.hybaid.com

Leitz/Leica UK Ltd.

Milton Keynes

Buckinghamshire

http://www.leica.com

Merck Ltd.

Lutterworth

Leicestershire

http://www.merck-ltd.co.uk

MWG Biotech UK Ltd.

Peartree Bridge

Milton Keynes

http://www.mwgdna.com

National Diagnostics

Distributed by: Flowgen

Oncogene Science

Cambridge, MA

U.S.A.

http://www.oncogene.com

Oswel Research Products Ltd.

University of Southampton

Southampton

Hampshire

http://www.oswel.com

PE Applied Biosystems

Birchwood

Warrington

http://www.perkin-elmer.com

http://www.pedirect.co.uk

Polaroid

Distributed by: Sigma-Aldrich Company Ltd.

Promega UK

Southampton

Hampshire

http://www.euro.promega.com/uk

Qiagen Ltd.

Crawley

West Sussex

http://www.qiagen.com

Sanford Corporation

Bellwood

Illinois, U.S.A.

http://www.sanfordcorp.com

Sigma-Aldrich Company Ltd.

Fancy Road

Poole

Dorset

http://www.sigma-aldrich.com

Surgipath Europe Ltd.

Distributed by: Merck Ltd.

Ultra Violet Products Ltd.

Distributed by: GRI - Genetic Research Instruments Ltd.

Vector Laboratories Ltd.

Bretton

Peterborough

http://www.vectorlabs.com

REFERENCE LIST

Altschul, S.F., Gish, W., Miller, W., Myers, E.W., and Lipman, D.J. (1990). Basic Local Alignment Search Tool. J.Mol.Biol. *215*, 403-410.

An, S.F. and Fleming, K.A. (1991). Removal of inhibitor(s) of the polymerase chain reaction from formalin fixed, paraffin wax embedded tissues. J.Clin.Pathol. *44*, 924-927.

Ashwell, J.D. and Klausner, R.D. (1990). Genetic and mutational analysis of the T-cell antigen receptor. Annu.Rev.Immunol. *8*, 139-167.

Bagdi, E., Diss, T.C., Munson, P., and Isaacson, P.G. (1999). Mucosal intra-epithelial lymphocytes in enteropathy-associated T-cell lymphoma, ulcerative jejunitis, and refractory celiac disease constitute a neoplastic population. Blood *94*, 260-264.

Baumforth, K.R.N., Nelson, P.N., Digby, J.E., O'Neil, J.D.O., and Murray, P.G. (1999). Demystified... The polymerase chain reaction. J.Clin.Pathol.: Mol.Pathol. *52*, 1-10.

Bennett, W.P., Hollstein, M.C., Metcalf, R.A., Welsh, J.A., He, A., Zhu, S., Kusters, I., Resau, J.H., Trump, B.F., Lane, D.P., and Harris, C.C. (1992). p53 mutation and protein accumulation during multistage human oesophageal carcinogenesis. Cancer Research *52*, 6092-6097.

Bentley, G.A. and Mariuzza, R.A. (1996). The structure of the T cell antigen receptor. Annu.Rev.Immunol. *14*, 563-590.

Bodmer, J.G., Marsh, S.G.E., Albert, E.D., Bodmer, W.F., Bontrop, R.E., Dupont, B., Erlich, H.A., Hansen, J.A., Mach, B., Mayr, W.R., Parham, P., Petersdorf, E.W., Sasazuki, T., Schreuder, G.M., Strominger, J.L., Svejgaard, A., and Terasaki, P.I. (1999). Nomenclature for factors of the HLA system, 1998. Eur.J.Immunogenet. *26*, 81-116.

Bosari, S., Marchetti, A., Buttitta, F., Graziani, D., Borsani, G., Loda, M., Bevilacqua, G., and Coggi, G. (1995). Detection of p53 mutations by single-strand

conformation polymorphisms (SSCP) gel electrophoresis. Diagnostic Molecular Pathology *4*, 249-255.

Bovo, D., Rugge, M., and Shiao, Y.-H. (1999). Origin of spurious multiple bands in the amplification of microsatellite sequences. J.Clin.Pathol.: Mol.Pathol. *52*, 50-51.

Brandtzaeg, P., Halstensen, T.S., Kett, K., Krajci, P., Kvale, D., Rognum, T.O., Scott, H., and Sollid, L.M. (1989). Immunobiology and immunopathology of human gut mucosa: humoral immunity and intraepithelial lymphocytes. Gastroenterology *97*, 1562-1584.

Brown, J.H., Jardetzky, T.S., Gorga, J.C., Stern, L.J., Urban, R.G., Strominger, J.L., and Wiley, D.C. (1993). Three-dimensional structure of the human class II histocompatibility antigen HLA-DR1. Nature *364*, 33-39.

Camozzi, M.L.P., Diss, T.C., Du, M., and Isaacson, P.G. (2000). P53 mutations in enteropathy-associated T-cell lymphomas (EATL). European Association for Haematopathology (EAHP) Meeting, London (Abstract).

Carbonnel, F., Grollet-Bioul, L., Brouet, J.C., Teilhac, M.F., Cosnes, J., Angonin, R., Deschaseaux, M., Chatelet, F.-P., Gendre, J.P., and Sigaux, F. (1998). Are complicated forms of celiac disease cryptic T-cell lymphomas? Blood *92*, 3879-3886.

Cataldo, F., Ventura, A., Lazzari, R., Balli, F., Nassimbeni, G., and Marino, V. (1995). Antiendomysium antibodies and coeliac disease: solved and unsolved questions. An Italian multicentre study. Acta Paediatrica *84*, 1125-1131.

Catassi, C., Goelz, S.E., Fabiani, E., Rossini, M., Bordicchia, F., Candela, F., Coppa, G., and Giorgi, P. (1994). Coeliac disease in the year 2000: exploring the iceberg. The Lancet *343*, 200-203.

Cattoretti, G., Pileri, S., Parravicini, C., Becker, M.H.G., Poggi, S., Bifulco, C., Key, G., D'Amato, L., Sabattini, E., Feudale, E., Reynolds, F., Gerdes, J., and Rilke, F.

(1993). Antigen unmasking on formalin-fixed, paraffin-embedded tissue sections. Journal of Pathology *171*, 83-97.

Celli, J., Duijf, P., Hamel, B.C.J., Bamshad, M., Kramer, B., Smits, A.P.T., Newbury-Ecob, R., Hennekam, R.C.M., van Buggenhout, G., van Haeringen, A., Woods, C.G., van Essen, A.J., de Waal, R., Vriend, G., Haber, D.A., Yang, A., McKeon, F., Brunner, H.G., and van Bokhoven, H. (1999). Heterozygous germline mutations in the p53 homolog p63 are the cause of EEC syndrome. Cell *99*, 143-153.

Cellier, C., Patey, N., Mauvieux, L., Jabri, B., Delabesse, E., Cervoni, J.-P., Burtin, M.-L., Guy-Grand, D., Bouhnik, Y., Modigliani, R., Barbier, J.P., Macintyre, E., Brousse, N., and Cerf-Bensussan, N. (1998). Abnormal intestinal intraepithelial lymphocytes in refractory sprue. Gastroenterology *114*, 471-481.

Cellier, C., Delabesse, E., Helmer, C., Patey, N., Matuchansky, C., Jabri, B., Macintyre, E., Cerf-Bensussan, N., and Brousse, N. (2000). Refractory sprue, coeliac disease, and enteropathy-associated T-cell lymphoma. The Lancet *356*, 203-208.

Cesarman, E., Chadburn, A., Inghirami, G., Gaidano, G., and Knowles, D.M. (1992). Structural and functional analysis of oncogenes and tumor suppressor genes in adult T-cell leukemia/lymphoma shows frequent p53 mutations. Blood *80*, 3205-3216.

Cesarman, E., Inghirami, G., Chadburn, A., and Knowles, D.M. (1993). High levels of p53 protein expression do not correlate with p53 gene mutations in anaplastic large cell lymphoma. American Journal of Pathology *143*, 845-856.

Cesarman, E., Liu, Y.F., and Knowles, D.M. (1994). The MDM2 oncogene is rarely amplified in human lymphoid tumours and does not correlate with p53 gene expression. International Journal of Cancer *56*, 457-458.

Chen, X. (1999). The p53 family: same response, different signals? Molecular Medicine Today *5*, 387-392.

Cheung, V.G. and Nelson, S.F. (1996). Whole genome amplification using a degenerate oligonucleotide primer allows hundreds of genotypes to be performed on less than one nanogram of genomic DNA. Proc Natl Acad Sci USA *93*, 14676-14679.

Chien, A., Edgar, D.B., and Trela, J.M. (1976). Deoxyribonucleic acid polymerase from the extreme thermophile *Thermus aquaticus*. J.Bacteriol. *127*, 1550-1557.

Chien, Y., Jores, R., and Crowley, M.P. (1996). Recognition by γ/δ T cells. Annu.Rev.Immunol. *14*, 511-532.

Cho, Y., Gorina, S., Jeffrey, P.D., and Pavletich, N.P. (1994). Crystal structure of a p53 tumor suppressor-DNA complex: understanding tumorigenic mutations. Science *265*, 346-355.

Chorzelsky, T.P., Beutner, E.H., Suley, J., Chorzewska, H.T., Jablonska, S., Kumar, V., and Kapuscinska, A. (1984). IgA antiendomysium antibody. A new immunological marker of dermatitis herpetiformis and coeliac disease. Br.J.Dermatol. *111*, 395-402.

Chou, Q., Russel, M., Birch, D.E., Raymond, J., and Bloch, W. (1992). Prevention of pre-PCR mis-priming and primer dimerization improves low-copy-number amplifications. Nucleic Acids Research *20*, 1717-1723.

Ciclitira, P.J. and Hall, M.A. (1990). Coeliac disease. Bailliere's Clinical Gastroenterology *4*, 43-59.

Cimino, G.D., Metchette, K., Isaacs, S.T., and Zhu, Y.S. (1990). More false-positive problems. Nature *345*, 773-774.

Collin, P., Maki, M., Keyrilainen, O., Hallstrom, O., Reunala, T., and Pasternack, A. (1992). Selective IgA deficiency and coeliac disease. Scand J Gastroenterol *27*, 367-371.

Congia, M., Cucca, F., Frau, F., Lampis, R., Melis, L., Clemente, M.G., Cao, A., and Virgilis, S.d. (1994). A gene dosage effect of the DQA1*0501/DQB1*0201 allelic combination influences the clinical heterogeneity of celiac disease. Human Immunology *40*, 138-142.

Connell, C., Fung, S., Heiner, C., Bridgham, J., Chakerian, V., Heron, E., Jones, B., Menchen, S., Mordan, W., Raff, M., Recknor, M., Smith, L., Springer, J., Woo, S., and Hunkapiller, M. (1987). Automated DNA sequence analysis. Biotechniques *5*, 342-348.

Corazza, G.R., Andreani, M.L., Biagi, F., Corrao, G., Pretolani, S., Giulianelli, G., Ghironzi, G., and Gasbarrini, G. (1997). The smaller size of the 'coeliac iceberg' in adults. Scand J Gastroenterol *32*, 917-919.

Cordon-Cardo, C., Latres, E., Drobnjak, M., Oliva, M.R., Pollack, D., Woodruff, J.M., Marechal, V., Chen, J., Brennan, M.F., and Levine, A.J. (1994). Molecular abnormalities of mdm2 and p53 genes in adult soft tissue sarcomas. Cancer Research *54*, 794-799.

Cordon-Cardo, C. and Richon, V.M. (1994). Expression of the retinoblastoma protein is regulated in normal human tissues. American Journal of Pathology *144*, 500-510.

Cuevas, E.C., Bateman, A.C., Wilkins, B.S., Johnson, P.A., Williams, J.H., Lee, A.H.S., Jones, D.B., and Wright, D.H. (1994). Microwave antigen retrieval in immunocytochemistry: a study of 80 antibodies. J.Clin.Pathol. *47*, 448-452.

Darnton, S.J. (1998). Demystified... p53. J.Clin.Pathol.: Mol.Pathol. *51*, 248-253.

de Bruin, P.C., Connolly, C.E., Oudejans, J.J., Kummer, J.A., Jansen, W., McCarthy, C.F., and Meijer, C.J.L.M. (1997). Enteropathy-associated T-cell lymphomas have a cytotoxic T-cell phenotype. Histopathology *31*, 313-317.

Deem, R.L., Shanahan, F., and Targan, S.R. (1991). Triggered human mucosal T cells release tumour necrosis factor-alpha and interferon-gamma which kill human colonic epithelial cells. Clin Exp Immunol *83*, 79-84.

Dieterich, W., Ehnis, T., Bauer, M., Donner, P., Volta, U., Riecken, E.O., and Schuppan, D. (1997). Identification of tissue transglutaminase as the autoantigen of celiac disease. Nature Medicine *3*, 797-801.

Dittmer, D., Pati, S., Zambetti, G., Chu, S., Teresky, A.K., Moore, M., Finlay, C., and Levine, A.J. (1993). Gain of function mutations in p53. Nature Genetics *4*, 42-46.

Dixon, M.F. (1996). Alimentary system. In General and Systematic Pathology. J.C.E. Underwood, ed. (Churchill Livingstone), pp. 401-448.

Djilali-Saiah, I., Schmitz, J., Harfouch-Hammoud, E., Mougenot, J.-F., Bach, J.-F., and Caillat-Zucman, S. (1998). CTLA-4 gene polymorphism is associated with predisposition to coeliac disease. Gut *43* , 187-189.

Donehower, L.A. and Bradley, A. (1993). The tumor suppressor p53. Biochimica et Biophysica Acta *1155*, 181-205.

Dowell, S.P. and Ogden, G.R. (1996). The use of antigen retrieval for immunohistochemical detection of p53 over-expression in malignant and benign oral mucosa: a cautionary note. J.Oral Pathol.Med. *25* , 60-64.

Du, M., Peng, H., Singh, N., Isaacson, P.G., and Pan, L.X. (1995). The accumulation of p53 abnormalities is associated with progression of mucosa-associated lymphoid tissue lymphoma. Blood *86*, 4587-4593.

El-Deiry, W.S., Harper, J.W., O'Connor, P.M., Velculescu, V.E., Canman, C.E., Jackman, J., Pietenpol, J.A., Burrell, M., Hill, D.E., Wang, Y., Wiman, K.G., Mercer, W.E., Kastan, M.B., Kohn, K.W., Elledge, S.J., Kinzler, K.W., and Vogelstein, B. (1994). Waf1/Cip1 is induced in p53-mediated G1 arrest and apoptosis. Cancer Research *54*, 1169-1174.

El-Deiry, W.S. (1998). Regulation of p53 downstream genes. Seminars in Cancer Biology *8*, 345-357.

Elledge, S.J. (1996). Cell cycle checkpoints: preventing an identity crisis. Science *274*, 1664-1671.

Fairley, N.H. and Mackie, F.P. (1937). The clinical and biochemical syndrome in lymphadenoma and allied diseases involving the mesenteric lymph glands. British Medical Journal *i*, 375-380.

Ferreira, M., Davies, S.L., Butler, M., Scott, D., Clark, M., and Kumar, P. (1992). Endomysial antibody: is it the best screening test for coeliac disease? Gut *33*, 1633-1637.

Forsthoefel, K.F., Papp, A.C., Snyder, P.J., and Prior, T.W. (1992). Optimization of DNA extraction from formalin-fixed tissue and its clinical application in Duchenne muscular dystrophy. American Journal of Clinical Pathology *98*, 98-104.

Foulkes, W.D., Black, D.M., Stamp, G.W.H., Solomon, E., and Trowsdale, J. (1993). Very frequent loss of heterozygosity throughout chromosome 17 in sporadic ovarian carcinoma. Int.J.Cancer *54*, 220-225.

Friedberg, E.C. (1985). DNA damage. In DNA Repair. E.C. Friedberg, ed. (New York: WH Freeman and Company), pp. 1-77.

Gaidano, G., Ballerini, P., Gong, J.Z., Inghirami, G., Neri, A., Newcomb, E.W., Magrath, J.T., Knowles, D.M., and Dalla-Favera, R. (1991). P53 mutations in human lymphoid malignancies:association with Burkitt lymphoma and chronic lymphocytic leukemia. Proc Natl Acad Sci USA *88*, 5413-5417.

Garboczi, D.N., Ghosh, P., Utz, U., Fan, Q.R., Biddison, W.E., and Wiley, D.C. (1996). Structure of the complex between human T-cell receptor, viral peptide and HLA-A2. Nature *384*, 134-141.

Gelfand, D.H. and White, T.J. (1990). Thermostable DNA polymerases. In PCR protocols:a guide to methods and applications. M.A. Innis, D.H. Gelfand, J.J. Sninsky, and T.J. White, eds. (Academic Press Inc), pp. 129-141.

Gillett, C.E. and Barnes, D.M. (1998). Demystified...cell cycle. J.Clin.Pathol.: Mol.Pathol. *51*, 310-316.

Goelz, S.E., Hamilton, S.R., and Vogelstein, B. (1985). Purification of DNA from formaldehyde fixed and paraffin embedded human tissue. Biochemical and Biophysical Research Communications *130*, 118-126.

Gottlieb, T.M. and Oren, M. (1996). p53 in growth control and neoplasia. Biochimica et Biophysica Acta *1287*, 77-102.

Gough, K.R., Read, A.E., and Naish, J.M. (1962). Intestinal reticulosis as a complication of idiopathic steatorrhoea. Gut *3*, 232-239.

Graeber, T.G., Osmanian, C., Jacks, T., Housman, D.E., Kock, C.J., Lowe, S.W., and Giaccia, A.J. (1996). Hypoxia-mediated selection of cells with diminished apoptotic potential in solid tumours. Nature *379*, 88-91.

Greenblatt, M.S., Bennett, W.P., Hollstein, M., and Harris, C.C. (1994). Mutations in the p53 tumor suppressor gene: clues to cancer etiology and molecular pathogenesis. Cancer Research *54*, 4855-4878.

Greer, C.E., Wheeler, C.M., and Manos, M.M. (1994). Sample preparation and PCR amplification from paraffin-embedded tissues. PCR Methods and Applications *3*, S113-S122.

Gruis, N.A., Abeln, E.C.A., Bardoel, A.F.J., Devilee, P., Frants, R.R., and Cornelisse, C.J. (1993). PCR-based microsatellite polymorphisms in the detection of loss of heterozygosity in fresh and archival tumour tissue. Br.J.Cancer *68*, 308-313.

Hansen, R. and Oren, M. (1997). P53; from inductive signal to cellular effect. Current Opinion in Genetics and Development *7*, 46-51.

Harper, K., Balzano, C., Rouvier, E., Mattei, M.G., Luciani, M.F., and Golstein, P. (1991). CTLA-4 and CD28 activated lymphocyte molecules are closely related in both mouse and human as to sequence, message expression, gene structure, and chromosomal location. J Immunol *147*, 1037-1044.

Harris, O.D., Cooke, W.T., Thompson, H., and Waterhouse, J.A.H. (1967). Malignancy in adult celiac disease and idiopathic steatorrhea. American Journal of Medicine *42*, 899-912.

Harris, S. and Jones, D.B. (1997). Optimisation of the polymerase chain reaction. British Journal of Biomedical Science *54*, 166-173.

Harvey, M., Vogel, H., Morris, D., Bradley, A., Bernstein, A., and Donehower, L.A. (1995). A mutant p53 transgene accelerates tumour development in heterozygous but not nullizygous p53-deficient mice. Nature Genetics *9*, 305-311.

Haupt, Y., Maya, R., Kazaz, A., and Oren, M. (1997). Mdm2 promotes the rapid degradation of p53. Nature *387*, 296-299.

Hayashi, K. (1991). PCR-SSCP: A simple and sensitive method for detection of mutations in the genomic DNA. PCR Methods and Applications *1*, 34-38.

Heichman, K.A. and Roberts, J.M. (1994). Rules to replicate by. Cell *79*, 557-562.

Hollstein, M., Sidransky, D., Vogelstein, B., and Harris, C.C. (1991). P53 mutations in human cancers. Science *253*, 49-53.

Hollstein, M., Rice, K., Greenblatt, M.S., Soussi, T., Fuchs, R., Sorlie, T., Hovig, E., Smith-Sorensen, B., Montesano, R., and Harris, C.C. (1994). Database of p53 gene somatic mutations in human tumors and cell lines. Nucleic Acids Research *22*, 3551-3555.

Holmes, G.K.T., Prior, P., Lane, M.R., Pope, D., and Allan, R.N. (1989). Malignancy in coeliac disease - effect of a gluten free diet. Gut *30*, 333-338.

Houlston, R.S. and Ford, D. (1996). Genetics of coeliac disease. Q J Med *89*, 737-743.

Howdle, P.D. and Losowsky, M.S. (1987). The immunology of coeliac disease. Bailliere's Clinical Gastroenterology *1*, 507-529.

Howell, W.M. and Jones, D.B. (1995). The role of human leucocyte antigen genes in the development of malignant disease. J.Clin.Pathol.: Mol.Pathol. *48*, M302-M306.

Howell, W.M., Leung, S.T., Jones, D.B., Nakshabendi, I., Hall, M.A., Lanchbury, J.S., Ciclitira, P.J., and Wright, D.H. (1995). HLA-DRB, DQA and DQB polymorphism in celiac disease and enteropathy-associated T-cell lymphoma: common features and additional risk factors for malignancy. Human Immunology *43*, 29-37.

Hsu, S.-M. and Soban, E. (1982). Color modification of diaminobenzidine (DAB) precipitation by metallic ionsand its application for double immunohistochemistry. The Journal of Histochemistry and Cytochemistry *30*, 1079-1082.

Innis, M.A. and Gelfand, D.H. (1990). Optimization of PCRs. In PCR protocols:a guide to methods and applications. M.A. Innis, D.H. Gelfand, J.J. Sninsky, and T.J. White, eds. (Academic Press Inc), pp. 3-12.

Isaacson, P. and Wright, D.H. (1978). Intestinal lymphoma associated with malabsorption. The Lancet *i*, 67-70.

Isaacson, P.G., Spencer, J., Connolly, C.E., Pollock, D.J., Stein, H., O'Connor, N.T.J., Bevan, D.H., Kirkham, N., Wainscoat, J.S., and Mason, D.Y. (1985). Malignant histiocytosis of the intestine: a T-cell lymphoma. The Lancet *ii*, 688-691.

Isaacson, P.G. (1999). Gastrointestinal lymphomas of T- and B-cell types. Mod Pathol *12*, 151-158.

Janeway, C.A., Jr. (1992). The T cell receptor as a multicomponent signalling machine: CD4/CD8 coreceptors and CD45 in T cell activation. Annu.Rev.Immunol. *10*, 645-674.

Janeway, C.A., Jr. and Travers, P. (1997). Antigen recognition by T lymphocytes. In Immunobiology - the immune system in health and disease. C.A. Janeway, Jr. and P. Travers, eds. (Current Biology Ltd., Churchill Livingstone, Garland Publishing Inc), pp. 4:1-4:49.

Johansen, B.H., Vartdal, F., Eriksen, J.A., Thorsby, E., and Sollid, L.M. (1996). Identification of a putative motif for binding of peptides to HLA-DQ2. International Immunology *8*, 177-182.

Jones, M.H. and Nakamura, Y. (1992). Detection of loss of heterozygosity at the human *TP53* locus using a dinucleotide repeat polymorphism. Genes Chrom Cancer *5*, 89-90.

Kaelin, W.G., Jr. (1999). The emerging p53 gene family. J Natl Cancer Inst *91*, 594-598.

Kaghad, M., Bonnet, H., Yang, A., Creancier, L., Biscan, J.-C., Valent, A., Minty, A., Chalon, P., Lelias, J.-M., Dumont, X., Ferrara, P., McKeon, F., and Caput, D. (1997). Monoallelically expressed gene related to p53 at 1p36, a region frequently deleted in neuroblastoma and other human cancers. Cell *90*, 809-819.

Kagnoff, M.F. (1990). Understanding the molecular basis of coeliac disease. Gut *31*, 497-499.

Kamer, J.H.v.d., Weijers, H.A., and Dicke, W.K. (1953). Coeliac Disease. Acta Paediatrica *42*, 223-231.

Kastan, M.B., Onyekwere, O., Sidransky, D., Vogelstein, B., and Craig, R.W. (1991). Participation of p53 protein in the cellular response to DNA damage. Cancer Research *51*, 6304-6311.

Kelly, C.P., Feighery, C.F., Gallagher, R.B., Gibney, M.J., and Weir, D.G. (1991). Mucosal and systemic IgA anti-gliadin antibody in celiac disease. Digestive Diseases and Sciences *36*, 743-751.

Keuning, J.J., Pena, A.S., Leeuwen, A.v., Hooff, J.P.v., and Rood, J.J.v. (1976). HLA-DW3 associated with coeliac disease. The Lancet *i*, 506-508.

Ko, L.J. and Prives, C. (1996). P53: puzzle and paradigm. Genes and Development *10*, 1054-1072.

Kocialkowski, S., Pezzella, F., Morrison, H., Jones, M., Laha, S., Harris, A.L., Mason, D.Y., and Gatter, K.C. (1995). Mutations in the p53 gene are not limited to classic 'hot spots' and are not predictive of p53 protein expression in high-grade non-Hodgkin's lymphoma. British Journal of Haematology *89*, 55-60.

Koreth, J., Bakkenist, C.J., and McGee, J.O. (1998). Microsatellite analysis in human disease. In Clinical Applications of PCR. Y.M.D. Lo, ed. (Totowa: Humana Press Inc.), pp. 321-339.

Kubbutat, M.H.G., Jones, S.N., and Vousden, K.H. (1997). Regulation of p53 stability by Mdm2. Nature *387*, 299-303.

Ladinser, B., Rossipal, E., and Pittschieler, K. (1994). Endomysium antibodies in coeliac disease: an improved method. Gut *35*, 776-778.

Lamb, P. and Crawford, L. (1986). Characterization of the human p53 gene. Molecular and Cellular Biology *6*, 1379-1385.

Lane, D.P. (1992). p53, guardian of the genome. Nature *358*, 15-16.

Lauritzen, A.F., Vejlsgaard, G.L., Hou-Jensen, K., and Ralfkiaer, E. (1995). p53 protein expression in cutaneous T-cell lymphomas. British Journal of Dermatology *133*, 32-36.

Levine, A.J., Momand, J., and Finlay, C.A. (1991). The p53 tumour suppressor gene. Nature *351*, 453-456.

Levine, A.J. (1995). Tumor suppressor genes. Scientific American Science and Medicine *3*, 28-37.

Levine, A.J. (1997). p53, the cellular gatekeeper for growth and division. Cell *88*, 323-331.

Li, G., Chooback, L., Wolfe, J.T., Rook, A.H., Felix, C.A., Lessin, S.R., and Salhany, K.E. (1998). Overexpression of p53 protein in cutaneous T cell lymphoma: relationship to large cell transformation and disease progression. J Invest Dermatol *110*, 767-770.

Lo, Y.M.D. (1998a). Introduction to the polymerase chain reaction. In Clinical Applications of PCR. Y.M.D. Lo, ed. (Totowa: Humana Press Inc), pp. 3-10.

Lo, Y.M.D. (1998b). PCR for the detection of minority DNA populations. In Clinical Applications of PCR. Y.M.D. Lo, ed. (Totowa: Humana Press Inc), pp. 101-107.

Lo, Y.M.D. (1998c). Amplification from archival materials. In Clinical Applications of PCR. Y.M.D. Lo, ed. (Totowa: Humana Press Inc), pp. 21-25.

Loda, M. (1994). PCR-based methods for the detection of mutations in oncogenes and tumor suppressor genes. Human Pathology *25*, 564-571.

Loeb, L.A. (1998). Cancer cells exhibit a mutator phenotype. Advances in Cancer Research *72*, 25-56.

Logan, R.F.A., Rifkind, E.A., Busuttil, A., Gilmour, H.M., and Ferguson, A. (1986). Prevalence and 'incidence' of celiac disease in Edinburgh and the Lothian region of Scotland. Gastroenterology *90*, 334-342.

Logan, R.F.A., Rifkind, E.A., Turner, I.D., and Ferguson, A. (1989). Mortality in celiac disease. Gastroenterology *97*, 265-271.

Lundin, K.E.A., Scott, H., Hansen, T., Paulsen, G., Halstensen, T.S., Fausa, O., Thorsby, E., and Sollid, L.M. (1993). Gliadin-specific, HLA-DQ(α1*0501,β1*0201) restricted T cells isolated from the small intestinal mucosa of celiac disease patients. Journal of Experimental Medicine *178*, 187-196.

Lundin, K.E.A., Scott, H., Fausa, O., Thorsby, E., and Sollid, L.M. (1994). T cells from the small intestinal mucosa of a DR4,DQ7/ DR4,DQ8 celiac disease patient preferentially recognize gliadin when presented by DQ8. Human Immunology *41*, 285-291.

Lundin, K.E.A., Sollid, L.M., Anthonsen, D., Noren, O., Molberg, O., Thorsby, E., and Sjostrom, H. (1997). Heterogeneous reactivity patterns of HLA-DQ-restricted, small intestinal T-cell clones from patients with celiac disease. Gastroenterology *112*, 752-759.

MacLennan, K. (1996). Lymph nodes, thymus and spleen. In General and Systematic Pathology. J.C.E. Underwood, ed. (Churchill Livingstone), pp. 657-682.

Marin, M.C., Jost, C.A., Irwin, M., DeCaprio, J.A., Caput, D., and Kaelin, W.G., Jr. (1998). Viral oncoproteins discriminate between p53 and the p53 homolog p73. Molecular and Cellular Biology *18*, 6316-6324.

Marsh, M.N. (1992). Gluten, major histocompatibility complex, and the small intestine. Gastroenterology *102*, 330-354.

Martinez-Delgado, B., Robledo, M., Arranz, E., Infantes, F., Echezarreta, G., Marcos, B., Sanz, C., Rivas, C., and Benitez, J. (1997). Correlation between mutations in p53 gene and protein expression in human lymphomas. American Journal of Hematology *55*, 1-8.

Martinez, J.C., Piris, M.A., Sanchez-Beato, M., Villuendas, R., Orradre, J.L., Algara, P., Sanchez-Verde, L., and Martinez, P. (1993). Retinoblastoma (Rb) gene product

expression in lymphomas. Correlation with Ki67 growth fraction. Journal of Pathology *169*, 405-412.

Martinez, J.C., Mateo, M., Sanchez-Beato, M., Villuendas, R., Orradre, J.L., Algara, P., Sanchez-Verde, L., Garcia, P., Lopez, C., Martinez, P., and Piris, M.A. (1995). MDM2 expression in lymphoid cells and reactive and neoplastic lymphoid tissue. Comparative study with p53 expression. Journal of Pathology *177*, 27-34.

Mathus-Vliegen, E.M.H. (1996). Coeliac disease and lymphoma: current status. Netherlands Journal of Medicine *49*, 212-220.

Matsushima, A.Y., Cesarman, E., Chadburn, A., and Knowles, D.M. (1994a). Post-thymic T-cell lymphomas frequently overexpress p53 protein but infrequently exhibit p53 gene mutations. American Journal of Pathology *144*, 573-584.

Matsushima, A.Y., Cesarman, E., and Knowles, D.M. (1994b). Mutations are not detected outside p53 gene exons 5 to 9 in lymphoid tumors. Laboratory Investigation *70*, 115A(Abstract).

McKee, P.H., Hobbs, C., and Hall, P.A. (1993). Antigen retrieval by microwave irradiation lowers immunohistological detection thresholds. Histopathology *23*, 377-379.

Mercer, W.E. and Baserga, R. (1985). Expression of the p53 protein during the cell cycle of human peripheral blood lymphocytes. Exp.Cell Res. *160*, 31-46.

Merlo, G.R., Cropp, C.S., Callahan, R., and Takahashi, T. (1991). Detection of loss of heterozygosity in tumor DNA samples by PCR. Biotechniques *11*, 166-171.

Mies, C. (1994). Molecular biological analysis of paraffin-embedded tissues. Human Pathology *25*, 555-560.

Milner, B.J., Allan, L.A., Eccles, D.M., Kitchener, H.C., Leonard, R.C.F., Kelly, K.F., Parkin, D.E., and Haites, N.E. (1993). p53 mutation is a common genetic event in ovarian carcinoma. Cancer Research *53*, 2128-2132.

Molberg, O., Kett, K., Scott, H., Thorsby, E., Sollid, L.M., and Lundin, K.E.A. (1997). Gliadin specific, HLA DQ2-restricted T cells are commonly found in small intestinal biopsies from coeliac disease patients, but not from controls. Scand J Immunol *46*, 103-108.

Molberg, O., McAdam, S., Korner, R., Quarsten, H., Kristiansen, C., Madsen, L., Fugger, L., Scott, H., Noren, O., Roepstorff, P., Lundin, K.E.A., Sjostrom, H., and Sollid, L.M. (1998). Tissue transglutaminase selectively modifies gliadin peptides that are recognized by gut-derived T cells in celiac disease. Nature Medicine *4*, 713-717.

Momand, J., Zambetti, G.P., Olson, D.C., George, D., and Levine, A.J. (1992). The mdm-2 oncogene product forms a complex with the p53 protein and inhibits p53-mediated transactivation. Cell *69*, 1237-1245.

Moskaluk, C.A. and Kern, S.E. (1997). Microdissection and polymerase chain reaction amplification of genomic DNA from histological tissue sections. American Journal of Pathology *150*, 1547-1552.

Murray, A., Cuevas, E.C., Jones, D.B., and Wright, D.H. (1995). Study of the immunohistochemistry and T-cell clonality of enteropathy associated T-cell lymphomas. American Journal of Pathology *146*, 509-519.

Nasmyth, K. (1996). Viewpoint: putting the cell cycle in order. Science *274*, 1643-1645.

Newton, C.R. and Graham, A. (1997a). Instrumentation, Reagents and Consumables. In PCR. D. Billington, ed. (Bios Scientific Publishers Ltd), pp. 9-28.

Newton, C.R. and Graham, A. (1997b). Amplifying the correct product. In PCR. D. Billington, ed. (Bios Scientific Publishers Ltd), pp. 29-46.

Newton, C.R. and Graham, A. (1997c). Sequencing PCR products. In PCR. D. Billington, ed. (Bios Scientific Publishers Ltd), pp. 85-99.

Nigro, J.M., Baker, S.J., Preisinger, A.C., Jessup, J.M., Hostetter, R., Cleary, K., Bigner, S.H., Davidson, N., Baylin, S., Devilee, P., Glover, T., Collins, F.S., Weston, A., Modali, R., Harris, C.C., and Vogelstein, B. (1989). Mutations in the p53 gene occur in diverse human tumour types. Nature *342*, 705-708.

Nilsen, E., Lundin, K.E.A., Krajci, P., Scott, H., Sollid, L.M., and Brandtzaeg, P. (1995). Gluten specific, HLA-DQ restricted T cells from coeliac mucosa produce cytokines with Th1 or Th0 profile dominated by interferon γ. Gut *37*, 766-776.

Nilsen, E., Jahnsen, F., Lundin, K.E.A., Johansen, F.-E., Fausa, O., Sollid, L.M., Jahnsen, J., Scott, H., and Brandtzaeg, P. (1998). Gluten induces an intestinal cytokine response strongly dominated by interferon gamma in patients with coeliac disease. Gastroenterology *115*, 551-563.

Nurse, P. (1994). Ordering S phase and M phase in the cell cycle. Cell *79*, 547-550.

O'Farrelly, C., Feighery, C., O'Brian, D., Stevens, F., Connolly, C., McCarthy, C., and Weir, D.G. (1986). Humoral response to wheat protein in patients with coeliac disease and enteropathy-associated T cell lymphoma. British Medical Journal *293*, 908-910.

Oberhuber, G., Vogelsang, H., Stolte, M., Muthenthaler, S., Kummer, A.J., and Radaszkiewicz, T. (1996). Evidence that intestinal intraepithelial lymphocytes are activated cytotoxic T cells in celiac disease but not in giardiasis. American Journal of Pathology *148*, 1351-1357.

Oliner, J.D., Kinzler, K.W., Meltzer, P.S., George, D.L., and Vogelstein, B. (1992). Amplification of a gene encodig a p53-associated protein in human sarcomas. Nature *358*, 80-83.

Orita, M., Iwahana, H., Kanazawa, H., Hayashi, K., and Sekiya, T. (1989a). Detection of polymorphisms of human DNA by gel electrophoresis as SSCP. Proc Natl Acad Sci USA *86*, 2766-2770.

Orita, M., Suzuki, Y., Sekiya, T., and Hayashi, K. (1989b). Rapid and sensitive detection of point mutations and DNA polymorphisms using the polymerase chain reaction. Genomics *5*, 874-879.

Paggi, M.G., Baldi, A., Bonetto, F., and Giordano, A. (1996). Retinoblastoma protein family in cell cycle and cancer: a review. Journal of Cellular Biochemistry *62*, 418-430.

Pan, L.X., Diss, T.C., and Isaacson, P.G. (1995). The polymerase chain reaction in histopathology. Histopathology *26*, 201-217.

Panja, A. and Mayer, L. (1996). Antigen presentation in the intestine. Bailliere's Clinical Gastroenterology *10*, 407-425.

Patey-Mariaud de Serre, N., Cellier, C., Jabri, B., Delabesse, E., Verkarre, V., Roche, B., Lavergne, A., Briere, J., Mauvieux, L., Leborgne, M., Barbier, J.P., Modigliani, R., Matuchansky, C., Macintyre, E., Cerf-Bensussan, N., and Brousse, N. (2000). Distinction between coeliac disease and refractory sprue: a simple immunohistochemical method. Histopathology *37*, 70-77.

Pescarmona, E., Pignoloni, P., Santangelo, C., Naso, G., Realacci, M., Cela, O., Lavinia, A., Martelli, M., Russo, M., and Baroni, C. (1999). Expression of p53 and retinoblastoma gene in high-grade nodal peripheral T-cell lymphomas: immunohistochemical and molecular findings suggesting different pathogenetic pathways and possible clinical implications. Journal of Pathology *188*, 400-406.

Phelps, M., Wilkins, B.S., and Jones, D.B. (2000). Selective genetic analysis of p53 immunostain positive cells. J.Clin.Pathol.: Mol.Pathol. *53*, 159-161.

Picarelli, A., Maiuri, L., Frate, A., Greco, M., Auricchio, S., and Londei, M. (1996). Production of antiendomysial antibodies after in-vitro gliadin challenge of small

intestine biopsy samples from patients with coeliac disease. The Lancet *348*, 1065-1067.

Piris, M.A., Villuendas, R., Martinez, J.C., Sanchez-Beato, M., Orradre, J.L., Mateo, M.S., and Martinez, P. (1995). p53 expression in non-Hodgkin's lymphomas: a marker of p53 inactivation? Leukemia and Lymphoma *17*, 35-42.

Ploski, R., Ek, J., Thorsby, E., and Sollid, L.M. (1993). On the HLA-DQ(α1*0501,β1*0201)-associated susceptibility in celiac disease:a possible gene dosage effect of DQB1*0201. Tissue Antigens *41*, 173-177.

Polak, J.M. and Norden, S.v. (1997a). Requirements for immunocytochemistry. In Introduction to Immunocytochemistry. J.M. Polak and S.v. Norden, eds. (Bios Scientific Publishers Ltd), pp. 13-36.

Polak, J.M. and Norden, S.v. (1997b). Methods. In Introduction to Immunocytochemistry. J.M. Polak and S.v. Norden, eds. (Bios Scientific Publishers Ltd), pp. 37-54.

Pomerantz, J., Schreiber-Agus, N., Liegeois, J., Silverman, A., Alland, L., Chin, L., Potes, J., Chen, K., Orlow, I., Lee, H.-W., Cordon-Cardo, C., and DePinho, R.A. (1998). The Ink4a tumor suppressor gene product, $p19^{Arf}$, interacts with MDM2 and neutralizes MDM2's inhibition of p53. Cell *92*, 713-723.

Prives, C. and Hall, P.A. (1999). The p53 pathway. Journal of Pathology *187*, 112-126.

Rainbow, R.D. (1996). Immunohistochemistry. In Laboratory Histopathology - a complete reference. A.E. Woods and R.C. Ellis, eds. (Churchill Livingstone), pp. 8.2-1-8.2-72.

Reifenberger, G., Liu, L., Ichimura, K., Schmidt, E.E., and Collins, V.P. (1993). Amplification and overexpression of the MDM2 gene in a subset of human malignant gliomas without p53 mutations. Cancer Research *53*, 2736-2739.

Rosenblum, B.B., Lee, L.G., Spurgeon, S.L., Khan, S.H., Menchen, S.M., Heiner, C.R., and Chen, S.M. (1997). New dye-labeled terminators for improved DNA sequencing patterns. Nucleic Acids Research *25*, 4500-4504.

Russell, G.J., Winter, H.S., Fox, V.L., and Bhan, A.K. (1991). Lymphocytes bearing the γδT-cell receptor in normal human intestine and celiac disease. Hum Pathol *22*, 690-694.

Said, J.W., Barrera, R., Shintaku, I.P., Nakamura, H., and Koeffler, H.P. (1992). Immunohistochemical analysis of p53 expression in malignant lymphomas. American Journal of Pathology *141*, 1343-1348.

Salter, D.M., Krajewski, A.S., and Dewar, A.E. (1986). Immunophenotype analysis of malignant histiocytosis of the intestine. J.Clin.Pathol. *39*, 8-15.

Sambrook, J., Fitsch, E.F., and Maniatis, T. (1989). Gel electrophoresis of DNA. In Molecular cloning - a laboratory manual. J. Sambrook, E.F. Fitsch, and T. Maniatis, eds. (Cold Springer Harbor Laboratory Press), pp. 6.1-6.62.

Sander, C.A., Yano, I., Clark, H.M., Harris, C., Longo, D.L., Jaffe, E.S., and Raffeld, M. (1993). p53 mutation is associated with progression in follicular lymphomas. Blood *82*, 1994-2004.

Sanger, F., Nicklen, S., and Coulson, A.R. (1977). DNA sequencing with chain-terminating inhibitors. Proc Natl Acad Sci USA *74*, 5463-5467.

Sarkar, G. and Sommer, S. (1990). More light on PCR contamination. Nature *347*, 340-341.

Selivanova, G. and Wiman, K.G. (1995). p53: a cell cycle regulator activated by DNA damage. Advances in Cancer Research *66*, 143-180.

Sheffield, V.C., Beck, J.S., Kwitek, A.E., Sandstrom, D.W., and Stone, E.M. (1993). The sensitivity of SSCP analysis for the detection of single base substitutions. Genomics *16*, 325-332.

Sherr, C.J. (1994). G1 phase progression: cycling on cue. Cell *79*, 551-555.

Sherr, C.J. (1996). Cancer cell cycles. Science *274*, 1672-1677.

Shi, S.T., Feng, B., Yang, G.-Y., Wang, L.-D., and Yang, C.S. (1996). Immunohistoselective sequencing (IHSS) of p53 tumor suppressor gene in human oesophageal precancerous lesions. Carcinogenesis *17*, 2131-2136.

Shibata, D., Hawes, D., Li, Z.-H., Hernandez, A.M., Spruck, C.H., and Nichols, P.W. (1992). Specific genetic analysis of microscopic tissue after selective ultraviolet radiation fractionation and the polymerase chain reaction. American Journal of Pathology *141*, 539-543.

Shibata, D. (1994). Extraction of DNA from paraffin-embedded tissue for analysis by polymerase chain reaction: new tricks from an old friend. Human Pathology *25*, 561-563.

Shibata, D. (1998). The SURF technique - Selective genetic analysis of microscopic tissue heterogeneity. In PCR in Bioanalysis. S.J. Meltzer, ed. (Totowa: Humana Press Inc.), pp. 39-47.

Shieh, S.-Y., Ikeda, M., Taya, Y., and Prives, C. (1997). DNA damage-induced phosphorylation of p53 alleviates inhibition by MDM2. Cell *91*, 325-334.

Sjostrom, H., Lundin, K.E.A., Molberg, O., Körner, R., McAdam, S., Anthonsen, D., Quarsten, H., Noren, O., Roepstorff, P., Thorsby, E., and Sollid, L.M. (1998). Identification of a gliadin T-cell epitope in coeliac disease: general importance of gliadin deamidation for intestinal T-cell recognition. Scand J Immunol *48*, 111-115.

Slatko, B.E. (1996). Thermal cycle dideoxy DNA sequencing. Molecular Biotechnology *6*, 311-322.

Soini, Y., Paakko, P., Alavaikko, M., and Vahakangas, K. (1992). p53 expression in lymphatic malignancies. Journal of Clinical Pathology *45*, 1011-1014.

Sollid, L.M., Markussen, G., Ek, J., Gjerde, H., Vartdal, F., and Thorsby, E. (1989). Evidence for a primary association of celiac disease to a particular HLA-DQ α/β heterodimer. Journal of Experimental Medicine *169*, 345-350.

Sollid, L.M. and Thorsby, E. (1993). HLA susceptibility genes in celiac disease: genetic mapping and role in pathogenesis. Gastroenterology *105*, 910-922.

Soto, D. and Sukumar, S. (1992). Improved detection of mutations in the p53 gene in human tumours as single-stranded conformation polymorphisms and double-stranded heteroduplex DNA. PCR Methods and Applications *2*, 96-98.

Spencer, J., Cerf-Bensussan, N., Jarry, A., Brousse, N., Guy-Grand, D., Krajewski, A.S., and Isaacson, P.G. (1988). Enteropathy-associated T cell lymphoma (malignant histiocytosis of the intestine) is recognized by a monoclonal antibody (HML-1) that defines a membrane molecule on human mucosal lymphocytes. American Journal of Pathology *132*, 1-5.

Spencer, J., MacDonald, T.T., Diss, T.C., Walker-Smith, J.A., Ciclitira, P.J., and Isaacson, P.G. (1989). Changes in intraepithelial lymphocyte subpopulations in coeliac disease and enteropathy associated T cell lymphoma (malignant histiocytosis of the intestine). Gut *30*, 339-346.

Stokes, P.L., Asquith, P., Holmes, G.K.T., Mackintosh, P., and Cooke, W.T. (1972). Histocompatibility antigens associated with adult coeliac disease. The Lancet *ii*, 162-164.

Stott, F.J., Bates, S., James, M.C., McConnell, B.B., Starborg, M., Brookes, S., Palmero, I., Ryan, K., Hara, E., Vousden, K.H., and Peters, G. (1998). The alternative product from the human CDKN2A locus, $p14^{ARF}$, participates in a regulatory feedback loop with p53 and MDM2. EMBO J *17*, 5001-5014.

Sun, F., Arnheim, N., and Waterman, M.S. (1995). Whole genome amplification of single cells: mathematical analysis of PEP and tagged PCR. Nucleic Acids Research *23*, 3034-3040.

Swinson, C.M., Hall, P.J., Bedford, P.A., and Booth, C.C. (1983a). HLA antigens in coeliac disease associated with malignancy. Gut *24*, 925-928.

Swinson, C.M., Slavin, G., Coles, E.C., and Booth, C.C. (1983b). Coeliac disease and malignancy. The Lancet *i*, 111-115.

Telenius, H., Carter, N.P., Bebb, C.E., Nordenskjold, M., Ponder, B.A.J., and Tunnacliffe, A. (1992). Degenerate oligonucleotide-primed PCR (DOP-PCR): general amplification of target DNA by a single degenerate primer. Genomics *13*, 718-725.

Thomas, L., Young, J., Searle, J., Ward, M., and Leggett, B. (1995). Loss of heterozygosity analysis in colorectal cancers by PCR using microsatellite markers: Technical considerations. Australian Journal of Medical Science *16*, 71-75.

Tighe, M.R. and Ciclitira, P.J. (1995). The gluten-host interaction. Bailliere's Clinical Gastroenterology *9*, 211-230.

Torinsson, A., Gudjonsdottir, A., Nilsson, S., Samuelson, L., Martinsson, T., Ascher, H., Kristiansson, B., and Wahlstrom, J. (1999). The CTLA 4 gene (2q33) is associated with coeliac disease in Scandinavia. Eighth International Symposium on Coeliac Disease, Naples, Italy (Abstract).

Tosi, R., Vismara, D., Tanigaki, N., Ferrara, G.B., Cicimarra, F., Buffolano, W., Follo, D., and Auricchio, S. (1983). Evidence that celiac disease is primarily associated with a DC locus allelic specificity. Clinical Immunology and Immunopathology *28*, 395-404.

Trejdosiewicz, L.K. and Howdle, P.D. (1995). T-cell responses and cellular immunity in coeliac disease. Bailliere's Clinical Gastroenterology *9*, 251-272.

Trier, J.S., Falchuk, K.R., Carey, M.C., and Schreiber, D.S. (1978). Celiac sprue and refractory sprue. Gastroenterology *75*, 307-316.

Troncone, R. and SIGEP Working Group on Latent Coeliac Disease (1995). Latent coeliac disease in Italy. Acta Paediatrica *84*, 1252-1257.

Tzardi, M., Kouvidou, Ch., Panayiotides, I., Stefanaki, K., Rontogianni, D., Zois, E., Koutsoubi, K., Eliopoulos, G., Delides, G., and Kanavaros, P. (1996). p53 protein expression in non-Hodgkin's lymphoma. Comparative study with the wild type p53 induced proteins mdm2 and p21/waf1. J.Clin.Pathol.: Mol.Pathol. *49*, M278-M282.

Unsworth, D.J. and Brown, D.L. (1994). Serological screening suggests that adult coeliac disease is underdiagnosed in the UK and increases the incidence by up to 12%. Gut *35*, 61-64.

van de Wal, Y., Kooy, Y.M.C., van Veelen, P.A., Pena, S.A., Mearin, L.M., Molberg, O., Lundin, K.E.A., Sollid, L.M., Mutis, T., Benckhuijsen, W.E., Drijfhout, J.W., and Koning, F. (1998a). Small intestinal T cells of celiac disease patients recognize a natural pepsin fragment of gliadin. Proc Natl Acad Sci USA *95*, 10050-10054.

van de Wal, Y., Kooy, Y., van Veelen, P., Pena, S., Mearin, L., Papadopoulos, G., and Koning, F. (1998b). Cutting edge: Selective deamidation by tissue transglutaminase strongly enhances gliadin-specific T cell reactivity. The Journal of Immunology *161*, 1585-1588.

Varon, R., Vissinga, C., Platzer, M., Cerosaletti, K.M., Chrzanowska, K.H., Saar, K., Beckmann, G., Seemanova, E., Cooper, P.R., Nowak, N.J., Stumm, M., Weemaes, C.M.R., Gatti, R.A., Wilson, R.K., Digweed, M., Rosenthal, A., Sperling, K., Concannon, P., and Reis, A. (1998). Nibrin, a novel DNA double-strand break repair protein, is mutated in Nijmegen Breakage Syndrome. Cell *93*, 467-476.

Vartdal, F., Johansen, B.H., Friede, T., Thorpe, C.J., Stevanovic, S., Eriksen, J.E., Sletten, K., Thorsby, E., Rammensee, H.-G., and Sollid, L.M. (1996). The

peptide binding motif of the disease associated HLA-DQ (α1*0501, β1*0201) molecule. Eur.J.Immunol. *26*, 2764-2772.

Vidalpuig, A. and Moller, D.E. (1994). Comparative sensitivity of alternative single-strand conformation polymorphism (SSCP) methods. Biotechniques *17*, 490-496.

Villuendas, R., Piris, M.A., Orradre, J.L., Mollejo, M., Algara, P., Sanchez, L., Martinez, J.C., and Martinez, P. (1992). p53 protein expression in lymphomas and reactive lymphoid tissue. Journal of Pathology *166*, 235-241.

Villuendas, R., Piris, M.A., Algara, P., Sanchez-Beato, M., Sanchez-Verde, L., Martinez, J.C., Orradre, J.L., Garcia, P., Lopez, C., and Martinez, P. (1993). The expression of p53 protein in non-Hodgkin's lymphomas is not always dependent on p53 gene mutations. Blood *82*, 3151-3156.

Viney, J., MacDonald, T.T., and Spencer, J. (1990). Gamma/delta T cells in the gut epithelium. Gut *31*, 841-844.

Volta, U., Molinaro, N., Fusconi, M., Cassani, F., and Bianchi, F.B. (1991). IgA antiendomysial antibody test. Digestive Diseases and Sciences *36*, 752-756.

Wang, L.T., Smith, A., Iacopetta, B., Wood, D.J., Papadimitriou, J.M., and Zheng, M.H. (1996). Nested PCR-SSCP assay for the detection of p53 mutations in paraffin wax embedded bone tumours: improvement of sensitivity and fidelity. J.Clin.Pathol.: Mol.Pathol. *49*, M176-M178.

Warford, A., Pringle, J.H., Hay, J., Henderson, S.D., and Lauder, I. (1988). Southern blot analysis of DNA extracted from formol-saline fixed and paraffin wax embedded tissue. Journal of Pathology *154* , 313-320.

Watanabe, T., Ichikawa, A., Saito, H., and Hotta, T. (1996). Overexpression of the MDM2 oncogene in leukemia and lymphoma. Leukemia and Lymphoma *21*, 391-397.

Weinberg, R.A. (1996). How cancer arises. Scientific American *275*, 32-40.

Wieser, H. (1995). The precipitating factor in coeliac disease. Bailliere's Clinical Gastroenterology *9*, 191-207.

Wright, D.H., Jones, D.B., Clark, H., Mead, G.M., Hodges, E., and Howell, W.M. (1991). Is adult-onset coeliac disease due to a low-grade lymphoma of intraepithelial T lymphocytes? The Lancet *337*, 1373-1374.

Wright, D.H. (1995). The major complications of coeliac disease. Bailliere's Clinical Gastroenterology *9*, 351-369.

Wright, D.H. (1997). Enteropathy associated T cell lymphoma. Cancer Surveys *30*, 249-261.

Wu, X., Bayle, J.H., Olson, D., and Levine, A.J. (1993). The p53-mdm2 autoregulatory feedback loop. Genes and Development *7*, 1126-1132.

Yamaguchi, K., Sugano, K., Fukayama, N., Nakashima, Y., Saotome, K., Yokoyama, T., Yokota, T., and Ohkura, H. (1997). Polymerase chain reaction-based approaches for detection of allelic loss in the *p53* tumor suppressor gene in colon neoplasms. The American Journal of Gastroenterology *92*, 307-312.

Yin, Y., Tainsky, M.A., Bischoff, F.Z., Strong, L.C., and Wahl, G.M. (1992). Wild-type p53 restores cell cycle control and inhibits gene amplification in cells with mutant p53 alleles. Cell *70*, 937-948.

Zhang, L., Cui, X., Schmitt, K., Hubert, R., Navidi, W., and Arnheim, N. (1992). Whole genome amplification from a single cell: implications for genetic analysis. Proc Natl Acad Sci USA *89*, 5847-5851.

Zhang, Y., Xiong, Y., and Yarbrough, W.G. (1998). ARF promotes MDM2 degradation and stabilizes p53: ARF-INK4a locus deletion impairs both the Rb and p53 tumor suppression pathways. Cell *92*, 725-734.

Zhong, F., McCombs, C.C., Olson, J.M., Elston, R.C., Stevens, F.M., McCarthy, C.F., and Michalski, J.P. (1996). An autosomal screen for genes that predispose to celiac disease in the western counties of Ireland. Nature Genetics *14*, 329-333.